Estación Experimental de Aula Dei

Consejo Superior de Investigaciones Científicas

(CSIC)

Zaragoza

Tesis Doctoral

MECANISMOS DE TOLERANCIA AL EXCESO DE COBRE EN SUSPENSIONES CELULARES DE SOJA. CARACTERIZACIÓN DEL TRANSPORTADOR DE COBRE HMA8.

Memoria presentada por Dña. María Bernal Ibáñez

Licenciada en Bioquímica, para optar al grado de Doctor en Ciencias

Zaragoza, Julio 2006

MINISTERIO
DE EDUCACIÓN Y
CIENCIA

CONSEJO SUPERIOR
DE INVESTIGACIONES
CIENTÍFICAS

ESTACIÓN EXPERIMENTAL
DE AULA DEI

Dña. Mª INMACULADA YRUELA GUERRERO, Científico Titular del Consejo Superior de Investigaciones Científicas (CSIC) adscrita a la Estación Experimental de Aula Dei de Zaragoza

CERTIFICA:

Que la Tesis Doctoral **"*Mecanismos de tolerancia al exceso de cobre en suspensiones celulares de soja. Caracterización del transportador de cobre HMA8***" ha sido realizada por la licenciada MARÍA BERNAL IBÁÑEZ en el Departamento de Nutrición Vegetal de la Estación Experimental de Aula Dei (CSIC) de Zaragoza bajo su dirección y que reúne, a su juicio, las condiciones requeridas para optar al grado de Doctor en Ciencias.

Zaragoza, Julio de 2006

Fdo.: Mª Inmaculada Yruela Guerrero

A Fernando

A mi familia

A mi abuela María

“La sabiduría suprema es tener sueños lo bastante grandes

para no perderlos de vista mientras se persiguen”

William Faulkner

AGRADECIMIENTOS

Quisiera aprovechar estas primeras líneas para expresar mi gratitud a todas aquellas personas que, de una u otra forma, han hecho posible la realización de esta Tesis Doctoral, y especialmente:

A la Dra. Inmaculada Yruela, directora de esta Tesis Doctoral, por su ayuda, dedicación y profesionalidad. Mi más sincero agradecimiento.

Al Prof. Rafael Picorel, por darme la oportunidad de trabajar en su laboratorio y realizar esta Tesis, por su confianza y apoyo mostrado en todo momento.

Al Dr. Miguel Alfonso, por el tiempo dedicado, su ayuda con los experimentos de Biología Molecular, sus sugerencias e ideas y por su amistad.

A la Prof. Mª Carmen Risueño y a la Dra. Pilar Sánchez Testillano del Centro de Investigaciones Biológicas (CIB), por permitirme trabajar en su laboratorio y aprender nuevas técnicas. Por el trato recibido y el cariño mostrado en todo momento. Quiero también agradecer su ayuda y colaboración al resto de los miembros del laboratorio, a Ivett, Mª José, Pablo, Carlos, Josefina, Hong y Nandini, que hicieron que mi estancia en el CIB fuera tan agradable.

A la Prof. Salomé Prat del Centro Nacional de Biotecnología (CNB), por su disposición y ayuda.

A las Profs. Mª Luisa Peleato y Mª Francisca Fillat de la Universidad de Zaragoza, por sus consejos y colaboración.

A Mariví Ramiro, por su ayuda, sus buenos consejos y amistad.

Al Consejo Superior de Investigaciones Científicas, por la beca predoctoral que me ha permitido realizar este trabajo.

A todas las personas que trabajan en la Estación Experimental de Aula Dei y, en especial, en el Departamento de Nutrición Vegetal.

De manera especial quiero agradecer a mis compañeras de laboratorio, Raquel, Marian, Sara Sagasti, Vanesa y Sara López, su apoyo, compañerismo y amistad. Para mí son las mejores compañeras que se puede tener. Con ellas he compartido risas, alegrías, penas, complicidades e incontables horas de trabajo. Gracias por los buenos momentos vividos, tanto fuera como dentro del laboratorio. Os voy a echar de menos.

A mis compañeros de despacho, Ricardo y, especialmente a Sergio, por su apoyo y compañerismo en estos últimos meses.

A mis compañeros de Aula Dei, Mariví López, Sofía, María Solanas, Ruth, Rubén, Ana Flor, Ana Álvarez, Fermín, Aurora, Victoria, Victor, Piluca, Irene, Ade, Tere, Carmen, Concha, MC, Jorge Loscos, Loreto, Manu, Carmen Pérez, Javier, María Clemente, David Moret, Jorge Álvaro, Manuel, Pepa, María Muñoz, Merche, Meriam, Olfa y Ana Pina (del SIA) por todos los momentos compartidos dentro y fuera de Aula Dei.

A mis amigas de siempre, Ana, Silvia, Loreto, Myriam, Noelia, Celia, Conchi, Mª Pilar, Elena, Chus, Ibana y Ana.

A mis padres, por su amor, apoyo y comprensión en todos los momentos de mi vida. Por la educación recibida y enseñarme a ver siempre la botella medio llena y no medio vacía.

A mi hermano Alejandro, cómplice y amigo, tanto en la infancia como en la madurez. Gracias por estar siempre ahí.

A mis abuelos, especialmente a mi abuela María, gracias a su esfuerzo y lucha son responsables de la gran cantidad de oportunidades que he tenido.

A Fernando, por su amor y cariño. Por la comprensión, ayuda y paciencia incondicional mostradas durante todos estos años sin las cuales no habría sido capaz de concluir este trabajo. Este esfuerzo también es suyo.

A todos ellos, GRACIAS

ABREVIATURAS

AO	Ascorbato oxidasa
APX	Ascorbato peroxidasa
ATP	Trifosfato de adenosina
ATP sintasa	Adenosina 5'-trifosfato sintasa
BCB	Dominio de unión a cobre
BCDS	Ácido Na_2-2,9-dimetil-4,7-difenil-1,10-fenantrolindisulfónico
BPDS	Ácido Na_2-batofenantrolindisulfónico
BSA	Seroalbúmina bovina
CAO	Amino oxidasa de cobre
cit	Citocromo
Chl	Clorofila
CLSM	Microscopía laser confocal
COX	Citocromo c oxidasa
CSD	Superóxido dismutasa de Cu y Zn
CP43	Complejo antena de 43 kDa del fotosistema II
CP47	Complejo antena de 47 kDa del fotosistema II
D1	Polipéptido del centro de reacción del fotosistema II
D2	Polipéptido del centro de reacción del fotosistema II
DAPI	4',6-diamidino-2-fenilindol diclorhidrato
DCBQ	2, 6-diclorobenzoquinona
DEPC	Dietilpirocarbonato
DHAR	Dehidroascorbato reductasa
DIC	Contraste interdiferencial de Nomarski
EDTA	Ácido etilen-diamino tetra-acético
EDX	Espectroscopia de dispersión de rayos X
F	Fluorescencia
FAD	Dinucleótido de riboflavina y adenina
Fd	Ferredoxina
FNR	Ferredoxin-NADP reductasa
FRO	Óxido reductasa de hierro
GFP	Proteína de fluorescencia verde

GR	Glutatión reductasa
HEPES	N-2-(hidroxi-etil) piperazine-N'-(ácido 2-etanosulfónico)
LC	Lacasa
LHCII	Complejo de antena extrínseca del fotosistema II
LTSEM	Microscopía electrónica de barrido a baja temperatura
MCO	Oxidasas multicobre
MDHAR	Monodehidroascorbato reductasa
MES	Ácido 2-(N-morfolino) etano sulfónico
MT	Metalotioneína
NA	Nicotianamina
$NADP^+$	2'-fosfodinucleótido de nicotianamida y adenina oxidado
NADPH	2'-fosfodinucleótido de nicotianamida y adenina reducido
NBT	Nitroblue tetrazolium
OECC	Complejo mínimo que conserva la capacidad de desprendimiento de oxígeno
OEC33	Proteína extrínseca de 33 kDa del fotosistema II
Q_A	Primera quinona aceptora de electrones
Q_B	Segunda quinona aceptora de electrones
ORF	Marco de lectura abierta
PAGE	Electroforesis en gel de poliacrilamida
PBS	Tampón fosfato salino
PC	Plastocianina
PCR	Reacción en cadena de la polimerasa
Pheo	Feofitina
PPO	Polifenol oxidasa
PS	Fotosideróforo
PSI	Fotosistema I
PSII	Fotosistema II
PVDF	Fluoruro de polivinilideno
RACE	"Rapid amplification of cDNA ends"
RC	Centro de reacción
ROS	Especies reactivas de oxígeno
RT-PCR	PCR reversa
RuBisCo	Ribulosa 1,5-bisfosfato carboxilasa/oxigenasa

SDS	Dodecil sulfato de sodio
SOD	Superóxido dismutasa
TEMED	N, N, N', N'-tetrametil-etil-N-diamina
Tricina	N-tris(hydroximetil) metil glicina
Tris	(Tris)-hidroximetil-amino metano
UTR	Región no traducida
UV	ultravioleta
Y_Z	Tirosina Z de la proteína D1
Y_D	Tirosina D de la proteína D2

ÍNDICE

1. INTRODUCCIÓN GENERAL 1

1.1. BIOQUÍMICA DEL COBRE 3
1.1.1. PROPIEDADES FÍSICO-QUÍMICAS 3
1.2. FUNCIÓN DEL COBRE EN PLANTAS 5
1.2.1. PROTEÍNAS DE COBRE O CUPROPROTEÍNAS 5
1.2.1.1. Cuproproteínas que participan en el transporte de electrones 5
1.2.1.1.1. Proteínas azules de cobre o cuprodoxinas 5
1.2.1.1.2. Oxidasas azules o multicobre oxidasas (MCOs) 6
1.2.1.2. Cuproproteínas involucradas en el transporte y oxidación del oxígeno molecular y en la reducción de compuestos inorgánicos 7
1.2.1.3. Cuproproteínas con diversas funciones 8
1.2.2. DEFICIENCIA DE COBRE EN PLANTAS 10
1.2.3. TOXICIDAD DE COBRE EN PLANTAS 11
1.2.4. COBRE Y FOTOSÍNTESIS 14
1.2.4.1. Organización del cloroplasto 15
1.2.4.2. Función y toxicidad del cobre en el cloroplasto 17
1.2.5. MECANISMOS DE TOLERANCIA A COBRE EN PLANTAS 20
1.3. TRANSPORTE DE COBRE EN PLANTAS 22
1.3.1. TRANSPORTE DE COBRE A LARGA DISTANCIA 22
1.3.1.1. Biodisponibilidad y movilización de cobre en el suelo 22
1.3.1.2. Adquisición y transporte de cobre por la raíz 26
1.3.1.3. Transporte de cobre en el xilema 28
1.3.1.4. Transporte de cobre en la hoja 30
1.3.1.5. Transporte de cobre en el floema 31
1.3.2. HOMEOSTASIS INTRACELULAR DE COBRE EN PLANTAS 32
1.3.2.1. Transporte de cobre en el citoplasma celular 36
1.3.2.1.1. Cuprochaperonas 36
1.3.2.1.2. Metalotioneínas 38
1.3.2.2. Transporte de cobre a través de la membrana plasmática 38
1.3.2.2.1. Familia COPT 38
1.3.2.2.2. Familia YSL 39
1.3.2.2.3. Familia ZIP 39
1.3.2.2.4. Familia NRAMP 40
1.3.2.2.5. Familia P_{1B}-ATPasas 40
1.3.3. REGULACIÓN DE LA HOMEOSTASIS DE COBRE 44

2. OBJETIVOS 47

3. EXCESS COPPER EFFECT ON GROWTH, CHLOROPLAST ULTRASTRUCTURE, OXYGEN-EVOLUTION ACTIVITY AND CHLOROPHYLL FLUORESCENCE IN *Glycine max* CELL SUSPENSIONS 51

3.1. ABSTRACT 53
3.2. INTRODUCTION 53
3.3. MATERIALS AND METHODS 55
3.3.1. Cell suspension growth conditions 55
3.3.2. Cell growth 56
3.3.3. Isolation of thylakoid membranes 56
3.3.4. Oxygen evolution activity 57
3.3.5. Immunoblotting analysis 57
3.3.6. Microscopy imaging 58
3.3.7. Determination of macro and micronutrient elements 59
3.3.8. Energy-dispersive X-ray microanalysis 59
3.3.9. Fluorescence measurements 60
3.4. RESULTS 60
3.4.1. Soybean cell suspension growth 60
3.4.2. Oxygen evolution activity from cell suspensions and thylakoids 63
3.4.3. Effect of Cu on the OEC33 protein 65
3.4.4. Cu-uptake by cell suspensions and its intracellular distribution 67
3.4.5. Morphological and ultrastructural changes in chloroplasts from Cu-adapted cell suspensions 69
3.4.6. Fluorescence spectral changes induced by Cu treatments 72
3.4.7. Effect of Fe and Zn on chloroplast structure and oxygen evolution activity 72
3.5. DISCUSSION 73

4. EXCESS COPPER INDUCES STRUCTURAL CHANGES IN CULTURED PHOTOSYNTHETIC SOYBEAN CELLS 77

4.1. ABSTRACT 79
4.2. INTRODUCTION 79
4.3. MATERIALS AND METHODS 82
4.3.1. Cell culture conditions 82
4.3.2. Sample processing for microscopical structural analysis 83

4.3.3. Morphometric analysis of cell, chloroplast and vacuole size 83
4.3.4. Cytochemical stainings for starch and DNA 83
4.3.5. Copper determination 83
4.3.6. Organic acids analysis 84
4.3.7. Energy-dispersive X-ray microanalysis 84
4.3.8. Low Temperature Scanning Electron Microscopy (LTSEM) 85
4.4. RESULTS 86
4.5. DISCUSSION 94

5. FOLIAR AND ROOT CU SUPPLY AFFECT DIFFERENTLY FE AND ZN UPTAKE AND PHOTOSYNTHETIC ACTIVITY IN SOYBEAN PLANTS 101

5.1. ABSTRACT 103
5.2. INTRODUCTION 103
5.3. MATERIALS AND METHODS 105
5.3.1. Plant material and copper treatment 105
5.3.2. Cell suspension growth conditions 105
5.3.3. Isolation of thylakoid membranes 105
5.3.4. Oxygen evolution activity 106
5.3.5. Determination of micronutrient elements 106
5.3.6. Fluorescence measurements 107
5.4. RESULTS 107
5.4.1. Effect of Cu treatments on soybean plants 107
5.4.2. Effect of Cu treatments on soybean cell suspensions 109
5.4.3. Cu-uptake and its effect on other micronutrients 111
5.5. DISCUSSION 112

6. IDENTIFICATION AND SUBCELLULAR LOCALIZATION OF THE SOYBEAN COPPER P_{1B}-ATPase *Gm*HMA8 TRANSPORTER 115

6.1. ABSTRACT 117
6.2. INTRODUCTION 117
6.3. MATERIALS AND METHODS 119
6.3.1. "*In silico*" sequence analysis of plant P_{1B}-ATPases 119
6.3.2. Cell suspension growth conditions 119
6.3.3. RNA isolation and cDNA synthesis 120
6.3.4. Isolation of *GmHMA8* sequence 120
6.3.5. Isolation of intact chloroplasts and thylakoid membranes 121

6.3.6. *Gm*HMA8 antibody production 122
6.3.7. Immunoblotting analysis 122
6.3.8. Sample processing for microscopical structural analysis and immunofluorescence 122
6.3.9. Cytochemical stainings for starch and DNA 123
6.3.10. Immunofluorescence and Confocal Laser Microscopy 123
6.3.11. Low temperature processing for immunoelectron microscopy 124
6.3.12. Immunogold labelling 124
6.3.13. Quantitative evaluation of immmunogold labelling distribution: Clustering test 125
6.4. RESULTS 125
6.4.1. Isolation of *GmHMA8* cDNA 125
6.4.2. Production of a polyclonal antibody anti-*Gm*HMA8 130
6.4.3. Subcellular localization of *Gm*HMA8 by immunofluorescence labelling 132
6.4.4. Subcellular localization of *Gm*HMA8 by immunogold labelling 135
6.5. DISCUSSION 137

7. IDENTIFICATION OF TWO COPPER *HMA8* P-ATPase mRNAs IN SOYBEAN: ANALYSIS OF THEIR RESPONSE TO COPPER AND THEIR SPLICING REGULATORY MECHANISM 141

7.1. ABSTRACT 143
7.2. INTRODUCTION 143
7.3. MATERIALS AND METHODS 144
7.3.1. Cell suspension growth conditions 144
7.3.2. Plant material 145
7.3.3. Antioxidant isoenzyme assays 145
7.3.4. DNA isolation 146
7.3.5. RNA isolation and cDNA synthesis 146
7.3.6. Identification of two *GmHMA8* mRNAs 147
7.3.7. Expression analysis of two *GmHMA8* mRNAs 148
7.3.8. Northern Blot 148
7.3.9. Expresion analysis of *GmCCS* mRNA 149
7.3.10. Sequence analysis 149
7.4. RESULTS 150
7.4.1. Identification of two *HMA8* mRNAs in soybean 150
7.4.2. *GmHMA8* and *GmHMA8-T* mRNAs are alternatively spliced 155
7.4.3. Copper affects patterns of alternatively spliced *GmHMA8* and *GmHMA8-T* mRNAs 158

7.4.4. Copper increases CuZnSOD activity and *GmCCS* expression 162
7.5. DISCUSSION 163

8. DISCUSIÓN GENERAL 167

9. CONCLUSIONES 187

10. BIBLIOGRAFÍA 191

11. ANEXO 227

11.1. PUBLICACIONES 229

CAPÍTULO 1

INTRODUCCIÓN GENERAL

1.1. BIOQUÍMICA DEL COBRE

El cobre (Cu) es un elemento esencial para los organismos vivos ya que es un constituyente indispensable de un gran número de enzimas y agentes redox que intervienen en el metabolismo celular. Para entender las funciones que desempeña el Cu así como la maquinaria celular que regula su homeostasis consideraremos en primer lugar sus propiedades físico-químicas.

1.1.1. PROPIEDADES FÍSICO-QUÍMICAS

El Cu pertenece al grupo IB de la serie de metales de transición de la tabla periódica de elementos. Su estructura electrónica en estado fundamental es [Ar]$3d^{10}4s$, mientras que la de sus estados de oxidación más habituales, Cu^{+} y Cu^{2+} es $3d^{10}$ y $3d^{9}$, respectivamente.

Los cationes de la serie de elementos d, como el Cu, presentan alta afinidad para formar complejos de coordinación. Debido a su elevada afinidad electrónica, los cationes mono y divalentes de Cu son los iones más efectivos para la unión a moléculas orgánicas.

La geometría, la estequiometría y la estabilidad de los centros de coordinación en las moléculas orgánicas depende de la naturaleza de los ligandos y del estado de oxidación del metal. En el estado de oxidación +1, el ión cuproso (Cu^{+}) tiene todos los orbitales d ocupados, por tanto es diamagnético, y los números de coordinación más habituales son 2, 3 y 4 con geometría tetraédrica o trigonal. En el estado de oxidación +2, el ión cúprico (Cu^{2+}) posee un electrón desapareado en el orbital d, por tanto es paramagnético y los números de coordinación más habituales son 4, 5 y 6 con geometría cuadrada plana.

La geometría de coordinación del Cu y su proximidad a otros metales paramagnéticos han permitido definir tres tipo de centros de Cu^{2+} en las cuproproteínas (Kotch et al., 1997; Falconi y Desideri, 2002):

- Centros de tipo I: se caracterizan por tener una geometría de coordinación tetraédrica distorsionada. Este tipo de centro se encuentra, principalmente en las cuproproteínas azules (ej. plastocianina). El espectro de

absorción presenta una intensa banda de absorción a unos 600 nm, sola o asociada con otras, a la que debe su color azul.

- Centros de tipo II: presentan una geometría cuadrada distorsionada. Las proteínas que tienen este tipo de centro poseen propiedades espectroscópicas similares a las de otros muchos complejos ordinarios de Cu.
- Centros de tipo III: poseen dos átomos de Cu^{2+} coordinados piramidalmente. El sitio activo de estas proteínas contiene dos átomos de Cu muy próximos que se acoplan antiferromagnéticamente.

Actualmente, hay cada vez más estructuras de proteínas de Cu disponibles y se ha observado que además de los tres tipos de centros descritos, existen otros tres que no pueden ser incluidos en ninguno de los anteriores. Por tanto, además de los centros de tipo I, II y III, existen centros trinucleares (I+II+III), centros Cu_A y/o Cu_B y centros tipo metalotioneína (Kaim y Rall, 1996) (Tabla 1-1).

Generalmente las proteínas de Cu tienen un solo tipo de centro, pero es frecuente que en una misma proteína coexistan varios de ellos.

Tabla 1-1. Tipos de centros de Cu^{2+} existentes en las cuproproteínas

TIPO I	TIPO II	TIPO III	TRINUCLEAR	Cu_A	Cu_B
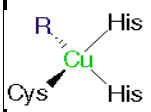	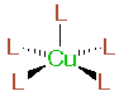	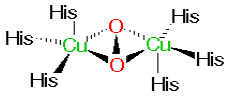	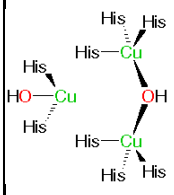	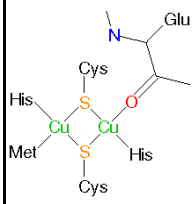	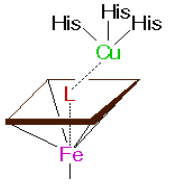

1.2. FUNCIÓN DEL COBRE EN PLANTAS

En plantas, el Cu es un cofactor que interviene en el transporte de electrones durante la fotosíntesis y la respiración, así como en el mecanismo de detoxificación de radicales libres generados en el metabolismo. Las funciones del Cu en la planta vienen determinadas por las enzimas que lo requieren para su funcionamiento, de modo que conocer este tipo de proteínas nos permitirá determinar cuales son las funciones de este metal en la planta.

1.2.1. PROTEÍNAS DE COBRE O CUPROPROTEÍNAS

Funcionalmente, las cuproproteínas se pueden clasificar en tres grupos (De Rienzo et al., 2000; Halcrow et al., 2001; Lindley, 2001a; 2001b; Vila y Fernández, 2001):

1.2.1.1. Cuproproteínas que participan en el transporte de electrones

1.2.1.1.1. Proteínas azules de cobre o cuprodoxinas

- Plastocianina (PC): Se encuentra en los organismos fotosintéticos (cianobacterias, algas y plantas superiores) y se cree que más del 50% del contenido de Cu en el cloroplasto está unido a esta proteína. Se caracteriza por tener en su secuencia un sólo dominio BCB ("blue-copper binding domain") (Nerssisian y Shipp, 2002). La PC es una óxido-reductasa de pequeño tamaño (10 kDa) que se asocia de modo extrínseco a la membrana tilacoidal en el lado del lumen y hace de puente redox entre el citocromo b_6f (cit b_6f) y el fotosistema I (PSI). El grupo prostético de esta proteína es un átomo de Cu ligado a cuatro aminoácidos (dos histidinas, una cisteína y una metionina) en una geometría casi tetraédrica y clasificado como centro de Cu tipo I, que exhibe en su forma oxidada el típico color azul de las proteínas de este grupo (azurina, amicianina, pseudoazurina, estelacianina) (Bonilla, 2000). La plastocianina está codificada por un gen nuclear (*petE*) de forma que se sintetiza en forma de preapoproteína en el citoplasma y se transporta post-traduccionalmente a través de la membrana del cloroplasto (en plantas superiores y algas) o hacia

el lumen del tilacoide (en cianobacterias), donde se une al Cu y forma la holoproteína. Esta cuproproteína es esencial para la fotosíntesis.

En algunas algas y cianobacterias, la biosíntesis de la plastocianina está controlada por la disponibilidad de Cu en el medio de cultivo. Si el contenido de Cu en el medio es inferior a la cantidad requerida para mantener la concentración necesaria de plastocianina, se inicia la transcripción del gen *petJ* que codifica al citocromo c_6. En estas condiciones, este citocromo sustituye a la plastocianina en la cadena de transporte electrónico fotosintético (Merchant, 1998; Molina-Heredia et al., 2003). En plantas superiores se ha identificado una proteína homóloga (citocromo c_{6A}) al citocromo c_6 de cianobacterias y algas (Wastl et al., 2002; 2004; Weigel et al., 2003a; Howe et al., 2006; Schlarb-Ridley et al., 2006), pero se ha demostrado que no realiza la misma función (Weigel et al., 2003b).

- Plantacianina: Pertenece a la familia de fitocianinas. Tiene un tamaño de aproximadamente 10 kDa. Se caracteriza por tener en su secuencia un sólo dominio BCB (Nerssisian y Shipp, 2002). Recientemente se ha demostrado que esta proteína desempeña un papel importante en el desarrollo de la antera y en la polinización en *Arabidopsis thaliana* (Dong et al., 2005).

1.2.1.1.2. Oxidasas azules o multicobre oxidasas (MCOs)

- Ascorbato oxidasa (AO, EC 1.10.3.3): Es una glicoproteína que posee tres dominios BCB. Cataliza la oxidación de ácido ascórbico a ácido dehidroascórbico. Esta enzima contiene ocho átomos de Cu por molécula que se asignan a dos centros de Cu tipo I, dos tipo II y dos tipo III. Se encuentra ampliamente distribuida en los tejidos (Chichiricco et al., 1989; Hayashi y Morohashi, 1993), encontrándose en tallos, flores, frutos y semillas tanto en etapas tempranas como tardías del desarrollo y en células diferenciadas y no diferenciadas. A nivel celular, se ha localizado en la pared celular y en el citoplasma (Nerssisian y Shipp, 2002). Puede actuar como oxidasa terminal de la cadena respiratoria o en combinación con la enzima polifenol oxidasa. La expresión de la ascorbato oxidasa se induce por la luz y por la aparición de heridas por lo que se cree que actúa en los mecanismos de defensa frente a

oxidantes relacionados con el ascorbato o la vitamina C (Nakamura y Go, 2005).

- Lacasa (LC, EC 1.10.3.2): Esta enzima posee tres dominios BCB y contiene ocho átomos de Cu por molécula que se asignan a dos sitios de Cu tipo I, dos tipo II y dos tipo III. Cataliza la oxidación de diversas sustancias fenólicas e inorgánicas. En plantas, participa en mecanismos de respuesta a la herida y en la síntesis de lignina (Nerssisian y Shipp, 2002; Nakamura y Go, 2005).

1.2.1.2. Cuproproteínas involucradas en el transporte y oxidación del oxígeno molecular y en la reducción de compuestos inorgánicos

- Citocromo c oxidasa (COX, EC 1.9.3.1): Es una oxidasa terminal de la cadena de transporte electrónico mitocondrial que cataliza la transferencia de electrones. La energía que se produce tras este proceso es utilizada para bombear protones hacia el exterior de la membrana mitocondrial y sintetizar ATP. Contiene dos átomos de Cu y dos átomos de Fe (hemo). Cuando esta enzima se inhibe existe otra oxidasa llamada “oxidasa alternativa” que proporciona una ruta de oxidación alternativa en la mitocondria. En esta vía no se produce el bombeo de protones al exterior por lo que toda la energía producida se pierde en forma de calor. Esta oxidasa alternativa contiene Cu pero no Fe (Marschner, 1995).

- Diamino oxidasa (CAOs, EC 1.4.3.6): Es una flavoproteína que pertenece a la familia de amino oxidasas que contienen Cu en su estructura (CAO, “copper containing amine oxidases”). Su función consiste en catalizar la oxidación aeróbica de poliaminas a aldehídos. Esta familia de proteínas se ha descrito en un amplio rango de organismos (bacterias, levaduras, plantas, y mamíferos). Todas las CAOs caracterizadas son proteínas homodiméricas, cada subunidad tiene un peso molecular de 70-95 kDa y un átomo de Cu y un grupo carbonilo como cofactor (Halcrow et al., 2001).

En plantas, la enzima diamino oxidasa se encuentra localizada en el apoplasto de la epidermis y en el xilema de tejidos maduros donde se ha propuesto que funciona como sistema liberador de agua oxigenada, necesaria para la actividad peroxidasa en el proceso de lignificación y suberización

(Marschner, 1995). En general, las amino oxidasas de plantas participan en el crecimiento y desarrollo de la planta, y en los mecanismos de defensa a través de la formación de metabolitos secundarios (Cona et al., 2006).

- Polifenol oxidasa (PPO): Es una metaloenzima que contiene un centro de unión de Cu tipo III y es homóloga a la enzima hemocianina encontrada en moluscos. La PPO puede tener actividad cresolasa (EC 1.14.18.1) utilizando el oxígeno molecular para catalizar la oxidación de varios monofenoles a *o*-difenoles) y actividad catecolasa (EC 1.10.3.1, oxidación de *o*-difenoles a *o*-quinonas). El sitio activo de todas las PPO es un centro dinuclear formado por dos átomos de Cu, cada uno de ellos coordinado a tres histidinas **(**Gerdemann et al., 2002).

Las PPOs de plantas están codificadas por genes nucleares y contienen un péptido señal que dirige la proteína al lumen tilacoidal donde se encuentra en forma soluble o débilmente unida a la membrana tilacoidal (Sommer et al., 1994). El peso molecular de la preproteína está en el rango de 55-70 kDa y la proteína madura se obtiene tras la ruptura proteolítica de un fragmento de 15-20 kDa del extremo C-terminal (Marusek et al., 2006). Las PPOs son abundantes en la pared celular, donde participan en la biosíntesis de lignina, y en las membranas tilacoidales donde se ha propuesto que se requieren para la síntesis de pigmentos (betalainas) y para la detoxificación de especies reactivas de oxígeno (Marschner, 1995; Marusek et al., 2006).

1.2.1.3. Cuproproteínas con diversas funciones

En plantas, las proteínas que pertenecen a esta familia son las cuprozinc superóxido dismutasas (CuZnSODs), las cuprochaperonas (ver 1.3.2.1.1), las metalotioneínas (ver 1.3.2.1.2) y las Cu-ATPasas (ver 1.3.2.2.5) (Lindley, 2001b).

- CuZnSOD (SOD, EC 1.15.1.1): Es una enzima ubicua en todos los organismos aerobios y constituye una de sus defensas primarias frente a las especies reactivas de oxígeno. Esta enzima cataliza la dismutación del radical superóxido (O_2^-) a peróxido de hidrógeno (H_2O_2). El H_2O_2 generado como producto de la reacción es eliminado por la catalasa o por la ascorbato peroxidasa (APX) en el ciclo ascorbato-glutatión. Mediante la eliminación del

radical O_2^-, la SOD disminuye el riesgo de formación del radical hidroxilo (·OH) a través de la reacción de Haber-Weiss. La CuZnSOD de plantas está formada generalmente por homodímeros de ~ 30-33 kDa. Se localiza en el apoplasto, citosol, cloroplastos, glioxisomas, núcleo y espacio intermembrana mitocondrial. Las dos isoenzimas mayoritarias son la CuZnSOD citosólica y la CuZnSOD cloroplástica; esta última puede encontrarse tanto en el estroma (forma soluble) como en los tilacoides (asociada a membrana). Los átomos de Cu y Zn de su centro activo están directamente involucrados en los mecanismos de detoxificación de radicales O_2^- generados durante la fotosíntesis.

Tabla 1-2. Resumen de las principales características de las cuproproteínas en plantas

PROTEÍNA	TIPO DE CENTRO	FUNCIÓN
Plastocianina	I	Fotosíntesis
Plantacianina	I	Desarrollo antera y polinización
Ascorbato oxidasa	I+II+III	Metabolismo de pared celular Defensa antioxidante
Lacasa	I+II+III	Lignificación
Citocromo c oxidasa	Cu_A+Cu_B	Respiración aerobia
Diamino oxidasa	II	Lignificación Defensa
Polifenol oxidasa	III	Síntesis de pigmentos Defensa antioxidante Lignificación
Cu/Zn SOD	II	Defensa antioxidante
Cu-ATPasas	tipo metalotioneína	Distribución intracelular de Cu Detoxificación
Metalotioneínas	tipo metalotioneína	Detoxificación
Cuprochaperonas	tipo metalotioneína	Distribución intracelular de Cu

Recientemente, se ha descrito la función del Cu en la síntesis del cofactor de molibdeno (Mo) (Kuper et al., 2004). Este hecho permite relacionar el metabolismo del Cu con la asimilación de nitrógeno y la biosíntesis de fitohormonas (Mendel, 2005).

Todo lo expuesto indica que el Cu es un elemento esencial para el crecimiento y desarrollo normal de la planta (6-12 μg $Cu \cdot g^{-1}$ de tejido seco). Si el Cu suministrado a la planta se encuentra por debajo de los niveles fisiológicos (5 μg $Cu \cdot g^{-1}$ de tejido seco), ésta desarrollará síntomas de deficiencia y si por el contrario se encuentra por encima de los niveles fisiológicos, la planta desarrollará síntomas de toxicidad (20-30 μg $Cu \cdot g^{-1}$ de tejido seco) (Marschner, 1995).

1.2.2. DEFICIENCIA DE COBRE EN PLANTAS

La deficiencia de Cu se observa a menudo en plantas que crecen en suelos donde el nivel de Cu es bajo de forma inherente (ej. suelos calcáreos) y en suelos con alto contenido de materia orgánica donde el Cu está acomplejado (Marschner, 1995). En general, los primeros síntomas de deficiencia de Cu aparecen en las hojas jóvenes y están asociados a puntos cloróticos que se extienden desde la punta hacia los márgenes de la hoja (Schubert, 1982). Otro síntoma característico es una mala lignificación que ocurre incluso a niveles bajos de deficiencia. En estas condiciones, el tallo se dobla y se enrolla y las hojas se distorsionan debido a la insuficiente lignificación de los vasos del xilema (Fig.1-1). Estos fenómenos ocurren por un descenso severo de la actividad de las enzimas diamino oxidasa y polifenol oxidasa (Marschner, 1995).

Fig. 1-1. Síntomas de la deficiencia de Cu en mora (Tewari et al., 2006)

Por otro lado, el Cu es necesario para la lignificación de la antera. Su lignificación produce su rotura liberando de esta manera el polen. Así, en deficiencia de Cu este proceso no ocurre y el polen no es viable, además disminuye la formación de órganos reproductores. En estado reproductivo, las anteras y ovarios son los componentes de la planta con más Cu, esto pone de manifiesto la necesidad de fertilizar con Cu durante la época reproductiva para mejorar el rendimiento de la semilla y el fruto (Marschner, 1995).

La deficiencia de Cu también puede provocar: *i)* atrofiamiento; *ii)* clorosis; *iii)* necrosis; *iv)* retardo de la senescencia; *v)* disminución de la concentración de carbohidratos en el tejido vegetativo; *vi)* alteración de la composición lipídica de las membranas biológicas; *vii)* inhibición de actividades enzimáticas (lacasa, CuZnSOD, diamino oxidasa, ascorbato peroxidasa); *viii)* daño oxidativo; *ix)* bloqueo de la fotosíntesis a nivel del PSI (existe una correlación directa entre el contenido de Cu en la hoja, la concentración de plastocianina y la actividad del fotosistema I (PSI)); *x)* inhibición débil de la respiración a través de la inhibición parcial de la actividad de la enzima citocromo c oxidasa (Marschner, 1995).

La deficiencia de Cu puede corregirse con la aplicación de fertilizantes tanto en el suelo como a nivel foliar.

Recientemente, se ha comenzado el estudio a nivel molecular del efecto de la deficiencia de Cu en la regulación de la expresión génica de la maquinaria de homeostasis de Cu en plantas superiores (Wintz et al., 2003). Sin embargo, aún son escasos los trabajos realizados en este tema.

1.2.3. TOXICIDAD DE COBRE EN PLANTAS

Las mismas propiedades redox que explican el funcionamiento del Cu en la catálisis de múltiples reacciones biológicas y que, por tanto, hacen que sea un elemento esencial, son las responsables de su toxicidad (Halliwell y Gutteridge, 1989). El Cu puede cambiar de forma cíclica su estado de oxidación dentro de la célula cuando entra en contacto con productos intermediarios del metabolismo aerobio, conocidos como especies reactivas de oxígeno: radical superóxido (O_2^-), anión peróxido (O_2^{2-}), peróxido de hidrógeno

(H_2O_2) y radical hidroxilo (·OH). Estas especies reactivas son generadas por la reducción incompleta del oxígeno molecular durante la fotosíntesis y la respiración. En estas condiciones, el Cu en estado reducido puede generar radicales ·OH mediante la catálisis de la reacción de Fenton:

$$Cu^{+} + H_2O_2 \rightarrow Cu^{2+} + OH^{-} + \cdot OH$$

El Cu^{2+} se puede volver a reducir en presencia del radical superóxido:

$$Cu^{2+} + O_2^{-} \rightarrow Cu^{+} + O_2$$

Y el balance neto de estas dos reacciones es lo que se conoce como reacción de Haber-Weiss, en la cual el Cu cataliza la producción de radical ·OH a partir de radical O_2^{-} y de H_2O_2. El radical ·OH es uno de los oxidantes más poderosos que se conocen, capaz de reaccionar rápidamente con numerosos compuestos celulares esenciales, incluyendo lípidos de membranas, proteínas, carbohidratos y ADN (Halliwell y Gutteridge, 1989).

Otro hecho que hace que el Cu sea tóxico deriva de su capacidad de interaccionar inespecíficamente con cadenas laterales de aminoácidos (cisteína, metionina e histidina). Este efecto puede producir cambios conformacionales en las proteínas, bloqueo del sitio activo, y la inactivación de su función biológica.

Fig. 1-2. Síntomas de la toxicidad de Cu (5-100 ppm) en el crecimiento y desarrollo de plantas de girasol (modificado de www.crystalclay.com/copper.jpg).

Para la mayoría de las especies vegetales, la presencia de altas concentraciones de Cu en el medio de cultivo es tóxica para el crecimiento pudiendo provocar: *i)* clorosis; *ii)* necrosis; *iii)* atrofiamiento; *iv)* decoloración de las hojas; *v)* descenso en el contenido de clorofila; *vi)* interacción con otros iones esenciales; *vii)* reducción de biomasa e inhibición del crecimiento de la raíz (Lidon y Henriques, 1993; Maksymiec, 1997; Pätsikkä et al., 2002; Panou-Filotheou y Bosabalidis, 2004; Kopittke y Menzies, 2006) (Fig.1-2).

A nivel celular, la toxicidad de Cu puede ocasionar: *i)* la inhibición de actividades enzimáticas y de función de proteínas; *ii)* la peroxidación de lípidos (De Vos et al., 1993; Ouariti et al., 1997; Quartacci et al., 2001; Mithöfer et al., 2004); *iii)* estrés oxidativo (Navari-Izzo et al., 1998; Cuypers et al., 2000; Mithöfer et al., 2004); *iv)* alteraciones en la estructura cloroplástica y en la composición de la membrana tilacoidal (Baszynski et al., 1988; Lidon y Henriques, 1991, 1993; Ciscato et al., 1997; Pätsikkä et al., 1998; Quartacci et al., 2000); *v)* la modificación de la morfología de los cromosomas durante el proceso de división celular (Jiang et al., 2001).

Las plantas poseen una gran variedad de mecanismos de defensa frente al estrés oxidativo que incluyen a los sistemas antioxidantes enzimáticos (superóxido dismutasas, catalasas, guaiacol peroxidasas, polifenol oxidasa, glutatión peroxidasa, ciclo ascorbato-glutatión) y a los no enzimáticos (carotenoides, ascorbato, glutatión, α-tocoferol). En las plantas, el exceso de Cu provoca una respuesta inmediata de los sistemas antioxidantes debido a la generación de especies reactivas de oxígeno. Así, se han descrito cambios en la actividad y en el contenido de algunos de los componentes de la maquinaria antioxidante tales como ascorbato peroxidasa (APX), monodehidroascorbato reductasa (MDHAR), dihidroascorbato reductasa (DHAR), glutatión reductasa (GR), superóxido dismutasas (SODs) y guiacol peroxidasa (De Vos et al., 1992; Luna et al., 1994; Weckx y Clijsters, 1996; Kurepa et al., 1997; Navari-Izzo et al., 1998; Gupta et al., 1999; Drazkiewicz et al., 2003 y 2004; Tewari et al., 2006). Estos cambios se han observado tanto en hojas como en raíces y dependen de la concentración de Cu y del tiempo de exposición al mismo. También existen indicios de la participación del ciclo ascorbato-glutatión (Gupta et al., 1999; Drazkiewicz et al., 2003)

Por otro lado, las especies reactivas de oxígeno generadas por el exceso de Cu pueden provocar la peroxidación de lípidos. Así, se ha observado un descenso en el contenido de lípidos y una modificación de la composición de ácidos grasos de las membranas tilacoidales (Sandmann y Böger, 1980; Luna et al., 1994; Maksymiec et al., 1994). Como consecuencia, se han encontrado modificaciones en la movilidad del fotosistema II (PSII) en la membrana tilacoidal (Quartacci et al., 2000).

Otro efecto provocado por el exceso de Cu es la reducción de la enzima nitrato reductasa que es necesaria para la asimilación de nitrato. Este hecho se traduce en un menor contenido de nitrógeno total, así como de aminoácidos tanto en la raíz como en las hojas (Llorens et al., 2000).

Recientemente, Jonak et al. (2004) han observado que el exceso de Cu activa la cascada de MAPK quinasas ("mitogen-activated protein kinases"), de forma que estas proteínas están involucradas en la transducción de la señal inducida por metales pesados.

1.2.4. COBRE Y FOTOSÍNTESIS

La fotosíntesis es un proceso fundamental en la Naturaleza que tiene importantes repercusiones sobre la vida en la Tierra puesto que condiciona la evolución de los ecosistemas y la vida en nuestro planeta. La fotosíntesis oxigénica usa la energía solar para producir NADPH y ATP, que posteriormente se emplea como fuente de energía para elaborar hidratos de carbono a partir de dióxido de carbono (CO_2) y agua (H_2O); simultáneamente se libera oxígeno a la atmósfera como subproducto.

La reacción neta de la fotosíntesis en plantas, algas y cianobacterias puede formularse como:

$$nCO_2 + nH_2O \xrightarrow{luz} (CH_2O)_n + nO_2$$

donde $(CH_2O)_n$ son los hidratos de carbono. La fotosíntesis transcurre en dos fases: procesos unidos a membrana y procesos no unidos a membrana. En los primeros la clorofila y otros pigmentos de las células fotosintéticas (carotenos, xantofilas) absorben la energía lumínica y la transforman en energía química y poder reductor (ATP y NADPH), liberándose oxígeno. En los procesos no unidos a membrana, el ATP y NADPH producidos anteriormente se emplean

para reducir el CO_2 y formar glucosa y otros productos orgánicos en el Ciclo de Calvin (Hipkins y Baker, 1984). La formación de oxígeno y la reducción del CO_2 son por tanto procesos separados y distintos.

1.2.4.1. Organización del cloroplasto

La fotosíntesis en las plantas tiene lugar en unos orgánulos subcelulares llamados cloroplastos. La Fig. 1-3 muestra la organización estructural del cloroplasto en un corte transversal.

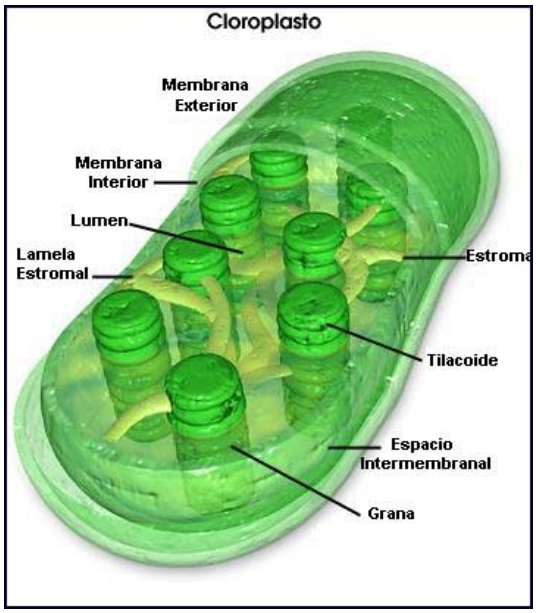

Fig. 1-3. Estructura del cloroplasto (modificado de linus.ajusco.upn.mx/fotosintesis/cloroplasto.html).

El cloroplasto está rodeado por una doble membrana. La membrana externa del cloroplasto es permeable a la mayor parte de metabolitos de bajo peso molecular, mientras que la membrana interna es prácticamente impermeable a la mayoría de las sustancias. Sin embargo, ambas membranas cloroplásticas son muy permeables al CO_2, sustrato de la síntesis de los hidratos de carbono. El espacio entre las membranas interna y externa se denomina espacio intermembranal. La región acuosa encerrada por la membrana interna se llama estroma. Las enzimas necesarias para catalizar las reacciones en las que el CO_2 se reduce para formar glucosa se localizan en el estroma. Suspendida en el interior del estroma existe una membrana continua

denominada membrana tilacoidal, que encierra un espacio interno conocido como lumen. La membrana tilacoidal contiene todos los pigmentos fotosintéticos del cloroplasto y todas las enzimas necesarias en las reacciones primarias dependientes de la luz. Esta membrana está muy plegada en un entramado de vesículas aplastadas, con forma de saco, que se disponen en apilamientos denominados grana o en vesículas individuales que atraviesan el estroma y conectan los grana. Las porciones de la membrana tilacoidal que se localizan dentro de los grana, y no están así expuestas al estroma, se llaman lamelas granales, mientras que las porciones de la membrana tilacoidal expuestas al estroma se conocen como lamelas estromales.

Embebidos en las membranas tilacoidales se localizan varios complejos multiproteicos: fotosistema I (PSI), fotosistema II (PSII), citocromo *b*$_6$*f* (cit *b*$_6$*f*) y ATP sintasa; cada uno de los cuales contribuye a la reacción fotosintética global (Fig. 1-4).

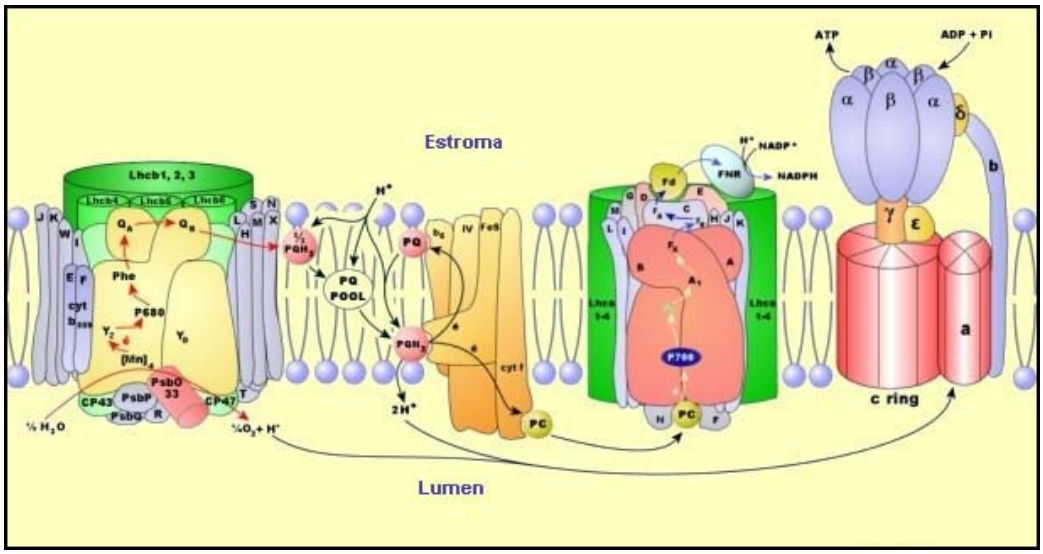

Fig. 1-4. Esquema de la cadena de transporte electrónico fotosintético (modificado de www.uqtr.ca/labcarpentier/eng/main.html)

Los fotosistemas I y II son complejos pigmento-proteína que contienen 200-250 moléculas de clorofila y 50 moléculas de carotenoides aproximadamente. Cada fotosistema está constituido por un centro de reacción (RC) y un complejo “antena”. El complejo “antena” capta la energía lumínica y transfiere la energía de excitación al RC donde se produce la separación de

cargas entre pigmentos que actúan como donador (clorofilas) y aceptor (feofitina) de electrones. Esta separación de cargas se estabiliza a través de aceptores secundarios de electrones y cataliza un transporte electrónico a través de la membrana fosfolipídica que proporcionará a la célula vegetal el poder reductor en forma de NADPH. Como consecuencia de estos procesos también se establece un gradiente de pH a través de la membrana que dará lugar a la formación de ATP catalizada por la ATP sintasa.

Ambos fotosistemas se encuentran conectados mediante un transporte electrónico no cíclico, denominado esquema Z, por medio del citocromo b_6f. Además de estos complejos de membrana también intervienen en este transporte electrónico proteínas solubles tales como la plastocianina (PC) que actúa como donador de electrones al PSI una vez reducida por el cit b_6f y la ferredoxina (Fd), aceptor de electrones del PSI, que reduce a la ferredoxina-NADP reductasa (FNR), la cual posteriormente reduce al $NADP^+$.

El transporte electrónico fotosintético es uno de los procesos biológicos más eficientes que se conocen.

1.2.4.2. Función y toxicidad del cobre en el cloroplasto

Los cloroplastos contienen una gran variedad de metales (Cu, Fe, Mn y Zn) que son esenciales para su función. En concreto, el Cu participa como cofactor redox en dos procesos básicos que tienen lugar en el cloroplasto: *i)* la cadena de transporte electrónico fotosintético, donde el Cu actúa como cofactor de la plastocianina en el lumen tilacoidal y *ii)* la detoxificación de radicales O_2^-, donde el Cu actúa como cofactor de la enzima CuZnSOD y de la polifenol oxidasa en el estroma y lumen cloroplástico, respectivamente (Raven et al., 1999). Estudios en algas han mostrado que el Cu participa en la regulación y síntesis de los complejos fotosintéticos (Moseley et al., 2002). También se ha propuesto que podría ser un componente estructural del PSII (Barón et al., 1995; Burda et al., 2002; 2003).

El cloroplasto es un orgánulo extremadamente sensible al estrés por exceso de Cu que puede ocasionar la pérdida de la actividad fotosintética (Droppa y Horváth, 1990; Barón et al., 1995; Quartacci et al., 2000). Esto

ocasiona una importante disminución de la productividad primaria de la célula vegetal que repercute en el desarrollo global de la planta.

La disminución en el contenido de clorofila es un síntoma común provocado por la toxicidad del Cu. Este efecto podría deberse al bloqueo de su biosíntesis en la etapa de formación del ácido δ-aminolevulénico (Stiborová et al., 1986). También se han descrito alteraciones en la estructura del cloroplasto y en la composición de la membrana tilacoidal (Baszynski et al., 1988; Lidon y Henriques, 1991 y 1993; Ciscato et al., 1997; Pätsikkä et al., 1998; Quartacci et al., 2000; Küpper et al., 2003) (Fig. 1-5). En particular, se ha observado que la toxicidad por Cu provoca: *i)* la degradación de las zonas apiladas y no apiladas de los cloroplastos; *ii)* el aumento en el número y en el tamaño de las plastoglobulinas; *iii)* la aparición de inclusiones intratilacoidales. Así se ha propuesto que el Cu puede interferir en la biosíntesis de la maquinaria fotosintética modificando la composición de los pigmentos y de las proteínas embebidas en el tilacoide (Lidon y Henriques, 1991; Maksymiec et al., 1994).

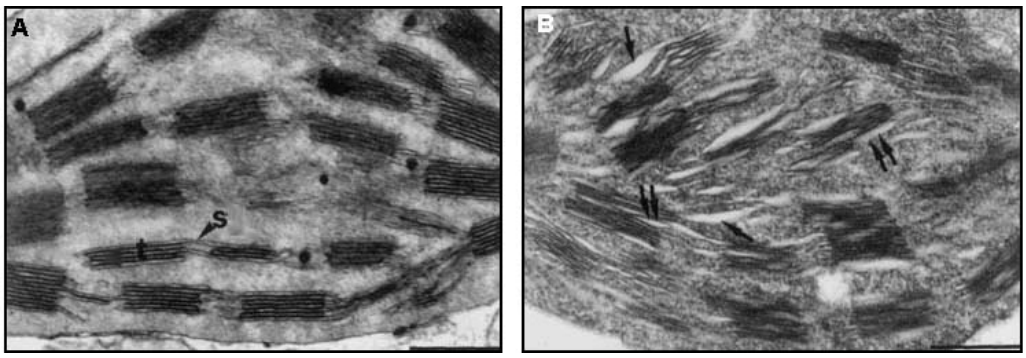

Fig. 1-5. Efecto de la toxicidad del Cu en la ultraestructura del cloroplasto. Cloroplastos de hojas tratadas con 10 μM (A) y 50 μM (B) de Cu. Tilacoides (t), estroma (s). Las flechas muestran cambios en los grana de la membrana tilacoidal. La barra corresponde a 0.5 μm (Quartacci et al., 2000).

Numerosos estudios *in vitro* han mostrado que la cadena de transporte electrónico fotosintético es muy sensible a la acción tóxica del Cu y en particular el PSII (Fig.1-6) (Droppa y Horváth, 1990; Barón et al., 1995).

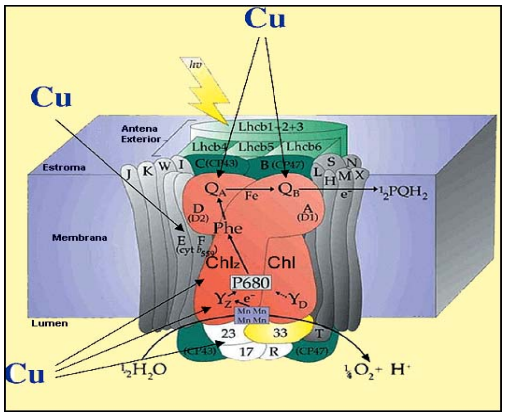

Fig. 1-6. Sitios de acción del ión Cu en el fotosistema II (modelo de Nield et al., 1995, modificado en Yruela, 2005).

En las plantas, el PSII está formado por al menos 22 subunidades proteicas entre las que se pueden distinguir las que forman parte de la antena extrínseca (LHCII), que es el complejo antena mayoritario, la antena interna (CP43 y CP47), el centro de reacción (D1, D2 y citocromo b_{559}) y los polipéptidos expuestos al lumen que estabilizan el complejo de manganeso que cataliza la oxidación del agua (33 kDa, 23 kDa y 16 kDa). Estas subunidades proteicas tienen asociados cofactores tales como quinonas (Q_A y Q_B), iones Ca^{2+}, Cl^- y HCO_3^-, clorinas (clorofila y feofitina), átomos metálicos (Mn, Fe), que son indispensables para las funciones de separación y estabilización de cargas, y fotooxidación del agua.

Tanto el lado donador como el lado aceptor de electrones del PSII han sido propuestos como lugares de acción del ión Cu. En el lado aceptor del PSII, el sitio de Q_B (Mohanty et al., 1989) y el dominio feofitina (Pheo)-Fe-Q_A (Yruela et al., 1991; 1992; 1993; 1996a) se han mostrado como los sitios más sensibles a la acción tóxica del Cu. En el lado donador del PSII, la tirosina Z (Y_Z) de la proteína D1 (Arellano et al., 1995), la tirosina D (Y_D) de la proteína D2 (Sersen et al., 1997), el complejo de manganeso y las proteínas extrínsecas que estabilizan el complejo de manganeso, son los lugares de acción tóxica del ión Cu propuestos.

Los diferentes sitios de acción del ión Cu descritos en la literatura dependen de la cantidad de Cu aplicada por unidad de centro de reacción (RC). Así, a concentraciones de Cu bajas (Cu/RC $\leq$ 250) se produce un

descenso del 50% en la actividad fotosintética y en la fluorescencia variable de clorofila *a,* sin que se observe modificación de la composición polipeptídica del PSII. Sin embargo, a concentraciones de Cu superiores (Cu/RC $>$ 250), las proteínas extrínsecas (33, 23 y 16 kDa) que estabilizan el complejo de manganeso que cataliza la oxidación del agua, se desprenden. Por otro lado, tanto el complejo antena (LHCII) como la proteína D1 del PSII, no se ven afectados por el ión Cu incluso a altas concentraciones (Yruela et al., 2000).

También se ha descrito que el Cu afecta las propiedades redox del citocromo b_{559} asociado al RC del PSII (Jegerschöld et al., 1995; Yruela et al., 1996b; 2000; Roncel et al., 2001; Burda et al., 2003; Bernal et al., 2004). Por otro lado, se ha comprobado que el Cu estimula los efectos adversos generados por la fotoinhibición (Aro et al., 1993). Se ha propuesto que esta estimulación es debida a que: *i)* el Cu cataliza la formación de radicales ·OH a partir del radical O_2^- producido en el lado aceptor de electrones durante el transporte electrónico (Yruela et al., 1996b); *ii)* el exceso de Cu provoca deficiencia de Fe y un descenso en el contenido de clorofila (Pätsikkä et al., 2001).

1.2.5. MECANISMOS DE TOLERANCIA A COBRE EN PLANTAS

En la última década se han descubierto plantas hiperacumuladoras, endémicas de suelos metalíferos, capaces de eliminar residuos tóxicos de suelos y aguas contaminadas. Estas plantas han desarrollado unos mecanismos de tolerancia específicos que están controlados por un número escaso de genes. Estos mecanismos actúan tanto a nivel externo (movilización y absorción) como a nivel interno (distribución y compartimentalización) (Macnair, 1993). Por lo que respecta a los mecanismos internos, el ritmo de absorción y de translocación a la parte aérea son dos factores que determinan el índice de acumulación y tolerancia a los metales. Un buen ejemplo lo constituyen las especies hiperacumuladoras que concentran los iones metálicos preferentemente en los órganos aéreos, contrariamente a las plantas no acumuladoras que lo hacen en las raíces (Brown et al., 1995).

Para resistir la toxicidad de los metales asimilados, estas plantas adoptan una serie de estrategias bioquímicas y moleculares, que incluyen: *i)* la reducción de la adquisición del metal por acción de micorrizas o de exudados extracelulares; *ii)* la estimulación de la entrada del metal a través de la membrana plasmática; *iii)* la formación de complejos con ácidos orgánicos, metalotioneínas, fitoquelatinas o proteínas de choque térmico; *iv)* la compartimentalización (Hall, 2002).

La excreción de ácidos orgánicos como citrato, malato y oxalato está correlacionada con la resistencia de las plantas superiores a los metales, especialmente al aluminio (Al) (Delhaize y Jones, 2001). En el caso del Cu, se ha observado que es un eficiente inductor de la exudación de ácidos orgánicos por la raíz (Yang et al., 2001), principalmente de citrato (Murphy et al., 1999). Además, la aplicación exógena de malonato y malato alivia la toxicidad derivada de la exposición a exceso de Cu (Parker et al., 2001).

Por otro lado, se ha propuesto que tanto las metalotioneínas como las fitoquelatinas participan en el mecanismo de tolerancia a Cu (Cobbet y Golsbrough, 2002). En el caso de las metalotioneínas existen evidencias claras de su participación: *i)* el nivel de expresión de las metalotioneínas de tipo II está estrechamente correlacionado con la tolerancia a Cu en un grupo de ecotipos de *A. thaliana* (Murphy y Taiz, 1995); *ii)* el nivel de expresión de las metalotioneínas (MT) de tipo II aumenta en el mutante *cup1-1* de *A. thaliana* que se caracteriza por acumular Cu (2-3 veces más) (van Vliet et al., 1995); *iii)* la tolerancia a Cu de la planta metalófila *Silene vulgaris* está relacionada con el aumento de expresión de las metalotioneínas de tipo II (van Hoof et al., 2001); *iv)* la transformación de plantas transgénicas de tabaco con el gen de la metalotioneína *MT CUP1* de levaduras contribuye a la fitoextracción de Cu de suelos contaminados (Thomas et al., 2003). Sin embargo, no se han encontrado datos que muestren que las fitoquelatinas actúen en el mecanismo de detoxificación de Cu.

Recientemente, se ha propuesto que tanto los transportadores de membrana como las cuprochaperonas también podrían participar en el mecanismo de tolerancia a Cu.

1.3. TRANSPORTE DE COBRE EN PLANTAS

1.3.1. TRANSPORTE DE COBRE A LARGA DISTANCIA

Tanto la deficiencia como la toxicidad de Cu pueden provocar alteraciones graves en el desarrollo y crecimiento de la planta. Por este motivo, su homeostasis debe estar altamente regulada. De este modo, al igual que la mayor parte de los macro- y micro- nutrientes, el Cu requiere la coordinación de cinco procesos (Clemens et al., 2002): *i)* biodisponibilidad y movilización en el suelo; *ii)* adquisición, transporte y almacenaje en la raíz; *iii)* transporte en el xilema; *iv)* transporte al interior de las hojas; *v)* transporte en el floema (Fig. 1-7).

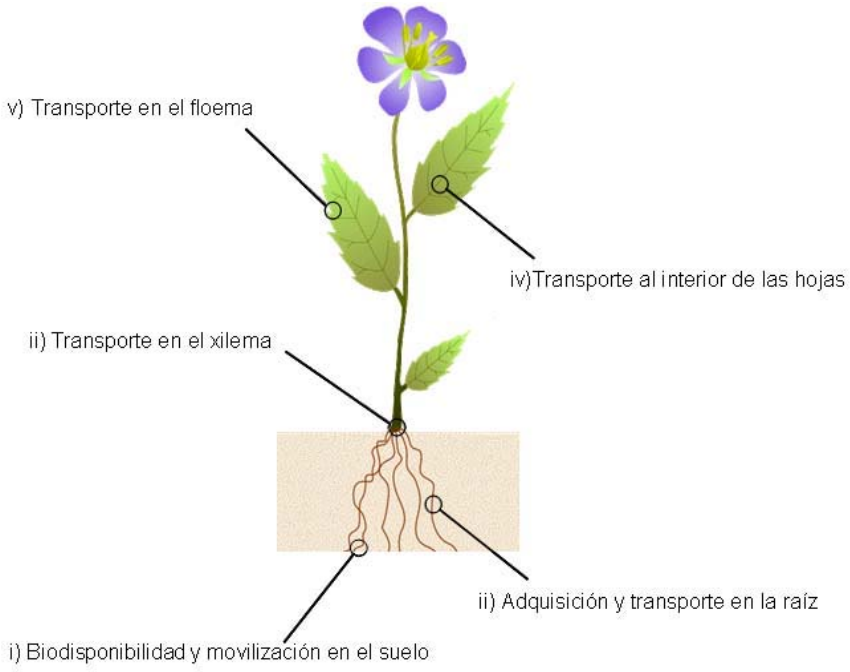

Fig. 1-7. Mecanismo de transporte de Cu a larga distancia (modificado de Clemens et al., 2002).

1.3.1.1. Biodisponibilidad y movilización de cobre en el suelo

Para sobrevivir y crecer, las plantas se tienen que adaptar a las variaciones existentes en la composición mineral del suelo y a la accesibilidad de sus nutrientes. La disponibilidad de un elemento mineral en concreto se define como la fracción de ese elemento que puede ser absorbida por las raíces de una determinada planta. Así, el término disponibilidad de nutrientes

implica definir el estado físico-químico del nutriente en el suelo así como las relaciones raíz-planta (Brun et al., 2001).

El Cu aparece en el suelo casi exclusivamente en forma divalente y está adsorbido a materia orgánica, óxidos de Fe y Mn, arcillas y a otros silicatos. La movilidad, disponibilidad y toxicidad potencial del Cu en el suelo depende de: *i)* las propiedades físico-químicas del suelo (pH, textura, materia orgánica, microorganismos, etc); *ii)* la concentración existente en la solución del suelo; *iii)* la naturaleza de su asociación con otras especies iónicas; *iv)* la liberación de Cu de la fase sólida a la solución del suelo (Lepp, 2004).

La disponibilidad natural de los micronutrientes en la solución del suelo suele estar limitada. Por ejemplo, en suelos alcalinos y calcáreos (30% de la superficie terrestre), el Fe se encuentra en forma de óxidos e hidróxidos de muy baja solubilidad y, por tanto, poco disponible para la planta, y el 98% del Cu de la solución del suelo (10^{-4} a 10^{-5} M) está acomplejado por compuestos orgánicos de bajo peso molecular (Fox y Guerinot, 1998).

Para resolver estas dificultades, las plantas tienen diversas estrategias que modifican las características de la rizosfera y movilizan los nutrientes del suelo que son poco accesibles de forma natural. Estas estrategias son: *i)* la solubilización de los nutrientes de la fase sólida del suelo; *ii)* la movilización de estas especies iónicas hacia la superficie de la raíz; *iii)* la mejora de los mecanismos de absorción que incluye: 1) la acidificación de la rizosfera mediante excreción de H^+ que favorece la solubilización de los micronutrientes; 2) la excreción de compuestos de bajo peso molecular que facilitan la movilización de los micronutrientes.

Así como los mecanismos de adquisición de Fe por la raíz son los más conocidos a nivel fisiológico (Estrategia II en gramíneas y Estrategia I en monocotiledóneas no gramíneas y dicotiledóneas) (Marschner, 1995), en el caso del Cu se desconocen. Existen evidencias experimentales contradictorias en relación a la reducción del metal como requisito previo a su asimilación por la planta. Podría ocurrir que la estrategia utilizada varíe en función de la especie en consideración. Así, se ha observado que las deficiencias de Fe y de Cu, pero no de otros iones metálicos, inducen la actividad reductasa en raíces de guisante y de soja (Welch et al., 1993; Norvell et al., 1993; Cohen et al., 1997) y que la inducción de esta enzima provoca una acumulación de Cu y Mn

en las raíces y en la parte aérea de guisante (Welch et al., 1993). Cohen et al. (1997) realizaron estudios cinéticos en raíces de guisante en deficiencia de Fe y de Cu para averiguar si se inducía la misma reductasa, o si por el contrario eran distintas. Estos autores observaron que la reducción de Cu, al igual que la de Fe, se ajusta a una cinética de tipo Michaelis-Menten con un pH óptimo para la reducción de ambos de 5,5-6,0, y plantearon la existencia de una única reductasa en la raíz para ambos tipos de deficiencias. Estos resultados son compatibles con un modelo en el que el estado nutricional del Fe y del Cu regule la actividad reductasa variando la cantidad de enzima que se localiza en la membrana plasmática. A la vista de la posible reducción de Cu^{2+} a Cu^{+}, se ha propuesto que la liberación de Cu^{+} a la superficie de la raíz podría ser una forma de desestabilizar los complejos que forma el Cu^{2+} en la rizosfera del suelo, de la misma manera que ocurre tras la liberación de Fe^{2+} (Bienfait, 1988).

Estos resultados se corresponden bien con los observados en otros organismos (algas, levaduras). En ambos casos, tanto el Fe^{3+} como el Cu^{2+} son reducidos por unas reductasas presentes en la membrana plasmática antes de entrar a la célula (Hasset y Kosman, 1995; Hill et al., 1996). Además, existe una conexión entre el metabolismo del Cu y del Fe a nivel del transportador de Fe de alta afinidad de la membrana plasmática. Este transportador necesita Cu para su función.

Existen también datos experimentales que sugieren que la reducción de Cu no es necesaria para la absorción del metal por la raíz. Bell et al. (1991) estudiaron la absorción de Cu^{+} y Cu^{2+} mediante el uso de quelatos específicos de Cu^{+} (BCDS, ácido Na_2-2,9-dimetil-4,7-difenil-1,10-fenantrolindisulfónico) y Cu^{2+} (BPDS, ácido Na_2-batofenantrolindisulfónico) en raíces de maíz. Los resultados indicaron que la especie absorbida por la raíz era Cu^{2+} ya que el Cu^{+} se absorbía con una eficiencia muy baja. A este respecto hay que señalar que el maíz es una gramínea que adquiere el Fe como Fe^{3+}-fitosideróforo (PS) mediante la estrategia II, sin necesidad de reducirlo, por lo que algo similar podría ocurrir con la adquisición del Cu. Por otro lado, en el mutante *frd1* ("ferric reductase defective") de *A. thaliana,* que se caracteriza por no tener inducida la actividad reductasa en condiciones de deficiencia de Fe, se ha observado que

no se reduce su capacidad de acumular Cu en la parte aérea de la planta (Yi y Guerinot, 1996).

Robinson et al. (1999) identificaron en *A. thaliana* el primer gen que codifica a la reductasa férrica responsable de la reducción de Fe (III) en la superficie de la raíz (*AtFRO2,* "ferric reductase oxidase") y que se induce en condiciones de deficiencia de Fe. Este gen también ha sido identificado en tomate (*LeFRO1*; Li et al., 2004), guisante (*PsFRO1*; Waters et al., 2002) y en *Medicago truncatula* (*MtFRO1*; López-Millán et al., 2005). Estos genes pertenecen a una superfamilia de flavocitocromos cuyos miembros contienen en su secuencia sitios de unión a FAD y NADPH, de acuerdo con su función en la transferencia de electrones desde los nucleótidos de pirimidina citosólicos a los quelatos férricos del lado opuesto de la membrana. Recientemente, se han identificado siete miembros más de esta familia de reductasas en *A. thaliana* (*AtFRO1-8*) (Mukherjee et al., 2006). Cada uno de ellos tiene una expresión diferencial en función de la parte de la planta analizada y del estado nutricional de Fe y Cu en el que se encuentre. Estos autores han propuesto que estos genes podrían participar en la homeostasis de Fe y Cu a lo largo de toda la planta. También han observado que varios miembros de la familia FRO (*AtFRO3* y *AtFRO6*) tienen una regulación dependiente del nivel de Cu, esto indica un posible papel de estos enzimas en la homeostasis de Cu en la planta. Sin embargo, al mismo tiempo no está claro que la reducción de Cu sea fisiológicamente relevante, es posible que las reductasas férricas sean capaces de reducir Cu pero que esta función no sea importante para el transporte de este elemento a las células vegetales.

Por otro lado, existen evidencias experimentales de que la deficiencia de Cu estimula la extrusión de protones provocando la acidificación de la rizosfera. Esta acidificación varía con el tratamiento y no siempre está correlacionada con el aumento de la actividad de la reductasa férrica. Grusak y Pezeshgi (1996) demostraron una separación temporal en la expresión de las dos respuestas, en la cual la elevada extrusión de protones precede en varios días al comienzo del aumento de la actividad reductasa. Además, la localización de la actividad reductasa y de la extrusión de protones a lo largo de la raíz no es la misma por lo que existe una separación espacial de las dos respuestas. También se ha visto que el mutante *frd1* de *A. thaliana* tiene una acidificación normal de la

rizosfera en condiciones de deficiencia de Fe. Esto sugiere que el producto del gen *FRD1* no está involucrado en la acidificación de la rizosfera y que, por tanto, las dos respuestas podrían estar reguladas de forma independiente (Cohen et al., 1997; Yi y Guerinot, 1996).

Finalmente, las raíces también pueden liberar compuestos orgánicos a la rizosfera que solubilicen el Cu y en consecuencia aumenten su disponibilidad para las plantas (Mench et al., 1988; 1990; Treeby et al., 1989).

1.3.1.2. Adquisición y transporte de cobre por la raíz

Una vez que los iones son movilizados y alcanzan la zona de absorción de la raíz por difusión a través de la solución salina del suelo, son arrastrados por el movimiento del agua hacia la raíz o entran en contacto con las zonas de absorción de la raíz a medida que ésta crece (Fernández y Maldonado, 2000). La raíz primaria es el órgano especializado en la absorción de agua y de nutrientes del suelo, pero no todas las partes de la raíz son igualmente eficientes en la realización de este proceso. El perfil de absorción a lo largo del eje longitudinal de la raíz varía según el tipo de ión, el estado nutricional de la planta y la especie considerada (Marschner, 1995). La tendencia general en el caso de dicotiledóneas y plantas perennes es que el ritmo de entrada de iones por unidad de longitud decrece a medida que aumenta la distancia al ápice de la raíz. En el caso del Cu, se ha visto que en maíz la entrada es uniforme a lo largo de la raíz y sólo en condiciones de deficiencia aumenta la absorción en la zona apical pero no en la basal (Bell et al., 1991).

Una vez en el interior de las raíces, los nutrientes minerales se distribuyen por toda la planta a través del xilema, impulsados por la corriente ascendente de agua que genera el flujo de transpiración. Así, de la misma manera que el agua, los iones se transportan radialmente en la raíz para alcanzar el xilema a través de dos vías: 1) vía apoplástica y 2) vía simplástica (Fig.1-8).

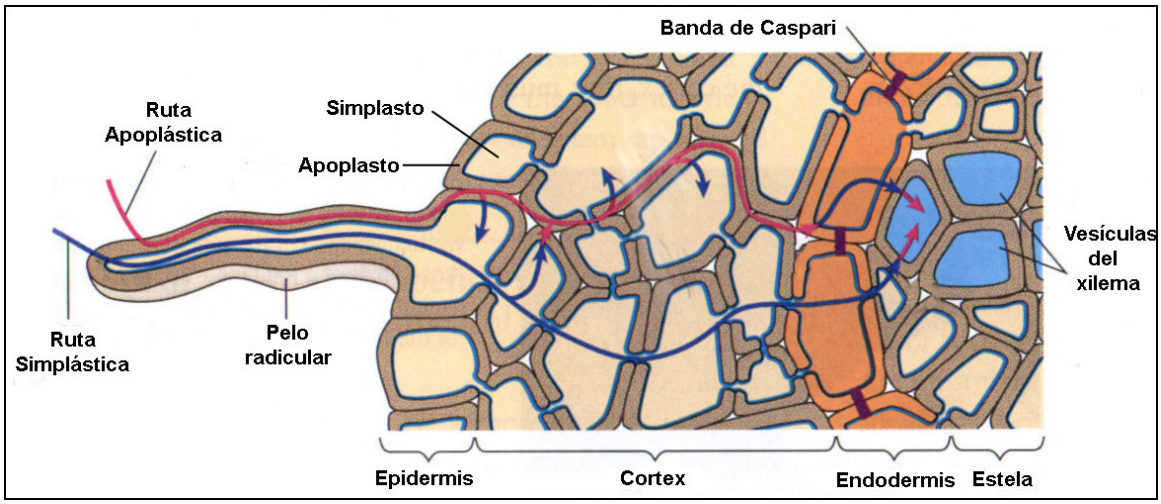

Fig. 1-8. Esquema del transporte radial de nutrientes en la raíz (modificado de www.uvm.edu/~dbarring/bio2atlas.html).

1) Vía apoplástica: las células vegetales están separadas por la pared celular que forma una matriz porosa contínua denominada espacio libre aparente, espacio periplásmico o apoplasto. A lo largo de este recorrido, los iones pueden ser absorbidos tanto por las células del cortex como de la epidermis. Sin embargo, la existencia de la banda de Caspari en las células de la endodermis supone una barrera infranqueable en el camino hacia el xilema, por tanto, los iones deben atravesar obligatoriamente la membrana plasmática de las células que componen la endodermis. La permeabilidad, selectividad y afinidad de los canales y transportadores localizados en esta membrana plasmática determinan, en última instancia, qué iones y a qué velocidad se incorporan o liberan. Además, los grupos carboxilo de las paredes celulares actúan como intercambiadores catiónicos de baja afinidad y selectividad que restringen el libre movimiento de solutos cargados, reteniendo los cationes y excluyendo los aniones.

2) Vía simplástica: los iones son primero incorporados a las células de la epidermis o del cortex y luego son transportados, célula a célula, a través del cortex, la endodermis y el periciclo hasta el xilema.

Recientemente, se ha visto que el transporte de Cu en la raíz de *A. thaliana* se realiza a través de un transportador de Cu llamado *At*COPT1 (ver 1.3.2.2.1) (Sancenón et al., 2004). Estos autores han demostrado que *At*COPT1 está localizado en la membrana plasmática de raíz, concretamente

en la zona apical e interviene en el transporte de Cu de alta afinidad en raíces. Posiblemente, como ocurre en levaduras (Puig y Thiele, 2002), existe un sistema de transporte de baja afinidad mediado también por un transportador de esta familia (Sancenón et al., 2004).

Otros transportadores que podrían intervenir en la adquisición de Cu en la raíz de *A. thaliana* son *At*ZIP2 y *At*ZIP4. Pertenecen a la familia de transportadores ZIP (ver 1.3.2.2.3) y se ha descrito que los genes que los codifican están regulados positivamente en deficiencia de Cu (Wintz et al., 2003; Mukherjee et al., 2006).

Una vez en el interior de las células de la raíz, se ha propuesto que el Cu es transportado radialmente por vía simplástica unido a nicotianamina (NA) formando el complejo Cu^{2+}-NA (Pich et al., 1994). En el momento en el que este complejo Cu^{2+}-NA llega al cilindro vascular de la raíz se descarga a los vasos del xilema (Sancenón et al., 2004).

Las ventajas de usar la zona apical de la raíz para la absorción de cationes metálicos se pueden resumir en: 1) una mejor regulación de la adquisición del catión metálico debida a una mayor regulación del transportador correspondiente y 2) mayor facilidad de entrada del catión metálico al cilindro vascular por no existir banda de Caspari en esta zona (Sancenón et al., 2004).

1.3.1.3. Transporte de cobre en el xilema

En las plantas superiores un medio de transporte adecuado de los micronutrientes entre los lugares de adquisición y los de consumo es esencial. Esto es debido a que si los micronutrientes (al igual que el agua) absorbidos por los pelos radicales de la raíz y que atraviesan la endodermis continuaran pasando de célula a célula el transporte sería muy lento. Sin embargo, existen dos tipos de tejidos conductores: xilema y floema que facilitan este transporte. El xilema se encarga del transporte ascendente de agua e iones desde la raíz. El floema transporta la materia orgánica de las partes verdes a los distintos órganos. En este proceso de transporte, el agua juega un papel determinante ya que los micronutrientes son translocados hacia la parte aérea de la planta gracias a la tasa de transpiración generada por el transporte de agua desde la raíz hasta las hojas.

La forma por la que el Cu es transportado al interior del xilema aún se desconoce, pero probablemente se realiza a través de un transportador llamado OPT3 (Wintz et al., 2003). Este transportador, que ha sido identificado en *A. thaliana,* pertenece a la familia de transportadores oligopeptídicos OPT (Yen et al., 2001) y es homólogo a los transportadores de Fe^{2+} de la familia YSL en Arabidopsis e YS1 de maíz (ver 1.3.2.2.2). El descubrimiento de la existencia de estos transportadores en plantas de Estrategia I, como Arabidopsis, es sorprendente ya que entre las plantas superiores sólo las gramíneas sintetizan y excretan fitosideróforos (PS), el sustrato del transportador YS1. Como todas las plantas producen nicotianamina (NA), y esta molécula es muy similar tanto en estructura como en su capacidad de unir Fe a los fitosideróforos, se podría especular una posible función transportadora para las proteínas YSL similar a la de los complejos Fe^{2+}-NA en plantas no gramíneas. Del mismo modo, podría especularse con una función transportadora de complejos Cu^{2+}-NA para la proteína OPT3 tanto en dicotiledóneas como monocotiledóneas. La expresión del gen *AtOPT3* aumenta en condiciones de deficiencia de Cu. Además, es capaz de reestablecer el crecimiento normal de las levaduras tras complementar el mutante Δ*ctr1* (CTR1, "copper transporter 1"). Esto sugiere que este transportador podría ser un componente de la maquinaria de transporte de Cu en *A. thaliana* (Wintz et al., 2003). Stacey et al. (2002) han observado que la expresión de este gen aumenta en el tejido vascular de las plantas lo que sugiere que este transportador podría participar en el transporte de Cu a larga distancia.

Una vez en el interior del xilema, el Cu se transporta como complejo Cu^{2+}-NA. Tiffin (1972) encontró en el exudado del xilema de 4 dicotiledóneas que el Cu estaba presente en forma de uno o más complejos cargados negativamente y que posiblemente estos complejos estaban formados por aminoácidos. Posteriormente, Graham (1979) mostró que más del 99% del Cu total del xilema de girasol estaba acomplejado con compuestos de carga negativa. Sin embargo, hasta la década de los 90 no se conoció qué molécula actuaba como quelante de Cu en el xilema. Pich y Scholz (1996) demostraron que la NA juega un papel determinante en el transporte de Cu en el xilema basándose en resultados obtenidos en un mutante de tomate llamado *chloronerva* que se caracteriza por no tener NA. En este mutante, el Cu se

acumula en las raíces y apenas es transportado a la parte aérea de la planta por lo que el transporte de Cu en el xilema es ineficiente. Sin embargo, tras aplicar NA en las raíces o en las hojas, el transporte de Cu aumenta de forma proporcional a la concentración aplicada. Estos datos conducen a la teoría de que la NA está involucrada en la translocación de Cu^{2+} desde la raíz hasta la parte aérea de la planta formando complejos Cu^{2+}-NA. Sin embargo, la NA no tiene por qué ser el único translocador de Cu^{2+} en el xilema. Liao et al. (2000) demostraron que el Cu^{2+} que no se encuentra unido a NA se encuentra coordinado con histidina. En el exudado del xilema el Cu se ha encontrado en un amplio rango de concentraciones, desde cantidades traza hasta altas concentraciones del orden de 14 mmol m^{-3} (Loneragan, 1981). Además, los niveles de Cu en el xilema pueden variar en función de las condiciones ambientales.

1.3.1.4. Transporte de cobre en la hoja

El mecanismo de transporte de Cu desde la savia del xilema hasta las hojas todavía no se conoce en profundidad. Se ha propuesto que el transportador implicado en esta descarga sea *At*YSL2 aunque son necesarios más estudios para confirmar este hecho. *At*YSL2 es capaz de transportar Fe^{2+} y Cu^{2+} cuando están quelados por NA (preferentemente Fe^{2+}). Se supone que estos metales entran en la célula como complejos con NA. Este transportador podría intervenir en el movimiento lateral de Cu y Fe en el tejido vascular por lo que podría ser el encargado de transportar estos metales desde el xilema a la hoja. Sin embargo, también se ha visto que no está regulado transcripcionalmente por Cu por lo que se cree que su función en el transporte de Cu no es tan importante (DiDonato et al., 2004; Schaaf et al., 2005).

Una vez que el Cu llega al apoplasto, éste entra en la hoja y se distribuye a los diferentes orgánulos subcelulares, principalmente al cloroplasto, a través de diversos mecanismos de homeostasis intracelular (ver 1.3.2). El exceso de Cu, al igual que el de Zn, Ni y Mn, se acumula principalmente en las vacuolas de las raíces de forma acomplejada con ácidos orgánicos. Sin embargo, tanto en condiciones de exceso de Cu como en el caso de plantas hiperacumuladoras, el Cu se acumula en la base de los tricomas y en las

vacuolas de células de la epidermis de la hoja unido a diversos quelantes principalmente ácidos orgánicos. Esta localización preferencial en células de la epidermis minimiza su efecto tóxico manteniendo el metal lo más lejos posible de las células del mesófilo, donde se realiza la fotosíntesis.

De la misma manera que existe controversia con la necesidad de reducir el Cu^{2+} a Cu^{+} antes de ser incorporado por la raíz, no se sabe si el Cu se reduce en el apoplasto antes de entrar a la célula del mesófilo. Se ha propuesto que una reductasa (*At*FRO6) podría reducir el Cu^{2+} a Cu^{+} en la membrana plasmática de las células del mesófilo (Mukherjee et al., 2006).

1.3.1.5. Transporte de cobre en el floema

El floema es el tejido vegetal encargado del transporte a larga distancia, desde los órganos de producción, principalmente hojas maduras, hasta los tejidos en crecimiento y órganos reproductivos o de almacenamiento. En angiospermas está constituido por tubos cribosos, floema parenquimático y, en algunos tejidos, fibras floemáticas. En el floema secundario, los elementos de los tubos cribosos se encuentran asociados a células parenquimáticas especializadas denominadas células de compañía (García Luís y Guardiola, 2000). En los elementos de los tubos cribosos existen unas terminaciones conocidas como placas cribosas. Los elementos de los tubos cribosos son las células más características de este tejido. Durante su madurez funcional estas células pierden el núcleo aunque conservan su citoplasma. Las células de compañía mantienen vivo dicho citoplasma permitiendo el transporte de sustancias.

El transporte de Cu en el floema se estudió inicialmente mediante: *i)* el análisis del exudado del xilema; *ii)* estudios de translocación con $^{64}Cu^{2+}$ radiactivo tras su aplicación en hojas; *iii)* la observación de la variación del contenido de Cu en las hojas a lo largo del tiempo. El Cu se ha encontrado en el floema en un rango de concentraciones de 3-140 mmol m^{-3} (Loneragan, 1981).

Se considera que el Cu es un elemento de movilidad intermedia en la planta (Loneragan, 1981; Kochian, 1991; Marschner, 1995). Generalmente, el Cu está inmóvil en el floema a menos que esté asociado al proceso de

senescencia donde es móvil (Loneragan, 1981). Para explicar este fenómeno se ha propuesto que cuando el Cu entra en la hoja se une a proteínas y deja de estar disponible para su retranslocación vía floema incluso en deficiencia de Cu, hasta que la hoja senesce y estas proteínas se hidrolizan. En este momento el Cu sale de la hoja unido a complejos nitrogenados provenientes de la hidrólisis proteica. Existen evidencias de que el Cu se transporta en el floema unido a NA (Pich et al., 1994). Además, se ha observado que en condiciones de senescencia el Cu puede transportarse en el floema unido a distintas metalotioneínas (ver 1.3.2.1.2) (Guo et al., 2003) y a la chaperona de Cu CCH (ver 1.3.2.1.1) (Mira et al. 2001a). Hasta la fecha ésta es la única chaperona descrita que interviene en el transporte a larga distancia y probablemente transporta Cu de hojas que mueren a hojas que están creciendo. Las metalotioneínas también están implicadas en el transporte de Cu en el floema en condiciones de senescencia ya que aumentan su expresión en estas condiciones.

1.3.2. HOMEOSTASIS INTRACELULAR DE COBRE EN PLANTAS

La regulación de la concentración de micronutrientes a nivel intracelular es crucial para el crecimiento de la planta e implica varias estrategias. Desde un punto de vista bioquímico o molecular, el control de la homeostasis supone una red compleja de mecanismos que incluyen el paso del micronutriente a través de la membrana plasmática por medio de una serie de transportadores más o menos específicos. La reactividad y solubilidad limitada de la mayoría de los micronutrientes metálicos hace que estén constantemente inmovilizados, una vez que han llegado al citoplasma, por la formación de complejos con aminoácidos, proteínas o metabolitos. Estos complejos contribuyen por un lado a evitar los efectos tóxicos del metal y por otro ayudan a su distribución a los sitios en los que es requerido y a los compartimentos diana. Por último, intervienen en la detoxificación mediante el almacenamiento del exceso en la vacuola o mediante extrusión del metal al exterior celular (Williams et al., 2000; Clemens, 2001; Hall, 2002; Pilon et al., 2006).

Debido a la alta toxicidad del Cu, éste no puede encontrarse de forma libre en la célula. En levaduras, la concentración de Cu libre es < 10^{-18} M, es

decir, menos de un átomo de Cu por célula, mientras que la concentración total de Cu es de 70 μM (Rae et al., 1999). Por este motivo, este metal se transporta en el citosol unido a unas proteínas llamadas chaperonas de Cu o cuprochaperonas y a metalotioneínas, y dirigido a los distintos compartimentos subcelulares a través de diversos tipos de transportadores de membrana.

El uso de la levadura *Saccharomyces cerevisiae* como herramienta genética y bioquímica ha permitido investigar los mecanismos moleculares implicados en la homeostasis de Cu en las células eucariotas (Puig y Thiele, 2002). En la Tabla 1-3 se resumen los principales componentes de las rutas de transporte, distribución y detoxificación del ión Cu en levaduras y plantas. En la figura 1-9 se presenta un esquema de la homeostasis de Cu en una célula de *A. thaliana* (Pilon et al., 2006). Es de señalar que hasta la fecha la mayoría de los estudios realizados se restringen a esta especie vegetal.

Tabla 1-3. Proteínas que participan en la homeostasis de Cu en levaduras y plantas.

<table>
<tr><th>PROTEÍNA/ORGANISMO</th><th colspan="2">LEVADURAS</th><th colspan="2">PLANTAS</th></tr>
<tr><td>REDUCTASAS</td><td colspan="2">FRE1-7</td><td colspan="2">AtFRO1-8</td></tr>
<tr><td rowspan="3">METALOCHAPERONAS</td><td colspan="2">CCS</td><td colspan="2">CCS</td></tr>
<tr><td colspan="2">COX17</td><td colspan="2">COX17</td></tr>
<tr><td colspan="2">ATX1</td><td colspan="2">CCH</td></tr>
<tr><td rowspan="4">METALOTIONEÍNAS</td><td colspan="2">CUP1</td><td colspan="2">MT-1</td></tr>
<tr><td colspan="2" rowspan="3">CRS5</td><td colspan="2">MT-2</td></tr>
<tr><td colspan="2">MT-3</td></tr>
<tr><td colspan="2">MT-4</td></tr>
<tr><td rowspan="10">TRANSPORTADORES DE MEMBRANA</td><td rowspan="2">Alta afinidad</td><td>ScCTR1</td><td>COPT</td><td>AtCOPT 1-6</td></tr>
<tr><td rowspan="2">ScCTR3</td><td rowspan="2">YSL</td><td>AtOPT3</td></tr>
<tr><td rowspan="8">Baja afinidad</td><td>AtYSL2</td></tr>
<tr><td rowspan="2">FET4</td><td rowspan="2">ZIP</td><td>AtZIP2</td></tr>
<tr><td>AtZIP4</td></tr>
<tr><td>SMF1/2</td><td>NRAMP</td><td>AtNRAMP1</td></tr>
<tr><td rowspan="5">ScCTR2</td><td rowspan="5">P_{1B}-ATPasa</td><td>AtRAN1</td></tr>
<tr><td>AtHMA1</td></tr>
<tr><td>AtHMA5</td></tr>
<tr><td>AtHMA6</td></tr>
<tr><td>AtHMA8</td></tr>
<tr><td rowspan="2">FACTORES DE TRANSCRIPCIÓN</td><td colspan="2">ACE1</td><td colspan="2" rowspan="2"></td></tr>
<tr><td colspan="2">MAC1</td></tr>
</table>

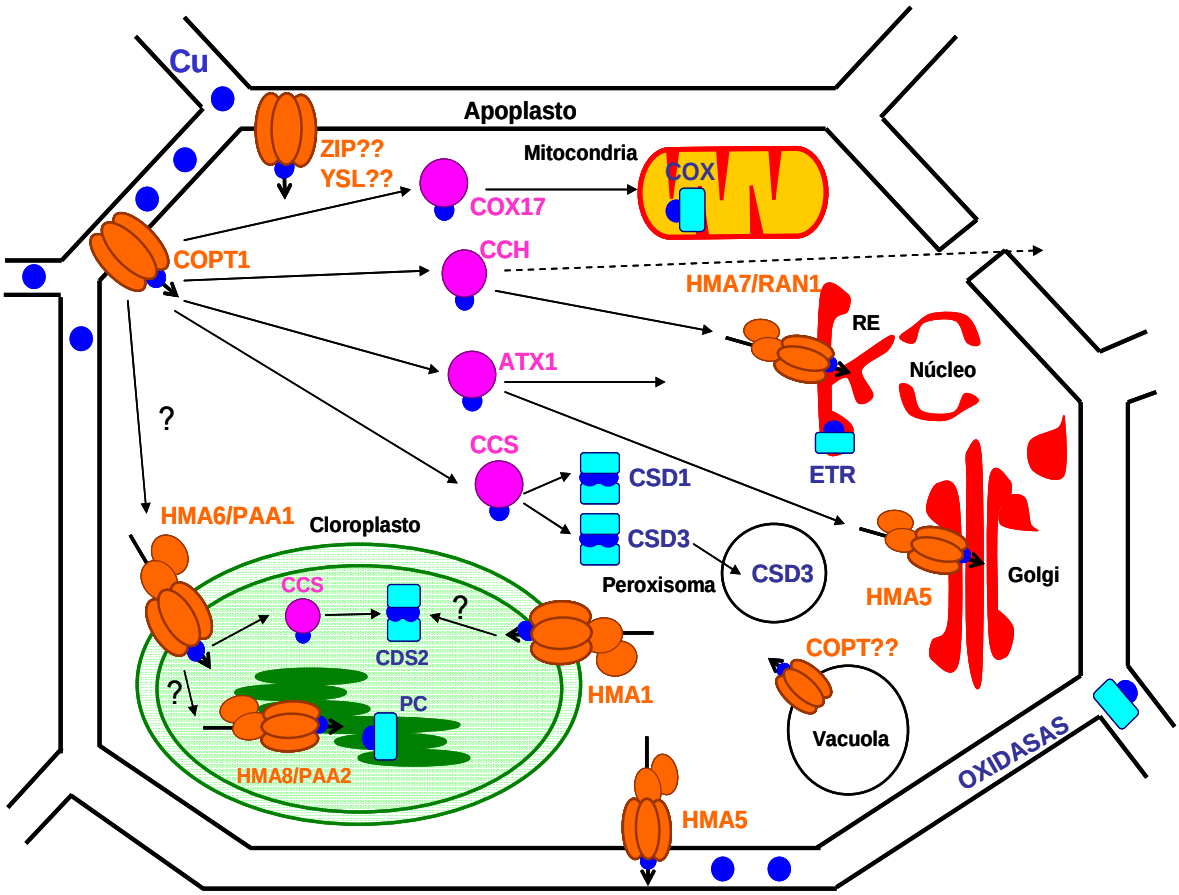

Fig. 1-9. Homeostasis de Cu en una célula de *A. thaliana*. El cobre extracelular es transportado al interior celular por el transportador COPT1 donde se distribuye a través de las cuprochaperonas COX17, CCH, ATX1 y CCS y de transportadores de membrana específicos, como las P_{1B}-ATPasas HMA1, HMA5, HMA6 (PAA1), HMA7 (RAN1), HMA8 (PAA2) y los transportadores de alta afinidad de la familia COPT, hasta llegar a las diferentes cuproproteínas diana que son: la citocromo c oxidasa (COX); las enzimas CuZn superóxido dismutasas citosólica, peroxisomal y cloroplástica (CSD1, CSD2, CSD3); la plastocianina (PC); el receptor de etileno (ETR) y las oxidasas apoplásticas. La flecha discontinua indica la participación de la chaperona CCH en el transporte de Cu a larga distancia. El Cu se muestra con un círculo azul, los transportadores de membrana aparecen marcados en naranja, las cuprochaperonas en rosa y las cuproproteínas diana en azul. Los interrogantes indican mecanismos que permanecen todavía sin identificar. Este modelo se ha realizado en base al conocimiento actual de la homeostasis de Cu en *A. thaliana*.

1.3.2.1. Transporte de cobre en el citoplasma celular

1.3.2.1.1. Cuprochaperonas

Las cuprochaperonas pertenecen a una familia de pequeñas proteínas citosólicas encargadas de la distribución intracelular de Cu a los diferentes compartimentos subcelulares y a las proteínas que requieren Cu en su grupo prostético. Esta familia de proteínas se encuentra en un amplio rango de organismos, desde bacterias hasta humanos.

En plantas, se han identificado las siguientes cuprochaperonas (Wintz y Vulpe, 2002):

- CCH ("copper chaperone"): Fue la primera chaperona identificada en plantas (*A. thaliana*) y es homóloga a la chaperona ATX1 ("antioxidant protein 1") de levaduras (Himmelblau et al., 1998). Posee un extremo C-terminal exclusivo de plantas de estructura y función desconocida (Mira et al., 2001b). Está involucrada en: *i)* transportar el Cu en la ruta secretora hasta la ATPasa de Cu, RAN1 (HMA7) ("responsive to antagonist 1"), y activar la síntesis de los receptores de etileno (ETR) (Hiramaya et al., 1999); *ii)* proteger a la célula frente al estrés oxidativo (Company y González-Bosch, 2003); *iii)* transportar el Cu por el simplasto del floema desde las hojas viejas en estado de senescencia hasta las hojas jóvenes (Mira et al., 2001a).

- ATX1: Esta chaperona es similar a la chaperona CCH. Tiene una secuencia más corta en la que le falta el dominio C-terminal. Mediante la técnica de doble híbrido, Andrés-Colás et al. (2006) han demostrado que esta chaperona ATX1 interviene en el transporte de Cu en la ruta secretora interaccionando con RAN1 (HMA7) y HMA5. La chaperona CCH sólo interacciona débilmente con RAN1 (HMA7) y HMA5 cuando se elimina el extremo C-terminal. Estos datos sugieren que el extremo C-terminal de CCH podría desempeñar un papel regulador en la interacción de la misma con ambas ATPasas. Sin embargo, teniendo en cuenta que la CCH está presente en el floema, no puede descartarse la posibilidad de que este extremo C-terminal sea el responsable de su función en el transporte de Cu a larga distancia a través de los plasmodesmos.

- CCS ("copper chaperone for superoxide dismutase"): Es homóloga a la chaperona LYS7 de levaduras y se ha identificado en tomate

(*Lycopersicom esculentum*), en patata (*Solanum tuberosum*), maíz (*Zea mays*) y *A. thaliana* (Zhu et al., 2000; Ruzsa y Scandalios, 2003; Trindade et al., 2003; Chu et al., 2005; Abdel-Ghany et al., 2005a). Su función es la de suministrar Cu a la enzima CuZnSOD. Esta chaperona tiene un peso molecular de 30-35 kDa y está formada por tres dominios: el dominio I o extremo N-terminal, homólogo a ATX1, donde se encuentra un sitio de unión a Cu MxCxxC; el dominio II que es homólogo a la SOD y el dominio III o extremo C-terminal que incluye otro sitio de unión a Cu CxC (Markossian y Kurganov, 2003). Recientemente, se ha demostrado que en el genoma de *A. thaliana* sólo existe una copia del gen *AtCCS.* Por otro lado también se ha propuesto que dentro del marco de lectura (ORF) de este gen existen dos ATGs que podrían generar dos sitios de inicio de la transcripción produciendo dos formas de la chaperona *At*CCS, una citosólica y otra cloroplástica, que participarían en suministrar el Cu a la enzima CuZnSOD citosólica y cloroplástica, respectivamente (Abdel-Ghany et al., 2005a; Chu et al., 2005). En *A. thaliana,* la expresión de este gen se induce por exceso de Cu, de la misma manera que se induce la expresión de los genes *CSD1* y *CSD2* que codifican a la CuZnSOD citosólica y cloroplastica, respectivamente.

- SCO1, COX11 y COX17 ("cytochrome oxidase"): estas tres chaperonas han sido identificadas en *A. thaliana* y son homólogas a las chaperonas SCO1, COX11 y COX17 de levaduras. El transporte de Cu a la citocromo c oxidasa de la cadena de transporte electrónico mitocondrial se realiza en dos pasos: COX17 transporta el Cu a SCO1 y COX11 y posteriormente estas chaperonas lo transportan a la enzima citocromo c oxidasa. La expresión del gen *AtCOX17* se activa por niveles tóxicos de Cu, ácido salicílico, infecciones y tratamientos que generen óxido nítrico y peróxido de hidrogeno que inhiben la respiración mitocondrial. Así, se ha propuesto que esta chaperona participaría en la estabilización del complejo COX restringiendo así la producción de ROS (Balandín y Castresana, 2002).

Además de estas seis cuprochaperonas se cree que pueden existir más debido a la especilazación de las células vegetales. Por ejemplo, las cuproproteínas presentes en el lumen tilacoidal como la plastocianina y la polifenol oxidasa necesitarán que una cuprochaperona les suministre el Cu necesario para formar la holoproteína y ser funcionalmente activas. A este

respecto, Tottey et al. (2002) identificaron y caracterizaron una chaperona en la cianobacteria *Synechocystis* PCC 6803 que transporta Cu desde la Cu-ATPasa CtaA a la Cu-ATPasa PacS y que, posteriormente, lo transporta a la plastocianina. Sin embargo, todavía no se ha identificado la chaperona que realiza esta función en plantas.

1.3.2.1.2. Metalotioneínas

Las metalotioneínas (MT) son proteínas de bajo peso molecular (4-8 kDa) que tienen un alto contenido en cisteínas. Se encargan de acomplejar el Cu (y otros metales pesados, principalmente Cd) cuando se encuentran en exceso en la célula e intervienen en su detoxificación. Atendiendo a su secuencia de aminoácidos se clasifican en dos grupos: Clase I (en mamíferos) y clase II (con miembros en plantas, hongos e invertebrados). En plantas, las MT de clase II se subclasifican en 4 grupos según la organización de las cisteínas (MT1, MT2, MT3, MT4). Las diferencias en su expresión y localización hacen pensar que tienen distintas funciones en las plantas. Las metalotioneínas actúan en los mecanismos de tolerancia a Cu, en el proceso de senescencia y se sobreexpresan en los tricomas cuando hay exceso de Cu (Clemens, 2001; Cobbet y Goldsbrough, 2002).

1.3.2.2. Transporte de cobre a través de la membrana plasmática

Las principales familias de transportadores de membrana que participan en el transporte de Cu en plantas son:

1.3.2.2.1. Familia COPT

Los transportadores COPT ("copper transporter family") son homólogos a los transportadores de Cu CTR de levaduras. Estructuralmente, poseen tres hélices transmembrana y un alto contenido en metioninas que podrían participar en el proceso de translocación del Cu. Todavía no está claro cómo funcionan estos transportadores, pero es probable que el Cu sea incorporado al citosol celular como Cu^{+}. En Arabidopsis se han identificado seis miembros de esta familia (*At*COPT1-6) que se encargan de transportar Cu a través de las

membranas plasmáticas de diferentes tejidos y compartimentos subcelulares (Sancenón et al., 2003).

En concreto, *At*COPT1 es un transportador de Cu de alta afinidad que se localiza en la membrana plasmática de la raíz, estomas, tricomas, polen y embriones por lo que participa en: *i)* la adquisición del Cu del suelo; *ii)* en el desarrollo del polen; *iii)* los mecanismos de elongación de la raíz (Sancenón et al., 2004). El gen *AtCOPT1* está regulado por Cu de forma negativa. *At*COPT2 y *At*COPT6 están en la membrana plasmática mientras que *At*COPT3 y *At*COPT5 están localizados en la membrana cloroplástica y en la ruta secretora, respectivamente. Por otro lado, no se conoce una relación directa entre *At*COPT4 y el transporte de Cu (Sancenón et al., 2003).

1.3.2.2.2. Familia YSL

Los transportadores YSL ("yellow stripe like") pertenecen a una familia de transportadores oligopeptídicos OPT (Yen et al., 2001). Recientemente, se ha descrito un transportador de esta familia, *At*YSL2, que podría transportar el complejo Cu^{2+}-NA desde la savia del xilema al apoplasto de las hojas (Didonato et al., 2004), aunque todavía se desconoce su relevancia fisiológica. Otro transportador de esta familia es *At*OPT3 que participaría en el transporte de Cu desde la raíz hasta los vasos del xilema (Wintz et al., 2003).

1.3.2.2.3. Familia ZIP

Los transportadores de esta familia ("zrt1-irt1-like proteins") deben su nombre a los dos primeros miembros descritos de la misma: IRT1 ("iron responsive transporter 1") de *A. thaliana* (Eide et al., 1996) y ZRT1 ("zinc responsive transporter") de *S. cerevisiae* (Zhao y Eide, 1996). Actualmente, se conocen varias decenas de transportadores de esta familia que se encuentran ampliamente distribuidos en los organismos eucariotas (Guerinot, 2000). Todos los ZIPs que se han identificado hasta la fecha se caracterizan por transportar cationes divalentes al citoplasma (Zn, Mn, Fe, Co, Cd). La función que realizan estos transportadores está relacionada con la absorción de los metales del medio extracelular. Recientemente, se ha propuesto que dos de ellos, *At*ZIP2 y

*At*ZIP4, podrían intervenir en el proceso de adquisición de Cu por la raíz (Wintz et al., 2003).

1.3.2.2.4. Familia NRAMP

La familia NRAMP ("natural resistance macrophage associated proteins") participa en el transporte de una gran variedad de metales de transición. Se han identificado al menos tres miembros en arroz (*Os*NRAMP1-3) y cinco miembros en Arabidopsis (*At*NRAMP1-5) (Williams et al., 2000). Shingles et al. (2004) han propuesto que *At*NRAMP1 podría transportar Cu^{2+} a través de la membrana tilacoidal, sin embargo son necesarios más estudios para poder corroborar esta función de *At*NRAMP1.

Las proteínas de esta familia constituyen una conexión entre los cationes metálicos y la señalización intercelular. El gen *EIN2* ("ethylene-insensitive 2"), que participa en la transducción de la señal del etileno, codifica una proteína con un dominio N-terminal hidrofóbico que presenta homología con los transportadores de la familia NRAMP y con un dominio C-terminal hidrofílico que estimula la expresión de genes involucrados en la respuesta frente al estrés oxidativo, jasmonato y etileno (Alonso et al., 1999). Se piensa que el dominio N-terminal podría actuar como sensor de metales divalentes mientras que el dominio C-terminal actuaría en la transducción de la señal.

1.3.2.2.5. Familia P_{1B}-ATPasas

Los transportadores P_{1B}-ATPasas (Williams et al., 2000), también conocidos como CPx-ATPasas (Solioz y Vulpe, 1996) o HMAs ("heavy metal ATPases") (Axelxen y Palmgrem, 2001) se han identificado en diversos organismos (bacterias, algas y eucariotas) y se caracterizan por transportar metales pesados a través de las membranas biológicas. Esta familia de proteínas pertenece a la superfamilia de ATPasas de tipo P que usan ATP para bombear un amplio rango de cationes a través de las membranas biológicas en contra del gradiente electroquímico (Kühlbrandt, 2004). Estructuralmente, las P_{1B}-ATPasas poseen 8 hélices transmembrana y tienen características comunes a las P-ATPasas, como el dominio de unión a ATP (GDxxNDxP) o el

dominio de fosforilación (DKTGT), y características específicas (Tabla 1-4) (Fig. 1-10).

Tabla 1-4. Características estructurales de las P-ATPasas y P_{1B}-ATPasas (Williams et al., 2000; Kühlbrandt, 2004; Williams y Mills, 2005).

CARACTERÍSTICA ESTRUCTURAL	P-ATPasas	P_{1B}-ATPasas	FUNCIÓN
Nº de regiones TM antes del primer dominio citoplasmático	2	4	
Nº de regiones TM después del segundo dominio citoplasmático	4-5	2	
Segundo dominio citoplasmático		150 aminoácidos menos que en P-ATPasas	Esta diferencia se utiliza para identificarlas por PCR
DKTGTLT	Conservado	Conservado	Dominio de fosforilación (D es fosforilado por el ATP en un ciclo de reacción)
GDGxNDx	Conservado	Conservado	Dominio de unión a ATP
TGD	Conservado	Conservado	Fosforilación
KGAPE, DPPR	Específico		
PxxK	Conservado	Conservado	Estabilización de carga
HP		Específico	Interacción proteína-proteína
CxxC, $(CC)_n$, $(HH)_n$		Específico	Sitio de unión del metal
CPx		Específico	Transducción del metal
PGD, PAD, TGES	Conservado	Conservado	Transducción de la energía

La familia de P_{1B}-ATPasas se subdivide en seis grupos según un análisis filogenético (P_{1B-1}-P_{1B-6}) (Axelsen y Palmgrem, 1998; Argüello, 2003). A su vez, se pueden agrupar en dos grupos en base a un análisis preliminar de la especificidad por el metal transportado, así podemos distinguir las P_{1B}-ATPasas que transportan Cu^+ y Ag^+ (grupos 3-6), y las P_{1B}-ATPasas que transportan $Zn^{2+}/Co^{2+}/Cd^{2+}/Pb^{2+}$(grupos 1-2). Estas últimas P_{1B} -ATPasas sólo se encuentran en organismos procariotas y en organismos eucariotas fotosintéticos (plantas y algas).

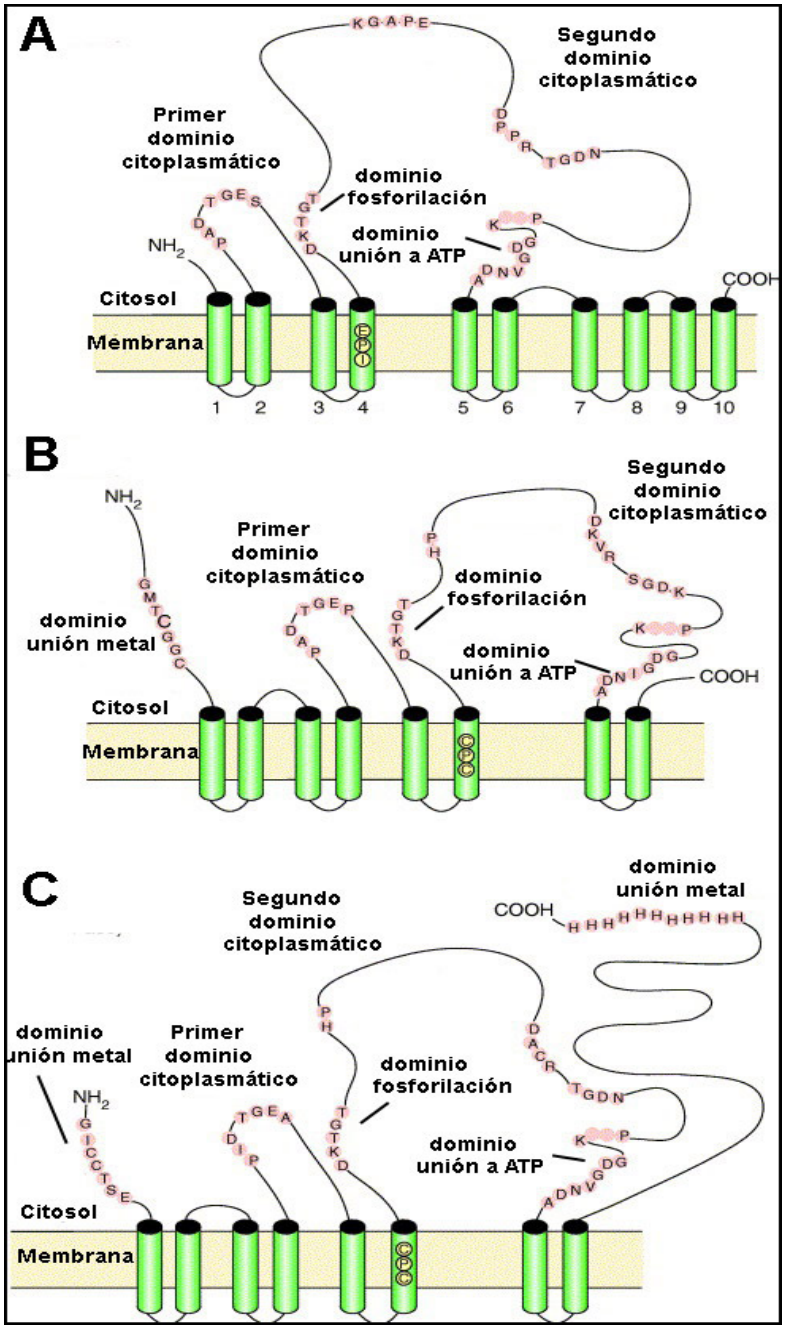

Fig. 1-10. Comparación entre la topología de la Ca^{2+}-P-ATPasa SERCA1A (A) de mamíferos y la de la familia de P_{1B}-ATPasas de plantas (B, C). Pueden observarse las características comunes y específicas enumeradas en la Tabla 1-4. En las P_{1B}-ATPasas de plantas se han descrito dos tipos de dominios de unión a metal. (B) El primero de ellos se conoce como HMA (Heavy Metal Associated domain), tiene la secuencia consenso CxxC y se encuentra localizado en el extremo N-terminal del transportador, este tipo de dominio se ha encontrado en HMA6 y HMA8. (C) El segundo dominio de unión a metal son regiones ricas en cisteína e histidina que se encuentran localizadas tanto en el extremo N-terminal como en el C-terminal del transportador, este tipo de dominio se ha encontrado en HMA4 (Modificado de Williams y Mills, 2005).

El número de P_{1B}-ATPasas en el genoma de plantas superiores (*A. thaliana*, *Oryza sativa*) es relativamente alto en comparación con otros organismos, esto puede ser debido a una diversificación en las funciones que desempeñan, ya que, además de participar en la detoxificación de metales del citoplasma celular, participan en el transporte de metales a larga distancia vía xilema y su posterior distribución a los compartimentos diana.

En *A. thaliana* se han identificado ocho miembros (*At*HMA1-8, http://mips.gsf.de) que difieren en su estructura, función, localización y en el metal transportado (Williams y Mills, 2005).

En particular, las P_{1B}-ATPasas *At*HMA1, *At*HMA6 (PAA1, "P-type ATPase for arabidopsis"), *At*HMA7 (RAN1) y *At*HMA8 (PAA2) transportan Cu a diferentes compartimentos subcelulares (Hiramaya et al., 1999; Shikanai et al., 2003; Abdel-Gahny et al., 2005b; Seigneurin-Berny et al., 2006); mientras que las P_{1B}-ATPasas *At*HMA2-4 y *At*HMA5 desempeñan un papel en la nutrición mineral y en la detoxificación de Zn, Cd y Pb (Mills et al., 2003; 2005; Eren y Argüello, 2004; Gravot et al., 2004; Verret et al., 2004; 2005) y Cu (Andrés-Colás et al., 2006), respectivamente.

La primera P_{1B}-ATPasa que se caracterizó funcionalmente en plantas fue *At*HMA7 ó RAN1 (Hirayama et al., 1999). Se ha propuesto que *At*HMA7 (RAN1) transporta Cu al receptor de etileno en el retículo endoplásmico y participa en: *i)* la activación de los receptores de etileno (Hirayama et al., 1999; Rodríguez et al, 1999); *ii)* la interrupción de la liberación de Cu a otra cuproenzima apoplástica (ej. ascorbato oxidasa) implicada en la expansión celular (Woeste y Kieber, 2000); *iii)* la movilización del Cu durante el proceso de senescencia (Himelblau y Amasino, 2001).

Recientemente, se ha identificado y caracterizado el transportador *At*HMA5 que se expresa principalmente en raíces y flores (Andrés-Colás et al., 2006). Estos autores han demostrado su especificidad por Cu y han propuesto dos funciones para este transportador según el nivel de Cu existente en el medio de crecimiento. A concentraciones bajas, este transportador estaría localizado en el aparato de Golgi, y a concentraciones altas, cambiaría de localización y actuaría en el mecanismo de detoxificación del Cu del citoplasma celular. Por otro lado, *At*HMA5 también podría intervenir en la expansión celular como ocurre con RAN1 (*At*HMA7) (Andrés-Colás et al., 2006).

*At*HMA4 fue el primer transportador que se caracterizó del subgrupo P_{1B-2}. Está localizado en el cilindro vascular de la raíz y participa en el mecanismo de detoxificación de Zn (Mills et al., 2003 y 2005). *At*HMA2, interviene en la detoxificación de Zn. Hussain y Verret et al. (2004) demostraron mediante el mutante doble *hma2hma4* de *A. thaliana* que las funciones de ambos transportadores se solapan. Por otro lado, se han propuesto otras funciones para estos transportadores: *i)* papel en la translocación de Zn vía xilema y floema (Hussain et al., 2004); *ii)* detoxificación de otros iones metálicos (Cd, Co) cuando están en exceso (Mills et al., 2003 y 2005; Verret et al., 2004).

*At*HMA3 es otro transportador del subgrupo de P_{1B-2} que podría participar en la detoxificación de Cd y Pb en la vacuola.

Recientemente, se han identificado tres miembros de la familia P_{1B}-ATPasa involucrados en la homeostasis de Cu en el cloroplasto: *At*HMA1, *At*HMA6 (PAA1) y *At*HMA8 (PAA2) (Shikanai et al., 2003; Abdel-Gahny et al., 2005b; Seigneurin-Berny et al., 2006). Estos transportadores participan en el transporte de este metal hasta la plastocianina y la CuZnSOD cloroplástica. Por este motivo, se ha propuesto que estos transportadores son de vital importancia para la fotosíntesis y la defensa frente al estrés oxidativo en el cloroplasto. Sin embargo, son necesarios más estudios para entender la homeostasis de Cu en este orgánulo.

1.3.3. REGULACIÓN DE LA HOMEOSTASIS DE COBRE

La regulación de la concentración de Cu a nivel intracelular es crucial para el crecimiento y desarrollo normal de la planta (ver apartado 1.3.2). Por este motivo, es necesaria una maquinaria de regulación que asegure un control eficaz de los niveles intracelulares de este metal y garantice una distribución adecuada que prevenga su acumulación.

En la levadura *S. cerevisiae* se ha descrito que esta regulación se produce a dos niveles. El primero de ellos es una regulación a nivel transcripcional que se caracteriza por actuar directamente sobre la expresión de los genes que controlan la adquisición y detoxificación del Cu, mientras que el segundo es una regulación a nivel postranscripcional que actúa sobre la

localización y estabilidad de las proteínas implicadas. En la regulación a nivel transcripcional, se han descrito dos factores de transcripción Ace1 y Mac1 (Tabla 1-3) (Jungmann et al., 1993). En condiciones tóxicas de Cu, la proteína Ace1 induce la expresión de genes implicados en la detoxificación de Cu (MTs y CuZnSOD) tras unirse a los elementos de respuesta a metales (MREs, "metal response elements") localizados en los promotores de estos genes, mientras que en condiciones de deficiencia de Cu, la proteína Mac1 activa la transcripción de los transportadores de Cu de alta afinidad (CTR1 y CTR3) tras unirse a los elementos *cis* de respuesta a Cu (CuREs, "Cu-responsive elements") localizados en los promotores de estos genes. A nivel postranscripcional se ha observado la degradación de CTR1 en condiciones tóxicas de Cu (De Freitas et al., 2003).

De forma análoga, en el alga verde *Chlamydomonas reinhardtii* se ha descrito un mecanismo de regulación transcripcional a través de un factor de transcripción llamado Crr1 ("copper-responsive regulator 1") que induce la expresión de genes implicados en la deficiencia de Cu, como por ejemplo el citocromo c_6, tras unirse a un elemento CuRE localizado en su promotor (Moseley et al., 2000; Merchant et al., 2004).

La regulación de la homeostasis de Cu en plantas superiores es un área de investigación que ha empezado a desarrollarse en los últimos años. A día de hoy se conoce la regulación por Cu a nivel transcripcional de algunos genes involucrados en la homeostasis de Cu en plantas superiores (*COPT1*, *HMA5*, *CCH*, *CCS*, etc) (Himelblau et al., 1998; Mira et al., 2002; Sancenón et al., 2003, 2004; Abdel-Ghany et al., 2005b). Sin embargo, tanto los factores de transcripción como los elementos *cis* y *trans* implicados en esta regulación transcripcional son desconocidos. Del mismo modo, los mecanismos de regulación postranscripcional también son desconocidos. A este respecto, se ha especulado que podrían ser similares a los que tienen lugar en levaduras.

CAPÍTULO 2

OBJETIVOS

En la Introducción de esta Memoria de Tesis Doctoral se ha destacado la importancia que tiene el cloroplasto para el desarrollo y crecimiento de las plantas, así como su alta sensibilidad al estrés por exceso de cobre (Cu). Se han revisado los estudios realizados acerca del efecto de este metal en plantas superiores que se centran principalmente en su efecto tóxico. Estos trabajos analizan los daños que ocasiona el Cu en los tejidos y orgánulos celulares y los mecanismos que la planta utiliza para tolerar de forma global este tipo de estrés.

Sin embargo, se conocen poco los mecanismos de respuesta y de adaptabilidad del cloroplasto en general y del aparato fotosintético en particular al exceso de Cu a pesar de su importancia, tal como se refleja en la Introducción de esta Memoria. Otro aspecto no bien conocido es la homeostasis de Cu en el cloroplasto, a pesar de que es un aspecto importante para entender los mecanismos de respuesta antes mencionados. Por ello, el objetivo general de la presente Tesis Doctoral ha sido profundizar en el conocimiento de estos mecanismos y de las bases moleculares de la homeostasis de Cu en el cloroplasto.

Para abordar este objetivo general se han utilizado suspensiones de células fotosintéticas de soja que permiten estudiar a nivel celular el efecto del Cu de forma controlada y plantas de soja crecidas en medio hidropónico para realizar un análisis comparativo de los resultados.

Para alcanzar este objetivo general se plantearon los siguientes objetivos específicos:

1. Estudio fisiológico, estructural y bioquímico de la influencia del exceso de Cu en la línea celular *Glycine max* var. Corsoy.
2. Identificación, localización y caracterización del transportador de Cu HMA8 en soja (*Gm*HMA8).
3. Estudio de la regulación del transportador de Cu *Gm*HMA8.

CAPÍTULO 3

EXCESS COPPER EFFECT ON GROWTH, CHLOROPLAST ULTRASTRUCTURE, OXYGEN-EVOLUTION ACTIVITY AND CHLOROPHYLL FLUORESCENCE IN *Glycine max* CELL SUSPENSIONS

3.1. ABSTRACT

The influence of excess copper on soybean photosynthetic cell suspensions was investigated. The cell suspensions grew well in the presence of 5-20 μM $CuSO_4$ and developed tolerance to even higher levels of $CuSO_4$ (*i.e.*, up to 50 μM), indicating that copper was not toxic to the cells at that high concentrations. Cu-adapted cell suspensions grew faster than the control in limiting light conditions and had higher content of chlorophyll per dry weight of cells. Copper was accumulated within the cells and this event was accompanied by *i)* increase oxygen evolution activity; *ii)* increased number of chloroplasts per cell, smaller chloroplasts, increased thylakoid stacking and grana size; *iii)* higher fluorescence emission of photosystem II antenna complexes and *iv)* stimulation of plastocyanin protein synthesis compared with untreated cells. Microanalysis of cross-sections revealed an increase of copper content in chloroplasts as well as vacuole, cytoplasm and cell wall in Cu-adapted cells. No antagonist interaction between copper and iron uptake took place in these cell suspensions. On the other hand, copper at subtoxic concentrations stimulated oxygen evolution activity in thylakoids from control cells, but this event did not take place in those from Cu-adapted ones. Furthermore, the loss of activity by copper inhibitory action at toxic concentrations was two-fold slower in thylakoids from Cu-adapted cells compared with the control ones. The data strongly indicate that copper plays a specific positive role on photosynthesis and stimulates the growth and the oxygen evolution activity in soybean cell suspensions.

3.2. INTRODUCTION

Copper (Cu) is an essential micronutrient for all photosynthetic organisms (*i.e.,* cyanobacteria, algae and plants) and plays an important role in numerous metabolic processes. In chloroplasts, Cu is a cofactor of several enzymes and metalloproteins that catalyze redox reactions (*i.e.,* plastocyanin, Cu/Zn superoxide dismutase and polyphenol oxidase) (Sadmann and Böger, 1983; Droppa and Horváth, 1990; Raven et al., 1999). The optimal average

composition of Cu in plant tissue is 10 μg g^{-1} dry weight (Baker and Senef, 1995). At concentrations above those required for optimal growth Cu was shown to inhibit growth and to interfere with important cellular processes such as photosynthesis and respiration (Marschner, 1995; Prasad and Strzałka, 1999; Yruela 2005). Plant grown in the presence of high levels of Cu (3-100 μM) normally showed reduced biomass and chlorotic symptoms. A lower content of chlorophyll (Chl) and alterations of chloroplast structure and thylakoid membrane composition have been found in leaves of spinach, rice (*Oryza sativa L.*), wheat (*Triticum durum* cvs *Adamello* and *Ofanto*) and bean (*Phaseolus L.* and *Phaseolus coccineus L.* cv. *Piekny*) in such growth conditions (Baszyński et al., 1988; Lidon and Henriques, 1991, 1993; Ciscato et al., 1997; Pätsikkä et al., 1998; Quartacci et al., 2000). In particular, degradation of grana stacking and stroma lamellae, increase in the number and size of plastoglobuli, and appearance of intrathylakoidal inclusions were observed. It was proposed that Cu interferes with the biosynthesis of the photosynthetic machinery modifying the pigment and protein composition of photosynthetic membranes (Lidon and Henriques, 1991; Maksymiec et al., 1994). Pätsikkä et al. (2002) attributed the reduction of Chl content to a Cu-induced Fe deficiency. The substitution of the central Mg ion of chlorophyll by Cu *in vivo* has also been proposed as an important damage mechanism leading to inhibition of photosynthesis (Küpper et al., 1996; 2003). Besides, lipid peroxidations, decrease of lipid content and changes in fatty acid composition of thylakoid membranes were also shown (Sandmann and Böger, 1980; Luna et al., 1994; Maksymiec et al., 1994). As a consequence of those modifications, an alteration of photosystem II (PSII) membrane fluidity was found (Quartacci et al., 2000). The mechanism of Cu toxicity on photosynthetic electron transport has extensively been studied *in vitro* and it was found that PSII is the most sensitive site to Cu toxicity. Both the acceptor and the donor sides of PSII were suggested as the main targets of Cu toxic action (Mohanty et al., 1989; Yruela et al., 1993; Schröder et al., 1994; Jegerschöld et al., 1995). Copper also increased susceptibility to photoinhibition in isolated thylakoids (Pätsikkä et al., 2001) or PSII-enriched membrane preparations (Yruela et al., 1996b). Considering copper is an efficient catalyst in the formation of reactive oxygen

species (ROS) we suggested that the toxicity associated with this metal in plants was due, at least in part, to oxidative damage.

On the other hand, it has been reported that Cu is involved in photosynthetic reactions of PSII non-dependent of plastocyanin (a chloroplastic Cu-containing protein) (Lightbody and Krogmann, 1967; Barr and Crane, 1976). These authors reported the probably presence of a Cu-binding site close to the oxygen-evolving complex, which was sensitive to the action of Cu-chelators or the existence of a Cu-protein within PSII, respectively. More recently, Burda et al. (2002) found that Cu in an equimolar concentration to PSII reaction center stimulated *in vitro* the oxygen evolution activity of PSII. Nevertheless, little information in this respect exists *in vivo*.

Most of the studies dealing with the effect of excess Cu in higher plants show that its toxicity on growth and photosynthetic activity are the most general influences of excess Cu in higher plants. Studies on cell cultures from higher plants grown under stress conditions are limited and in particular little information is available on the effects of Cu on cell suspensions. In this respect, the present work is a significant contribution to this field and may provide relevant information to advance in our knowledge of physiological aspects of leaf cells. The results are discussed in terms of the positive role of Cu on the structure/function of PSII *in vivo*.

3.3. MATERIALS AND METHODS

3.3.1. Cell suspension growth conditions

Photosynthetic cell suspensions from soybean (G*lycine max* var. Corsoy) SB-P line were grown as described by Rogers et al. (1987) with some modifications. These cell suspensions were established in our laboratory in 1990. Cell suspensions were grown in liquid cultures as follows: *a)* photomixotrophically under continuous low light (30 $\pm$ 5 μE m^{-2} s^{-1}); *b)* photomixotrophically under continuous normal growth light (65 $\pm$ 5 μE m^{-2} s^{-1}); *c)* photoautotrophically under continuous low light (30 $\pm$ 5 μE m^{-2} s^{-1}); *d)* photoautotrophically under continuous normal light (65 $\pm$ 5 μE m^{-2} s^{-1}). It has been reported that this kind of cultures grow optimally with 65-75 μE m^{-2} s^{-1}

(Rogers et al., 1987; Alfonso et al., 1996) and that high light cause photoinhibitory effects in these cell suspensions (personal communication; Alfonso et al., 1996). On the other hand, it is known that Cu is a potential toxic element and its toxicity enhances with light. Thus, first of all we decided to assay a low-light regime (30 ± 5 μE m^{-2} s^{-1}) following the light conditions used in previous works studying the copper-stress effect on cell cultures (Gori et al., 1998) and compared the results with those obtained using control light regime. To assay the Cu effect on cell growth the media were supplemented with 5, 10, 20, and 50 μM $CuSO_4 \cdot 5H_2O$. Control medium corresponded to 0.1 μM $CuSO_4 \cdot 5H_2O$. To assay the Fe and Zn effect on cell growth, the media were supplemented with 10 μM $FeSO_4 \cdot 7H_2O$ and 10 μM $ZnSO_4 \cdot 7H_2O$, respectively. All cell suspensions were grown under an atmosphere with 5% CO_2 at 24 ºC on a rotatory shaker (TEQ, model OSFT-LS-R) at 110 rpm in 125 ml Erlenmeyer flasks filled up to 50 ml and illuminated with cool-white fluorescent lamps (Alfonso et al., 1996). It is worth mentioning that this kind of cultures demands for an elevated CO_2 concentration, at least 1% CO_2 (Rogers et al., 1987; Roitsch and Sinha, 2002) and that CO_2 was not directly bubbled into the flasks. Cells used for physiological and biochemical experiments were collected from cultures after 18-21 days of growth.

3.3.2. Cell growth

Cell suspension growth was measured by monitoring cell-packed volume and Chl concentration during the first 21 consecutive days of culture after the transfer (Alfonso et al., 1996). Cell-packed volume determination consisted in transferring 1 ml of cell suspension to an eppendorf tube and measuring the cell volume after sedimentation. Chlorophyll concentration was measured as described by Arnon (1949).

3.3.3. Isolation of thylakoid membranes

Soybean cells from 18-day-old cultures were collected, filtered through a layer of Miracloth (Boehringer) and weighted. Cells were then resuspended in buffer containing 400 mM NaCl, 2 mM $MgCl_2$, 0.2% (w/v) sucrose, and 20 mM Tricine, pH 8.0 at a cell to buffer ratio of 1:2 (w/v) and broken with a Teflon

homogeneizer during 10 min with 2-min delay every 2 min homogeneization to avoid sample heating at 4 ºC in darkness. Broken cells were gently stirred for 10 min and centrifuged at 300 x g for 2 min. The supernatant (hereafter called cell extract fraction) was centrifuged at 13,000 x g for 10 min and the resultant sediment resuspended in buffer containing 150 mM NaCl, 5 mM $MgCl_2$, and 20 mM Tricine, pH 8.0 and centrifuged at 13,000 x g for 10 min. The pellet (thylakoids) was resuspended in buffer containing 400 mM sucrose, 15 mM NaCl, 5 mM $MgCl_2$, and 50 mM 2-(N-morpholino)ethanesulfonic acid (MES)-NaOH, pH 6.0 and the supernatant fractions were concentrated. For Cu(II) inhibition experiments 25 mM N-2-hydroxyethylpiperazine-N'-2-ethanesulphonic acid (HEPES)-NaOH, pH 7.8 instead of Tricine, pH 8.0 was used to avoid chemical interference with Cu (II) (Renganathan and Bose, 1990). The thylakoid fractions were frozen in liquid nitrogen and stored at -80 ºC. Chlorophyll determination was done as described by Arnon (1949).

3.3.4. Oxygen evolution activity

Oxygen evolution activity was measured with a Clark-type oxygen electrode at 23 ºC. The heat-filtered white light intensity on the surface of the cuvette was 3,000 $\mu E\ m^{-2}\ s^{-1}$. Cells (15 μg Chl ml^{-1}) and thylakoids (10 μg Chl ml^{-1}) were diluted in 3 ml buffer containing 10 mM NaCl, 300 mM sucrose, and 25 mM MES-NaOH, pH 6.5. For cation stimulation and Cu-inhibition effect on oxygen evolution activity experiments thylakoids were incubated with $CaCl_2$, $CuCl_2$, $FeCl_3$, and $ZnCl_2$ for 2 min at 23 ºC under constant stirring in the dark before exposing the samples to heat-filtered white light. The temperature was maintained at 23 ºC by circulating water from a temperature-controlled waterbath around the Clark cell. Cell and thylakoid activities were measured in the absence and presence of 0.5 mM 2,6-dichlorobenzoquinone (DCBQ) as artificial electron acceptor, respectively. DCBQ was dissolved in ethanol.

3.3.5. Immunoblotting analysis

The analyses of plastocyanin were done in cell-extract fractions. LHCII antenna complex and OEC33 proteins of PSII were assayed in intact and washed thylakoid membranes. Washed thylakoids were prepared from intact

thylakoids by washing twice with 250 mM NaCl, 5 mM $MgCl_2$, and 50 mM MES-NaOH, pH 6.0. It is worth mentioning that the surfactant sucrose was eliminated in this buffer. The solutions used contained pefabloc (100 $\mu g\ ml^{-1}$) as a protease inhibitor. The electrophoretic separation of PSII proteins was performed by sodium dodecyl sulphate (SDS)-poliacrylamide gel electrophoresis using 12.5% (w/v) acrylamide gels containing 6 M urea according basically to Laemmli (1970). Gels were electroblotted to a nitrocellulose membrane with a BioRad transfer system and the immunodetection was done with a rabbit antibodies against plastocyanin from *Scenedesmus vacuolatus* (a kind gift from Dr. M.L. Peleato, Biochemistry and Cellular and Molecular Biology Department, Zaragoza University, Zaragoza, Spain), D1 protein of PSII from a synthetic peptide homologous to the N-terminus, and LHCII antenna complex and OEC33 proteins of PSII from spinach (kindly provided by Dr. M. Barón, Estación Experimental del Zaidín, Granada, Spain). A goat anti-rabbit IgG coupled to horseradish peroxidase as a secondary antibody. Bands were revealed by the peroxidase method. The blots were scanned with a Studio Scan II Si (AGFA) and the intensity of the bands was quantified by densitometry using US National Institute of Health Software (NIH IMAGE) available at http://www.ncbi.nih.gov.

3.3.6. Microscopy imaging

Images were obtained with a confocal laser scanning microscope (Zeiss, Mod. LSM 310) and a transmission electron microscope (Zeiss, Mod. EM 910). Cells were collected from suspension cultures, passed 20 times through a hypodermic syringe to disperse most cell aggregates. For confocal laser scanning microscopy excitation was generated with an argon laser at 488 nm and the resultant emission was filtered through a long-pass filter >515 nm. The three-dimensional images were made up of several confocal sections at 0.5-1 μm increments through the sample by computer-assisted microscopy. For transmission electron microscopy cells were fixed in 2.5% (w/v) glutaraldehyde (dissolved in 30 mM sodium phosphate buffer, pH 7.4) during 2 h at 25 ºC. Then, cells were washed twice with sodium phosphate buffer, pH 7.4 and subsequently treated with 1% (w/v) osmium tetroxide solution, dehydrated through a series of acetone solutions, and embedded in Durcupan ACM (Fluka)

epoxy resin. After polymerization during 48 h at 60 ºC ultra-thin sections were obtained using a diamond knife ultramicrotome, and post-stained with lead citrate.

3.3.7. Determination of macro and micronutrient elements

Cells from 20-day-old suspensions were washed twice with 3 mM EDTA and once with destilled H_2O to remove free cations. After washing, cells were filtered through a layer of Miracloth (Calbiochem) and dried in a ventilated oven at 60 ºC for 48 h. Analyses were performed in an atomic absorption spectrometer (UNICAN 969).

3.3.8. Energy-dispersive X-ray microanalysis

Cells from 20-day-old suspensions were cry fixed using a high-pressure freezer (Leica EMPact; Leica Microsystems, Gladesville, Australia) and were then stored in liquid nitrogen until freeze substitution. Frozen cells were freeze substituted with diethyl ether containing 10% acrolein with freshly activated 5 Å molecular sieve (Baker Analyzed) for 4 days at -90 ºC, 2 days at -70 ºC and 1 day at -30 ºC. Subsequently, samples were gradually brought to 4 ºC by raising the temperature for 1.5 h. Diethyl ether was the freeze-substitution solvent chosen because it does not lead to redistribution of ions, even for highly diffusible elements (Bidwell et al., 2004). The freeze-substituted cells were infiltrated with Araldite resin over 4 days. Araldite contains negligible levels of elements detectable by energy-dispersive spectrometry (Pålsgård et al., 1994). Cell sections were cut dry at 0.25, 0.5 and 1.0 μm using an ultramicrotome (Leica Ultracut UCT) and mounted directly onto titanium grids (75 mesh) that were coated with formvar. Sections were stored in a desiccator under vacuum until analysis to prevent absorption atmospheric water and hence possible redistribution of ions.

Unstained sections were analysed at room temperature in a carbon holder by energy-dispersive X-ray microanalysis using a transmission electron microscope (model H-800-MT, Hitachi) and X-ray EDX Quantum detector (model 3600, Kevex). The detector was interfaced to a signal processing unit (Röntec). The electron microscope was operated at 100 kV in STEM mode with

a spot size 10-15 nm and a beam current 15 μA. The spatial resolution of analysis in a 0.5 μm section at 120 kV was estimated to be better that in a 0.25 μm and 1.0 μm sections. The spectral data from individual cells and compartments in each section were collected using selected area analysis with an acquisition time of 300 s. Analyses were carried out by Quantax 1.5 program (Röntec). Spectra were normalized at titanium peak used as internal standard.

3.3.9. Fluorescence measurements

Thylakoid membranes isolated from 18-day-old suspensions were resuspended in 400 mM sucrose, 20 mM NaCl, 5 mM $MgCl_2$, and 50 mM MES-NaOH, pH 6.0, placed in a 3-mm quartz tube and frozen in liquid nitrogen. Fluorescence spectra were obtained at 77 K by exciting the samples with a 1,000 W ORIEL 66187 tungsten halogen lamp and a double 0.22 m SPEX 1680B monochromator. Excitation was carried out at 470 nm. Fluorescence was detected through a 0.5 JARREL-ASH monochromator with a Hamamatsu R928 photomultiplier tube. All the measurements were corrected from the system response. The spectral linewidths (FWHM) for the excitation and the emission were 3.6 nm and 1.92 nm, respectively.

3.4. RESULTS

3.4.1. Soybean cell suspension growth

The influence of Cu on soybean photosynthetic cell suspension growth was investigated under two different conditions; *i.e.*, low-sucrose content medium (photomixotrophic growth) and minimal medium with CO_2 as the sole carbon source (photoautotrophic growth). Addition of 5, 10, and 20 μM $CuSO_4$ to the control media that already contained a sufficient amount of Cu for culture growth did not reduce cell growth rate under both 30 ± 5 μE m^{-2} s^{-1} (low light) and 65 ± 5 μE m^{-2} s^{-1} (control light) illumination regimes. Control and Cu-treated cell cultures showed the same doubling time and Chl content rate during the first 22 days of growth (equivalent to one transfer, data not shown). Interestingly, a different feature was observed after two transfers in media

containing excess $CuSO_4$ (5-20μM) and under low light illumination. In these light conditions cells grew faster either photomixotrophically (Fig. 3-1A) or photoautotrophically (Fig. 3-1C). It is worth mentioning that the average volume of individual cell did not change with Cu treatment (data not shown). During the growth exponential phase, the Chl content of these Cu-treated cultures was also 2.5-3.0 fold that of control suspensions (Fig. 3-1B, D). These findings were independent on the presence of sucrose in the medium; therefore the participation of a sucrose-dependent mechanism in this faster growth could be discounted. No enhancement of growth rate was observed in the same conditions under 65 ± 5 μE m^{-2} s^{-1} which corresponded to the normal illumination in our cell suspension growth conditions (Alfonso et al., 1996). Control and Cu-treated cells exhibited similar growth rate and Chl content under normal illumination grown either photomixotrophically (Fig. 3-1E, F) or photoautotrophically growth (data not shown). Higher $CuSO_4$ concentrations up to 50 μM were somewhat toxic as reflected by a change of colour and slower growth (Fig. 3-1A, B), but tolerance to up 50 μM $CuSO_4$ was achieved in cultures previously grown in 20 μM $CuSO_4$ for twenty transfers (Fig. 3-1A, B, dashed line). As the results indicate that Cu stimulates the growth of soybean cell suspensions after two transfers under limiting illumination, the rest of the results of the present work correspond to those obtained under these conditions of growth (hereafter called Cu-adapted cells) unless stated otherwise.

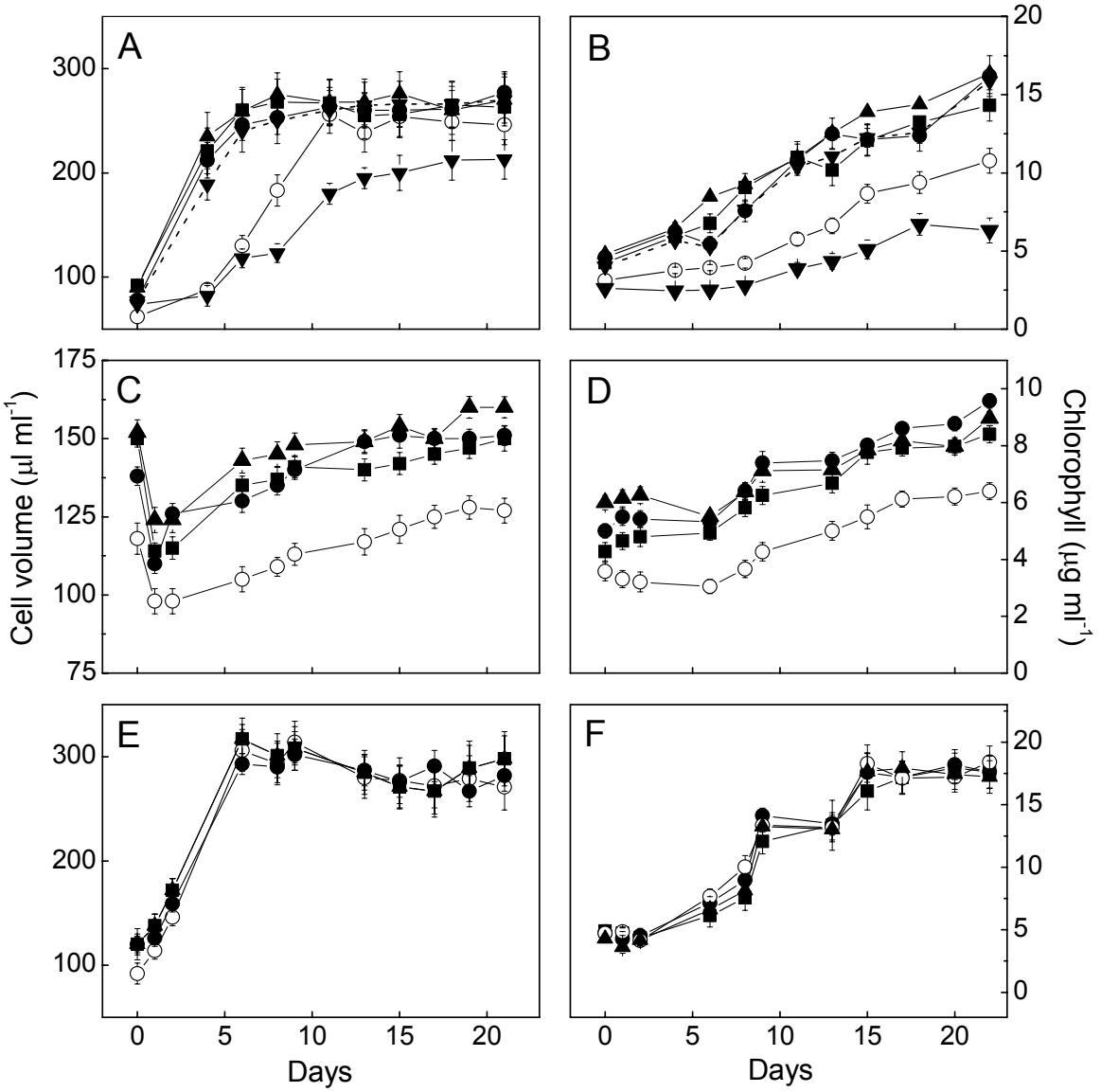

Fig. 3-1. Cell volume (A, C and E) and chlorophyll content (B, D and F) of soybean cell cultures growing under low light (A-D) and control light (E and F) illumination photomixotrophycally (A, B, E and F) and photoautotrophycally (C and D) in the absence and presence of excess Cu(II). ○, ●, ▲, ■, ▼ correspond to 0.1 (control), 5, 10, 20, and 50 μM $CuSO_4 \cdot 5H_2O$, respectively. Dashed line corresponds to culture previously adapted to 20 μM Cu(II) and subsequently grown in medium supplemented with 50 μM Cu(II). Data are representative of four independent experiments.

3.4.2. Oxygen evolution activity from cell suspensions and thylakoids

Oxygen evolution activity measurements were performed in cell suspensions and thylakoids from those cells. Cells from control and Cu-adapted 18-day-old cultures exhibited 57 ± 5 and 74 ± 5 μmol O_2 mg^{-1} Chl h^{-1}, respectively, with no artificial electron acceptor added to the reaction mixture. Similar activity values have been reported in intact chloroplasts and alga cells (Rai et al., 1991). A similar difference ratio was observed in thylakoids from the cell suspensions. Indeed, thylakoids from cells exposed to high content Cu showed on average a 30-45% increase of oxygen evolution activity compared to the control using 2,6-dichloro-*p*-benzoquinone (DCBQ) as artificial electron acceptor to PSII (Table 3-1).

Table 3-1. Photosynthetic parameters of thylakoids from soybean cell suspensions.

Samples	Chlorophyll (mg g^{-1} dry weight)	Oxygen evolution (μmol O_2 mg^{-1} Chl h^{-1})	Chl *a*/Chl *b*	F_{735}/F_{685}	F_{735}/F_{695}
Soybean cell suspension[a]					
Photomixotrophic growth					
Control	3.16 ± 0.5	189 ± 7	3.1	3.1	3.0
5 μM Cu(II)	3.93 ± 0.3	243 ± 12	3.1	2.9	2.8
10 μM Cu(II)	3.85 ± 0.6	248 ± 11	3.1	2.4	2.5
20 μM Cu(II)	3.76 ± 1.1	245 ± 14	3.0	2.3	2.4
Photoautotrophic growth					
Control	3.06 ± 0.7	152 ± 9	3.0	2.4	2.6
5 μM Cu(II)	3.68 ± 0.6	216 ± 8	3.0	2.3	2.5
10 μM Cu(II)	3.98 ± 0.6	232 ± 4	3.0	1.7	2.0
20 μM Cu(II)	3.89 ± 0.6	198 ± 9	2.9	1.6	2.0
10 μM Fe(II)	4.24 ± 0.5	184 ± 2	2.9	2.5	2.6
10 μM Zn(II)	4.12 ± 0.6	179 ± 4	2.8	2.5	2.5

[a]*Soybean cell cultures were grown in media supplemented with $CuSO_4 \cdot 5H_2O$, $FeSO_4 \cdot 7H_2O$ or $ZnSO_4 \cdot 7H_2O$. Cells were analysed after 18 days of growth. Data were obtained from four independent cultures for each condition.*

As no modifications in the PSII/PSI ratio took place in such growth conditions as indicated by the Chl*a*/Chl*b* ratio, the observed results could respond to a specific positive role of Cu on the structure/function of the PSII. This point was investigated in thylakoid membranes isolated from control and Cu-adapted cell suspensions. The results showed a 20% increase of oxygen evolution activity when control thylakoids were incubated with 1.0 μM Cu(II) (Fig. 3-2A). This oxygen evolution stimulation was somewhat lower than that observed *in vivo* may be due to different cation accessibility in isolated thylakoids and intact cells. To know whether this phenomenon is specific to Cu(II) or the response to a more general cation effect, we also measured the oxygen evolution activity in control thylakoids incubated with other cations such as Ca(II), Fe(III), and Zn(II). It is known that Ca participates in the oxygen-evolving complex and stimulates its activity. On the other hand, Fe and Zn can inhibit the oxygen evolution activity by production of reactive oxygen species (ROS) through Fenton's reaction and by dissociation of extrinsic proteins of the oxygen-evolving complex, respectively (Rashid et al., 1994; Yruela et al., 1996b). All the cations assayed stimulated the thylakoid oxygen evolution activity up to a maximum of 15-18% (Fig. 3-2A), although the range of cation concentrations varied for each element being in the same order of magnitude for Ca(II) and Cu(II), somewhat lower for Fe(III) and higher for Zn(II). Interestingly, *in vitro* cation stimulation was not found in thylakoids isolated from Cu-adapted cells (data not shown) indicating that Cu already has a specific positive role on oxygen evolution activity *in vivo*.

The effect of addition of toxic Cu(II) concentrations (10-100 μM) on the oxygen evolution activity of thylakoid preparations was also examined (Fig. 3-2B). A 50% inactivation occurred with approximately 24 μM Cu(II) and approximately 50 μM Cu(II) in thylakoids from control and Cu-adapted cells, respectively. The 50% inactivation in thylakoids from control cells was similar to that previously reported in spinach thylakoids (Yruela et al., 2000). The loss of activity by Cu(II) inhibitory action at toxic concentrations was two-fold slower in thylakoids from Cu-adapted cells compared with those from control ones.

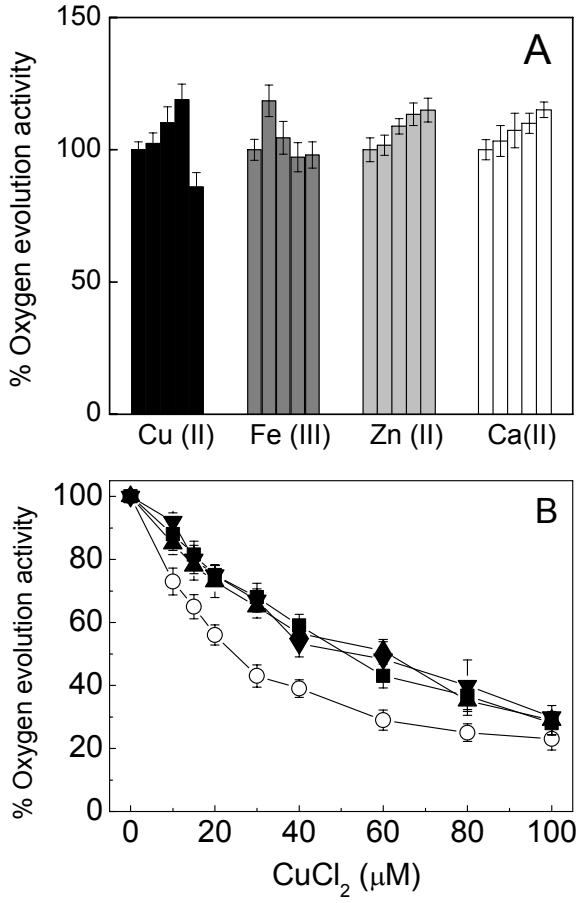

Fig. 3-2. (A) Oxygen evolution activities of thylakoid membranes from control 18-day-old soybean cells incubated with $CuCl_2$ (0, 0.5, 0.75, 1.0 and 1.5 μM), $FeCl_3$ (0, 0.05, 0.1, 0.2 and 0.5 μM), $ZnCl_2$ (0, 0.75, 1.0, 2.0 and 10.0 μM) and $CaCl_2$ (0, 0.05, 0.1, 0.75 and 1.0 μM). (B) Inhibition of oxygen evolution activity of thylakoid membranes from control (○) and 5 μM (■), 10 μM (▲), 20 μM (▼) Cu-treated cells in the presence of 10-100 μM $CuCl_2$. The activity was measured in the presence of 0.5 mM DCBQ. One hundred percent activity corresponded to 198, 258, 269, 268 μmol O_2 mg^{-1} Chl h^{-1} in thylakoids from control and Cu-treated cells, respectively. Cells were grown under low light illumination. Data are representative of four independent experiments.

3.4.3. Effect of Cu on the OEC33 protein

The composition of LHCII antenna complex, D1 protein, and OEC33 extrinsic protein of PSII in thylakoid preparations from control and Cu-adapted cells before and after twice washing steps was assayed (for details see Materials and Methods). The immunoblot analyses showed that the OEC33 extrinsic protein partially released after washing of thylakoids from control cells

(Fig. 3-3, *lane 5). A minor OEC33 loss was detected in thylakoids from cells grown with 5 μM Cu(II) (Fig. 3-3, lane 6). Indeed, no effect of washing steps on OEC33 protein was observed in thylakoids from cells grown with 10 μM and 20 μM Cu(II) (Fig. 3-3, lane 7 and 8). LHCII antenna complex and D1 protein of PSII composition did not vary in all the conditions assayed. Assuming that ratio of OEC33/ LHCII proteins is 1:1 in intact PSII preparations, the OEC33/LHCII ratio calculated was 0.63 ± 0.11, 0.89 ± 0.16, 1.0 ± 0.18 and 1.0 ± 0.14 in control (lane 5) and 5 μM, 10 μM and 20 μM Cu-adapted (lanes 6-8) thylakoids, respectively, after washing. A ratio value of 1.0 was calculated for either control or Cu-adapted thylakoids assayed before washing steps (Fig. 3-3, lanes 1-4). OEC33/D1 ratios varied with the same trend.

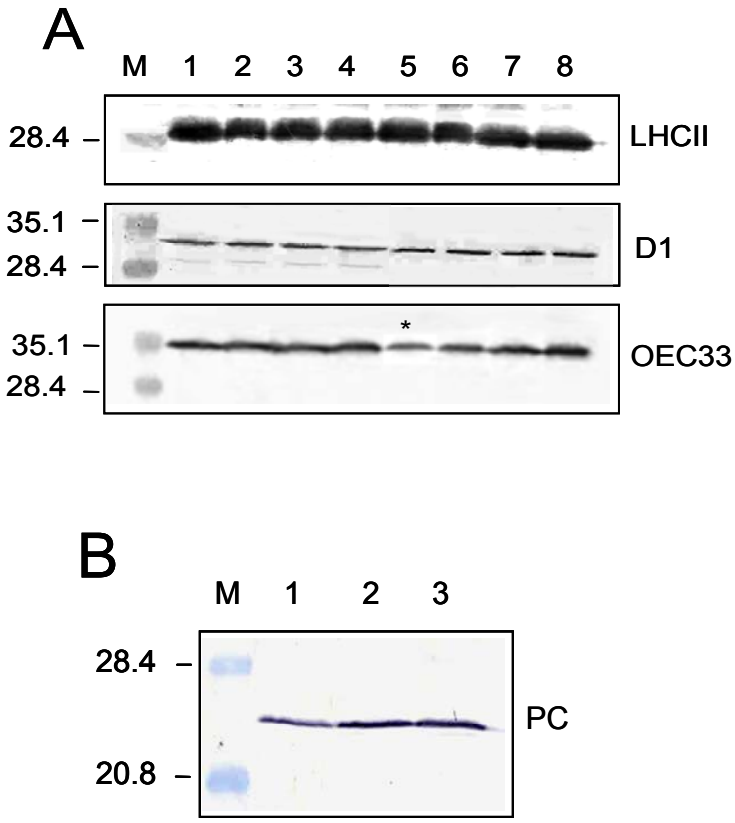

Fig. 3-3. A) Immunoblots with antiserum anti-LHCII antenna complex, anti-D1 and anti-OEC33 extrinsic proteins of intact (lanes 1-4) and twice washed (lanes 5-8) thylakoid membranes. Lanes (1 and 5) control; (2 and 6) 5 μM Cu(II); (3 and 7) 10 μM Cu(II); (4 and 8) 20 μM Cu(II). (B) Immunoblot with anti-plastocyanin (PC) serum. Lanes (1) control; (2) 5 μM Cu(II); (3) 20 μM Cu(II). The same amount of protein [25 μg in (A) and 16 μg in (B)] was loaded in each gel lane. Cells were grown in medium supplemented with the Cu(II) concentrations specified above. Data are representative of three independent experiments. Other experimental conditions as in Fig.3-2.

3.4.4. Cu-uptake by cell suspensions and its intracellular distribution

At this stage of development of the work, it would be important to know how much Cu did really enter into the cells used in the above described experiments. Determination of Cu demonstrated that this element is accumulated in the cells during treatments. The Cu concentration increased on average from 6 μg g^{-1} dry weight in the control to 350 μg g^{-1} dry weight in the highest Cu concentration treatment (Table 3-2).

Table 3-2. Micronutrient content (μg g^{-1} dry weight) in soybean cell suspensions.

Samples	Cu	Fe	Mn	Zn
Soybean cell suspensions[a]				
Photomixotrophic growth				
Control	5.9 ± 1.6	282.2 ± 7.0	23.2 ± 0.3	351.1 ± 8.3
5 μM Cu(II)	136.8 ± 2.7	319.5 ± 4.7	23.9 ± 0.2	164.9 ± 3.3
10 μM Cu(II)	209.5 ± 5.3	328.1 ± 4.3	21.9 ± 0.3	161.3 ± 4.3
20 μM Cu(II)	351.2 ± 7.5	389.8 ± 3.9	23.8 ± 0.2	174.3 ± 3.2
Photoautotrophic growth				
Control	9.8 ± 2.3	715.1 ± 9.3	31.3 ± 0.4	395.4 ± 4.3
5 μM Cu(II)	99.4 ± 2.2	754.0 ± 4.7	31.0 ± 0.1	226.0 ± 6.3
10 μM Cu(II)	148.4 ± 4.3	1411.9 ± 8.3	36.4 ± 0.3	197.3 ± 3.3
20 μM Cu(II)	221.2 ± 5.5	1197.5 ± 4.8	40.5 ± 0.2	179.3 ± 5.2
10 μM Fe(II)	9.1 ± 2.0	1372.3 ± 9.3	17.0 ± 0.4	413.7 ± 5.3
10 μM Zn(II)	13.8 ± 2.1	1690.7 ± 9.3	147.5 ± 0.4	299.1 ± 4.3

[a] *Soybean cell cultures were grown in media supplemented with $CuSO_4 \cdot 5H_2O$, $FeSO_4 \cdot 7H_2O$ and $ZnSO_4 \cdot 7H_2O$. Cells were analysed after 20 days of growth. Data were obtained from four independent cultures for each condition.*

The data showed certain differences between photomixotrophic and photoautotrophic cultures. Cells grown photomixototrophically accumulate much higher Cu upon Cu treatment. We also found that Fe- and Zn-uptake was affected in the same and opposite direction, respectively. The concentration of Fe increased on average 1.4-fold in the cells treated with 20 μM $CuSO_4$, whereas Zn content was on average 2.0 fold lower in that condition. Interactions between micronutrients affecting absorption and bioavailability have also been reported (Sandström, 2001). On the other hand, Mn (Table 3-2) and Ca, Mg, K and P (data not shown) content was not influenced by Cu accumulation.

Elemental analysis of cell cross-sections revealed that Cu is predominantly localized in the chloroplast of control cells (Fig. 3-4A, a) and that Cu content increases in this organelle of Cu-adapted cells (Fig. 3-4B, a). The results also showed that Cu content increases in all the subcellular compartments of the Cu-adapted cells analyzed. Overall, Cu appeared to be distributed in chloroplasts, vacuole, cytoplasm and cell wall of Cu-adapted cells (Fig. 3-4B, b-d). No accumulation of electrodense material was observed in the cells analyzed. The data also showed an increase of Fe within Cu-adapted cells compared to control ones that preferentially was localized in cytoplasm and wall cell compartments. These results are in agreement with micronutrient content analysis (Table 3-2).

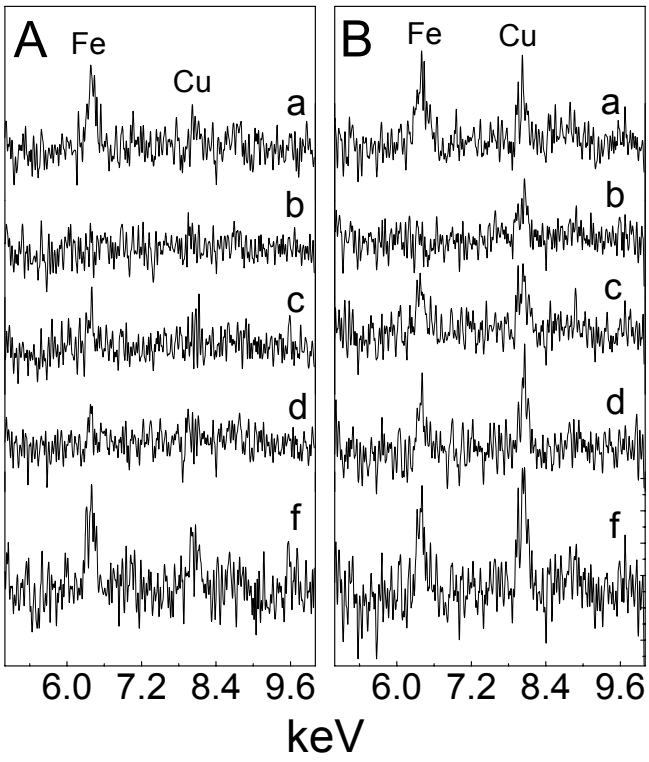

Fig. 3-4. Energy dispersive X-ray spectra in the 4.0-10.0 keV range of different subcellular compartments of individual cells from 18-old-day cell suspensions grown with 0.1 μM (control) (A) and 10 μM (B) $CuSO_4 \cdot 5H_2O$. (*a*) chloroplast, (*b*) vacuole, (*c*) cytoplasm, (*d*) cell wall, (*f*) sum of *a, b, c* and *d* spectrum. Spectra were normalized at titanium peak intensity as internal standard. Typically, eight cells of each type were analysed. Each spectrum represents the mean of four spectra of each cell analysed. Y-axe scale for *f* was double. Other experimental conditions as in Fig. 3-2.

3.4.5. Morphological and ultrastructural changes in chloroplasts from Cu-adapted cell suspensions

The presence of high Cu concentration was apparently not toxic to the cells, but it would be interesting to know if the high accumulation of Cu within the cells induced some changes in the morphology and ultrastructure of chloroplasts. Confocal laser scanning microscopy experiments on 18-day-old cells treated with excess Cu showed that the size of chloroplasts was altered by the treatment. Chloroplasts from Cu-adapted cells were more numerous and smaller than that from control cells and showed brighter autofluorescence compared with control ones (Fig. 3-5A, B). Transmission electron micrographs of chloroplasts from 18-day-old Cu-adapted cells were consistent with these findings and showed that changes in the organelle morphology were accompanied by ultrastructure modifications (Fig. 3-5C, D). Cells grown in the presence of excess Cu exhibited more thylakoid stacking than the control. Analysis of micrographs (Table 3-3) showed that the thylakoid/chloroplast area ratio was somewhat higher in Cu-adapted cells. A 20% increase of thylakoid area ratio was reached in the presence of 10-20 μM $CuSO_4$.

Table 3-3. Morphometric analysis of chloroplasts from soybean cell suspensions[a].

Measurement	Control	+ Cu(II)			+ Fe(II)	+ Zn(II)
		5 μM	10 μM	20 μM	10 μM	10 μM
Photomixotrophic growth						
Chloroplast surface, (μm^2)	3.7 ± 0.5	2.9 ± 0.1	2.6 ± 0.3	2.6 ± 0.5	3.5 ± 0.2	3.7 ± 0.3
Thylakoid/Plastid surface	0.41 ± 0.08	0.42 ± 0.08	0.48 ± 0.07	0.54 ± 0.04	0.41 ± 0.1	0.39 ± 0.1
Photoautotrophic growth						
Chloroplast surface, μm^2	2.9 ± 0.5	2.7 ± 0.6	2.6 ± 0.5	1.7 ± 0.4	3.3 ± 0.8	3.0 ± 0.8
Thylakoid/Plastid surface	0.37 ± 0.03	0.45 ± 0.05	0.46 ± 0.08	0.44 ± 0.04	0.40 ± 0.05	0.41 ± 0.04

[a]Soybean cell cultures were grown in media supplemented with $CuSO_4 \cdot 5H_2O$, $FeSO_4 \cdot 7H_2O$ or $ZnSO_4 \cdot 7H_2O$. Cells were analyzed after 18 days of growth. Data were obtained on average from 10 images from three independent cultures for each condition.

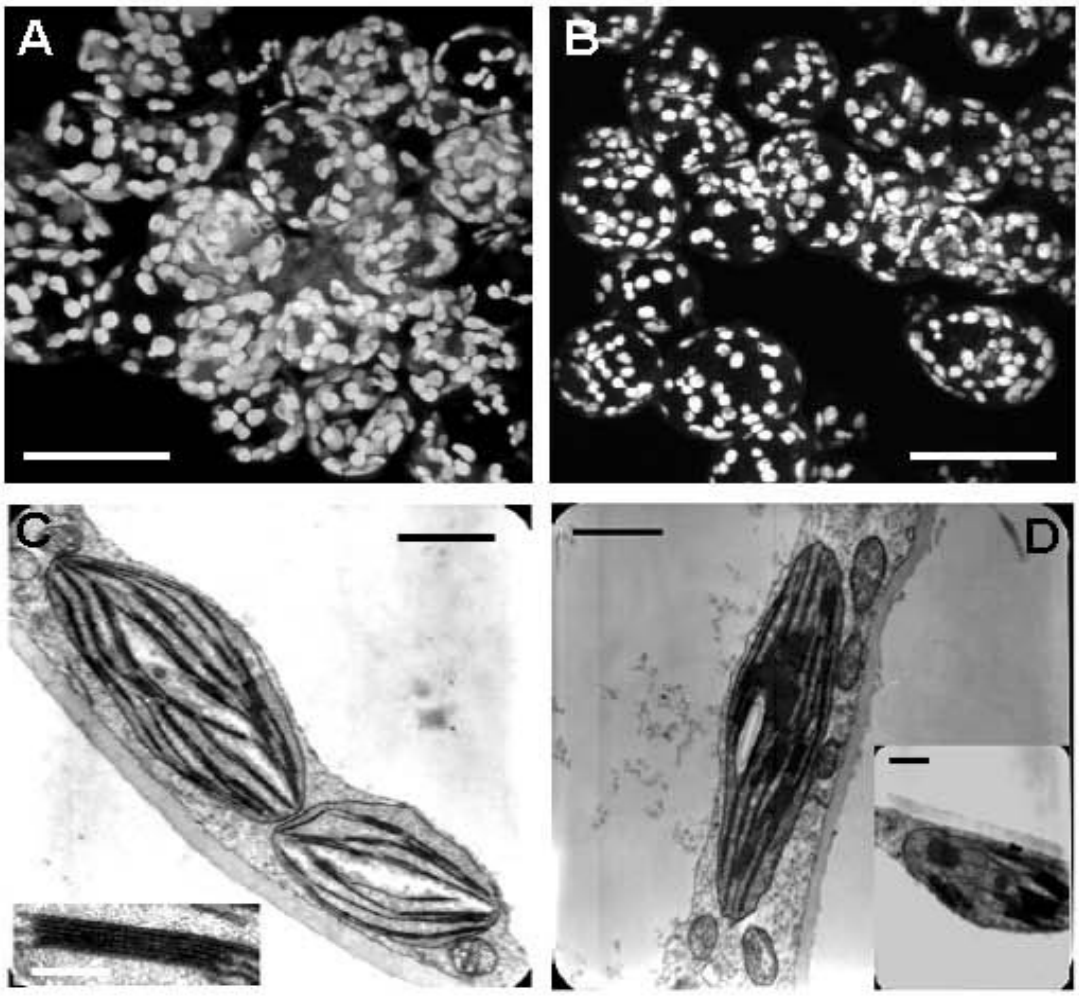

Fig. 3-5. Confocal laser scanning images of cells (A and B) and transmission electron micrographs of chloroplasts (C and D). Control cells and chloroplasts (A and C), cells and chloroplasts in the presence of 10 μM $CuSO_4 \cdot 5H_2O$ (B, D). For confocal images excitation wavelength was 488 nm and focal distance was 1 μm. White bar in A and B correspond to 35.7 μm; black bar in C and D is 1.2 μm; bars in insets are 0.16 μm. Images are representative of four independent experiments. Other experimental conditions as in Fig. 3-2.

On the other hand, significant changes of granal distribution were observed upon growth in the presence of excess Cu(II) (Fig. 3-6). Cu-adapted cells had wider grana than control cells. It is worth mentioning that the cells used for transmission electron microscopy were fixed within 12-min period because changes in irradiance can rapidly initiate modifications of granal appression (Rozak et al., 2002).

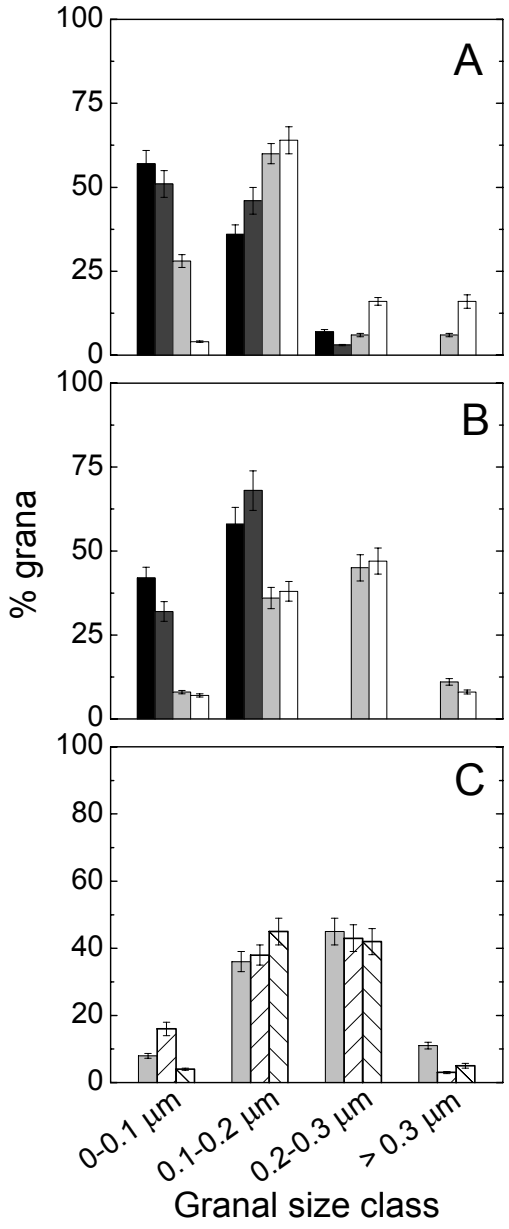

Fig. 3-6. Granal size distribution changes in chloroplasts from 18-day-old soybean cells grown in photomixotrophic (A) and photoautotrophic (B, C) conditions under low light illumination. Control (black), 5 μM $CuSO_4 \cdot 5H_2O$ (dark grey), 10 μM $CuSO_4 \cdot 5H_2O$ (light grey), 20 μM $CuSO_4 \cdot 5H_2O$ (white), 10 μM $FeSO_4 \cdot 7H_2O$ (right dash), 10 μM $ZnSO_4 \cdot 7H_2O$ (left dash). Data were obtained on average from 10 images from three independent cultures for each condition.

Other chloroplast characteristics were also modified in Cu-adapted cells. For instance, total Chl content per cell dry weight on average was 25% higher Table 3-1). The activation of Cu/ZnSOD synthesis (data not shown) and an increase of plastocyanin content (another chloroplastic Cu-containing protein) (Fig. 3-3B) was observed. Thylakoids had a higher content of C18:2 and C18:3 fatty acids while C16:0, C18:0, and C18:1 levels were lower in comparison with control membranes. These findings could be related to the higher thylakoid stacking observed in Cu-adapted cells.

3.4.6. Fluorescence spectral changes induced by Cu treatments

Fluorescence spectra at 77K are often used to monitor ultrastructural changes in thylakoid membranes as a response to environmental condition variations (Anderson, 1999; Rozak et al., 2002). Thus, the F_{735}/F_{685} and F_{735}/F_{695} ratios can be used as a probe for the amount of antenna Chls unconnected to each photosystem (Van Dorssen et al., 1987; Alfonso et al., 1994). Cells treated with excess Cu normally had the lowest F_{735}/F_{685} ratio values, whereas higher values were found in control cells, independently of growth conditions (Table 3-1). Similar variations were found for the F_{735}/F_{695} ratio. The data indicate that the presence of Cu induces a higher fluorescence emitted mainly by antenna complexes associated to PSII compared to the control.

3.4.7. Effect of Fe and Zn on chloroplast structure and oxygen evolution activity

To know if Fe and Zn have a similar influence as Cu *in vivo*, excess of these cations was supplemented to the growth media. Cells grown in medium supplemented with 10 μM $FeSO_4$ or 10 μM $ZnSO_4$ under low light illumination exhibited a slightly faster growth rate compared with the control but slightly slower one compared with those grown in the presence of excess $CuSO_4$ (data not shown). Oxygen evolution activity of thylakoid membranes from Fe- and Zn-treated cells was only about 5-10% higher than the control but 20-25% lower than that measured in thylakoids from Cu-adapted cells (Table 3-1). On the other hand, no significant differences in Chl*a*/Chl*b* ratio values and F_{735}/F_{685} and

F_{735}/F_{695} ratios were found after 18 days of growth but higher Chl content compared to the control was observed (Table 3-1). Determination of micronutrients (Table 3-2) showed that Fe is accumulated by cells grown either in the presence of 10 μM $FeSO_4$ or 10 μM $ZnSO_4$ while Cu-uptake is not significantly influenced. Fe accumulation by cells on average was 2-fold the control value. The data also showed that *i)* Zn treatment results in high increase of Fe accumulation (exceeding that under Fe treatment) with concomitant decrease of Zn content and increase of Mn content and *ii)* the increase of Fe accumulation induced by Fe treatment was accompanied by increase in Zn accumulation and decrease of Mn. These changes in Mn level contrast with those taking place with Cu treatment. Analysis of micrographs revealed differences between chloroplasts from cells grown in the presence of excess Cu(II), Fe(II), and Zn(II). Fe- and Zn-treated cells showed that: *i)* the thylakoid per chloroplast area ratio was somewhat lower; and *ii)* grana were slightly narrower compared with those from Cu-adapted cells (Table 3-3).

3.5. DISCUSSION

Our data demonstrated that, in contrast to what commonly happens in whole plants, the supplementation of excess Cu to the soybean SB-P line cell suspensions caused a high accumulation of this element within the cells but that such Cu content was apparently not toxic. Soybean cell suspensions used in this study grew well in 5-20 μM $CuSO_4$. Indeed, they develop tolerance to even higher levels of Cu (*i.e.*, up to 50 μM). Only a few works have been published concerning to excess Cu effect on plant cell suspensions. Several of them showed tolerance to Cu (80-100 μM) in cell suspension cultures from *Nicotiana plumbaginifolia, Nicotiana tabacum L.,* and *Acer pseudoplatanus L.* (sycamore) (Kishinami and Widholm, 1986; 1987; Turner and Dickinson, 1993; Gori et al., 1998; Raeymaekers et al., 2003). These works were limited and they partially report physiological aspects of this subject. Thus, the extensive study presented in this paper with soybean cell suspensions can be useful to understand some of the mechanisms underlying Cu acclimatation or tolerance in cells of higher plants established from leaves.

Soybean Cu-adapted cells showed a higher growth rate than the control under limiting illumination after an adaptive period of one transfer. The increase in measured cell volume can be explained by additional cell division, because the volume of individual cell did not change with Cu treatment (data not shown). The higher growth was accompanied by a higher Chl content probably due to a Cu stimulation of Chl synthesis under low light compensating the effect of light limitation. Recently, the role of Cu as a regulatory element of Chl synthesis has been described (Moseley et al., 2002; Tottey et al., 2003). It is well known that Fe is essential for an optimal formation of the photosynthetic apparatus (Raven et al., 1999). Therefore, the fact that Fe uptake slightly increased in Cu-adapted cells could in principle explain the significant increase of Chl content, thylakoid appresion and grana size and photosynthetic activity observed in these cells. However, the stimulation of the oxygen evolution activity (30-45%) observed in Cu-adapted cells cannot be only explained by the Fe level increase. In this sense our *in vitro* experiments of cation-stimulating effect of PSII activity and *in vivo* experiments supplying excess Cu(II), Fe(II), and Zn(II) to the growth media are in agreement with that. It is worth mentioning that: *i) in vitro* cation stimulation was not found in thylakoids isolated from Cu-adapted cells; *ii)* Fe was accumulated in cells exposed to excess of either Cu(II), Fe(II), or Zn(II) but the oxygen evolution activity of PSII was preferentially activated in thylakoids from Cu-adapted cells where Cu uptake was significantly increased. Interestingly, no increase of Cu uptake was observed in cells exposed to excess Fe(II) or Zn(II). Therefore, the data indicate that Cu has a specific positive role in photosynthesis and particularly in the structure/function of PSII. The presence of higher Cu content within chloroplasts of Cu-adapted cells supports this picture. It is clear therefore that the high Cu content in these cells is not toxic but modulates photosynthesis at least at levels Chl synthesis, PSII activity and plastocyanin content. In support of our findings, it has been described that leaves of Cu-deficient plants and *A. thaliana* mutants defective in Cu-transport into the chloroplast (Shikanai et al., 2003) exhibited reduced Chl content and photosynthetic electron transport. Cu-adapted cells also showed a higher fluorescence emission of PS II antenna complexes compared to untreated cells in all the conditions assayed. This finding could respond to: *i)* a higher PSII/PSI ratio; or *ii*) a higher level of stacking and aggregation of PSII surrounding

antenna complexes due to non-specific electrostatic interactions between membrane and protein negative-charged surfaces and Cu(II) cations reducing repulsion effects (Izawa and Good, 1966; Chow et al., 1980). The first hypothesis can be discounted, becames the determined Chl*a*/Chl*b* ratio was 3.0 ± 0.1 for all the cultures conditions assayed (Table 3-1). Thus, our results are more in agreement with the second hypothesis. An increase of fluorescence from the purified LHCII antenna complex has been reported in the presence of cations (Kirchhoff et al., 2003).

It is known that organization of PSII in granal and stromal membranes present important differences. PSII exists in a dimeric form in granal membranes while only a monomeric form of PSII is found in stroma lamellae (Bassi et al., 1995). It has been also found that the polypeptide composition of the oxygen-evolving core complexes (OECC) in both PSII forms is similar except that the level of OEC33 extrinsic protein associated to monomeric PSII forms is lower (Bassi et al., 1995; Hankamer et al., 1997). Furthermore, isolated dimeric OECC preparations are more stable, contain higher levels of Chl and exhibit a higher oxygen-evolution activity than monomeric OECC preparations (Hankamer et al., 1997). Taking into account the above considerations, our results would be in agreement with a higher presence of dimeric PSII complexes in the thylakoids of Cu-adapted cells, associated with the higher level of granal membranes observed in these cells. In that case the proportion of monomeric PSII forms should be higher in control cells. Considering this scenario, the partial release of the OEC33 extrinsic protein by washing steps in thylakoids from control cells could be explained by the presence of a certain amount of OEC33 proteins not firmly bound to PSII complexes in stromal membranes. The presence of the surfactant sucrose in the buffer might favour the precipitation of these not firmly bound OEC33 proteins in the thylakoid fraction, and the washings with buffer without sucrose release that. In this respect, it is worth mentioning that the OEC33 protein is synthesized as a precursor protein in the cytoplasm, it binds to PSII cores or minimal PSII complexes in the stromal regions and then it migrates to the grana (Hashimoto et al., 1997). Nevertheless further experiments are needed to clarify this issue.

In the past, the structural role of Cu in PSII was discussed extensively (Barón et al., 1995) but no definitive conclusions were attained. Accordingly to

Burda et al. (2002) we observed that Cu(II) at subtoxic concentrations increases oxygen evolution activity *in vitro* in isolated thylakoids from control cells, but it has no effect on thylakoids from Cu-adapted cells. Interestingly, inhibition of oxygen evolution activity by concentrations of 10 μM Cu and above was 2-fold less in thylakoids from Cu-adapted cells than from control ones. This finding could be explained by: *i)* a Cu-binding site less accessible in the former case probably due to conformational changes in the neighbour of the Cu-binding site; *ii)* an extra metal sequestering or chelating capacity developed in Cu-adapted cells; *iii*) less capacity of Cu ions to damage due to changes in membrane lipids or ultrastructure. Kruk et al. (2003) showed that the OEC33 protein contains a low-affinity binding site for several cations, *i.e.,* Ca, and certain lanthanides and that this metal binding induces protein conformational changes that would stabilize the optimal conformation of PSII reaction center proteins involved in Mn-Ca coordination. In this respect Burda et al. (2002) showed that Ca, lanthanides and low Cu concentrations similarly stimulate *in vitro* the oxygen evolution activity of PSII membranes.

In conclusion, the photosynthetic soybean cell cultures established from leaves used in this study can accumulate high content of Cu in the cells with no apparent toxicity. The high Cu content accumulated by cells stimulates cell growth and Chl synthesis under low irradiance probably due to a Cu stimulation. In addition, Cu-adapted cells showed higher photosynthetic activity and some morphological changes in chloroplast and thylakoid ultrastructures. The data support the picture of Cu as a positive element affecting and mediating *in vivo* the structure/function of PSII.

CAPÍTULO 4

EXCESS COPPER INDUCES STRUCTURAL CHANGES IN CULTURED PHOTOSYNTHETIC SOYBEAN CELLS

4.1. ABSTRACT

Soybean cell suspensions have the capacity to develop tolerance to excess copper, constituting a convenient system for studies on the mechanisms of copper tolerance. The functional cell organization changes observed in these cell cultures after both a short-term (stressed cells) and a long-term (adapted cells) 10 μM $CuSO_4$ exposure are reported by using a structural, cytochemical and microanalytical approach. Cells grown in the presence of 10 μM $CuSO_4$ shared some main structural features with control cells such as: *i)* a large cytoplasmic vacuole; *ii)* chloroplasts along the thin layer of cytoplasm; *iii)* nucleus in a peripheral location exhibiting circular-shaped nucleolus and a decondensed chromatin pattern; *iv)* presence of Cajal bodies in the cell nuclei. In addition, cells exposed to 10 μM $CuSO_4$ exhibited important differences compared with control cells: *i)* chloroplasts displayed rounded shape and smaller size with a denser structured internal membranes specially in Cu adapted cells; *ii)* no starch granules were found within chloroplasts; *iii)* cytoplasmic vacuole was larger specially after a long-term copper exposure; *iv)* the levels of citrate and malate increased. Extracelullar dark deposits attached at the outer surface of the cell wall with high copper content were only observed after a short-time response in Cu-stressed cells as a differential feature. Structural cell modifications, mainly affecting chloroplasts, accompanied the short-term copper induced response and were maintained as a stable character during the adaptive period to excess copper. Vacuolar changes rather accompanied the long-term copper response. The results indicate that the first response of soybean cells to excess copper avoids its entrance to the cell by its immobilization in the cell wall, and after an adaptative period copper acclimation may be mainly due to vacuolar sequestration.

4.2. INTRODUCTION

Copper is an essential micronutrient for plants. Copper acts as a structural element in certain metalloproteins, many of which are involved in electron transport in mitochondria and chloroplasts, and oxidative stress

response. It also participates in cell wall metabolism, hormone signalling, protein trafficking machinery, transcription signalling and iron mobilization (for reviews see Marschner, 1995; Raven et al., 1999; Gratão et al., 2005; Yruela, 2005; Pilon et al., 2006). Nevertheless, it can also be a toxic element at a tissue concentration slightly higher (20-30 $\mu g\ g^{-1}$ dry weight) than the optimal one (6-12 $\mu g\ g^{-1}$ dry weight) (Baker and Senef, 1995; Marschner, 1995). Although normally copper binds to proteins, it may be released and become free to catalyze the formation of highly reactive hydroxyl radicals *via* Fenton-type reactions. Thus, copper has capacity to initiate oxidative damage and interfere with important cellular events such as photosynthesis, pigment synthesis, plasma membrane permeability and other metabolic mechanisms causing a strong inhibition of plant development (Küpper et al., 2003; Bertrand and Poirier, 2005; Yruela, 2005). Since copper is both an essential cofactor and a toxic element their uptake and cellular concentrations must be strictly regulated. Thus, plants use different strategies to appropriately regulate copper homeostasis as a function of its environmental level (Krämer and Clemens, 2006; Pilon et al., 2006).

At present, there is an increasing concern about copper toxicity in agriculture and health since copper is considered a major heavy metal contaminant that results from fertilizers accumulation, the application of pig and poultry slurries rich in copper, fungicides, industrial and urban activities, mining or metal processing (Kabata-Pendias and Pendias, 2001; Pilon-Smits and Pilon, 2002). Copper concentration in non-contaminated soils and natural waters is *ca*. 20-30 $mg\ kg^{-1}$ and 2 $\mu g\ kg^{-1}$, respectively but in contaminated soils and waters can reach levels one hundred times higher (Fernandes and Henriques, 1991). Some plant species or ecotypes are sensitive to metals, whereas others are tolerant showing little growth inhibition or damage even if they grow in severely polluted soils and accumulate high concentrations of these elements in their tissues. It was demostrated that the plant *Silene vulgaris* exhibits tolerance to different metals (Zn, Cd or Cu) (Schat and Vooijs, 1997; Van Hoof et al., 2001). Different response to excess copper were observed in four Australian tree species, *Acacia holosericea*, *Eucalyptus crebra*, *Eucalyptus camaldulensis* and *Melaleuca leucadendra* (Reichman et al., 2006). Nowadays, mechanisms of

heavy metal tolerance in plants are of interest and numerous works have been conducted on this subject. In general, control of metal uptake, excretion of accumulated metals and intracellular immobilization of those are the main mechanisms that operate alone or in concert to protect plants from toxic effects (Ernst et al., 1992; Clemens, 2001; Hall and Williams, 2003; Krämer and Clemens, 2006). However, in some cases the mechanisms underlying the tolerance to metals are not fully understood and in particular those mechanisms related to copper tolerance. In soybean seedlings treated with excess copper it has been reported that the enhancement in peroxidasa and laccase activities was accompanied by a rapid increase of lignin contents in the copper treated tissues (Lin et al., 2005). The increase in phenolic compounds, related enzymes and lignin was observed in root suspension cultures of *Panax gingseng* in response to copper stress (Ali et al., 2006). Intraspecific and interspecific differences in sensitivity to copper do occur between different plant species. On the other hand, with regard to mechanisms allowing a copper tolerance, a question of interest is whether this tolerance is constitutive in each species or depends on previous long-term exposure to metal.

Plant cell cultures are widely used as suitable model system to analyse metabolic signalling pathways, developmental process and cell stress response and adaptation, among many other studies on plant physiology (Roitsch and Sinha, 2002; Allan et a., 2006; Zuppini et al., 2006). Plant cell cultures can be a useful tool for studying the characteristics and mechanisms of heavy metal tolerance in plants at cellular level. In this respect, only a few studies concerning heavy metal tolerance in plant cell suspensions exist. Selection and characterization of various cell cultures from *Nicotiana* tolerant to aluminium, cadmium, copper and zinc have been reported (Kishinami and Widholm, 1986; 1987; Gori et al., 1998). Cadmium stress has been studied in sugar cane callus cultures (Fornazier et al., 2002). However, a very little information exists from cell suspensions of other species. Since the cell culture used in this work comes from mesophyll cells, the results presented here may provide information to advance in our knowledge of physiological aspects of leaf cells in plants. In chapter 3 (Bernal et al., 2006) we reported that soybean cell suspensions have capacity to develop tolerance up to 50 μM $CuSO_4$ after a long-time copper exposure. In this work we investigated more in detail the functional structural

cellular changes induced by excess copper on soybean cell suspensions. The comparison between a short-term and a long-term copper exposure is presented.

4.3. MATERIALS AND METHODS

4.3.1. Cell culture conditions

Photosynthetic cell cultures from soybean (*Glycine max* var. Corsoy) SB-P line were grown as described by Rogers et al. (1987) with some modifications. These cell cultures were established in our laboratory in 1990. Cell suspensions were grown in liquid cultures photomixotrophically (KN^1 medium) under continuous low light (30 $\pm$ 5 $\mu E\ m^{-2}\ s^{-1}$). The KN^1 medium contained thiamine (0.1 mg/L), kinetin (0.2 mg/L), naphthalene acetic acid (1 mg/L) and sucrose (1% w/v) as organic components. It has been reported that this kind of cultures grow optimally with 65-75 $\mu E\ m^{-2}\ s^{-1}$ (Alfonso et al., 1996) and that high light cause photoinhibitory effects in these cell suspensions (personal communication; Alfonso et al., 1996). On the other hand, it is known that Cu is a potential toxic element and its toxicity enhances with light. Thus, we decided to assay a low light regime (30 $\pm$ 5 $\mu E\ m^{-2}\ s^{-1}$) following the light conditions used in previous works studying the copper stress effect on cell cultures (Gori et al., 1998; Bernal et al., 2006). To assay the Cu effect on cell growth the media were supplemented with 10 μM $CuSO_4 \cdot 5H_2O$. Control medium corresponded to 0.1 μM $CuSO_4 \cdot 5H_2O$. Cell suspensions were subcultured at 23 day intervals. For experiments cells exposed to excess copper were collected after the first 21 days of treatment (Cu-stressed cells) and after 22 transfers in the presence of excess copper (Cu-adapted cells). For microscopical structural analysis, soybean cells were grown in 1.5% (w/v) agar plates with KN^1 medium at 24 ºC and atmosphere with 5% CO_2. Cells cultured in these conditions were easier to handle during the fixation and sectioning procedures than liquid suspensions.

4.3.2. Sample processing for microscopical structural analysis

Soybean cells were fixed overnight at 4 ºC in 4% (w/v) formaldehyde in phosphate buffered saline solution (PBS), pH 7.3. Then, they were washed in PBS and dehydrated through an acetone series (30%, 50%, 70% and 100% (v/v)) at 4 ºC. The samples were infiltrated and embedded in Historesin 8100 at 4 ºC. Semithin sections (1 µm thickness) were obtained and used for light microscopy observations. Toluidine-blue stained semithin sections were observed under bright field and phase contrast field for structural analysis in a Leitz microscope fitted with a digital camera Olympus DP10.

4.3.3. Morphometric analysis of cell, chloroplast and vacuole size

Random sampling was carried out over toluidine-stained micrographs of the three cultures. The number of micrographs to be taken was determined using the progressive mean test, with a maximum confidence limit of $p \leq 0.05$. The cell, chloroplast and vacuolar area was measured in μm^2 using a square lattice composed by 40 x 57 squares of 5 x 5 mm (cell and vacuole) or 65 x 96 squares of 3 x 3 mm (chloroplast) each. For each culture, the mean area per cell was estimated and the results were compared among the cultures. Duncan's multiple range test ($p \leq 0.05$) was used to compare the data among the cultures.

4.3.4. Cytochemical stainings for starch and DNA

Starch was detected by I_2KI staining (O'Brien and McCully, 1981) on Historesin semithin sections and observed under bright field (Barany et al., 2005). DAPI staining for DNA was applied to semithin sections (Testillano et al., 1995) and observed under UV light in a Zeiss Axiophot epifluorescence microscope fitted with a CCD camera.

4.3.5. Copper determination

Cells were harvested and washed twice with 3 mM EDTA and once with distilled H_2O to remove free cations. After washing, cells were filtered through a layer of Miracloth (Calbiochem, EMD Biosciences Inc, San Diego, CA, USA) and dried in a ventilated oven at 60 ºC for 48 h. Dried samples were treated

using a standard procedure (Abadía et al., 1985). Analyses were performed in an atomic absorption spectrometer (UNICAN 969).

4.3.6. Organic acids analysis

Cells were harvested on Miracloth layer (Calbiochem, EMD Biosciences Inc, San Diego, CA, USA), washed three times with cold distilled water and then homogenized in 70% (v/v) ethanol in a Teflon homogenizer. The homogenate was centrifuged at 10,000 x g for 10 min at 4 ºC and the pellet was washed with 70% (v/v) ethanol three times. The supernatants were combined and dried under vacuum at 35 ºC in SPD Speed Vac model SPD111V (Thermo Savant, Holbrook, NY, USA). The residue was resuspended in 0.1% (v/v) formic acid and filtered with 0.2 μm nylon filter (Tecknokroma, Barcelona, Spain), taken to a final volume of 0.5 ml and stored at -80 ºC until analysis. Organic acids were analysed by HPLC-ESI/MS with a BioTOF® II (Bruker Daltonics, Billerica, MA, US) coaxial multipass time of flight mass spectrometer (MS (TOF)) equipped with an Apollo electrospray ionization source (ESI), and coupled to a Waters Alliance 2795 HPLC system (Waters Corp., Mildford, MA, US) with a Supelcogel H 250 x 4,6 mm column. The mobile phase was 0.1% (v/v) formic acid. Duncan's multiple range test ($p \leq 0.05$) was used to compare the data among the cultures.

4.3.7. Energy-dispersive X-ray microanalysis

Cells were cry fixed using a high-pressure freezer (Leica EMPact; Leica Microsystems, Gladesville, Australia) and were then stored in liquid nitrogen until freeze-substitution. Frozen cells were freeze-substituted with diethyl ether containing 10% acrolein with freshly activated 5 Å molecular sieve (Baker Analyzed) for 4 days at -90 ºC, 2 days at -70 ºC and 1 day at -30 ºC. Subsequently, samples were gradually brought to 4 ºC by raising the temperature for 1.5 h (Bidwell et al., 2004). The freeze-substituted cells were infiltrated with Araldite resin over 4 days. Araldite contains negligible levels of elements detectable by energy-dispersive spectrometry (Pålsgård et al., 1994). Cell sections were cut dry at 0.5 μm using an ultramicrotome (Leica Ultracut UCT) and mounted directly onto titanium grids (75 mesh) that were coated with

formvar. Sections were stored in a desiccator under vacuum until analysis to prevent absorption atmospheric water and hence possible redistribution of ions.

Unstained sections were analysed at room temperature in a carbon holder by energy-dispersive X-ray microanalysis using a transmission electron microscope (model H-800-MT, Hitachi) and X-ray EDX Quantum detector (model 3600, Kevex). The detector was interfaced to a signal processing unit (Röntec, Ltd, Normanton, UK). The electron microscope was operated at 100 kV in STEM mode with a spot size 10-15 nm and a beam current 15 μA. The spectral data from individual cells and compartments in each section were collected using selected area analysis with an acquisition time of 300 s. Analyses were carried out by Quantax 1.5 program (Röntec Ltd, Normanton, UK). Spectra were normalized at titanium peak used as an internal standard, which came from the grid material.

4.3.8. Low Temperature Scanning Electron Microscopy (LTSEM)

Samples were examined by using the Low Temperature Scanning Electron Microscopy LTSEM technique (De los Ríos et al., 2004). Cells were mechanically fixed onto the specimen holder of a cryotransfer system (Oxford CT1500), plunged into subcooled liquid nitrogen, and then transferred to a preparation unit via an air lock transfer device. The frozen specimens were cryofractured and transferred directly via a second air lock to the microscope cold stage, where they were etched for 2 min at -90 °C. After ice sublimation, the etched surfaces were sputter coated with gold in the preparation unit. Samples were subsequently transferred onto the cold stage of the scanning electron microscope chamber. Fractured surfaces were observed with a DSM 960 Zeiss scanning electron microscope at -135 °C.

4.4. RESULTS

The main features of the cell structure in the soybean photosynthetic cell cultures grown in control medium (control cells) and in the presence of 10 μM $CuSO_4$ after either the first 21 days of copper treatment (Cu-stressed cells), or 22 transfers (Cu-adapted cells) were analysed (for details see Materials and Methods). Cells accumulated copper during the first 21 days of growth in the presence of 10 μM $CuSO_4$ and the copper concentration in Cu-adapted cells even slightly increased during the 10 μM $CuSO_4$ treatment (Fig. 4-1).

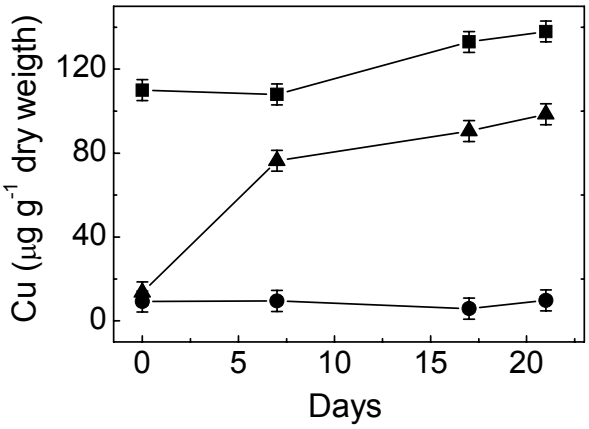

Fig. 4-1. Cu content in soybean photosynthetic cells during 21 days of growth. Control cells (●); Cu-stressed cells (▲); Cu-adapted cells (■). For details see Materials and Methods.

Semithin sections were observed at light microscopy after different staining and cytochemical procedures (Figs. 4-2, 4-3, 4-4): *i)* toluidine blue for general structural analysis; *ii)* iodide-based staining to reveal starch and *iii)* DAPI for DNA. The observations revealed common and differential features in the structural organization of cells from different cultures assayed. Scanning electron microscopy observations are also shown in Fig. 4-5.

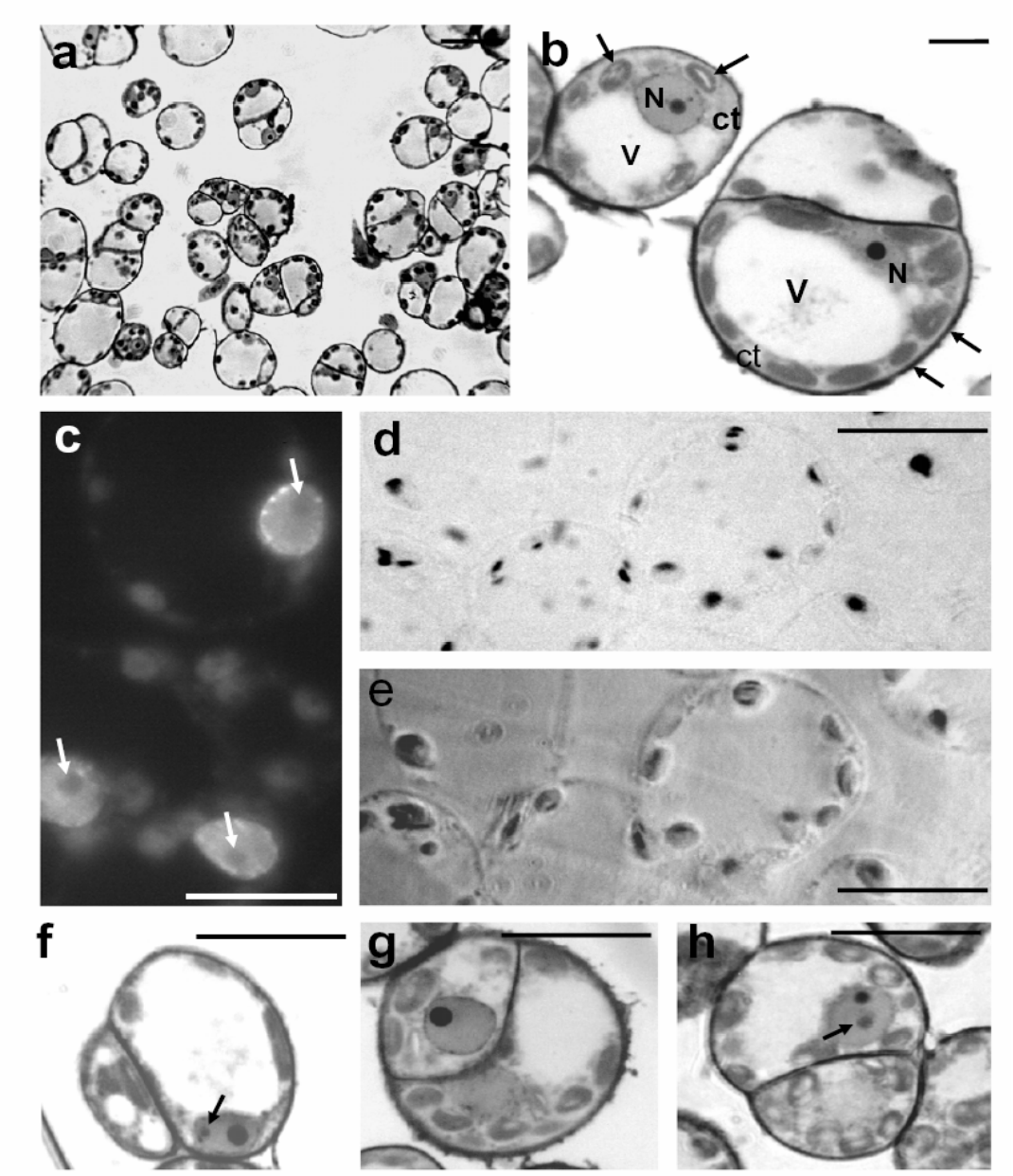

Fig. 4-2. Structural organization of soybean photosynthetic cells of control cultures. Historesin semithin sections after toluidine blue staining (a, b, f-h), DAPI staining for DNA (c) and I_2IK staining for starch (d, e). (a) Panoramic view of the cells in the culture, isolated and in two-cell groups. (b) Cell structure observed at higher magnification, cells show large vacuoles (v), perypheric nucleus (N) with one nucleolus each, cytoplasm (ct) with ellipsoid chloroplasts, many of them containing clear starch deposits (arrows). (c) Chromatin pattern showed by DAPI staining: nuclei exhibit a homogeneous medium-bright fluorescence and several brighter small spots aligned at the nuclear periphery, corresponding to condensed chromatin patches. The nucleoli appear as dark areas (arrows). (d and e) Starch grains revealed as dark inclusions by iodide-base cytochemistry, observed under bright field (d) and phase contrast (e). (f-h) Several two-cell structures showing different asymmetric position of the dividing cell wall and some details of the cell organization. In some nuclei, Cajal-like bodies (arrows) can be observed. Bars represent 10 μm.

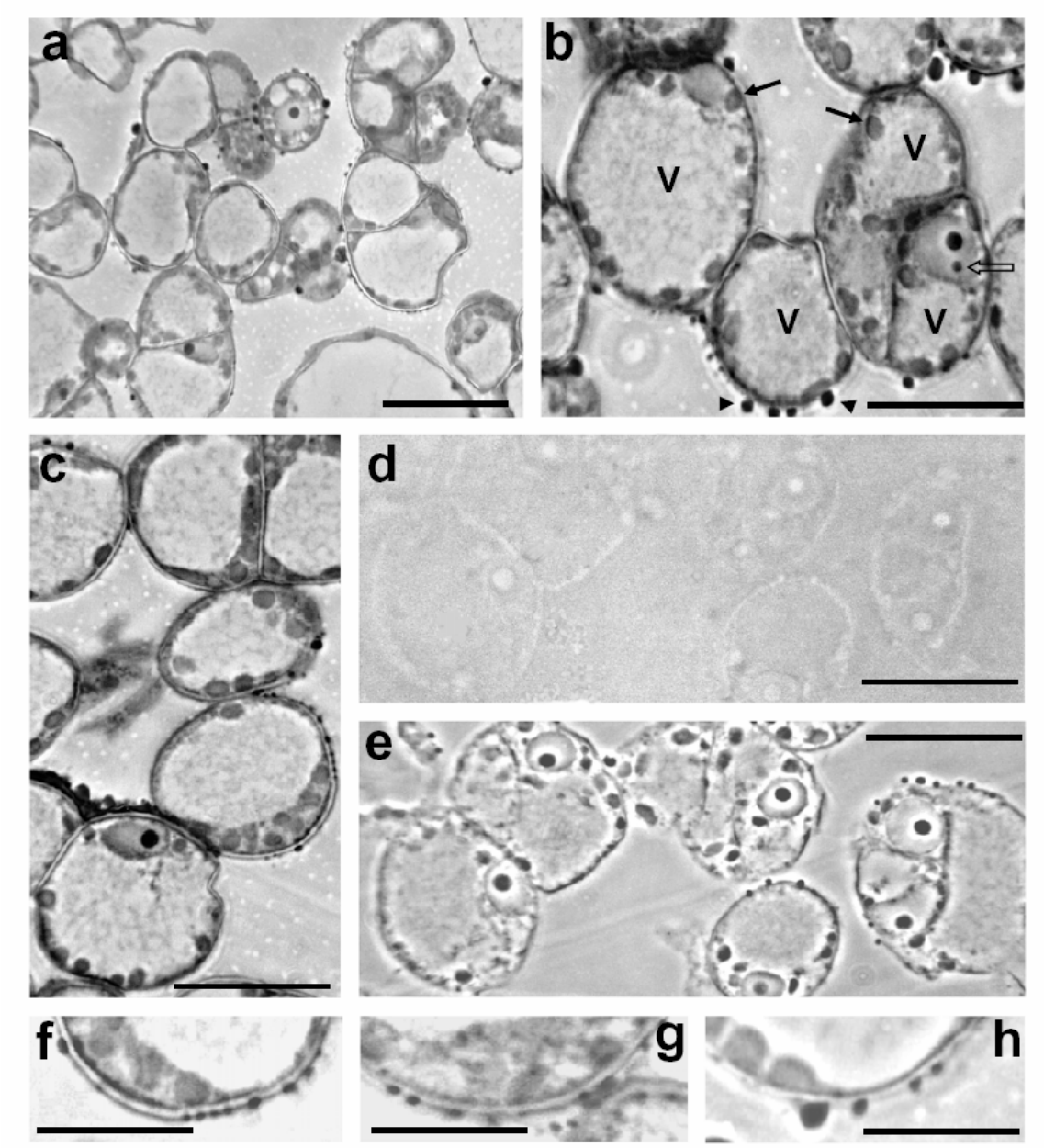

Fig. 4-3. Structural organization of soybean photosynthetic cells of Cu-stressed cultures. Historesin semithin sections after toluidine blue staining (a, b, c, f-h), and I_2IK staining for starch (d, e). (a) Panoramic view of the cells in the culture, isolated and in two-cell groups, showing high vacuolation. (b and c) Cell structure observed at higher magnification: the chloroplasts (arrows) appear dense and rounded, with no clear areas inside. The nuclei exhibit small dark nucleoli each and some of them Cajal-like bodies (open arrow). Extracellular dark deposits (arrowheads) are observed in contact with the outer face of the cell walls in many cells. (d and e) Iodide-based cytochemistry revealed no presence of starch deposits in the chloroplasts, observed under bright field (d) and phase contrast (e). (f-h) Extracellular deposits of different sizes and shapes (rounded and ellipsoid) are found on the cell walls. Bars in a, b, c, d, e represent 10 μm; bars in f, g, h represent 5 μm.

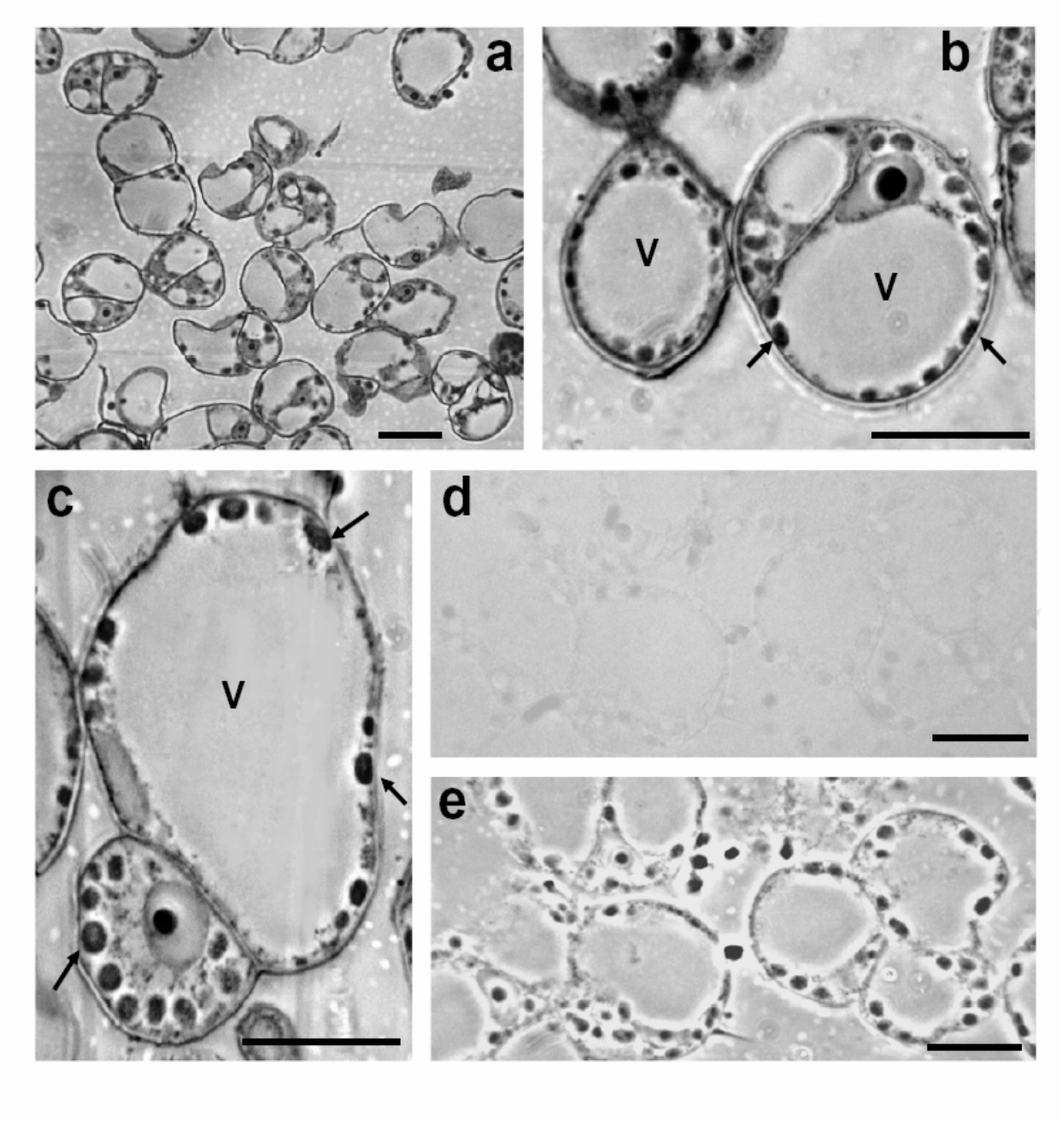

Fig. 4-4. Structural organization of soybean photosynthetic cells of Cu-adapted cultures. Historesin semithin sections after toluidine blue staining (a, b, c), and I_2IK staining for starch (d, e). (a) Panoramic view of the culture, cells appear isolated and in two-cell groups with a cell wall in asymmetric position. (b and c) Higher magnification of the cell organization details: the cytoplasmic vacuole (v) appears very large in most cells, the peripheral layer of cytoplasm is thin and contains rounded and dense chloroplasts (arrows), with no clear areas inside. (d and e) Iodide-based cytochemistry for starch does not provide any contrast under bright field (d) revealing no presence of starch deposits in the chloroplasts which are observed under phase contrast (e). Bars represent 10 μm.

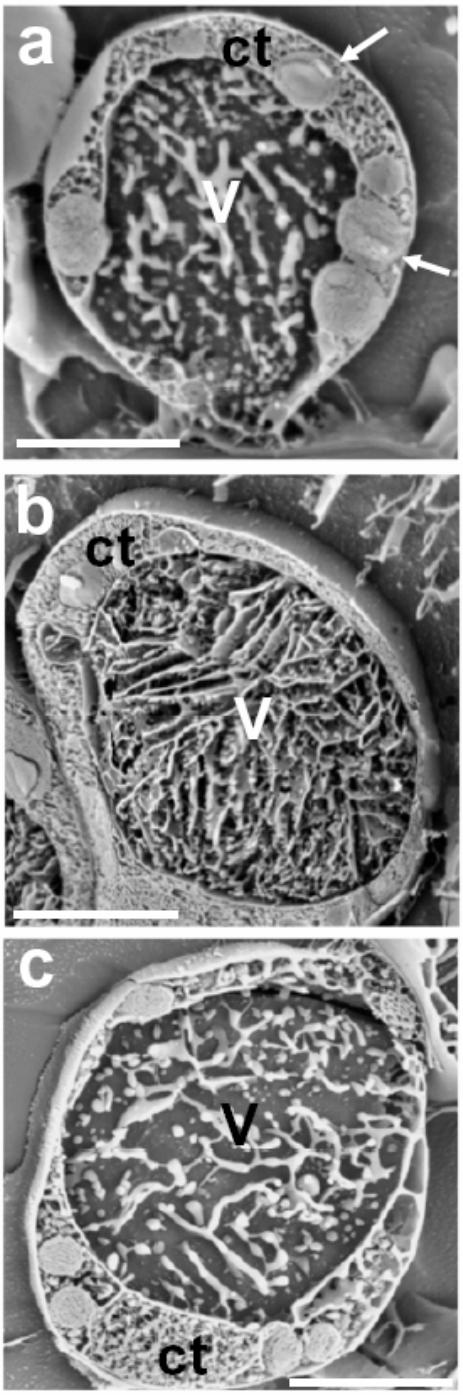

Fig. 4-5. Low Temperature Scanning Electron micrographs of soybean photosynthetic cells of control (a), Cu-stressed (b) and Cu-adapted (c) cultures. Etching of frozen native samples. The aqueous content of the vacuole (v) appears forming a reticulum due to the freezing. In the peripheral layer of cytoplasm (ct) the chloroplasts are observed as spherical structures, in non-treated cultures, most of them contain inner large structures, starch grains (arrows in a). Bars represent 5 μm.

Cells of the three types of *in vitro* cultures studied, with different copper concentrations and times (control, Cu-stressed and Cu-adapted), shared some main structural features and exhibited several differences, which characterized their structural organization. Control cells (Figs. 4-2, 4-5a), Cu-stressed cells (Figs. 4-3, 4-5b) and Cu-adapted cells (Fig. 4-4, 4-5c) showed rounded shape, most of them with a large cytoplasmic vacuole occupying a high proportion (*ca.* 50-60%) of the cellular volume; the rest of the cytoplasm appeared as a thin peripheral layer containing numerous chloroplasts. Cells grown under the three culture conditions assayed were found either isolated or forming spherical structures with two cells; the two-cell structures were divided by a straight cell wall located in a lateral position, probably originated by the asymmetric division of individual isolated cells (Figs. 4-2a, b, f-h; 4-3a; 4-4a, b). The nucleus was observed in a peripheral location exhibiting a patent and circular-shaped nucleolus (Figs. 4-2b, f-h; 4-3b, c; 4-4b, c), and a pattern of chromatin mostly decondensed, with several small patches of heterochromatin in linear arrays along to the nuclear envelope, as clearly seen by DAPI staining (Fig. 4-2c). Nuclear bodies were frequently observed in the cell nuclei of the photosynthetic cultures as small rounded structures of medium contrast in toluidine-blue stained preparations (arrows in Figs. 4-2f, h, and open arrow in Fig. 4-3b). Their size, localization and presence were similar to that of Cajal bodies, ribonucleoprotein structures found in most eukaryotic cells and also described in plants (Risueño and Medina, 1986; Beven et al., 1995). They are typical structures of metabolically-active and proliferating plant cells (Beven et al., 1995; Testillano et al., 2005; Seguí-Simarro et al., 2006). Morphometric analysis revealed a similar cellular size in control, Cu-stressed and Cu-adapted cells, with no statistically significant differences (Table 4-1).

The main differences observed among the cellular types of the three cultures affected chloroplasts, starch granules, vacuoles and extracellular deposits. Chloroplasts of control cells were ellipsoids (Fig. 4-2a, b, f-h) and most of them contained large starch deposits, as revealed by the iodide-based cytochemistry (Fig. 4-2d, e); the starch granules were clearly observed at LTSEM occupying large volumes in the chloroplast (Fig. 4-5a). In contrast, chloroplasts of Cu-stressed and Cu-adapted cells lost the ellipsoidal shape and displayed rounded shape (Figs. 4-3b, c; 4-4b, c; 4-5b, c). The chloroplast size in

these cells was on average 2-fold and 3-fold smaller, respectively, compared with those of control cells (Table 4-1). Moreover, chloroplasts of Cu-adapted cells appeared more numerous with denser structured internal membrane compared with control cells (Fig. 4-4b, c). These observations are in agreement with those previously reported by Bernal et al. (2006) (chapter 3). No starch granules could be found after iodide cytochemistry in control cells (Figs. 4-3d, e; 4-4d, e). The cells of Cu-adapted cultures showed larger cytoplasmic vacuoles than the control cells and Cu-stressed cells, exhibiting a vacuole size 34% larger (Figs. 4-4a-c; 4-5c; Table 4-1). In Cu-stressed cells, numerous dark and small rounded deposits were observed attached at the outer surface of the cell wall (Fig. 4-3a, b, c, f-h). The cells of the other cultures did not show similar extracellular features (Figs. 4-2, 4-4). EDX microanalyses revealed a high copper content in these attached dark deposits (Fig. 4-6B). These measurements also showed that in Cu-stressed cells copper is mainly localized in such deposits whereas copper accumulation was not detected in vacuoles, cytoplasm and chloroplasts. A different feature was observed in Cu-adapted cells where copper content increased in several subcellular compartments such as chloroplast and vacuole (Fig. 4-6C) in comparison with control cells (Fig. 4-6A).

Table 4-1. Morphometric analysis of cell, chloroplast and vacuole size (μm^2) from soybean cell cultures grown in control media, media supplemented with 10 μM $CuSO_4$ during 21 days of growth (Cu-stressed) and after 22 transfers (Cu-adapted).

Cell cultures	Cell	Chloroplast	Vacuole
Control	209.6 ^{a} ± 34.8	7.5 ^{a} ± 1.2	103.8 ^{a} ± 22.2
Cu-stressed	185.4 ^{a} ± 26.2	3.7 ^{b} ± 0.7	111.4 ^{a} ± 17.4
Cu-adapted	220.6 ^{a} ± 38.0	2.3 ^{c} ± 0.5	138.0 ^{b} ± 25.4

^{a,b,c} For the same column, different letters indicate significant differences at $p \leq 0.05$. Data were obtained on average from 15 images for each condition.

Since low molecular weight metal complexes could be organic acid-metal chelates (Kishinami and Widholm, 1987), the levels of citrate and malate were determined in the three types of *in vitro* cultures studied (Table 4-2). In Cu-adapted cells, both citrate and malate content increased to levels 2-3 fold and 3-4 fold higher, respectively, compared with control cells. Interestingly, in Cu-stressed cells citrate increased to levels 3-4 fold those of control cells, level somewhat higher than in Cu-adapted cells.

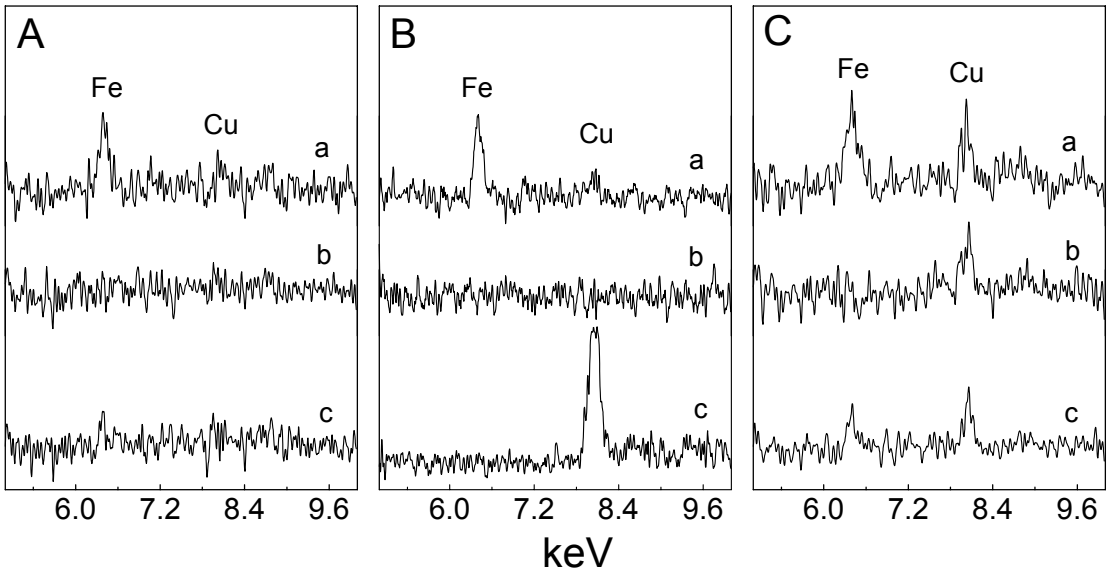

Fig. 4-6. Energy dispersive X-ray spectra of soybean photosynthetic cells of control (A), Cu-stressed (B) and Cu-adapted (C) cultures. (a) chloroplast; (b) vacuole; (c) extracellular dark deposits attached at the cell wall in (B) and cell wall in (A) and (C). Spectra were normalized at titanium peak intensity as internal standard. Typically, 6 cells of each type were analysed. Y-axis scale for B, c was double.

Table 4-2. Organic acid content (μmoles g^{-1} fresh weight) of cells from soybean cell cultures grown in control media, media supplemented with 10 μM $CuSO_4$ during 21 days of growth (Cu-stressed) and after 22 transfers (Cu-adapted).

Cell cultures	Citrate[1]	Malate[1]
Control	$2.4^{a} \pm 0.2$	$0.3^{a} \pm 0.1$
Cu-stressed	$7.6^{b} \pm 0.3$	n.d.
Cu-adapted	$5.9^{c} \pm 0.2$	$1.1^{b} \pm 0.3$

[a,b,c] For the same column, different letters indicate significant differences at $p \leq 0.05$. Data were obtained on average from 15 images for each condition.

4.5. DISCUSSION

In the present work we compare the effect of 10 μM $CuSO_4$ on the functional cellular structure of soybean cell cultures after different copper exposure times. This study provided information about which Cu-induced effects on soybean cell structure accompany a short-term and a long-term response associated to adaptive processes. Cells accumulated high copper concentration when they were grown in medium supplemented with 10 μM $CuSO_4$ with no toxicity symptoms, in agreement with previous results (chapter 3; Bernal et al., 2006). Tolerance to increased concentrations of copper has been induced in the laboratory in several strains of the algae *Scenedesmus* and *Chlrorella* (Küpper et al., 2003). The green algae *Scenedesmus quadricaula* was capable of developing a reversible (i.e. not generally fixed) high resistance to copper. The results reported here show that the general functional cell organization pattern of the control cultures is maintained by the cells after the copper treatments. Moreover, cell features typical of proliferating cells were found not only in the control cultures but also in both short- and long-term treated cultures such as nuclear Cajal-like bodies (Beven et al., 1995, Testillano et al., 2005, Seguí-Simarro et al., 2006) or straight thin cell walls dividing spherical two-cell structures (Satpute et al., 2005). The results also showed that the copper exposure induced changes in specific subcellular structures. The

main target of copper effect was the chloroplast compartment. Indeed, smaller chloroplasts with a rounded shape were observed in soybean cells grown in the presence of 10 μM $CuSO_4$ compared with control ones. This modification was observed either in Cu-stressed or Cu-adapted cells indicating that this event is a fast Cu-induced response in soybean cell cultures. This finding contrasts with certain observations reported in the literature. For instance, no significant alterations in chloroplast size and shape were found in 100 μM Cu-tolerant cultures of *Nicotiana tabacum* (Gori et al., 1998) and mesophyll cells from *Triticum durum* seeds exposed to 10-50 μM Cu (Ciscato et al., 1997; Quartacci et al., 2000). Chloroplasts of seven-week-old *A. thaliana* plants exposed to 50 μM Cu during 2-14 days showed similar size that the control ones but rather circular than ellipsoidal shape (Wójcik and Tukiendorf, 2003). Different chloroplast response has been found by exposure to other metals, *i.e.*, cadmium (Cd) stress increased the chloroplast size in *Myriophyllum spicatum* (Stoyanova and Tchakalova, 1997) and *Raphanus sativus* (radish) (Vitória et al., 2004). Our results also showed that chloroplasts in Cu-adapted cells were more numerous in agreement with Bernal et al (2006) (see chapter 3). This higher chloroplast number could maintain a constant plastid to mesophyll cell volume, which could compensate for the reduced chloroplast size. Recently, it has been reported that *A. thaliana* mutants altered in the accumulation and replication of chloroplasts (*arc* mutants) present reduced chloroplast number and increased plastid size due to a compensatory mechanism (Austin II and Webber, 2005).

After copper exposure, starch accumulation in chloroplasts was especially affected either in Cu-stressed or in Cu-adapted cells. No accumulation of starch was observed in those cells. This finding contrasts with the significant increase in starch observed in seven-week-old *A. thaliana* and cucumber plants exposed to excess copper (100 μM and 20 μg g^{-1}, respectively) (Wójcik and Tukiendorf, 2003; Alaoui-Sossé et al., 2004). Similarly, cadmium or nickel stress was accompanied by an increase in carbohydrate contents in rice seedlings (Moya et al., 1993). Such discrepancies could be due to differences in starch metabolism between plants and cell cultures. The relationship between starch accumulation in leaves and

chloroplasts from stressed plants and inhibition of photosynthesis is well documented (Foyer, 1988; Moya et al., 1993). Starch accumulation may result from a fall in the rate of utilisation of assimilates in the sink organs. Decrease in chlorophyll and sugars, and increase in starch was observed in the medicinal plant *Phyllanthus amarus* exposed to cadmium stress (Rai et al., 2005). On the contrary, the absence of starch accumulation may be attributed to a faster metabolism of assimilates. In this respect, previous results (chapter 3; Bernal et al., 2006) demonstrated that Cu-adapted soybean cell suspensions have a higher growth rate as consequence of additional cell division. Starch consuming could be also required for an enhanced antioxidant activity. It has been reported that induction of glucose-6-phosphate dehydrogenase (G6PDH) could contribute to antioxidant activity by providing more NADPH, which is required for the detoxification of ROS and peroxides (Kuo and Tang, 1998; Ali et al., 2006). In this respect we observed no significantly differences in the ascorbato peroxidase (APX) and total superoxide dismutase (SOD) enzyme activities between Cu-treated and control cells although Cu/ZnSOD activity was stimulated en cells exposed to excess copper (data not shown). On the other hand, the photosynthetic oxygen-evolution activity, which generates ROS and peroxides, was stimulated in Cu.adapted cells in comparison with control cells (chapter 3; Bernal et al., 2006) but it was not the case in Cu-stressed cells. Thus, a clear direct correlation between Cu-induced effect on starch reduction, antioxidant activity and photosynthesis cannot be established in these cell cultures. Interestingly, a correlation between the size of chloroplasts and the content of starch granules could be established. It is worth mentioning that starch accumulation strongly decreased in both Cu-stressed and Cu-adapted cells and this event accompanied the reduction of chloroplast size of those cells. These phenomena were independent of the copper exposure time and they were rather a short-term response than a long-term response as consequence of the excess copper adaptative period. Recently, it has been probed that manipulation of *FtsZ* expression levels, a key structural component of the chloroplast division machinery, can result in a modified size distribution of starch granules (De Parter et al., 2006). Further investigations are necessary to understand starch metabolism in chloroplasts of soybean cells and its relation with chloroplast division structure.

The strategies for avoiding heavy metal toxicity are diverse. A first barrier against copper stress can be the immobilization of copper by means of cell wall and extracellular compounds such as organic acids (citrate and malate), carbohydrates, proteins or peptides enriched in cysteine or hystidil groups. However, the importance of these mechanisms may vary in accordance with the concentration of metal supplied, the plant species involved and the exposure time. Dark deposits attached at the outer surface of the cell wall containing high level of copper were observed in Cu-stressed cells. Similar deposits have been observed in plants grown under metal stress conditions (Vitória et al., 2006). Interestingly, those dark deposits were not observed in Cu-adapted cells indicating that their presence is really a short-term response, which disappears with a longer time exposure. Extracellular chelation by organic acids such as citrate and malate is a mechanism of metal tolerance (Rauser, 1999). The secretion of organic acids is reasonably well stablished as a mechanism for aluminium tolerance (Kochian et al., 2004; Mariano et al., 2005), but there is very little number of studies in support of organic acids mechanism for copper tolerance.

In this work we show that the accumulation of higher levels of citrate and malate takes places in Cu-adapted cells. Similar levels of citrate and malate in Cu- tolerant *Nicotiana plumbaginifolia* cells have been reported (Kishinami and Widholm, 1987). It is worth mentioning that citrate increased in Cu-stressed cells and remained or slightly decreased in Cu-adapted ones. This fact could indicate that citrate synthesis is preferentially stimulated during the first time of copper exposure in these soybean cells, being one of the fastest responses to copper exposure. Two organic acids exudation responses differing in time have been observed in roots of aluminium resistant plants (for review see Mariano et al. 2005). In the former response organic acids release is rapidly activated after aluminium exposure and the rate of release remains constant with time. In this case it has been suggested that aluminium activates a constitutive mechanism of organic acids transport in the plasma membrane and the activation of genes is not necessary. Aluminium can activate anion channels, which have been proposed as the mediators of organic acids transport across the cell membranes. In the second one there is a delay in the organic acids release after the addition of aluminium and this release increases with time. In this case

the activation of genes related to the metabolism and membrane transport of organic acids might be required. According to that, the rapid induction of citrate in Cu-stressed cells might correspond to a mechanism similar to that taking place in the former response. On the other hand, the slower induction of malate observed in Cu-adapted cells might rather correspond to the second mechanism mentioned above. In this point it is clear that further experiments varying time of copper exposure are necessary to define and understand the mechanisms involved in organic acid respond to excess copper in these cells.

Vacuole was also affected by copper treatments. Accumulation of metals in vacuoles is known as a detoxification mechanism to maintain lower metal concentrations in other subcellular compartments (chloroplast, cytoplasm, nucleus). The results showed that the cytoplasmic vacuole area increased in Cu-adapted cells in comparison with control and Cu-stressed ones. This fact can be associated with an accumulation of copper within the vacuole. Indeed, previous results showed a higher level of copper in vacuoles of Cu-adapted cells compared with those control ones (chapter 3; Bernal et al., 2006). Furthermore, the analyses did not reveal the copper accumulation in vacuoles of Cu-stressed cells. Vacuole modifications can be associated to dynamic conversion between lytic and storage functions (Murphy et al., 2005). Our observations could indicate that in the adapted state the detoxification relies on compartmentation through active copper pumping into the vacuole rather than on complexation by ligands, or exclusion by an active efflux or reduced uptake. The results are in agreement with a picture where the first response of soybean cells to excess copper exposure avoids its entrance to the cell by its immobilization in the cell wall, probably through citrate copper chelates among other mechanisms. Then, after an adaptive long-term exposure, the Cu-acclimatation would be mainly due to vacuolar sequestration. Further research is underway to determine whether the copper tolerance developed by the soybean cell cultures is really a stable character. As preliminary result we found that the suppression of excess copper in the growth medium of Cu-adapted cells during four subsequent transfers did not alter the pattern of this cell culture, which was different to that of control one (data not shown).

In summary our results indicate that the functional structural cell modifications, mainly affecting chloroplasts and starch, accompany a short-term Cu-induced response and they are maintained as a stable character during an adaptive period to those conditions, whereas vacuole changes accompany a long-term response.

CAPÍTULO 5

FOLIAR AND ROOT Cu SUPPLY AFFECT DIFFERENTLY Fe AND Zn UPTAKE AND PHOTOSYNTHETIC ACTIVITY IN SOYBEAN PLANTS

5.1. ABSTRACT

A comparative study on the effect of excess copper (Cu) supplied through leaves and root treatments in soybean plants is presented. Although Cu was accumulated in leaves upon both treatments, important differences were observed between Cu treatment of leaves and Cu supplementation in hydroponic medium supplemented with excess Cu. The application of 50 μM $CuSO_4$ on leaves increased chlorophyll content, oxygen evolution activity of thylakoids and fluorescence emission at 685 nm and 695 nm with respect to that at 735 nm compared with control plants. In contrast soybean plants grown in hydroponic medium supplemented with 50 μM $CuSO_4$ exhibited lower chlorophyll content, decreased oxygen evolution activity of thylakoids and decreased fluorescence emission at 685 nm and 695 nm compared with control plants. On the other hand, the elemental analysis of leaves showed differences between the two treatments investigated. The results indicated that no antagonist interaction between Cu- and Fe-uptake took place in leaves from plants where excess Cu was applied on the leaf surface but Cu compete with Fe-uptake in plants grown with excess Cu in the hydroponic medium. Furthermore, differences in Zn-uptake were also observed. Zn content decreased upon Cu treatment of leaves whereas the opposite was observed upon Cu treatment through roots. Interestingly, plants with Cu-treated leaves behaved similarly as cell suspensions grown in the presence of excess Cu. The results strongly indicate that different Cu-uptake and transport strategies are taking place in leaf cells compared with root cells.

5.2. INTRODUCTION

Plants normally take up nutrients from soils and sediments through their roots although nutrients can be also supplied to plants as fertilizers by foliar sprays. In that case nutrients are absorbed through leaves. It is known that accumulation of certain micronutrients in soils can be toxic for plants. In particular, copper (Cu), an essential micronutrient, can be toxic in excess for most plants with the exception of a few plant species that can hyperaccumulate

metals. Accumulation of Cu in soils resulting from the use of fertilizers, the application of pig and poultry slurries rich in Cu, fungicides, atmospheric deposition from industrial and urban activities, metaliferous mining or metal processing inhibibit plant growth and development (Prasad and Strzałka, 1999; Kabata-Pendias and Pendias, 2001). Additionally, leaf uptake of atmospheric heavy metal emission has also been identified as an important pathway of heavy metal contamination in plants (Friedland, 1990; Salim et al., 1992). Plants grown in the presence of high levels of Cu (> 20 $\mu g\ g^{-1}$ dry weight) show reduced biomass and chlorotic symptoms. Cu has capacity to initiate oxidative damage and interfere with important cellular functions such as photosynthesis, pigment synthesis, plasma membrane permeability and other metabolic disturbances that are responsible for a strong inhibition of plant development. Lower chlorophyll (Chl) content, alterations of chloroplast ultrastructure and thylakoid membrane composition and inhibition of photosynthetic activity have been found in leaves in such growth conditions (for reviews see Droppa and Horváth, 1990; Barón et al., 1995; Yruela et al., 2005). On the other hand, it has also been reported that Cu treatments of leaves increase Chl content and photosynthetic activity (Nagler, 1973; Jasiewicz, 1981; Tong et al., 1995). The question arises as whether these different observations found in the literature are due to differences among plants or is the response to a more general phenomenon. Acquisition of heavy metals by plants is a complex phenomenon, which involves several steps. At the root level this process includes metal transport across the plasma membrane of root cells, xylem loading and translocation, detoxification and sequestration of metal at cellular and whole plant levels. In leaves, the metal is absorbed by the epidermis, transported across the plasma membrane of cells and immobilized within the cells.

In the present work we compare the effects of an excess Cu supplementation in the hydroponic medium and a direct Cu-treatment of leaves on micronutrient uptake, plant growth, and photosynthetic activity. Very few comparative studies have been conducted in this respect using the same plant variety. For that we carried out a comparative study using hydroponically grown soybean plants treated with different amounts of Cu supplementation in the growth medium or added to the leaf surface. We also used soybean cell suspensions as confirmatory experiments. The results indicated that the effects

were different depending on which part of the plant was directly exposed to excess Cu.

5.3. MATERIALS AND METHODS

5.3.1. Plant material and copper treatment

Soybean plants (*Glycine max* cv. Volaina) were grown hydroponically in a growth chamber in half-Hoagland nutrient solution (Arnon, 1950) under 200 ± 20 μE m^{-2} s^{-1} from fluorescent and incandescent lamps at 24 ºC, 70% humidity and a 16-h photoperiod. Copper treatment was made by adding to the nutrient solution 10 and 50 μM $CuSO_4 \cdot 5H_2O$. Control medium corresponded to 0.12 μM $CuSO_4 \cdot 5H_2O$. The hydroponic medium was changed once a week. Copper treatment was also done in young leaves by painting once a day every 4 day period during 20 days of growth with 10 and 50 μM $CuSO_4 \cdot 5H_2O$ solutions.

5.3.2. Cell suspension growth conditions

Photosynthetic cell suspensions from soybean (G*lycine max* var. Corsoy) SB-P line were grown as described by Rogers et al. (1987) with some modifications. These cell suspensions were established in our laboratory in 1990. Cell suspensions were grown photomixotrophically in liquid cultures under continuous low light (30 ± 5 μE m^{-2} s^{-1}) (Bernal et al., 2006). To assay the Cu effect on cell growth the media were supplemented with 10 and 20 μM $CuSO_4 \cdot 5H_2O$. The control medium corresponded to 0.1 μM $CuSO_4 \cdot 5H_2O$. Cell suspensions were grown under an atmosphere with 5% CO_2 at 24 ºC on a rotatory shaker (TEQ, model OSFT-LS-R) at 110 rpm in 125 ml flasks filled up to 50 ml and illuminated with cool-white fluorescent lamps (Alfonso et al., 1996; Bernal et al., 2006). Cells used for physiological and biochemical experiments were collected from cultures after 18-21 days of growth.

5.3.3. Isolation of thylakoid membranes

Soybean leaves from 23-day-old plants were collected, washed twice with 2 mM EDTA solution and once with destilled H_2O, and cut into pieces. The

leaf pieces were ground in buffer containing 400 mM NaCl, 2 mM $MgCl_2$, 0.2% (w/v) bovine serum albumen (BSA), 40 mM ascorbate, and 20 mM Tricine, pH 8.0 at a leaves to buffer ratio of 1:2 (w/v). The mixture was filtered through a layer of Miracloth (Calbiochem) and centrifuged at 300 x g for 2 min. The supernatant was centrifuged at 13,000 x g for 10 min and the resultant sediment resuspended in buffer containing 150 mM NaCl, 5 mM $MgCl_2$**,** and 20 mM Tricine, pH 8.0 and centrifuged at 13,000 x g for 10 min. The pellet (thylakoids) was resuspended in buffer containing 400 mM sucrose, 15 mM NaCl, 5 mM $MgCl_2$, and 50 mM 2-(N-morpholino)ethanesulfonic acid (MES)-NaOH, pH 6.0 and the supernatant fractions were concentrated.

Soybean cells from 18-day-old cultures were collected, filtered through a layer of Miracloth and weighted. Cells were then resuspended in buffer containing 400 mM NaCl, 2 mM $MgCl_2$, 0.2% (w/v) sucrose*,* and 20 mM Tricine, pH 8.0 at a cell to buffer ratio of 1:2 (w/v), and broken with a teflon homogeneizer during 10 min with 2 min delay every 2 min homogeneization to avoid sample heating at 4 ºC in darkness. Broken cells were gently stirred for 10 min and centrifuged at 300 x g for 2 min. The following steps were the same as described for soybean leaves.

The supernatants were concentrated in Centripep-10 tubes (Amicon). The thylakoid fraction was frozen in liquid nitrogen and stored at -80 ºC. Chlorophyll determination was done as described by Arnon (1949).

5.3.4. Oxygen evolution activity

Oxygen evolution activity was measured with a Clark-type oxygen electrode at 23 ºC. The light intensity on the surface of the cuvette was 3,000 $\mu E\ m^{-2}\ s^{-1}$. Thylakoids (10 μg Chl ml^{-1}) were diluted in 3 ml buffer containing 10 mM NaCl, 300 mM sucrose, and 25 mM MES-NaOH, pH 6.5. Thylakoid activities were measured in the presence of 0.5 mM 2,6-dichlorobenzoquinone (DCBQ) as artificial electron acceptor. DCBQ was dissolved in ethanol.

5.3.5. Determination of micronutrient elements

Cells from 20-day-old suspensions and leaves from 23-day-old plants were washed twice with 3 mM EDTA and once with destilled H_2O to remove

free cations. After washing, cells were filtered through a layer of Miracloth and dried in a ventilated oven at 60 ºC for 48 h. Dried samples were treated using a standard procedure (Abadía et al., 1985). Analyses were performed in an atomic absorption spectrometer (UNICAN 969).

5.3.6. Fluorescence measurements

Thylakoid membranes were resuspended in 400 mM sucrose, 20 mM NaCl, 5 mM $MgCl_2$, and 50 mM MES-NaOH, pH 6.0, placed in a 3-mm quartz tube and frozen in liquid nitrogen. Fluorescence spectra were obtained at 77 K by exciting the samples with a 1,000 W ORIEL 66187 tungsten halogen lamp and a double 0.22 m SPEX 1680B monochromator. Excitation was carried out at 470 nm. Fluorescence was detected through a 0.5 JARREL-ASH monochromator with a Hamamatsu R928 photomultiplier tube. All the measurements were corrected from the system response. The spectral linewidths (FWHM) for the excitation and the emission were 3.6 nm and 1.92 nm, respectively.

5.4. RESULTS

5.4.1. Effect of Cu treatments on soybean plants

Soybean whole plants were exposed to excess Cu (10 μM and 50 μM $CuSO_4 \cdot 5\ H_2O$) during the growth at two levels: i) Cu was applied directly on leaves; ii) Cu was added to the hydroponic medium (for more details see Materials and Methods). Plants had different behaviour upon these two treatments. Plants with Cu-treated leaves showed similar growth development, even with 50 μM Cu(II) (Fig. 5-1). All plants reached similar biomass after a month of growth. A different pattern was observed in plants treated by supplementing the growth medium with excess Cu. In this case a 80% reduction of biomass was observed upon supplementation the hydroponic medium with 50 μM Cu(II) and a strong inhibition of the root development took place (Fig. 5-1, inset).

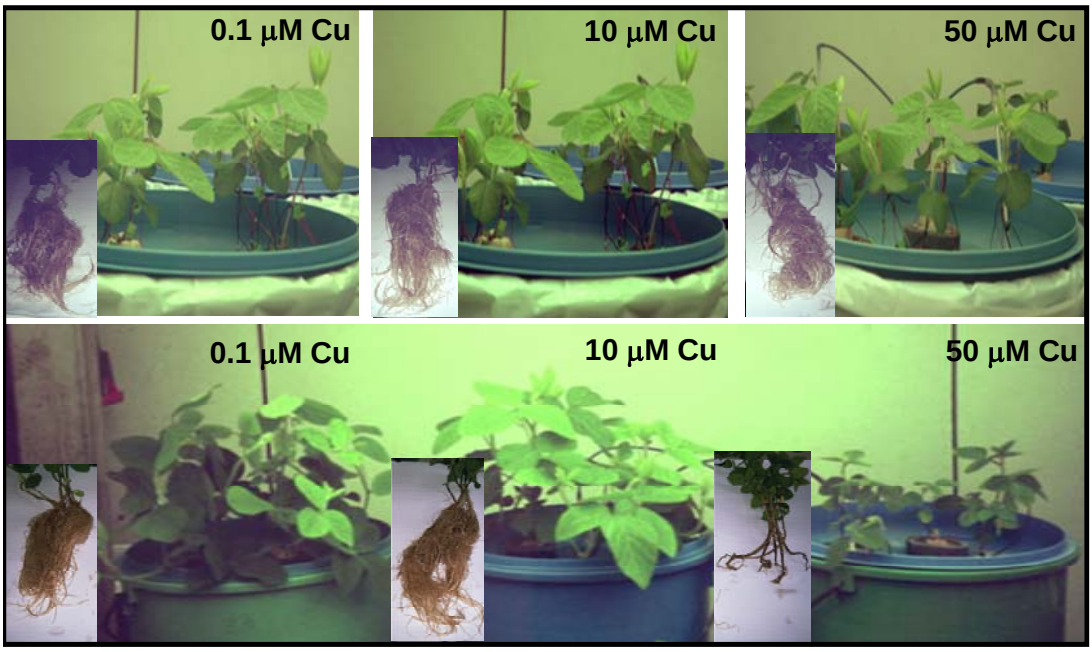

Fig. 5-1. Effect of excess Cu on soybean plants. Plants were treated with Cu at two levels: (a) young leaves were painted once every four day period with 10 μM and 50 μM $CuSO_4$ solutions (upper panel); (b) hydroponic medium was supplemented with 10 μM and 50 μM $CuSO_4$ (lower panel). Leaves were collected after a month of growth. For more details see Materials and Methods.

The results showed that Cu-treatment of leaves caused a Chl content increased by 35% and 60% upon 10 μM and 50 μM Cu-treatment, respectively. A 10% and 23% stimulation of the oxygen evolution activity in thylakoids isolated from those leaves was found upon 10 μM and 50 μM Cu-treatment, respectively (Table 5-1). On the other hand, fluorescence spectra at 77K with 470 nm excitation showed that F_{735}/F_{685} and F_{735}/F_{695} ratios decreased in thylakoids from Cu-treated leaves (Fig. 5-2, Table 5-1). Fluoresence spectra at 77K an often used to monitor ultraestructural changes in thylakoid membranes as a response to environmental condition variations. Thus F_{735}/F_{685} and F_{735}/F_{695} ratios can be used as a probe for the amount of antenna Chls connected to each photosystem (Van Dorssen et al., 1987; Alfonso et al., 1994). The antenna Chls of photosystem I emit maximum fluorescence at 735 nm whereas those of LHCII surrounding PSII emit at 685 nm. CP43 antenna complex and PSII reaction center complexes also contribute to 685 nm fluorescence maximum, and the band at 695 nm is associated to CP47 antenna complex. Different effects were observed in plants grown in hydroponic medium

supplemented with the same excess Cu. Plants exposed to 50 μM $CuSO_4$ in the hydroponic medium exhibited: *i)* a 2 fold Chl content reduction; *ii)* about 18% oxygen evolution activity decrease in thylakoids isolated from those plants; *iii)* F_{735}/F_{685} and F_{735}/F_{695} ratios increase.

Table 5-1. Photosynthetic parameters of thylakoids from soybean plant leaves and soybean cell suspensions[1].

Samples	Chlorophyll (mg g^{-1} dry weight)	Oxygen evolution (μmol O_2 mg^{-1} Chl h^{-1})	Chl *a*/Chl *b*	F_{735}/F_{685}	F_{735}/F_{695}
Soybean plant leaves					
Leaves treatment					
Control	4.6 ± 1.3	238 ± 12	3.5 ± 0.1	4.7 ± 0.2	4.8 ± 0.1
10 μM Cu(II)	6.3 ± 1.3	252 ± 15	3.5 ± 0.1	4.1 ± 0.1	4.2 ± 0.2
50 μM Cu(II)	7.5 ± 1.3	285 ± 12	3.5 ± 0.1	3.9 ± 0.0	3.8 ± 0.1
Hydroponic treatment					
Control	4.4 ± 1.3	242 ± 12	3.4 ± 0.1	4.4 ± 0.1	4.8 ± 0.1
10 μM Cu(II)	3.8 ± 0.3	220 ± 4	3.4 ± 0.1	5.4 ± 0.1	5.5 ± 0.2
50 μM Cu(II)	2.1 ± 0.1	197 ± 8	3.2 ± 0.1	5.6 ± 0.2	5.9 ± 0.1
Soybean cell suspension					
Control	3.16 ± 0.5	189 ± 7	3.1 ± 0.1	3.1 ± 0.1	3.0 ± 0.1
10 μM Cu(II)	3.90 ± 0.6	245 ± 11	3.1 ± 0.1	2.4 ± 0.1	2.5 ± 0.1
20 μM Cu(II)	3.96 ± 1.1	250 ± 14	3.1 ± 0.1	2.3 ± 0.1	2.4 ± 0.1

[1]Soybean plants were treated with excess Cu at two levels, a) young leaves were painted once a day every four day during the growth period with 10 μM and 50 μM $CuSO_4$ solutions; b) hydroponic medium was supplemented with 10 μM and 50 μM $CuSO_4$; media were changed weekly. Leaves were collected after a month of growth. Soybean cell cultures were grown in media supplemented with 10 μM and 20 μM $CuSO_4$. Cells were analysed after 21 days of growth. Data were obtained from three independent experiments. Values represent means ± SE (n=3).

5.4.2. Effect of Cu treatments on soybean cell suspensions

The influence of 10 μM and 20 μM $CuSO_4 \cdot 5\ H_2O$ on soybean photosynthetic cell suspension was investigated. Addition of excess Cu to the control media that already contained a sufficient amount of Cu for culture growth did not reduce cell growth rate under control light illumination regime (65 ± 5 μE m^{-2} s^{-1}) but indeed stimulated growth at limiting light conditions (30 ± 5

μE m^{-2} s^{-1}) being the doubling time of about 4-5 days compared to 8-9 days of control suspensions (chapter 3; Bernal et al., 2006). Soybean Cu-treated cells exposed to 10 μM and 20 μM $CuSO_4 \cdot 5H_2O$ in the medium after 20 days exhibited: *i)* about 23% Chl content increase; *ii)* about 25% oxygen evolution activity increase in thylakoids isolated from those cells; *iii)* F_{735}/F_{685} and F_{735}/F_{695} ratios decrease (Table 5-1, Fig. 5-2). It is worth mentioning that these parameters showed the same variation trend as in plants with Cu-treated leaves. Cu concentration of 20 μM was used instead that of 50 μM because soybean cells exposed to 50 μM Cu(II) did not show such growth stimulation (chapter 3; Bernal et al., 2006)

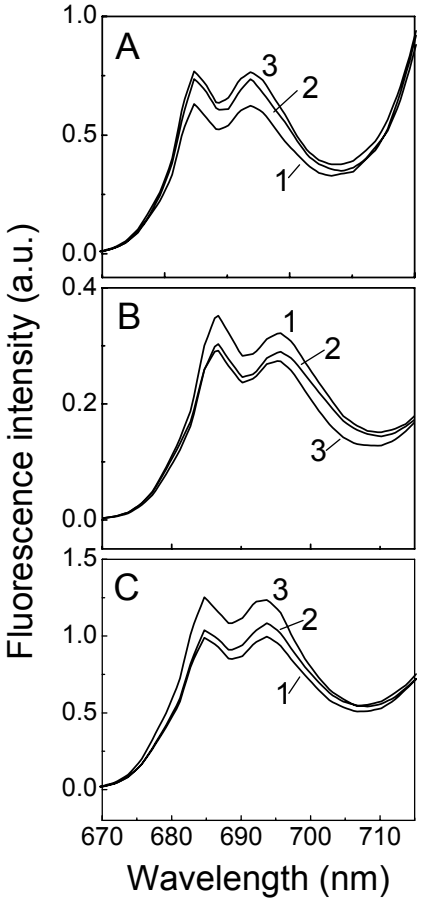

Fig. 5-2. Fluorescence emission spectra at 77K of thylakoid membranes from (A) leaves treated with Cu; (B) soybean plants grown in hydroponic medium supplemented with Cu; (C) Cu-treated soybean cells. (1) Control; (2) 10 μM $CuSO_4$; (3) 20 μM (C) or 50 μM $CuSO_4$ (A, B). Excitation wavelength was at 470 nm (for more details see Materials and Methods). Spectra were normalized at 739 nm (PSI emission band).

5.4.3. Cu-uptake and its effect on other micronutrients

Different elemental composition of leaves was found in Cu-treated leaves and plants grown in hydroponic medium supplemented with excess Cu. Although leaves from plants treated with 10 μM and 50 μM Cu(II) by either leaf treatment or hydroponic medium accumulated on average 2-3 fold higher Cu concentration when compared with control plants they differed in Fe and Zn content (Table 5-2). We found that Fe- and Zn-uptake was affected in the same and opposite direction, respectively. In plants with 50 μM Cu-treated leaves the concentration of Fe increased on average 1.4 fold whereas Zn content was on average 1.2 fold lower. The opposite was observed in plants grown in hydroponic medium supplemented with 50 μM $CuSO_4$ where the concentration of Fe decreased on average 2.5 fold whereas Zn content was on average 1.2 fold higher compared with the control. These elemental content variations are in the same order of magnitude than those found as consequence of Fe deficiency or Cu treatments in whole plants (Pätsikkä et al., 2002; Chen et al., 2004; Rombolà, et al., 2005).

Interestingly, the same trend as in plants with Cu-treated leaves was found in soybean cell suspensions. In cells grown in medium supplemented with 50 μM $CuSO_4$ the accumulation of Cu was accompanied by on the average 1.4 fold Fe increase whereas Zn content was on the average 2.0 fold lower than the control.

Table 5-2. Micronutrient content ($\mu g\ g^{-1}$ dry weight) in plant leaves and cell suspensions[1].

Samples	Cu	Fe	Zn
Soybean plant leaves			
Control	6.8 ± 1.8	90.2 ± 1.3	90.8 ± 1.3
Foliar treatment			
10 µM Cu(II)	11.5 ± 1.3	100.7 ± 1.2	85.1 ± 1.3
50 µM Cu(II)	13.5 ± 2.3	126.8 ± 4.3	77.7 ± 3.3
Hydroponic treatment			
50 µM Cu(II)	23.1 ± 2.3	38.2 ± 1.7	105.6 ± 2.4
Soybean cell suspensions			
Control	5.9 ± 1.6	282.2 ± 7.0	351.1 ± 8.3
10 M µCu(II)	209.5 ± 5.3	328.1 ± 4.3	161.3 ± 4.3
20 M µCu(II)	351.2 ± 7.5	389.8 ± 3.9	174.3 ± 3.2

[1]Soybean plants were treated with excess Cu at two levels, a) young leaves were painted once a day every four day during the growth period with 10 μM and 50 μM $CuSO_4$ solutions; b) hydroponic medium was supplemented with 10 μM and 50 μM $CuSO_4$; media were changed weekly. Leaves were collected after a month of growth. Soybean cell cultures were grown in media supplemented with 10 μM and 20 μM $CuSO_4$. Cells were analysed after 21 days of growth. Data were obtained from three independent experiments. Values represent means ± SE (n=3).

5.5. DISCUSSION

The results presented in this paper demonstrate that toxic concentrations of Cu can affect plants differently depending on what part of the plant is directly exposed to the element. In that sense, we observed that soybean plants behaved differently depending whether Cu supplementation was done through leaves or roots. Thus, soybean plants treated with the 50 µM Cu through roots were susceptible to reduce their biomass and exhibited decreased Chl content in leaves as well as lower oxygen evolution activity in thylakoids obtained from those leaves. A higher fluorescence emission at 685 nm and 695 nm respect to that at 735 nm was also observed compared with control plants. These findings

are in agreement with data reported in the literature where micromolar concentrations of Cu(II) in the range of 10 to 50 μM in the growth medium decreased the growth and inhibited the photosynthetic activity (Barón et al., 1995; Yruela et al., 2005). In the second case, no apparent changes in plant growth were observed and an increase of Chl content in leaves, a higher oxygen evolution activity in thylakoids and lower fluorescence emission at 685 nm and 695 nm compared with control plants were found. The results showed that the Cu-leaf treatment stimulates the Chl synthesis and the photosynthetic activity. This behaviour contrasts with that normally observed in other photosynthetic organisms such as algae and plants exposed to excess Cu (Franklin et al., 2002; Pätsikkä et al., 2002).

Our results clearly indicate that plants treated with excess Cu through leaves plants behave differently than plants by supplementing the growth medium with excess Cu. The different plant response observed upon these two Cu-treatments might be rationalized assuming different Cu-uptake strategies in leaf and root cells. Differences in Cu transport among, cyanobacteria, algae and whole plants have also been found (La Fontaine et al., 2002). Interstingly, Cu accumulation was accompanied by Fe increase and Zn decrease in leaves treated with Cu plants but the opposite was observed in leaves of plants treated by supplementing the growth medium with excess Cu. Interestingly, Cu accumulation induced a Fe-uptake increase and a Zn-uptake decrease in our soybean cell suspensions, similarly to that observed in plants with leaves treated with excess Cu.

Cation homeostasis is a very complex process. In plants relatively little is known about Cu transport into and within cells showing a dependence on Cu for Fe assimilation (for reviews see Fox and Guerinot 1998; Himelblau and Amasino, 2000). It was found that Cu and Fe compete in ion-uptake (Schmidt, 1999). Pätsikkä et al. (2002) observed that excess Cu in hydroponic medium induced a Fe-deficiency in bean plants. Chen et al. (2004) observed that Fe-deficiency induces Cu accumulation in *Commelina communis* plants. Furthermore, Rombolà et al. (2005) found that Fe-deficiency increased the Cu content and decrease the Zn content in leaf blades of sugar beet grown hydroponically. However, other organisms such as mammal cells, yeast or certain algae do not appear to manifest such a competition showing a

dependence on Cu for Fe assimilation (Franklin et al., 2002). A copper dependent iron assimilation pathway has been found in the unicellular green alga *Chlamydomonas reinhardtii* (La Fontaine et al., 2002). Additionally, an antagonist interaction between Cu and Zn was also observed in this alga (Herbik et al., 2002). The same scenario seems to appear in our soybean cell suspensions (Bernal et al., 2006; chapter 3). Thus, all the above considerations indicate that Cu-uptake strategies differ in root compared with leaf cells.

CAPÍTULO 6

IDENTIFICATION AND SUBCELLULAR LOCALIZATION OF THE SOYBEAN COPPER P_{1B}-ATPase *Gm*HMA8 TRANSPORTER

6.1. ABSTRACT

We have identified a copper P_{1B}-ATPase transporter in soybean (*Glycine max*), named as *Gm*HMA8, homologue to cyanobacterial PacS and *A. thaliana At*HMA8 (PAA2) transporters. A novel specific polyclonal anti-*Gm*HMA8 antibody raised against a synthetic peptide reacted with a protein of an apparent mass of around 180-200 kDa in chloroplast and thylakoid membrane preparations isolated from soybean cell suspensions. Immunoblot analysis with this antibody also showed a band with similar apparent molecular mass in chloroplasts from *Lotus corniculatus.* Immunofluorescence labelling with the anti-*Gm*HMA8 antibody and double immunofluorescence labelling with anti-*Gm*HMA8 and anti-RuBisCo antibodies revealed the localization of the *Gm*HMA8 transporter within the chloroplast organelle. Furthermore, the precise ultrastructural distribution of *Gm*HMA8 within the chloroplast subcompartments was demonstrated by using electron microscopy immunogold labelling. The *Gm*HMA8 copper transporter from soybean was localized in the thylakoid membranes showing a heterogeneous distribution in small clusters.

6.2. INTRODUCTION

Copper is an essential cofactor for enzymes required for a wide variety of biological processes in plants including redox reactions in photosynthetic electron transfer and detoxification of superoxide radicals. Nevertheless, copper can also be toxic at supraoptimal concentrations. Consequently, plants like other organisms have evolved a complex homeostasis network of metal trafficking pathways to: *i)* take up and distribute metals throughout the entire organism; *ii)* prevent high cytoplasmic concentrations of free heavy metal ions (Fox and Guerinot, 1998; Williams et al., 2000; Clemens, 2001; Hall and Williams, 2003; Krämer and Clemens, 2006). Membrane transport proteins play important roles in these processes and key roles have been identified for P_{1B}-ATPases, also known as CPx-ATPases (Solioz and Vulpe, 1996), metal P-type ATPases (Rensing et al., 1999) and heavy metal ATPase (HMAs) (Axelsen and Palmgren, 2001). These proteins transport transition metals such as copper,

zinc, cadmium, lead and cobalt across membranes. These transporters have been classified into six sub-groups (P_{1B1}-P_{1B6}) by analysing their amino acid sequences and topological arrangements, and combining this with their metal specificity (Axelsen and Palmgren, 1998; Argüello, 2003). Structurally, they are different from other P-ATPases and possess eight transmembrane regions, with a large cytoplasmic loop between transmembranes helices 6 and 7, a CPx/SPC motif, which is essential for metal transport, and putative heavy metal-binding domains at the N- and/or C-termini. The Arabidopsis genome encodes eight predicted P_{1B}-ATPases (*At*HMA1-*At*HMA8, http://mips.gsf.de) that differ in their structure, function and regulation but all of them are specialized in specific metal ion transport to cellular compartments and target proteins (for review see Williams and Mills, 2005). In particular *At*HMA1, *At*HMA6 (PAA1), *At*HMA7 (RAN1), and *At*HMA8 (PAA2) P_{1B}-ATPases are involved in copper transport to different cellular compartments (Hirayama et al., 1999; Woeste and Kieber, 2000; Shikanai et al., 2003; Abdel-Gahny et al., 2005b; Seigneurin-Berny et al., 2006). On the other hand, *At*HMA2-4 and *At*HMA5 P_{1B}-ATPases have roles in nutrition and metal detoxification, and are involved in zinc, cadmium and/or lead (Mills et al., 2003; 2005; Eren and Argüello, 2004; Gravot et al., 2004; Verret et al., 2004; 2005) and copper (Andrés-Colás et al., 2006) transport, respectively.

Understanding of chloroplast copper homeostasis is of particular interest because this metal is required for proteins, such as Cu/Zn superoxide dismutases (Cu/ZnSODs), polyphenol oxidase, and plastocyanin functioning in the stroma and thylakoid lumen, respectively. Since plastocyanin is targeted to the lumen compartment as apoprotein, a mechanism by which copper crosses the thylakoid membrane has to exist (Merchant and Dreyfuss, 1998). In cyanobacteria, the ancestor of chloroplasts, two Cu-transporting P-type ATPases, PacS and CtaA, were found in thylakoid and cytoplasmatic membranes, respectively (Kanamaru et al., 1994; Phung et al., 1994; Tottey et al., 2001). These proteins are required for copper transport to plastocyanin in the thylakoid lumen. At present, studies at a molecular level of copper homeostasis in plant chloroplasts are very limited and most of them are restricted to *A. thaliana.* Recently, two Cu-ATPases, PAA1 (*At*HMA6) and PAA2 (*At*HMA8), homologues to CtaA and PacS, have been identified in *A. thaliana* (Shikanai et al., 2003; Abdel-Gahny et al., 2005b). The authors proposed their

participation in copper transport across the chloroplast envelope and the thylakoid membrane, respectively. More recently, Seigneurin-Berny et al. (2006) have shown that the copper transporter *At*HMA1 is localized in the chloroplast envelope. The present work reports the identification of *Gm*HMA8, a copper P_{1B}-ATPase of soybean related to *At*HMA8 (PAA2), and its subcellular localization in the chloroplasts and more specifically in the thylakoid membranes. Results are discussed in terms of the possible transporter organization within the membrane.

6.3. MATERIALS AND METHODS

6.3.1. "*In silico*" sequence analysis of plant P_{1B}-ATPases

Search of the databases was done with BLAST programme (Altschul and Lipman, 1990) using previously identified PacS (sll1920) and CtaA (slr1950) sequences from *Synechocystis* PCC 6803. Alignments were done using ClustalW (Thompson et al., 1994) and theoretical subcellular location was predicted using with TargetIP and ChloroP programs (Emanuelsson et al., 1999). The complete gene sequence of *HMA8* from *Lotus corniculatus* var. *japonicus* genomic DNA (AP006090) was obtained with GenScan Web Server (Burge and Karlin, 1997). The location of possible transmembrane domains was determined using the programme ARAMEMNON at http://aramemnon.botanik.uni-koelm.de/ (Schwacke et al., 2003).

6.3.2. Cell suspension growth conditions

Photosynthetic cell suspensions from soybean (G*lycine max* var. Corsoy) SB-P line were grown as described by Rogers et al. (1987) with some modifications (Alfonso et al., 1996; Bernal et al., 2006). Liquid cultures were grown in photomixotrophic medium under continuous light (30 ± 5 µE m^{-2} s^{-1}) and atmosphere with 5% CO_2 at 24 ºC on a rotatory shaker (TEQ, model OSFT-LS-R) at 110 rpm. For immunolocalization experiments, soybean cells were grown on 1.5% (w/v) agar plates with KN^1 medium at 24 ºC and atmosphere with 5% CO_2. Cells cultured in these conditions were easier to handle during the fixation and sectioning procedures than liquid suspensions.

6.3.3. RNA isolation and cDNA synthesis

Cells (0.4 – 0.8 g wet weight) were washed with fresh KN[1] medium and pestled in liquid nitrogen. Then, a mixture of phenol:extraction buffer (0.1 M LiCl, 10 mM EDTA, 1% (w/v) SDS, 0.1 M Tris-HCl, pH 8.0) (1:1 v/v) was added to the powder (1.5 mL per 0.1 g of cells) and vortexed vigorously. Samples were centrifuged at 1,500 × g for 10 min at 4 ºC. The aqueous phase was washed first with an equal volume of phenol:chloroform (1:1 v/v) followed by an additional wash with an equal volume of chloroform:isoamyl alcohol (24:1). The RNA was then precipitated overnight at 8 ^{o}C with an equal volume of 4 M LiCl, centrifuged at 15,500 × g for 30 min at 4 ºC and then washed with cold 80% (v/v) ethanol. RNA was dried out with nitrogen and resuspended in sterile H_2O containing 1% (v/v) DEPC. The RNA concentration was determined by measuring the OD_{260nm}. cDNAs were synthetized from total RNA (5 μg) using 200 units of reverse transcriptase (M-MLV reverse trancriptase, Promega, Madison, WI, USA) and 1 μM oligo$(dT)_{12-18}$ from Invitrogen (Invitrogen Life Technologies, Carlsbad, CA, USA), according to the manufacturer's instructions. Total RNA for the 5'-RACE amplification was isolated and purified from soybean cells using a RNeasy Plant Mini Kit (Qiagen GmbH, Hiden, Germany). cDNA was synthetized at 54 ºC from total RNA (3 μg) using a *GmHMA8* specific-primer (2 pmol, GSP1) and 200 units of thermoscript reverse transcriptase (Invitrogen Life Technologies, Carlsbad, CA, USA) with the GeneRacer Kit (Invitrogen Life Technologies, Carlsbad, CA, USA) according to the manufacturer's instructions.

6.3.4. Isolation of *GmHMA8* sequence

The full-length *GmHMA8* cDNA was obtained by RT-PCR. Degenerated oligonucleotides, which could be used as primers for RT-PCR amplification, were designed from *in silico* sequence data analysis. The 24-mer oligonucleotides designed corresponded to the sequences of the phosphorylation domain FDKTGT(L/I)T (forward-ATPase) and hinge region GIND(S/A)P(S/A)L (reverse-ATPase) (Table 6-1) both located in the large cytoplasmatic loop of P_{1B}-ATPases. The *GmHMA8 3'*-end (including part of 3'-UTR) was obtained using a pair of primers designed the forward one from the

identified *GmHMA8* partial sequence (GmHMA8-1) and the reverse one designed from a GmHMA8 EST (UTRGmHMA8) (TC228758, TIGR Soybean Gene Index). The *GmHMA8* 5´-end (including part of 5'-UTR) was obtained using the GeneRacer Kit (Invitrogen Life Technologies, Carlsbad, CA, USA). The primary PCR was performed using an adaptator primer (GeneRacer 5' Primer) and a *GmHMA8* specific-primer (GSP2) followed by a nested PCR with a nested adaptator primer (GeneRacer 5' Nested Primer) and a nested *GmHMA8* specific-primer (GSP3) (Table 6-1). The PCR products were cloned into the pGEM-T Easy vector (Promega, Madison, WI, USA) and sequenced (CNIO service, Madrid, Spain) to check their identity.

Table 6-1. Primers used for the isolation of *GmHMA8*

Primer name	Forward/ Reverse	Primer sequence (5' → 3')
P-ATPase	forward	TT(TC)GA(TC)AA(AG)AC(TCA)GG(TCAG)AC(TCA)(TC)T(TCAG)AC(TCA)
	reverse	(GTCA)A(AG)(AGT)GC(AGT)GG(AGT)G(AG)TC(AG)TT(AT)AT(TCAG)CC'
UTRGmHMA8	reverse	CATGCTAGGATACTTCATGAGA
GmHMA8-1	forward	5'-GCTGAGTCATTAGAGTTGG
GSP1	reverse	ACCAATGATGCCTTCTCCTTCACG
GSP2	reverse	AGTTTCTGAATACTTTGAAGATGT
GSP3	reverse	GCACGCGCCGCACATCATCCC
5' GeneRacer primer	forward	CGACTGGAGCACGAGGACACTGA'
5' GeneRacer nested primer	forward	GGACACTGACATGGACTGAAGGAGTA'
UTRGmHMA8	reverse	CATGCTAGGATACTTCATGAGA

6.3.5. Isolation of intact chloroplasts and thylakoid membranes

Soybean cells from 18-day-old cultures were collected (3-4 g wet weight) and filtered through a layer of Miracloth (Calbiochem, EMD Biosciences Inc, San Diego, CA, USA). Cells were then resuspended in buffer containing 400 mM NaCl, 2 mM $MgCl_2$, 0.2% (w/v) sucrose, and 20 mM Tricine, pH 8.0 at a cell to buffer ratio of 1:2 (w/v) and broken with a teflon homogeneizer during 10 min with appropriate stops to avoid sample heating. Broken cells were gently stirred

for 10 min and centrifuged at 300 x g for 2 min. Intact chloroplasts and thylakoid membrane isolation were done as described in van Wijck et al. (1995) and Bernal et al. (2006), respectively. All procedures were carried out at 4 ºC under dim light. Chlorophyll determination was done as described by Arnon (1949). Protein determination was done as described by Bradford (1976).

6.3.6. GmHMA8 antibody production

The rabbit polyclonal antibody anti-*Gm*HMA8 was produced from a 15 amino acid synthetic peptide designed from the identified partial sequence of *Gm*HMA8 (Genosphere Biotechnologies, Paris, France). The selected peptide sequence was HERFQTRANPSDLTN, located within the putative large cytoplasmatic loop of *Gm*HMA8 (DQ418731).

6.3.7. Immunoblotting analysis

The electrophoretic separation of chloroplast and thylakoid proteins was performed by SDS-PAGE according to Laemmli (1970) using 15% and 12% (w/v) acrylamide gels containing 6 M urea as described in Bernal et al. (2006) with some modifications. Gels were electroblotted to a PVDF membrane with a BioRad transfer system and the immunodetection was done using the rabbit polyclonal antibody against *Gm*HMA8 described above. A goat anti-rabbit IgG coupled to horseradish peroxidase was used as a secondary antibody. Bands were revealed by the peroxidase method.

6.3.8. Sample processing for microscopical structural analysis and immunofluorescence

Soybean cells were fixed overnight at 4 ºC in formaldehyde 4% (w/v) in phosphate buffered saline solution (PBS), pH 7.3, and washed with PBS. Some samples were stored at 4 ºC for direct sectioning in a vibratome and further use for immunofluorescence. Other samples were dehydrated through an acetone series [30%, 50%, 70% and 100% (v/v)], infiltrated and embedded in Historesin 8100 at 4 ºC. Semithin sections (1 µm thickness) were obtained and used for light microscopy observations. Toluidine-blue stained semithin sections were

observed under bright and phase contrast field for structural analysis in a Leitz microscope fitted with a digital camera Olympus DP10.

6.3.9. Cytochemical stainings for starch and DNA

Starch was detected by I_2KI staining (O'Brien and McCully, 1981) on Historesin semithin sections and observed under bright field (Barany et al., 2005). DAPI staining for DNA was applied to semithin sections (Testillano et al., 1995) and observed under UV light in a Zeiss Axiophot epifluorescence microscope fitted with a CCD camera.

6.3.10. Immunofluorescence and Confocal Laser Microscopy

Immunofluorescence was performed on vibratome sections as previously described (Fortes et al., 2004). Vibratome sections of 30 µm (Vibratome1000, Formely Lancer) obtained from fixed soybean cells (see above) were placed onto 3-aminopropyltrietoxysilane coated slices and treated for permeabilization purposes. First, they were dehydrated [30%, 50%, 70%, 100% (v/v)] and rehydrated [100%, 70%, 50%, 30% (v/v)] in PBS:methanol series. Second, sections were treated with 2% (w/v) cellulase (Onozuka R-10) in PBS for 40 min at room temperature. After three washing in PBS for 5 min, sections were treated with 0.5% (v/v) Triton X-100 in PBS for 20 min and washed with PBS for 5 min. Subsequently, sections were incubated with 5% (w/v) bovine serum albumine (BSA) in PBS for 5 min and then in either anti-*Gm*HMA8 or anti-RuBisCo (large subunit, kindly provided by Dr. R.T. Besford from Horticultural Research International, Little Hampton, West Sussex, UK) polyclonal antibodies, diluted 1:10 and 1:25, respectively, in 1% (w/v) BSA for 1 h at room temperature. After washing twice with PBS for 10 min each, the signal was revealed with either ALEXA 488 (green fluorescence)- or ALEXA 546 (red fluorescence)-conjugated anti-rabbit antibodies (Molecular Probes, Eugene, OR) diluted 1:25 in 1% (w/v) BSA for 1 h in the dark at room temperature. Finally, the sections were washed twice with PBS for 10 min, stained with DAPI (4,6-diamidine-2-phenylindol; Serva, Heilderberg, Germany) for 10 min, washed with milli-Q H_2O and mounted with Mowiol 4-88 (Polysciences, Eppelheim, Germany).

A double immunofluorescence labelling with anti-RuBisCo and anti-*Gm*HMA8 polyclonal antibodies was also performed to assay the putative co-localization of both antigens. Double immunofluorescence was performed following a sequential incubation protocol, essentially as previously described (Silva et al., 2004). Controls replacing the first antibody by preimmune antiserum were also assayed. Immunofluorescence assays were observed in a Confocal Laser Microscopy (CLSM) (Leica TCS-SP2-AOBS) and Z-series of optical sections of 0.5-1.0 μm were collected. Images were taken from the projections of series of 15 to 20 optical sections. Differential Interference Contrast (DIC, Nomarski) images were also taken.

6.3.11. Low temperature processing for immunoelectron microscopy

Fixed soybean cells (see above) were cryoprotected by immersion in sucrose:PBS solution at the following concentrations and times: 0.1 M for 1 h, 1 M for 1 h, and 2.3 M overnight, at 4 ºC. Then, the specimens were put in cryoultramicrotomy pins and cryofixed by rapid plunging into nitrogen liquid at -190 ºC. After that, the samples were dehydrated by freeze substitution in an Automatic Freeze-substitution System (AFS, Leica, Vienna, Austria) essentially as described by us (Seguí-Simarro et al., 2005). Cryofixed samples were immersed in pure methanol containing 0.5% (w/v) uranyl acetate at -80 ºC for 3 days, and then the temperature was slowly (during 18 h) warmed to -30 ºC. After three washing in pure methanol, 30 min each, at -30 ºC, samples were infiltrated and embedded in Lowicryl K4M at -30 ºC, under UV. Ultrathin sections were obtained in an ultramicrotome (Ultracut Reichert, Vienna, Austria) and collected on 200-mesh nickel grids having a carbon-coated Formvar-supporting film.

6.3.12. Immunogold labelling

Nickel grids carrying ultrathin Lowicryl sections were sequentially floated in PBS, 5% (w/v) BSA in PBS, and undiluted anti-*Gm*HMA8 antibody, for 1 h. After several washes in 0.1% (w/v) BSA in PBS, the grids were incubated with a secondary antibody, anti-rabbit IgG conjugated to 10 nm gold particles (Biocell, Cardiff, UK) diluted 1:25 in 1% (w/v) BSA, for 1 h at room temperature, washed

in PBS and water, air dried, counterstained with uranyl acetate and lead citrate and observed in a JEOL 1010 EM at 80 kV. Controls were performed excluding the primary antibody.

6.3.13. Quantitative evaluation of immmunogold labelling distribution: Clustering test

To assess the distribution pattern of gold particles, a clustering test was performed. Sampling was carried out over a number of micrographs taken randomly from all the cells in different grids. The number of micrographs was determined using the progressive mean test with minimum confidence limit of α=0.05. Clustered particles were defined as 2 or more gold particles close to each other (Seguí-Simarro et al., 2003), taking into account the relative length of primary and secondary antibodies coupled to colloidal gold. For each micrograph, the isolated and clustered gold particles on chloroplasts were counted. The percentage of clustered particles versus the total number of particles was calculated.

6.4. RESULTS

6.4.1. Isolation of *GmHMA8* cDNA

In silico analysis using the sequences of PacS and CtaA from the cyanobacterium *Synechocystis* PCC 6803 identified homologue sequences in *A. thaliana* [At4g37270 (*At*HMA1); At1g63440 (*At*HMA5); At4g33520 (*At*HMA6 or PAA1); At5g44790 (*At*HMA7 or RAN1); At5g21930 (*At*HMA8 or PAA2)] and one homologous sequence in *Brassica napus* (AY045772) as possible orthologs of the P_{1B}-ATPase family in plants. All P_{1B}-ATPases identified with this analysis correspond to putative copper transporting ATPases Soybean cDNA amplification was done by RT-PCR using degenerated primers designed according to *in silico* data analysis (for details see Materials and Methods).

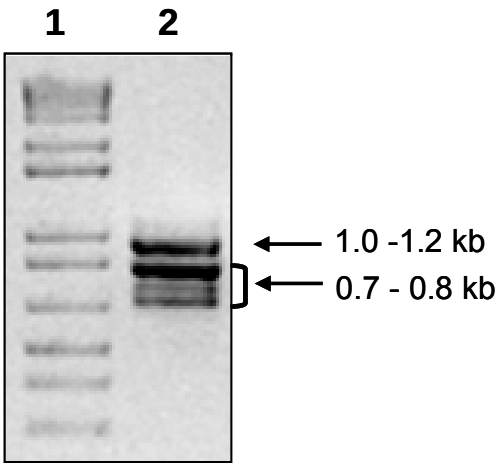

Fig. 6-1. Expression of *P-ATPase* family in soybean photosynthetic cell suspensions. *Lane* 1, 1.0 kb plus DNA ladder; *lane 2*, RT-PCR of *P-ATPase* family with degenerated primers: 1.0-1.2 kb bands correspond with classical *P-ATPases (Ca-ATPase, H^+-ATPase)* and 0.7-0.8 kb bands correspond with *P_{1B}-ATPases (Cu-ATPases).*

Two groups of cDNA bands were reproducibly amplified under these conditions (Fig. 6-1). One group of bands migrated at positions corresponding to 0.7-0.8 kb, and other group at positions above 1.0-1.2 kb. It is well-known that the large cytoplasmic loop of P_{1B}-ATPases is smaller than that of classical P-type ATPases. Between the phosphorylation and ATP binding domains, the Arabidopsis P_{1B} pumps have approximately 150 amino acid residues less than the Arabidopsis Ca^{2+} pump, *At*ECA1 (Williams et al., 2000). Thus, we assumed that the *ca.* 1.0 kb band encoded classical P-type ATPases, and the *ca.* 0.7-0.8 kb bands encoded P_{1B}-ATPases. Bands were cloned and positive clones were sequenced and analyzed. Eleven clones homologues to Cu-ATPases (lowest molecular size bands), and seven clones homologues to Ca-ATPases plus six clones homologous to H^+-ATPase (largest molecular size band) were obtained. Among those clones homologues to Cu-ATPases, only four encoded a desirable open-reading-frame (ORF) whose predicted amino acid sequence was highly similar to the corresponding regions of PacS and *At*HMA8. Sequence analysis revealed the identity of a 793 bp region as encoding a new copper transporter in soybean homologue to the copper transporters PacS and *At*HMA8, which we named as *Gm*HMA8. Subsequently, the full-length *GmHMA8* cDNA was obtained (for details see Materials and Methods). This provided us which a 2832 bp sequence of *GmHMA8* that contained part of the

3'-UTR and 5'-UTR regions of the gene. The sequence was deposited in GenBank as DQ418731.

Analysis of the predicted sequence of *Gm*HMA8 (908 aa) indicated that this protein belongs to Cu-transporting P-type ATPases. It is an integral membrane protein with an N-terminal chloroplast transit peptide, eight transmembrane (TM) domains (Fig. 6-2A,B) with a small cytoplasmatic loop between TM domains 4 and 5, and a large cytoplasmatic loop between TM domains 6 and 7 (Fig. 6-2C). Like all P-type ATPases, it has all the characteristic conserved domains: the ATP binding (GDGxNDx) and phosphorilation (DKTGTLT) domains in the large cytoplasmatic loop and a phosphatase domain in the small cytoplasmatic loop. *Gm*HMA8, have also the specific domains present in P_{1B}-ATPases: the GMxCxxC metal binding motif in the N-terminal region, the CPx ion transduction domain in the sixth TM domain and the HP domain that is involved in the translocation of copper (Fig. 6-2C) (Axelsen and Palmgrem, 2001; Argüello, 2003; Williams and Mills, 2005). The comparison of *Gm*HMA8 deduced amino acid sequence with the rest of the HMA8-related sequences available in databases indicated a 45% similarity to PacS, 83% to *At*HMA8, 75% to *Os*HMA8, and 88% to *Lc*HMA8 in the overlapping amino acids (Fig. 6-2A).

A

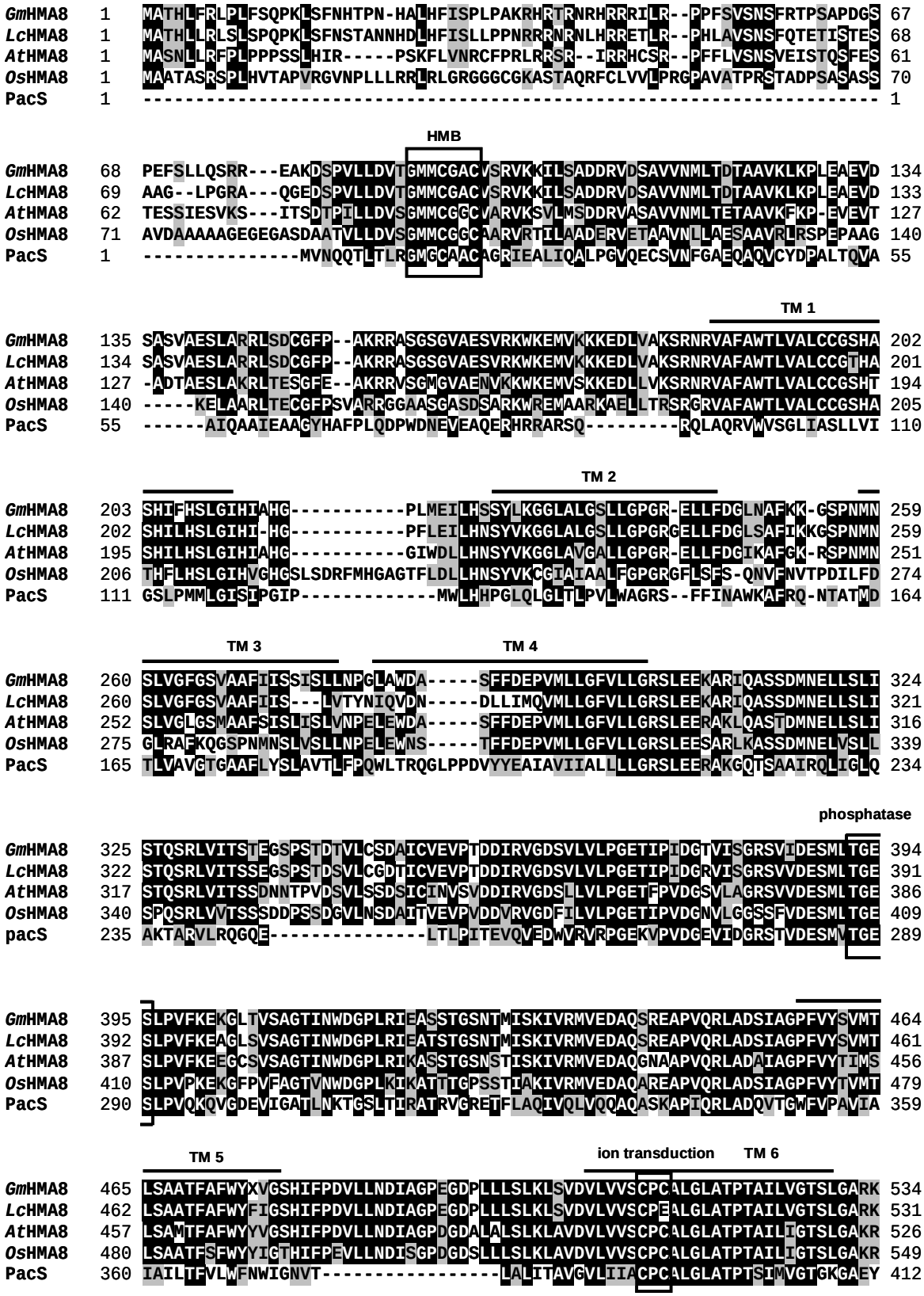
GmHMA8 1 MATHLFRLPLFSQPKLSFNHTPN-HALHFISPLPAKRHRTRNRHRRRILR--PPFSVSNSFRTPSAPDGS 67
LcHMA8 1 MATHLLRLSLSPQPKLSFNSTANNHDLHFISLLPPNRRRNRNLHRRETLR--PHLAVSNSFQTETISTES 68
AtHMA8 1 MASNLLRFPLPPPSSLHIR-----PSKFLVNRCFPRLRRSR--IRRHCSR--PFFLVSNSVEISTQSFES 61
OsHMA8 1 MAATASRSPLHVTAPVRGVNPLLLRRLRLGRGGGCGKASTAQRFCLVVLPRGPAVATPRSTADPSASASS 70
PacS 1 ---------- 1
HMB
GmHMA8 68 PEFSLLQSRR---EAKDSPVLLDVTGMMCGACVSRVKKILSADDRVDSAVVNMLTDTAAVKLKPLEAEVD 134
LcHMA8 69 AAG--LPGRA---QGEDSPVLLDVTGMMCGACVSRVKKILSADDRVDSAVVNMLTDTAAVKLKPLEAEVD 133
AtHMA8 62 TESSIESVKS---ITSDTPILLDVSGMMCGGCVARVKSVLMSDDRVASAVVNMLTETAAVKFKP-EVEVT 127
OsHMA8 71 AVDAAAAAGEGEGASDAATVLLDVSGMMCGGCAARVRTILAADERVETAAVNLLAESAAVRLRSPEPAAG 140
PacS 1 --------------MVNQQTLTLRGMGCAACAGRIEALIQALPGVQECSVNFGAEQAQVCYDPALTQVA 55
TM 1
GmHMA8 135 SASVAESLARRLSDCGFP--AKRRASGSGVAESVRKWKEMVKKKEDLVAKSRNRVAFAWTLVALCCGSHA 202
LcHMA8 134 SASVAESLARRLSDCGFP--AKRRASGSGVAESVRKWKEMVKKKEDLVAKSRNRVAFAWTLVALCCGTHA 201
AtHMA8 127 -ADTAESLAKRLTESGFE--AKRRVSGMGVAENVKKWKEMVSKKEDLLVKSRNRVAFAWTLVALCCGSHT 194
OsHMA8 140 -----KELAARLTECGFPSVARRGGAASGASDSARKWREMAARKAELLTRSRGRVAFAWTLVALCCGSHA 205
PacS 55 ------AIQAAIEAAGYHAFPLQDPWDNEVEAQERHRRARSQ---------RQLAQRVWVSGLIASLLVI 110
TM 2
GmHMA8 203 SHIFHSLGIHIAHG-----------PLMEILHSSYLKGGLALGSLLGPGR-ELLFDGLNAFKK-GSPNMN 259
LcHMA8 202 SHILHSLGIHI-HG-----------PFLEILHNSYVKGGLALGSLLGPGRGELLFDGLSAFIKKGSPNMN 259
AtHMA8 195 SHILHSLGIHIAHG-----------GIWDLLHNSYVKGGLAVGALLGPGR-ELLFDGIKAFGK-RSPNMN 251
OsHMA8 206 THFLHSLGIHVGHGSLSDRFMHGAGTFLDLLHNSYVKCGIAIAALFGPGRGFLSFS-QNVFNVTPDILFD 274
PacS 111 GSLPMMLGISIPGIP------------MWLHHPGLQLGLTLPVLWAGRS--FFINAWKAFRQ-NTATMD 164
TM 3
TM 4
GmHMA8 260 SLVGFGSVAAFIISSISLLNPGLAWDA-----SFFDEPVMLLGFVLLGRSLEEKARIQASSDMNELLSLI 324
LcHMA8 260 SLVGFGSVAAFIIS---LVTYNIQVDN-----DLLIMQVMLLGFVLLGRSLEEKARIQASSDMNELLSLI 321
AtHMA8 252 SLVGLGSMAAFSISLISLVNPELEWDA-----SFFDEPVMLLGFVLLGRSLEERAKLQASTDMNELLSLI 316
OsHMA8 275 GLRAFKQGSPNMNSLVSLLNPELEWNS-----TFFDEPVMLLGFVLLGRSLEESARLKASSDMNELVSLL 339
PacS 165 TLVAVGTGAAFLYSLAVTLFPQWLTRQGLPPDVYYEAIAVIIALLLLGRSLEERAKGQTSAAIRQLIGLQ 234
phosphatase
GmHMA8 325 STQSRLVITSTEGSPSTDTVLCSDAICVEVPTDDIRVGDSVLVLPGETIPIDGTVISGRSVIDESMLTGE 394
LcHMA8 322 STQSRLVITSSEGSPSTDSVLCGDTICVEVPTDDIRVGDSVLVLPGETIPIDGRVISGRSVVDESMLTGE 391
AtHMA8 317 STQSRLVITSSDNNTPVDSVLSSDSICINVSVDDIRVGDSLLVLPGETFPVDGSVLAGRSVVDESMLTGE 386
OsHMA8 340 SPQSRLVVTSSSDDPSSDGVLNSDAITVEVPVDDVRVGDFILVLPGETIPVDGNVLGGSSFVDESMLTGE 409
pacS 235 AKTARVLRQGQE--------------LTLPITEVQVEDWVRVRPGEKVPVDGEVIDGRSTVDESMVTGE 289
GmHMA8 395 SLPVFKEKGLTVSAGTINWDGPLRIEASSTGSNTMISKIVRMVEDAQSREAPVQRLADSIAGPFVYSVMT 464
LcHMA8 392 SLPVFKEAGLSVSAGTINWDGPLRIEATSTGSNTMISKIVRMVEDAQSREAPVQRLADSIAGPFVYSVMT 461
AtHMA8 387 SLPVFKEEGCSVSAGTINWDGPLRIKASSTGSNSTISKIVRMVEDAQGNAAPVQRLADAIAGPFVYTIMS 456
OsHMA8 410 SLPVPKEKGFPVFAGTVNWDGPLKIKATTTGPSSTIAKIVRMVEDAQAREAPVQRLADSIAGPFVYTVMT 479
PacS 290 SLPVQKQVGDEVIGATLNKTGSLTIRATRVGRETFLAQIVQLVQQAQASKAPIQRLADQVTGWFVPAVIA 359
TM 5
ion transduction
TM 6
GmHMA8 465 LSAATFAFWYXVGSHIFPDVLLNDIAGPEGDPLLLSLKLSVDVLVVSCPCALGLATPTAILVGTSLGARK 534
LcHMA8 462 LSAATFAFWYFIGSHIFPDVLLNDIAGPEGDPLLLSLKLSVDVLVVSCPEALGLATPTAILVGTSLGARK 531
AtHMA8 457 LSAMTFAFWYYVGSHIFPDVLLNDIAGPDGDALALSLKLAVDVLVVSCPCALGLATPTAILIGTSLGAKR 526
OsHMA8 480 LSAATFSFWYYIGTHIFPEVLLNDISGPDGDSLLLSLKLAVDVLVVSCPCALGLATPTAILIGTSLGAKR 549
PacS 360 IAILIFVLWFNWIGNVT----------------LALITAVGVLIIACPCALGLATPTSIMVGTGKGAEY 412

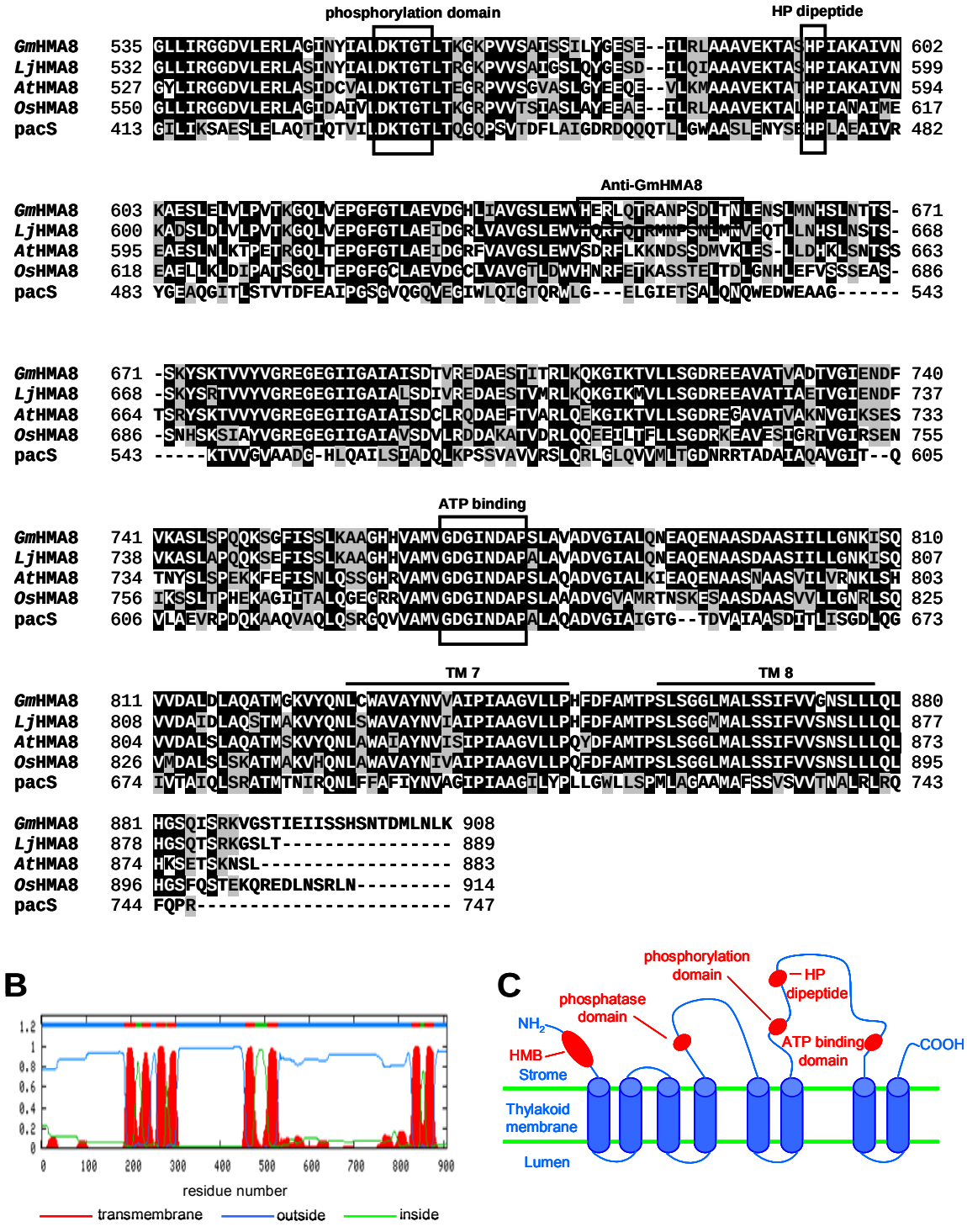

Fig. 6-2. A) Sequence alignment of soybean (*Glycine max*) *Gm*HMA8 (DQ418731) with HMA8 proteins from *Arabidopsis thaliana* (*At*HMA8/PAA2, At5g21930), *Oryza sativa* (rice) (*Os*HMA8, XP_470523), *Lotus corniculatus* (*Lc*HMA8) and *Synechocystis* PCC 6803 (PacS, sll1920). Identical residues are in black and similar residues are shaded. The eight putative transmembrane domains (TM1-TM8) for *Gm*HMA8 are underlined. Functional regions and 15 amino acid peptide sequence chosen to produce the specific antibody anti-*Gm*HMA8 are boxed. B) Hydrophobicity profiles of *Gm*HMA8. C) Topological model of *Gm*HMA8.

6.4.2. Production of a polyclonal antibody anti-*Gm*HMA8

A specific polyclonal anti-*Gm*HMA8 antibody was raised against a synthetic 15 aminoacid peptide corresponding to a region between the phosphorylation and ATP binding domains in the large cytoplasmatic loop of the *Gm*HMA8 protein sequence identified (Fig. 6-2A). This region was chosen to produce this antibody due to its high specificity for the *Gm*HMA8 protein; it is not present in the protein sequences of other HMA family members. Since a chloroplast target for this protein was predicted, we assayed the validity of this antibody in intact chloroplasts and thylakoid membranes isolated from soybean cell cultures. Figure 6-3A shows the polypeptide composition of the thylakoid fraction. Immunoblot analyses depicted a single band around 180-200 kDa in the chloroplast and thylakoid fractions assayed that may correspond to the *Gm*HMA8 protein (Fig. 6-3B, D, left pannel). The analyses revealed that the relative abundance of this band increased in those fractions enriched in thylakoid membranes (Fig. 6-3B). No signals were found with BSA extract protein and the preimmune antiserum (Fig. 6-3B, C) demonstrating the specificity of the antibody. To better validate the produced antibody we assayed it in chloroplasts isolated from soybean and *Lotus corniculatus* plants. As previously, immunoblot analyses showed a high molecular weight band that migrated slightly faster in the case of *Lotus* compared with soybean (Fig. 6-3D, right pannel). The apparent molecular mass revealed by immunoblot analysis was higher than the theoretical molecular mass predicted for *Gm*HMA8 and *Lc*HMA8 proteins based on its amino acid sequence, 97 kDa and 95 kDa, respectively. It is worth mentioning that according to our knowledge this is the first antibody raised against a HMA8 Cu-ATPase in plants and the third one available against a member of the P_{1B}-ATPases family (for details see Hussain et al., 2004; Seigneurin-Berny et al., 2006).

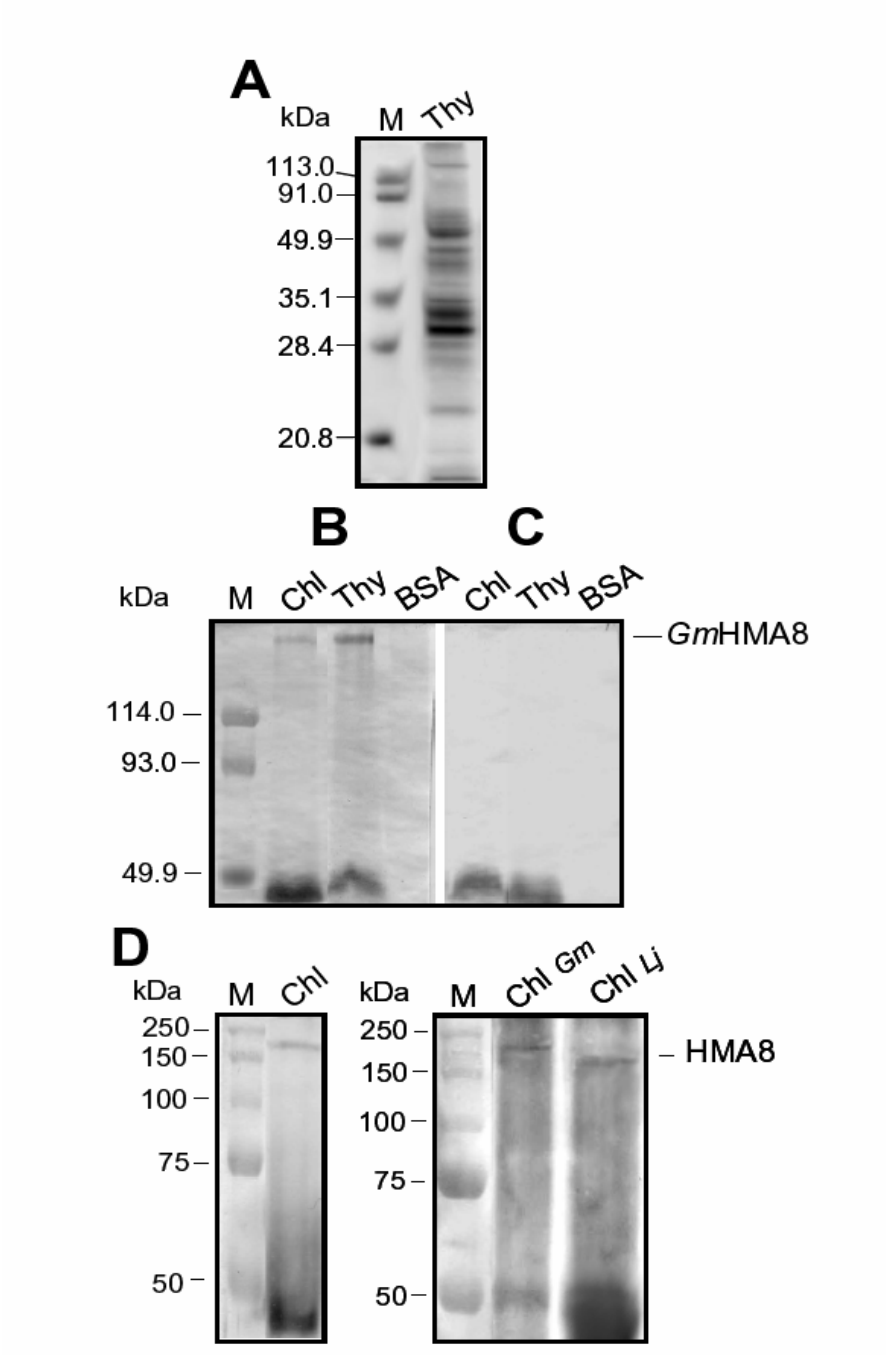

Fig. 6-3. (A) Protein composition of thylakoid membranes from soybean cells obtained by SDS-PAGE and visualized by Coomassie Blue. (B) Immunoblot with antiserum anti-*Gm*HMA8 protein (left pannel) and with preimmune antiserum (right pannel) of intact chloroplasts (Chl) and thylakoid membranes (Thy) from soybean cells, and bovine serum albumine protein (BSA). (C) Immunoblot with antiserum anti-*Gm*HMA8 of chloroplasts from soybean cells (Chl, left pannel), and chloroplasts from soybean plants (*Gm* Chl, right pannel) and *Lotus corniculatus* plants (*Lc* Chl, right pannel). Loading protein amount was 12 μg (A), 26 μg (B, C), 21 μg (D, Thy), 58 μg (D, *Gm* Chl, *Lc* Chl). Note the different MW markers for each electrophoresis.

6.4.3. Subcellular localization of *Gm*HMA8 by immunofluorescence labelling

The structural organization of soybean photosynthetic cells, as visualized in toluidine blue-stained semithin sections (Fig. 6-4A) was similar to that of mesophyll cells from young leaves. They showed a large and central cytoplasmic vacuole, chloroplasts distributed along the peripheral layer of the cytoplasm and an ellipsoid nucleus (Fig. 6-4A). Most chloroplasts contained large granules which appeared as clear inclusions in toluidine blue-stained sections visualized under bright field (Fig. 6-4A) and in unstained sections observed under phase contrast (Fig. 6-4E); the content of these inclusions was revealed by the iodide-based cytochemistry as starch (Fig. 6-4E, F).

Immunofluorescence experiments with anti-*Gm*HMA8 provided specific signals as intense green fluorescence in defined cytoplasmic spots (Fig. 6-4B). Labelling was not found in the nucleus that was revealed by DAPI with an intense blue fluorescence, or in the vacuole that appeared as a large dark central area (Fig. 6-4B). Confocal images of anti-*Gm*HMA8 immunofluorescence green signals were overlapped with the corresponding differential interference contrast (DIC) image of the section (Fig 6-4C). The result showed that the green fluorescence was localized on small rounded cytoplasmic structures, frequently at their periphery (Fig. 6-4C). This pattern of distribution of the immunofluorescence labelling and its comparison with the structural organization of the soybean cells strongly suggested the localization of the *Gm*HMA8 in the chloroplast. Controls with preimmune antiserum showed no labelling (Fig. 6-4D).

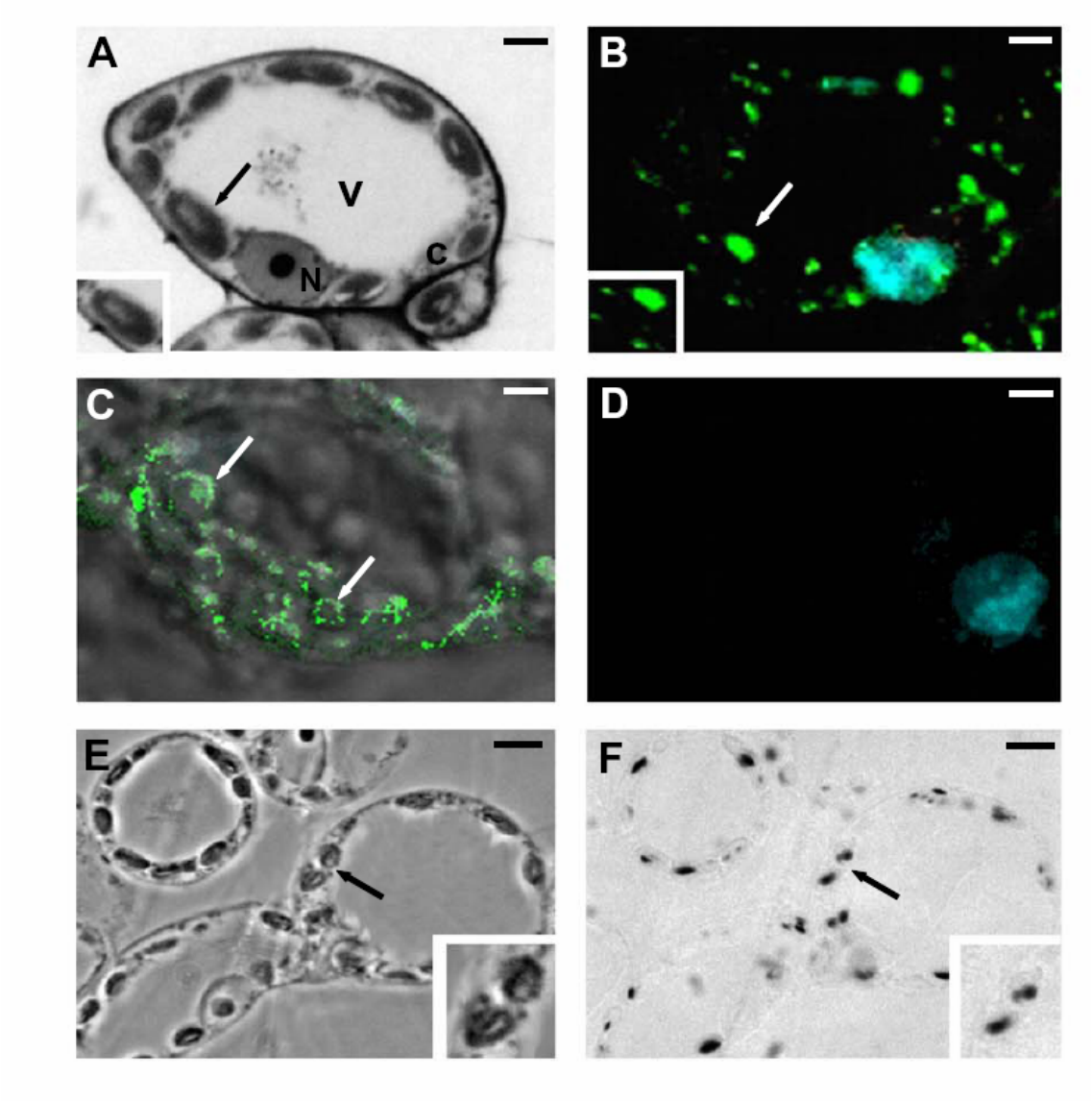

Fig. 6-4. (A) Structural organization of soybean photosynthetic cell cultures. Historesin semithin sections after toluidine blue staining. Vacuole (v), cytoplasm (c), and chloroplasts (arrows). (B) Immunofluorescence with anti-*Gm*HMA8 in soybean photosynthetic cells. Confocal laser microscopy observations of 30 μm vibratome sections. The images represent projections of 15-20 optical sections. Positive immunofluorescence (green) is observed in chloroplasts. Nuclear DNA was stained with DAPI (blue). (C) Overlap of Nomarski picture (grey) with anti-*Gm*HMA8 immunofluorescence (green). Arrows showed the chloroplast localization of *Gm*HMA8. (D) Preimmune antiserum immunofluorescence. (E) Cell structure with chloroplasts, many of them containing clear starch deposits (arrows). (F) Starch grains revealed as dark inclusions by iodide-base cytochemistry, observed under bright field. Bars in A, B, C and D represent 2.0 μm; bars in E and F represent 1.0 μm.

To further confirm the chloroplast localization of *Gm*HMA8 in soybean cells a double immunofluorescence labelling with anti-RuBisCo, a good chloroplastic marker, and with anti-*Gm*HMA8 antibodies was performed (Fig. 6-5). Anti-*Gm*HMA8 labelling, revealed by green fluorescence (Fig. 6-5A) and anti-RuBisCo labelling, visualized as red fluorescence (Fig. 6-5B) were specifically found in the same cytoplasmic rounded structures, the chloroplasts, showing a central dark area which probably corresponded with the starch deposits found in most chloroplasts (Fig. 6-5D, E). The overlay of both green and red fluorescence signals showed the co-localization of both antigens, as a yellow signal, in the chloroplast (Fig. 6-5C, F); some individual green and red small spots were also observed in the merged images (Fig. 6-5F) indicating that the co-localization was not complete.

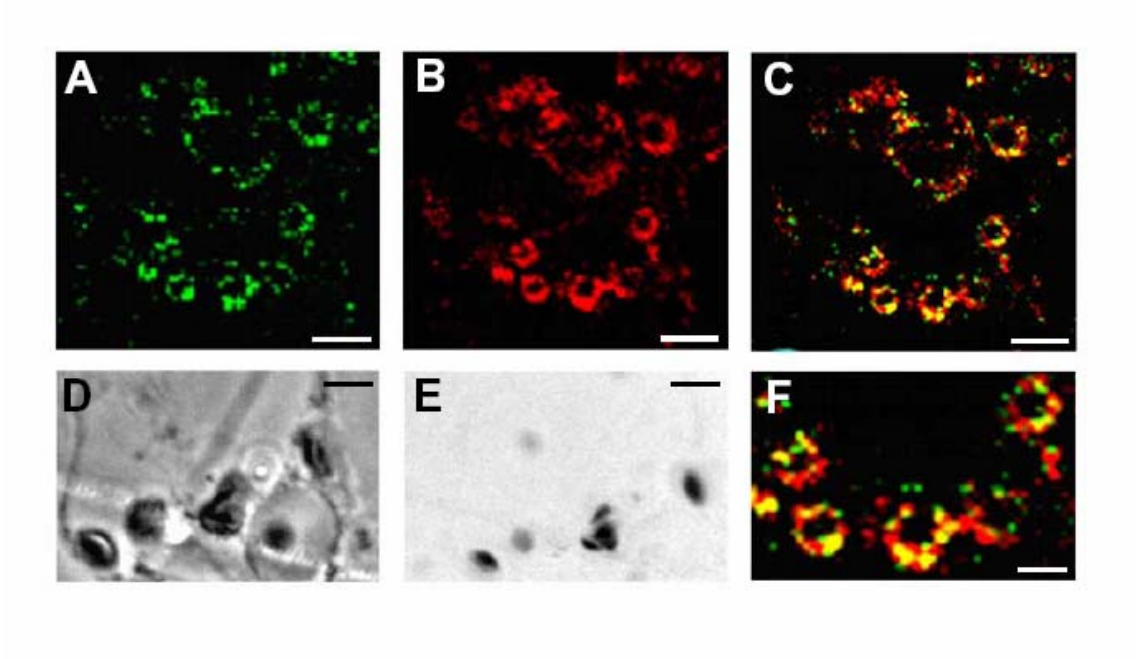

Fig. 6-5. Double immunofluorescence with anti-*Gm*HMA8 and anti-RuBisCo in soybean photosynthetic cell cultures. Confocal laser microscopy observations of 30 µm vibratome sections, the images represent projections of 15-20 optical sections. (A) Immumofluorescence with anti-*Gm*HMA8 and detected with anti-rabbit immunoglobulins labelled with Alexa 488. (B) Immunofluorescence with anti-RuBisCo and detected with anti-rabbit immunoglobulins labelled with Alexa 546. (C and F) Co-localization of staining for *Gm*HMA8 and RuBisCo (yellow). (D) Cell structure observed at higher magnification: cells show chloroplasts, many of them containing clear starch deposits. (E) Starch grains revealed as dark inclusions by iodide-base cytochemistry, observed under bright field. Images in A and B were taken with CLSM for the red channel reduced to zero and for the green channel reduced to zero, respectively. Images in C and F were obtained by simultaneous acquisition of data in both channels. Bars in A, B and C represent 1.0 µm; bars in D, E and F represent 2.0 µm.

6.4.4. Subcellular localization of *Gm*HMA8 by immunogold labelling

The resolution of the confocal microscope could not inform about the precise localization of the *Gm*HMA8 antigen inside the different chloroplast subcompartments. To go further on the ultrastructural distribution analysis of the *Gm*HMA8 protein, electron microscopy immunogold labelling was performed (Fig. 6-6). Cryofixation and freeze-substitution followed by low-temperature embedding in an acrylic resin were the most convenient processing methods to better preserve the cellular ultrastructure and the integrity of the membranes, as well as the antigenic reactivity of the cell. The results showed that the protocol used was adequate for soybean cell cultures, which maintain a good ultrastructural preservation of the different subcellular compartments, including chloroplasts and thylakoid membranes (Fig. 6-6A, B). Immunogold labelling was specifically found on the thylakoid membranes of chloroplasts (Fig. 6-6C, D). To assess the distribution pattern of immunogold particles, a quantitative clustering test was performed. Taking into account the labelling distribution observed, particles were considered clustered when two or more particles appeared close to each other. When considering the clusters of particles decorating the chloroplastic thylakoids, the clusters containing 2-4 particles were the most numerous and only a few of them displayed more than 4 particles. The percentages of clustered and isolated particles versus the total number of particles were calculated. Results showed that the percentage of clustered particles was much higher (73.92%) than the isolated ones (26.35%), indicating/suggesting a grouped distribution of the antigen in discrete locations of the chloroplastic thylakoids. No gold particles were observed in any other subcellular compartment. The preimmune serum did not provide any significant labelling (data not shown).

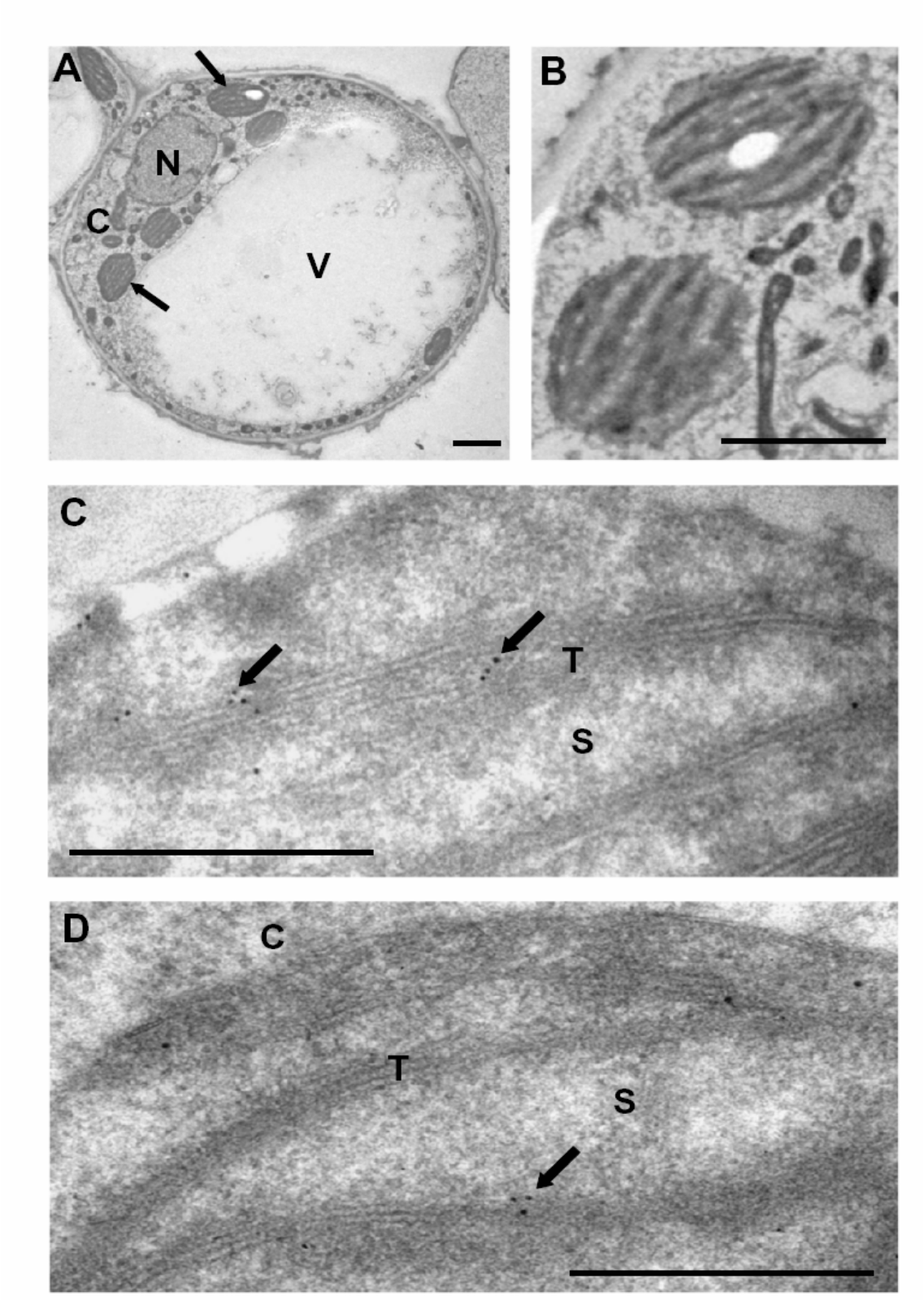

Fig. 6-6. Anti-*Gm*HMA8 immunogold labelling on soybean photosynthetic cells. Ultrathin Lowicryl sections. (A) General view of soybean cells. (B) General view of chloroplasts. (C) and (D) Gold particles are localized in thylakoid membranes (arrows) V (vacuole); N (nucleus); S (stroma); T (thylakoid membranes); C (cytoplasm). Bars in A, B represent 0.5 μm, and in C, D represent 200 nm.

6.5. DISCUSSION

In this paper we present the identification of a soybean Cu-transporting P-type ATPase, *Gm*HMA8, homologous to PacS and *At*HMA8 (PAA2) transporters that are members of Cu/Ag transporting group of P_{1B}-ATPases (Tottey et al., 2001; Abdel-Ghany et al., 2005b). Comparison of *Gm*HMA8 with sequences from other organisms showed that HMA8 protein sequences are evolutionary conserved, which may reflect a critical function for this protein. Immunoblot experiments using the specific antibody produced against this soybean copper P_{1B}-ATPase showed reaction against a single band around 180-200 kDa in chloroplasts and thylakoid membranes from soybean cells, which should correspond to the putative *Gm*HMA8 protein. Similarly, this antibody showed reaction against a band in chloroplasts from soybean and *Lotus corniculatus* plants demonstrating the validity of this antibody. In general, it has been reported that P-type ATPases have a molecular mass between 70 to 150 kDa (Kühlbrandt, 2004). The apparent molecular mass of both putative HMA8 proteins detected in soybean and *Lotus* chloroplasts was higher than the predicted theoretical molecular mass. This finding could be interpreted as *Gm*HMA8 protein might migrate differently in the electrophoretic gel that one expected (See and Jackowski, 1990). It is worth mentioning that no experimental evidence of the apparent size of other plant HMA8 transporters has been reported in the literature because of the absence of appropriate tools.

Immunofluorescence assays in soybean photosynthetic cells demonstrate that this soybean copper P_{1B}-ATPase is localized in chloroplasts. Double immunofluorescence labelling experiments with anti-*Gm*HMA8 and anti-RuBisCo antibodies showed the co-localization of both antigens with small differences in their distribution pattern. Our results are consistent with data reported for PAA2 (*At*HMA8) in protoplasts of *A. thaliana* using green fluorescence fusion proteins (PAA2-GFP) (Abdel-Ghany et al., 2005b). However, the level of resolution of the immunofluorescence signals does not allow visualize precisely their localization within the different chloroplast subcompartments: thylakoids, stroma, or thylakoid lumen. In fact, the immunofluorescence signal provided by the RuBisCo, a typical stromatic protein, could overlap with immunofluorescence signals from antigens localized

in the thylakoid membranes, as it seems to be the case of the *Gm*HMA8 protein. Thus, a high spatial resolution and a more precise demonstration of *Gm*HMA8 location is required to underscoring the subchloroplast location and then predicts the function of this protein as well as its possible role in photosynthesis.

Chloroplast is one of the most complex organelles in terms of ultrastructure, comprising three main different subcompartments: outer and inner interenvelope space, stroma and thylakoid lumen. In order to study the subchloroplast location of *Gm*HMA8 immunogold labelling assays were conducted using the specific antibody anti-*Gm*HMA8 that we produced. An accurate electron microscopy immunolocalization of membrane-associated antigens requires specific sample processing methods to preserve the chemical integrity, antigenic reactivity and ultrastructure of the membranes, which are highly affected by some chemically fixing and most dehydrating procedures. Cryofixation and freeze-substitution constitute an alternative and have been reported as very convenient processing methods for immunogold assays of membrane-associated antigens in plant cells (Risueño et al., 1998; Seguí-Simarro et al., 2003; 2005; review in Koster and Klumperman, 2003). Our results showed that the cryoprocessing method used was fully adequate for soybean cells, which displayed an excellent ultrastructural preservation of the chloroplastic membranes, distinguishing clearly among the other subcompartments of this organelle. A well-defined immunogold signal was found in the thylakoid membrane with no evidences of labelling in the chloroplast envelopes. Thus, the results demonstrated that *Gm*HMA8 is located in the thylakoid membrane. Our findings are in agreement with results reported by Abdel-Gahny et al. (2005b) for *At*HMA8 by using *in vitro* import protein experiments with a non-full length PAA2 (*At*HMA8) protein. It is worth mentioning that the approach presented here constitutes a direct method providing advantages to localize the full-length protein. The use of our specific antibody against *Gm*HMA8 is a valuable tool for this purpose and future studies. Interestingly, the labelling pattern frequently appeared in clusters of 2-3 gold particles. Quantitative analysis revealed that gold particles appeared 73.9% of total labelling in groups of 2-3 units, while 26.1% of labelling was as isolated particles. This type of distribution in cluster would indicate the presence of

*Gm*HMA8 transporter enriched sites within the thylakoid membrane. This finding is consistent with the current idea that thylakoid membranes are heterogeneous and contain domains or regions with specific functions. On the other hand, the observed distribution might suggest an oligomeric structure for this copper transporter. In this respect, it is worth mentioning that the apparent molecular mass of the *Gm*HMA8 protein detected in denaturing gel electrophoresis was around 2-fold higher than the predicted theoretical mass. At present, studies concerning to structural aspects of P-type ATPases are very limited (Kühlbrandt, 2004) and in particular those concerning to copper-transporting P_{1B}-ATPase subfamily. It is to note the great difficulties that in general membrane proteins present for structural studies. The X-ray structure of the sarcoplasmic reticulum Ca^{2+}-ATPase, a P_2-type ATPase, and the homology models of P-ATPases proposed provide a basis for understanding the molecular structure of these transporters (Toyoshima et al., 2000; Toyoshima and Nomura, 2002; Kühlbrandt, 2004). Based on those models, P-type ATPases of types II and III seem to form oligomeric structures (Kühlbrandt, 2004). Although this information cannot be straightforward extrapolated to members of P_{1B}-ATPases subfamily, since they differ in overall architecture, it might not be ruled out a similar organization for P-ATPases of type I. More recently, progress in structural characterization of P_{1B}-ATPases have been done, but these investigations were restricted to specific protein domains (Achila et al., 2006; Dmitriev et al., 2006; Sazinsky et al., 2006 a, b). Hence, information of the possible homodimerization or oligomerization for P_{1B}-ATPases is not still known. As for this possibility structural data of other copper transporters could be of interest.

Recently, the structure of the human copper transporter *h*CTR1, responsible for the initial uptake of copper into cells, and homologue to plant COPT transporters (Sancenón et al., 2003) has been reported by using electron crystallography of 2D protein crystals at 6 Å-resolution. The data revealed a symmetrical trimeric structure of *h*CTR1 that was <40 Å wide (Aller and Unger, 2006). The formation of a putative pore for metal ions at the interface of three identical subunits has been proposed, which could be related with its metal transport function. Further investigations are required to understand the

functional implications if any of the observed *Gm*HMA8 protein organization within the thylakoid membrane.

CAPÍTULO 7

IDENTIFICATION OF TWO COPPER *HMA8* P-ATPase mRNAs IN SOYBEAN: ANALYSIS OF THEIR RESPONSE TO COPPER AND THEIR SPLICING REGULATORY MECHANISM

7.1. ABSTRACT

We have identified two copper *HMA8* ATPase mRNAs in soybean, named as *GmHMA8* and *GmHMA8-T* that could correspond with two independent genes. *GmHMA8* corresponded with a fully spliced mRNA form and *GmHMA8-T* corresponded with a mRNA form containing a 7 bp deletion in comparison with *GmHMA8* mRNA sequence. This deletion leads to a change in the frame shift of the protein resulting in a putative truncated *Gm*HMA8 protein. At the transcript level, *GmHMA8* and *GmHMA8-T* are regulated by alternative splicing. The expression pattern was compared between control, Cu-stressed and Cu-adapted cells. The results showed that this pattern is diferentially regulated depending of copper exposure conditions. The effect of excess copper on *GmHMA8* and *GmHMA8-T* expression pattern was more pronounced in Cu-adapted cells in comparison with control ones. An up-regulation of non-spliced NSP transcripts and a down-regulation of spliced ones were observed in these conditions, accompanying to a long-term copper response. The results also showed that the expression pattern of *GmHMA8* and *GmHMA8-T* are regulated by growth media conditions.

7.2. INTRODUCTION

Copper functions within plant cells in a variety of processes, including electron transfer in photosynthesis and respiration, lignification of cell walls, hormonal signalling, antioxidant responses, senescence and biogenesis of molybdenum cofactor (Fox and Guerinot, 1998; Mira et al., 2002; Pilon et al., 2006). Because of its key role, intracellular levels of copper must be precisely regulated to prevent its potential toxicity (Raven et al., 1999). To that end, cells use a combination of compartmentalization, chelation and exclusion strategies to restrict deleterious effects of copper and to ensure that the correct metal species are delivered to their target proteins (Clemens, 2001; Hall and Williams, 2003).

Copper homeostasis has been well characterized in yeast and mammals. Recent molecular genetic analyses have allowed to identify components of the

pathways for intercellular and intracellular copper distribution in plants, including: *i)* the P_{1B}-ATPases RAN1/HMA7 (Hiramaya et al., 1999), HMA8/PAA2 (Abdel-Gahny et al., 2005b), HMA6/PAA1 (Shikanai et al., 2003), HMA5 (Andrés-Colás et al., 2006) and HMA1 (Seigneurin-Berny et al., 2006); *ii)* the COPT family (COPT1-6) (Sancenón et al., 2003; 2004); *iii)* the copper chaperones CCH (Mira et al., 2001a; b), CCS (Zhu et al., 2000; Ruzsa and Scandalios, 2003; Trindade et al., 2003; Chu et al., 2005; Abdel-Ghany et al., 2005a), COX17 (Balandín and Castresana, 2002) and ATX1 (Andrés-Colás et al., 2006). Thus, transmembrane metal-transporting proteins are crucial for transition metal homeostasis (Williams et al., 2000; Hall and Williams, 2003) and in particular key roles have been identified for P_{1B}-ATPases. The aim of this work was to study the molecular mechanisms that regulate copper ion uptake, storage and mobilization by plant chloroplasts. In a previous work (chapter 6), we identified a copper P_{1B}-ATPase in soybean (*Glycine max*), named as *Gm*HMA8, homologue to cyanobacterial PacS (Tottey et al., 2001) and *A. thaliana At*HMA8/PAA2 (Abdel-Gahny et al., 2005b) P_{1B}-ATPases. The *Gm*HMA8 transporter localized in the thylakoid membrane of chloroplast (chapter 6).

Here, we report the identification of two independent *GmHMA8* mRNAs that could correspond with two different Cu-ATPase proteins. The results indicated that these mRNAs are regulated by an alternative splicing mechanism. This is the first time that this type of regulation mechanism is proposed for P_{1B}-ATPase transporters in plants. This mechanism could be important in the control of copper homeostasis within chloroplasts.

7.3. MATERIALS AND METHODS

7.3.1. Cell suspension growth conditions

Photosynthetic cell suspensions from soybean (G*lycine max* var. Corsoy) SB-P line were grown as described by Rogers et al. (1987) with some modifications (Alfonso et al., 1996; Bernal et al., 2006). Cell suspensions were grown under continuous light (30 ± 5 μE m^{-2} s^{-1}) and atmosphere with 5% CO_2 at 24 ºC on a rotatory shaker (TEQ, model OSFT-LS-R) at 110 rpm. For gene

expression analysis cell suspensions were grown in the presence of 0.1 μM $CuSO_4 \cdot 5H_2O$ (control cells), 10 μM $CuSO_4 \cdot 5H_2O$ during the first 21 days of treatment that correspond with one transfer (Cu-stressed cells), during 49 transfers (Cu-adapted cells), and 5 nM $CuSO_4 \cdot 5H_2O$ during 21 days (Cu-deficient cells). Cu-adapted cells were also examined after suppression of excess Cu in the growth medium during five subsequent transfers (Cu-reverted cells). All these copper conditions were assayed either in photoautotrophic (KNº) and photomixotrophic (KN^1) medium. Cells used for experiments were collected from liquid cultures after 21 days of growth. Two to three repetitions were carried out for each treatment.

7.3.2. Plant material

Soybean plants (*Glycine max* cv. Volaina) were grown hydroponically in a growth chamber in half-Hoagland nutrient solution (Arnon, 1950) under 200 ± 20 μE m^{-2} s^{-1} from fluorescent and incandescent lamps at 24 ºC, 70% humidity and a 16-h photoperiod. Soybean leaves used for experiments were collected after 21 days of growth.

7.3.3. Antioxidant isoenzyme assays

SOD isoenzyme activities were assayed in the supernatant fractions obtained from the isolation procedure of thylakoid membranes (mainly chloroplast stroma fraction). All solutions used in the fractionation procedure contained 100 μg ml^{-1} pefablock as protease inhibitor. Fractions were concentrated by centrifugation with Centripep-10 and Centricon-10 (Amicon) tubes. Samples were loaded (30 μg total protein/well) on native PAGE, essentially as described by Laemmli (1970) except that SDS was omitted. Electrophoretic separation was performed at 4 ºC in 15% (w/v) polyacrilamide gels. SOD isoenzymes were detected in gels by the photochemical nitroblue tetrazolium (NBT) method as described by Beauchamp and Fridovich (1971). The different types of SODs were identified by incubating with specific inhibitors (KCN or H_2O_2). H_2O_2 inhibits the activity of both CuZnSOD and FeSOD while KCN only inhibits CuZnSOD activity. The MnSOD is insensitive to both inhibitors. After electrophoresis, gels were incubated with 50 mM sodium

phosphate buffer, pH 7.8 containing 3 mM KCN or 5 mM H_2O_2 for 1 h at 25 ºC in darkness. Gels were then incubated with 50 mM sodium phosphate buffer, pH 7.8 containing 0.48 mM NBT for 30 min and then with 30 µm riboflavin, 0.02% (v/v) TEMED, 50 mM sodium phosphate buffer pH 7.8 for 30 min. Gels were subsequently washed with 50 mM sodium phosphate buffer for 5 min and illuminated for 5-10 min.

7.3.4. DNA isolation

Soybean cells and leaves (4 g wet weight) were washed with fresh medium or with dionized sterile H_2O, respectively, and pestled in liquid nitrogen. Then, a mixture of extraction buffer (5 mM EDTA, 50 mM NaCl, 50 mM Tris-HCl pH 8.0) (5 mL per 1 g of green sample), 600 µg proteinase K and 1% (w/v) SDS was added to the powder and shaked carefully. Subsequently, the mixture was incubated with gently swirling at 55 °C for 2 hours. Then, the sample was centrifuged at 3,300 x g for 10 min at 4 ºC, the supernatant was extracted into a clean tube and 0.6 volumes of cold isopropanol were added yielding nucleic acids precipitate. The precipitate was fished out with a glass pipet, air dried and resuspended in dionized sterile H_2O. RNA traces were eliminated by incubation with 3 U of RNase H (Roche, Indianapolis, IN, USA) for 1 h at 37 ºC. DNA integrity was visually assessed on ethidium bromide-stained agarose gels. DNA was stored at -20 ºC.

7.3.5. RNA isolation and cDNA synthesis

Soybean cells and leaves (0.4 – 0.8 g wet weight) were washed with fresh medium or with dionized sterile H_2O, respectively, and pestled in liquid nitrogen. Then, a mixture of phenol:extraction buffer (0.1 M LiCl, 10 mM EDTA, 1% (w/v) SDS, 0.1 M Tris-HCl, pH 8.0) (1:1 v/v) was added to the powder (1.5 mL per 0.1 g of green sample) and vortexed vigorously. Samples were centrifuged at 1,500 × g for 10 min at 4 ºC. The aqueous phase was washed first with an equal volume of phenol:chloroform (1:1 v/v) followed by an additional wash with an equal volume of chloroform:isoamyl alcohol (24:1). The RNA was then precipitated overnight at 8 ºC with an equal volume of 4 M LiCl, centrifuged at 15,500 × g for 30 min at 4 ºC and then washed with cold 80%

(v/v) ethanol. RNA was dried out with nitrogen and resuspended in sterile H_2O containing 1% (v/v) DEPC. The RNA concentration was determined by measuring the OD_{260nm}. cDNAs were synthetized from total RNA (5 μg) using 200 units of reverse transcriptase (M-MLV reverse trancriptase, Promega, Madison, WI, USA) and 1 μM oligo$(dT)_{12-18}$ from Invitrogen (Invitrogen Life Technologies, Carlsbad, CA, USA), according to the manufacturer's instructions. Total RNA for the 5'-RACE amplification was isolated and purified from soybean cells using a RNeasy Plant Mini Kit (Qiagen GmbH, Hiden, Germany). cDNA was synthetized at 54 ºC from total RNA (3 μg) using a *GmHMA8* specific-primer (2 pmol, GSP1) and 200 units of thermoscript reverse transcriptase (Invitrogen Life Technologies, Carlsbad, CA, USA) with the GeneRacer Kit (Invitrogen Life Technologies, Carlsbad, CA, USA) according to the manufacturer's instructions.

7.3.6. Identification of two *GmHMA8* mRNAs

The full-length *GmHMA8* cDNA sequences were obtained by reverse transcription (RT) using cDNA prepared from soybean cell RNA in three steps: *i)* a pair of 24-mer degenerated oligonucleotides, designed from *in silico* sequence data analysis (see chapter 6, section 6.3.1), was used as primers for RT-PCR amplification. These oligonucleotides corresponded to the sequences of the phosphorylation domain FDKTGT(L/I)T (forward P-ATPase), and hinge region GIND(S/A)P(S/A)L (reverse P-ATPase), both located in the large cytoplasmatic loop of P_{1B}-ATPases; *ii)* the *GmHMA8 3'* end (including part of 3'-UTR) was obtained using a pair of primers, the forward one designed from the identified *GmHMA8* partial sequence (GmHMA8-1) and the reverse one designed from a *GmHMA8* EST (UTRGmHMA8) (TC228758, TIGR Soybean Gene Index); *iii)* the *GmHMA8 5´* end (including part of 5'-UTR) was obtained using the GeneRacer Kit (Invitrogen Life Technologies, Carlsbad, CA, USA). First, PCR was performed using an adaptator primer (GeneRacer 5' Primer) and a *GmHMA8* specific-primer (GSP2), after that a nested PCR with a nested adaptator primer (GeneRacer 5' Nested Primer) and a nested *GmHMA8* specific-primer (GSP3) was carried out (see Table 7-1). The PCR products

were cloned into the pGEM-T Easy vector (Promega, Madison, WI, USA) and sequenced (CNIO service, Madrid, Spain) to check their identity.

7.3.7. Expression analysis of two *GmHMA8* mRNAs

Total RNA extractions and first-strand cDNA synthesis were performed as described above. To examine the effect of copper in *GmHMA8* expression pattern equal amounts of RNA were used for RT-PCR. The housekeeping gene used was *actin* and the primers used were forward actin and reverse actin. For expression analysis, specific pair of primers were used: *i)* GmHMA8-1 and GmHMA8-2 to detect all *GmHMA8* mRNAs (*GmHMA8, GmHMA8-T, NSP GmHMA8, NSP GmHMA8-T*); *ii)* GmHMA8-1 and UTRGmHMA8 to detect *GmHMA8*; *iii)* GmHMA8-1 and NSPHMA8 to detect *NSP GmHMA8* and *iv)* GmHMA8-1 and NSPHMA8-T to detect *NSP GmHMA8-T* (Table 7-1). PCR reactions in *i)*, *iii)* and *iv)* were incubated for 3 min at 94 ºC and then 35 cycles of 30 s at 94 ºC, 30 s at 50 ºC, 45 s at 72 ºC were run. The last cycle was followed by an extended elongation step of 10 min at 72 ºC. The PCR conditions for *ii)* were the same except that the annealing (45 s, 52 ºC) and extending (1 min, 72 ºC) steps were optimised. The experiment was repeated twice on independently isolated material. PCR amplification was performed in a Perkin-Elmer thermal cycler (GeneAmp PCR system 9700, Applied Biosystems, Foster City, CA, USA). The resulting PCR products were cloned into the pGEM-T Easy vector (Promega, Madison, WI, USA) and sequenced (CNIO service, Madrid, Spain) to check their identity.

7.3.8. Northern Blot

For Northern Blot experiments, 30 µg of total RNA from control and Cu-adapted cell suspensions were denatured for 3 min at 65 ºC and separated by electrophoresis on a 1.2% (w/v) agarose gel containing formaldehyde as a denaturing agent. The gel was transferred onto a charged nylon membrane (Hybond-N^+, Amersham-Pharmacia Biotech, Buckinghamshire, UK) by capillary blotting and fixed by 5 min UV and 2 h at 80 ºC. The two *GmHMA8* probes were produced by amplifying a 350 bp fragment with the primers GmHMA8-1 and GmHMA8-2 (Table 7-1) and by excising a 793 bp fragment from the cloned

GmHMA8 by digestion with *Eco*RI, respectively. Radiolabeled probes were generated by random priming using ^{32}P-dCTP according to the manufacturer's instructions (ReadyPrime^{TM} labelling kit, Amersham Pharmacia, Biotech, Little Chalfont, UK). Blot prehibridazation was performed for 4 h at 42 ºC in prehibridazation buffer followed by 24 h at 42 ºC of hybridation in the same solution after addition of the *GmHMA8* probe. Blot was washed twice with 2 × SCC, 0.1% SDS (w/v) and with 0.1 × SCC, 0.1% SDS (w/v) for 5 min each at room temperature (Sambrook and Russel, 2001). Blot was exposed to x-ray film to obtain autoradiograms.

7.3.9. Expresion analysis of *GmCCS* mRNA

Specific gene primers were designed on the mRNA sequence of soybean *CCS* deposited in GenBanK (AF329816) (Table 7-1). The PCR mixture had 10 μl cDNA, 0.7 mM dNTPs, 4 mM $MgCl_2$, 0.5 μM primer 5', 1 μM primer 3' and 5 units of taq polimerase (platinum taq DNA polimerase, Invitrogen). The PCR procedure consisted of an initial denaturation step at 94 ºC and 35 cycles of the following steps: denaturation at 94 ºC for 30 s, annealing at 53 ºC for 30 s, and extension at 72 ºC for 1 min. A final elongation step was performed at 72 ºC for 10 min. The resulting PCR products were cloned into the pGEM-T Easy vector (Promega, Madison, WI, USA) and sequenced (CNIO service, Madrid, Spain) to check their identity.

7.3.10. Sequence analysis

Alignment of HMA8 sequences was performed using ClustalW programme (Thompson et al., 1994). The identification of putative introns in *GmHMA8* sequences was done with GenScan Web Server (Burge and Karlin., 1997). The percentage of identities and similarities at the amino acid level were calculated using the BLAST programme.

Table 7-1. Primers used for the isolation and characterization of *GmHMA8* and *GmHMA8-T*.

Primer name	Forward/ Reverse	Primer sequence (5' → 3')
P-ATPase	forward	TT(TC)GA(TC)AA(AG)AC(TCA)GG(TCAG)AC(TCA)(TC)T(TCAG)AC(TCA)
	reverse	(GTCA)A(AG)(AGT)GC(AGT)GG(AGT)G(AG)TC(AG)TT(AT)AT(TCAG)CC'
UTRGmHMA8	reverse	CATGCTAGGATACTTCATGAGA
GmHMA8-1	forward	5'-GCTGAGTCATTAGAGTTGG
GSP1	reverse	ACCAATGATGCCTTCTCCTTCACG
GSP2	reverse	AGTTTCTGAATACTTTGAAGATGT
GSP3	reverse	GCACGCGCCGCACATCATCCC
5' GeneRacer Primer	forward	CGACTGGAGCACGAGGACACTGA'
5' GeneRacer Nested Primer	forward	GGACACTGACATGGACTGAAGGAGTA'
UTRGmHMA8	reverse	CATGCTAGGATACTTCATGAGA
GmHMA8-2	reverse	AGTTGCAACTGCCTCTTCCC
NSPHMA8	reverse	TGAATTTGGCAGATGGCATAG
NSPHMA8-T	reverse	AGGGTGTATGTTACAATGATG
CCS1	foward	GGCATTTCTGAGGTCAATAGCA
CCS2	reverse	GGTAGAGCTGATGGGCGACAAT

7.4. RESULTS

7.4.1. Identification of two *HMA8* mRNAs in soybean

Soybean cDNA amplification was done by RT-PCR using degenerated primers designed from *in silico* data analysis (for details see Materials and Methods and chapter 6, section 6.3.1). Two groups of cDNA bands were reproducibly amplified under these conditions (Fig. 7-1, lane 1). One group migrated at positions corresponding to 1.0-1.2 kb, and other group at positions above 0.7-0.8 kb. As mentioned in chapter 6 (section 6.4.1), we assigned the *c.a* 0.7-0.8 kb band to P_{1B}-ATPases taking into account their structural characteristics. The sequence analysis of clones obtained from the 0.7-0.8 kb band yielded two nucleotide sequences that were highly similar (> 45%) to the

corresponding regions of PacS (sll1920) and *At*HMA8 (PAA2) (At5g21930). One of them (793 bp) corresponded with a region of the full-length *Gm*HMA8 protein identified previously (DQ418731).

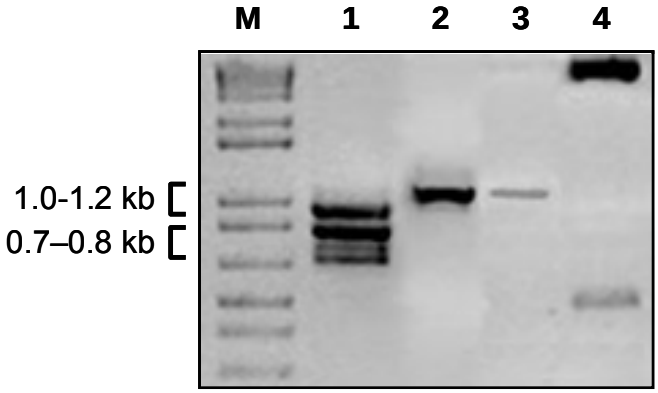

Fig. 7-1. Expression of *P-ATPase* family and *GmHMA8* in soybean photosynthetic cell suspensions. *Lane M*, 1.0 kb plus DNA ladder; *lane 1*, RT-PCR of *P-ATPase* family with degenerated primers: 1.0-1.2 kb bands correspond with classical *P-ATPases (Ca-ATPase, H^+-ATPase)* and 0.7-0.8 kb bands correspond with *P_{1B}-ATPases (Cu-ATPases); lane 2*, Amplification of 3'-end of *GmHMA8* including part of 3'-UTR; *lane 3*, *Acc*I digestion of band from *lane 2*; *lane 4*, positive control of *Acc*I digestion.

The analysis also revealed a 668 bp sequence with high homology to *GmHMA8* (Fig. 7-2) but presented certain differences compared with that. Such differences consisted in several base substitutions that resulted in amino acid changes and a 7-bp deletion (379-385 bp) (Fig. 7-2). This deletion leads to a change in the frame shift of the *Gm*HMA8 protein that resulted in a stop codon leading to premature termination of the *Gm*HMA8 protein. This 668 bp sequence namely as *GmHMA8-T* (*Gm*HMA8 truncated) was deposited in GenBank as DQ865164. The 7-bp deletion generates an *Acc*I restriction site in their sequence. This specific characteristic was used to identify the two mRNAs of *GmHMA8* found by digestion of PCR bands. The alignment of both mRNAs is shown (Fig. 7-2).

The derived partial amino acid sequences of *Gm*HMA8 and *Gm*HMA8-T proteins were aligned with the rest of the HMA8 polypeptides available in databases (Fig. 7-3). The *Gm*HMA8 protein resulted in a 45% similarity to PacS, 83% to *At*HMA8/PAA2, 84% to *Os*HMA8, and 88% to *Lc*HMA8 in the overlapping amino acids. *Gm*HMA8-T protein was more divergent and shared

only 30% similarity with PacS, 68% with *At*HMA8/PAA2, 56% with *Os*HMA8, and 76% with *Lc*HMA8 in the overlapping amino acids.

To further characterize *GmHMA8* and *GmHMA8-T* sequences we carried out a RT-PCR using a pair of primers, the forward one (GmHMA8-1) designed in the common sequence of both mRNAs and the reverse one (UTRGmHMA8) designed in the 3'-UTR region obtained from the *GmHMA8* EST (TC228758) (Table 7-1). These primers amplified a 971-bp product that corresponded well with the expected size (Fig. 7-1, lane 2). The band was purified and subsequently digested with *Acc*I. As shown in Fig. 7-1, lane 3, there was no digestion of the PCR product. The digestion positive control is shown in Fig. 7-1, lane 4. These results indicated that the primers used in this assay were specific of the full-length *GmHMA8* form and did not amplify the truncated one. This suggests that both mRNAs have different 3´-UTR sequences and thus could correspond with two independent genes. However, we cannot preclude the possibility that both sequences could correspond with two different alleles of a single copy gene, one of them corresponding to the mature form of *Gm*HMA8 and the other one corresponding to a null allele. The presence of null-alleles has been reported for the *At*HMA8 (PAA2) P_{1B}-ATPase (Abdel-Gahny et al., 2005b). Segregation experiments would be required to further confirm any of both hypotheses.

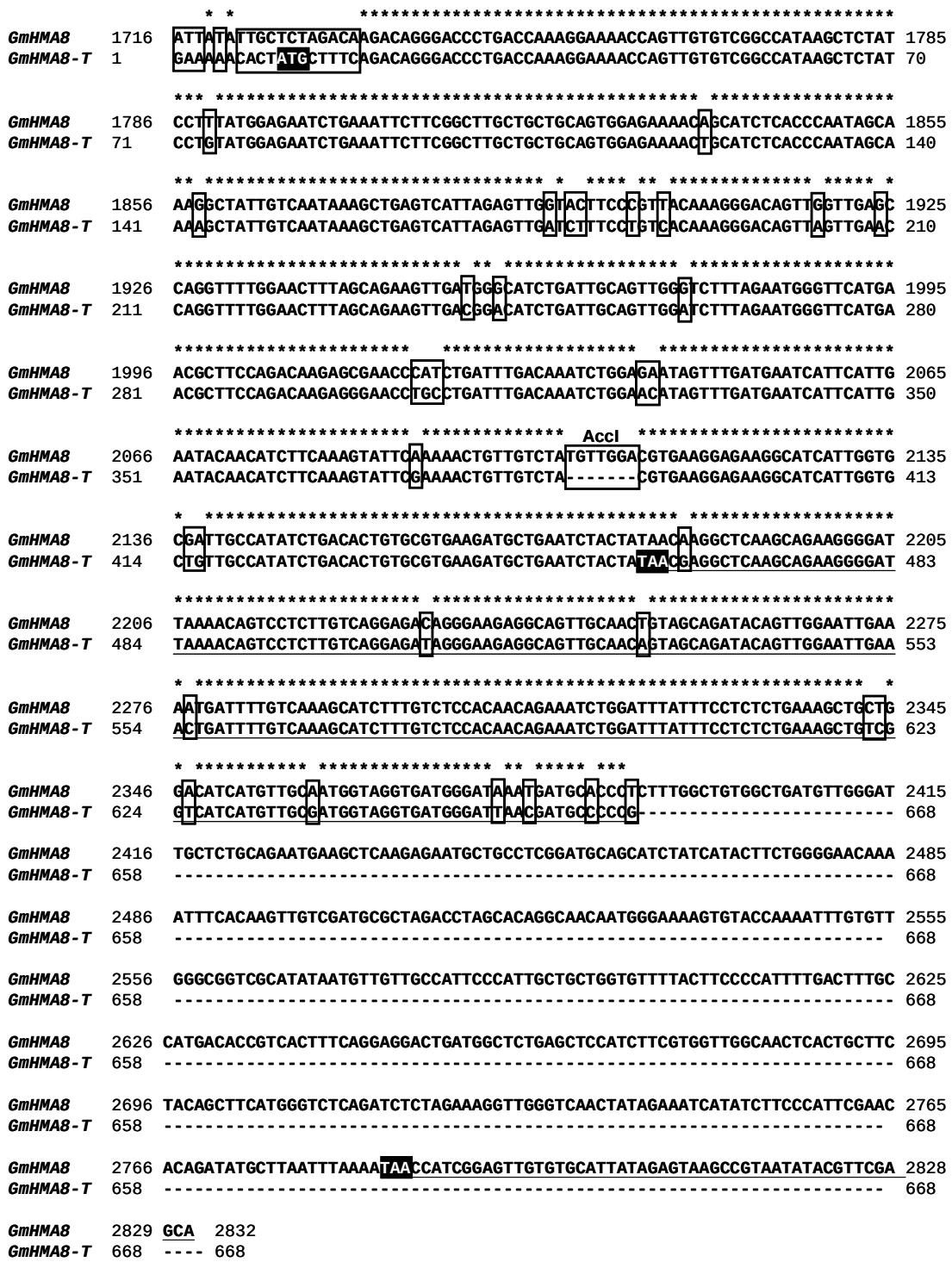

Fig. 7-2. Alignment of *GmHMA8* region (1716-2838 bp) and *GmHMA8-T* (1-668 bp). Identical bases are indicated by asterisks above the alignment. Start codon in *GmHMA8-T* and codon stops in both sequences are in black. The 3'-UTR regions are underlined. Different bases between both mRNA sequences are boxed.

```
                    * **+  + **    *       *****+*+* *+   ++   + +  +*  **++*  + **+* **+   +   +
GmHMA8          535 GLLIRGGDVLERLAGINYIAIDKTGTLTKGKPVVSAISSILYGESE--ILRLAAAVEKTASHPIAKAIVNKAESLELVLP 58
GmHMA8-T        1   -----------------KTLCFQTGTLTKGKPVVSAISSILYGESE--ILRLAAAVEKTASHPIAKAIVNKAESLELIFP 61
AtHMA8          527 GYLIRGGDVLERLASIDCVALDKTGTLTEGRPVVSGVASLGYEEQE--VLKMAAAVEKTATHPIAKAIVNEAESLNLKTP 604
OsHMA8          550 GLLIRGGDVLERLAGIDAIVLDKTGTLTKGRPVVTSIASLAYEEAE--ILRLAAAVEKTALHPIANAIMEEAELLKLDIP 627
LcHMA8          532 GLLIRGGDVLERLASINYIALDKTGTLTRGKPVVSAIGSLQYGESD--ILQIAAAVEKTASHPIAKAIVNKADSLDLVLP 609
PacS            413 GILIKSAESLELAQTIQTVILDKTGTLTQGQPSVTDFLAIGDRDQQQTLLGWAASLENYSEHPLAEAIVRYGEAQGITLS 492

                            ** *   ++++  + +*+  *+          + +                      +++  *  +*  +
GmHMA8           59 VTKGQLVEPGFGTLAEVDGHLIAVGSLEWVHERFQTRANPSDLTNLENSLMNHSLNTTS--SKYSKTVVYVGREGEGIIG 136
GmHMA8-T         59 VTKGQLVEPGFGTLAEVDGHLIAVGSLEWVHERFQTRGNLPDLTNLEHSLMNHSLNTTS—-SKYSET VVYVKEKASLVL 138
AtHMA8          605 ETRGQLTEPGFGTLAEIDGRFVAVGSLEWVSDRFLKKNDSSDMVKLES-LLDHKLSNTSSTSRYSKTVVYVGREGEGIIG 683
OsHMA8          628 ATSGQLTEPGFGCLAEVDGCLVAVGTLDWVHNRFETKASSTELTDLGNHLEFVSSSEAS--SNHSKSIAYVGREGEGIIG 705
LcHMA8          610 VTKGQLVEPGFGTLAEIDGRLVAVGSLEWVHQRFQTRMNPSNLMNVEQTLLNHSLNSTS--SKYSRTVVYVGREGEGIIG 687
PacS            493 TVTDFEAIPGSGVQGQVEGIWLQIGTQRWLG---ELGIETSALQNQWEDWEAAG----------KTVVGVAADG-HLQA 557

                       +   ++      +  *++  +   +*+**       +   ***        + * +*   ++ *+  *  *******
GmHMA8           137 AIAISDTVREDAESTITRLKQKGIKTVLLSGDREEAVATVADTVGIENDFVKASLSPQQKSGFISSLKAAGHHVAMVGDG 216
GmHMA8-T         139 LPYLTLCVKMLNLL ------------------------------------------------- ---------------152
AtHMA8           684 AIAISDCLRQDAEFTVARLQEKGIKTVLLSGDREGAVATVAKNVGIKSESTNYSLSPEKKFEFISNLQSSGHRVAMVGDG 763
OsHMA8           706 AIAVSDVLRDDAKATVDRLQQEEILTFLLSGDRKEAVESIGRTVGIRSENIKSSLTPHEKAGIITALQGEGRRVAMVGDG 785
LcHMA8           688 AIALSDIVREDAESTVMRLKQKGIKMVLLSGDREEAVATIAETVGIENDFVKASLAPQQKSEFISSLKAAGHHVAMVGDG 767
PacS             558 ILSIADQLKPSSVAVVRSLQRLGLQVVMLTGDNRRTADAIAQAVGIT--QVLAEVRPDQKAAQVAQLQSRGQVVAMVGDG 635

                    *****+** ****+*+      + *  *+ + *+   +  ++ *+ *+++**  + *** +*  **+  ******+* *
GmHMA8           217 INDAPSLAVADVGIALQNEAQENAASDAASIILLGNKISQVVDALDLAQATMGKVYQNLCWAVAYNVVAIPIAAGVLLPH 296
GmHMA8-T         152 ---------------------------------------------------------------------------- 152
AtHMA8           764 INDAPSLAQADVGIALKIEAQENAASNAASVILVRNKLSHVVDALSLAQATMSKVYQNLAWAIAYNVISIPIAAGVLLPQ 843
OsHMA8           786 INDAPSLAAADVGVAMRTNSKESAASDAASVVLLGNRLSQVMDALSLSKATMAKVHQNLAWAVAYNIVAIPIAAGVLLPQ 865
LcHMA8           768 INDAPALAVADVGIALQNEAQENAASDAASIILLGNKISQVVDAIDLAQSTMAKVYQNLSWAVAYNVIAIPIAAGVLLPH 847
PacS             636 INDAPALAQADVGIAIGTG--TDVAIAASDITLISGDLQGIVTAIQLSRATMTNIRQNLFFAFIYNVAGIPIAAGILYPL 713

                      + ++* *+
GmHMA8           297 FDFAMTPSLSGGLMALSSIFVVGNSLLLQLHGSQISRKVGSTIEIISSHSNTDMLNLK 908
GmHMA8-T         152 ------------------------------------------------------- 152
AtHMA8           844 YDFAMTPSLSGGLMALSSIFVVSNSLLLQLHKSETSKNSL------------------ 883
OsHMA8           866 FDFAMTPSLSGGLMALSSIFVVSNSLLLQLHGSFQSTEKQREDLNSRLN--------- 914
LcHMA8           848 FDFAMTPSLSGGMMALSSIFVVSNSLLLQLHGSQTSRKGSLT---------------- 889
PacS             714 LGWLLSPMLAGAAMAFSSVSVVTNALRLRQFQPR----------------------- 747
```

Fig. 7-3. Partial alignment of soybean *Gm*HMA8 (535-908 aa) (DQ418731) and GmHMA8-T (DQ865164) with HMA8 proteins from *A. thaliana* (527-883 aa) (*At*HMA8/PAA2, At5g21930), *Oryza sativa* (550-914) (*Os*HMA8, XP_470523), *Lotus corniculatus* var. *japonicus* (532-889 aa) (*Lc*HMA8) and *Synechocystis* PCC 6803 (413-747 aa) (PacS, sll1920). This alignment includes the large cytoplasmatic loop of P_{1B}-ATPases, the two last putative transmembrane regions and the C-terminal extreme. Identical residues are indicated by stars (*), and conservative residues are indicated by crosses (+). Functional regions are indicated in bold (DKTGT, phosphorylation domain; HP, HP dipeptide; GDGINDAP, ATP binding domain).

7.4.2. *GmHMA8* and *GmHMA8-T* mRNAs are alternatively spliced

To characterize the expression profile of *GmHMA8* and *GmHMA8-T* mRNAs, RT-PCR experiments were performed by using two specific primers (GmHMA8-1 and GmHMA8-2) (Table 7-1, Fig. 7-4). The sequence localization of both primers is shown in Fig. 7-6A. Two groups of cDNA bands were reproducibly amplified. One group of bands migrated at position corresponding to 685 bp and other group at 350 bp position (Fig. 7-4, lane 1). Sequence analysis revealed that clones from the higher band (685 bp) retained an intron of 292 bp in their sequence (2184-2470 bp) (Fig. 7-5, Fig. 7-6A). This sequence namely as *NSP GmHMA8* (non spliced *GmHMA8*) was deposited in GenBank as DQ865165. The presence of the intron in the *GmHMA8* mRNA sequence was also confirmed by PCR using genomic DNA from soybean cell suspensions and plants, and the same specific pair of primers (data not shown). The analysis also showed that the shorter RT-PCR band (350-bp) was identical to the *NSP GmHMA8* sequence, except for the absence of the intron. These results suggest that both transcripts were originated from the same gene. The shorter band (350-bp) was named as *GmHMA8*. This expression profile corresponds with a regulation by alternative splicing. Based on the alternative splicing classification it would correspond with the retained intron type, which is characterized by the intron inclusion or intron splicing in RNA sequence (Itoh et al., 2004).

In order to know if *GmHMA8-T* is regulated similarly to *GmHMA8* we analyzed their putative regulation by alternative splicing. For that, we used the specific *Acc*I restriction site found in *GmHMA8-T* sequence (Fig. 7-2, Fig. 7-6B). The higher (685 bp) and the shorter (350 bp) bands from RT-PCR experiment (Fig. 7-4, lane 1) were purified and subsequently digested with *Acc*I restriction enzyme, respectively (Fig. 7-4, lane 2 and 3). The digestion pattern demonstrated that *GmHMA8-T* is also regulated by alternative splicing. The retained intron for *GmHMA8-T* was 311 bp in length and it is located between 464-827 bp (Fig. 7-5, Fig. 7-6B). The fully-spliced and the non-spliced sequences were named as *GmHMA8-T* and *NSP GmHMA8-T*, respectively. The presence of this intron in the *GmHMA8-T* sequence was also confirmed by

PCR using genomic DNA from soybean cell suspensions and plants, the same specific pair of primers and subsequent digestion with *Acc*I (data not shown).

Interestingly, the results revealed two mRNA forms that corresponded with both fully-spliced and non-spliced transcripts for either *GmHMA8* or *GmHMA8-T*. Sequences of both non-spliced transcripts, *NSP GmHMA8* and *NSP GmHMA8-T*, are compared in Fig. 7-5. Introns from *NSP GmHMA8* and *NSP GmHMA8-T* transcripts belong to group II because follow the GT-AG rule (Sugiura and Takeda, 2000). As shown in Fig. 7-5, the intron sequences were different. This result supports the hypothesis that *GmHMA8* and *GmHMA8-T* could be two independent genes. Schematic representations of four identified transcripts are shown in Fig. 7-6.

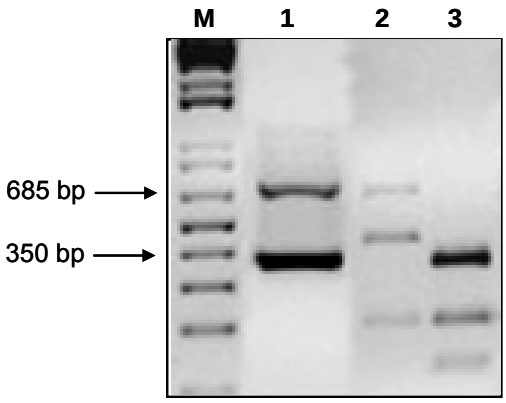

Fig. 7-4. Analysis of alternative splicing expression pattern of *GmHMA8* mRNAs in control soybean photosynthetic cell suspensions. Expression profile was determined by RT-PCR on RNA extracted from 21-days-old soybean cells. *Lane M*, 1.0 kb plus DNA ladder; *lane 1*, alternative splicing shown by RT-PCR; *lane 2*, *Acc*I digestion of the higher band (685 bp); *lane 3*, *Acc*I digestion of the shorter band (350 bp). Data shown are representative of at least two independent replicates.

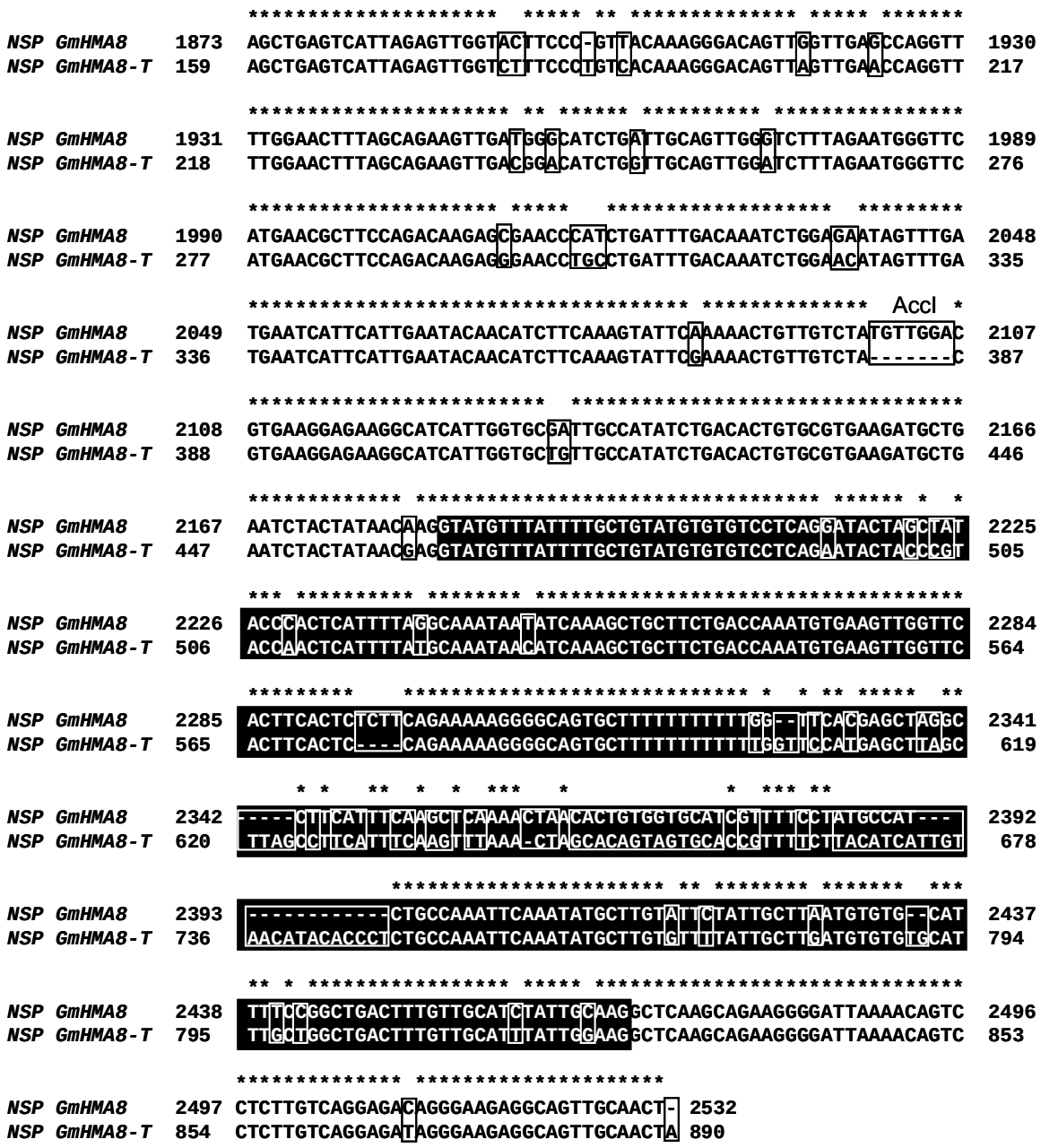

Fig. 7-5. Partial sequence alignment of non-spliced transcripts (*NSP GmHMA8* and *NSP GmHMA8-T*). Identical bases are indicated by asterisks above the alignment. Different bases between both mRNA sequences are boxed. Intron sequences are in black.

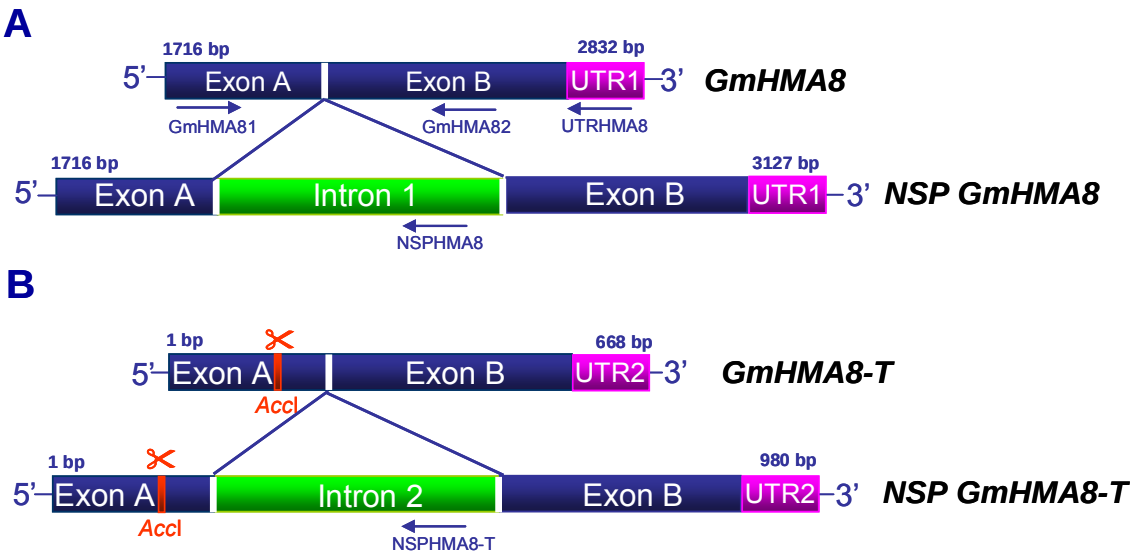

Fig. 7-6. Scheme of *GmHMA8* (A) and *GmHMA8-T* (B) mRNAs identified in soybean. The blue, green and pink boxes indicate the exon, intron and UTR regions, respectively. The red box indicates the 7-bp deletion sequence that is present in *GmHMA8-T* mRNA. The scissors shows the specific *Acc*I restriction site of *GmHMA8-T.* Primers for RT-PCR are shown with arrows indicating the polarity.

7.4.3. Copper affects patterns of alternatively spliced *GmHMA8* and *GmHMA8-T* mRNAs

The involvement of an alternative splicing mechanism in the biological function of either *GmHMA8* or *GmHMA8-T* was investigated. To that end, the expression of *GmHMA8* and *GmHMA8-T* and their respective non-spliced forms, *NSP GmHMA8* and *NSP-GmHMA8-T*, was assayed by RT-PCR in soybean photosynthetic cell suspensions treated with different copper concentrations and times (for details see Materials and Methods, section 7.3.7) In addition, the influence of copper on the four transcript expression in cell suspensions grown under two different growth conditions, photomixotrophically (KN^1) and photoautotrophically (KN^0), was also studied.

The expression pattern of the four *GmHMA8* transcripts is shown in Fig. 7-7A. The shorter band corresponded with spliced *GmHMA8* and *GmHMA8-T* mRNAs and the higher one with non-spliced *NSP GmHMA8* and *NSP GmHMA8-T* mRNAs (for details see scheme in Fig. 7-6). The results indicated that either copper or growth media conditions affect the expression of these four transcripts. The strongest changes were observed in Cu-adapted cells (Fig. 7-7A, lanes 3 and 6) in comparison with control ones (Fig.7-7A, lanes 1 and 4). Non-spliced transcripts were up-regulated while spliced ones were down-regulated independently of growth media conditions, although this effect was more pronounced in Cu-adapted cells grown photoautotrophically (Fig.7-7A, lane 6) compared with those grown photomixotrophically (Fig.7-7A, lane 3). Cu-deficient cells (Fig.7-7A, lane 7) also presented a similar regulation pattern although less pronounced, non-spliced transcripts were slightly up-regulated while spliced ones were slightly down-regulated in comparison with control cells. Surprisingly, in Cu-stressed cells such changes were not observed (Fig.7-7A, lanes 2 and 5). On the other hand, a different feature was observed in the expression pattern of Cu-reverted cells (Fig.7-7A, lanes 8, 9 and 10) where no significant presence of NSP transcripts were observed compared with control ones. Interestingly, Cu-reverted cells after five subsequently transfers without excess copper in the growth media showed that expression pattern turn a round to levels of control cells. Considering the above results, we can conclude that the alternative splicing pattern of *GmHMA8* and *GmHMA8-T* mRNAs mainly accompany to a copper long-term response. The presence of the four transcripts in all assayed conditions was confirmed by digestion with *Acc*I (Fig. 7-7B).

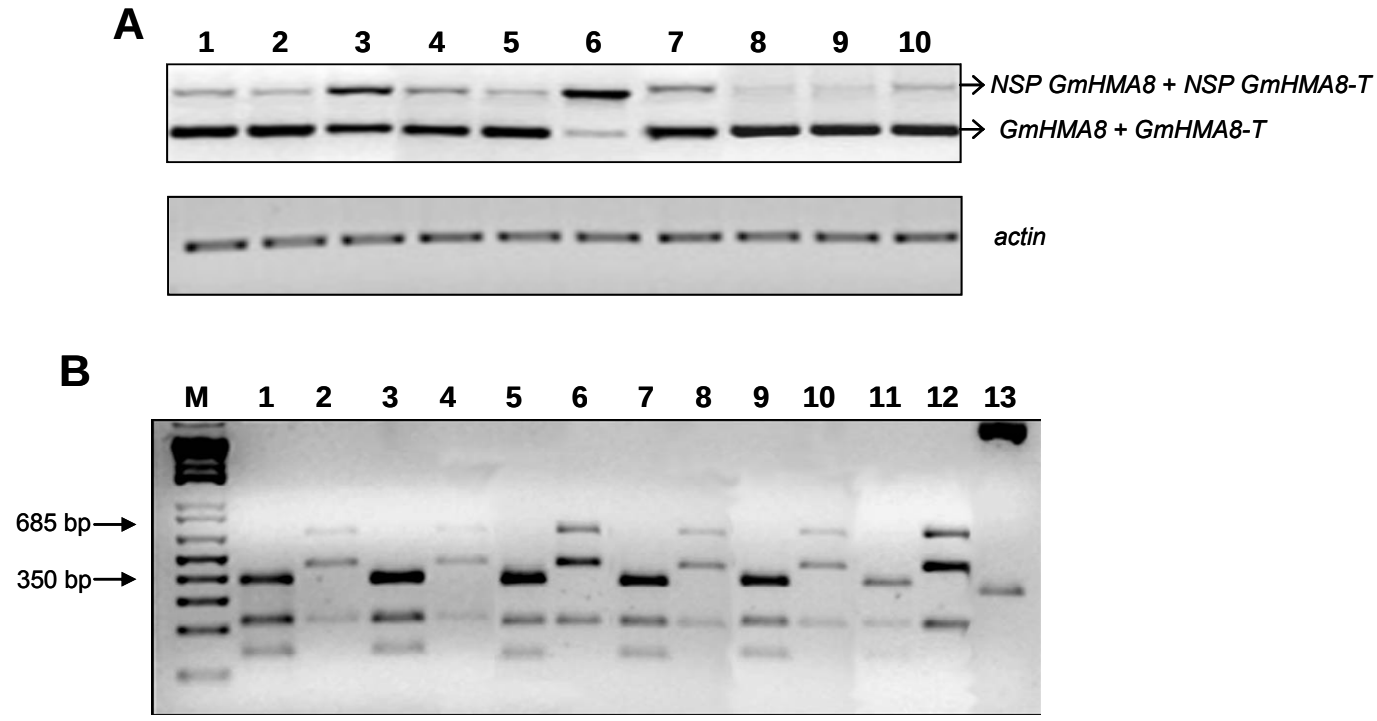

Fig. 7-7. A) Copper response of spliced *GmHMA8* (*GmHMA8* and *GmHMA8-T*) transcripts and their correspoding non-spliced transcripts (*NSP GmHMA8 and NSP GmHMA8-T*) respectively, in soybean photosynthetic cell suspensions. Expression profile of *GmHMA8* transcripts was determined by RT-PCR on RNA extracted from: *i)* control (*lane 1 and 4*); *ii)* Cu-stressed (*lane 2 and 5*); *iii)* Cu-adapted (*lane 3 and 6*); *iv)* Cu-deficient *(lane 7)*; *v)* Cu-reverted *(lanes 8, 9, 10)*. The influence of copper on *GmHMA8* expression in cells grown photomixotrophically (*lanes 1, 2, 3*) and photoautotrophically (*lanes 4, 5, 6*) is also compared. *Actin* is shown as an internal control. B) *Acc*I digestion of shorter band (350 bp) (*lanes 1, 3, 5, 7, 9, 11*) and higher band (685 bp) (*lanes 2, 4, 6, 8, 10, 12*) from: *i)* control cells (*lanes 1, 2, 7, 8*); *ii)* Cu-stressed cells (*lanes 3, 4, 9, 10*); *iii)* Cu-adapted cells (*lanes 5, 6, 11, 12*); The influence of copper on *GmHMA8* abundance transcripts is also compared in cells grown photomixotrophically (*lanes 1, 2, 3, 4, 5, 6*) and photoautotrophically (*lanes 7, 8, 9, 10, 11, 12*). *Lane M*, 1.0 kb plus DNA ladder. *Lane 13*, positive control digestion. Data shown are representative of at least two independent replicates. Note that different amounts of cDNA were loaded in each line to better visualize the digestion products.

To better analyze which of the four identified transcripts were more affected by the conditions assayed, we carried out RT-PCR experiments with specific pair of primers for each transcript except for *GmHMA8-T* (due to the high homology between *GmHMA8* and *GmHMA8-T*) (for details see Materials and Methods, section 7.3.7). The expression profile of *GmHMA8*, *NSP GmHMA8* and *NSP GmHMA8-T* are shown in Fig. 7-8A, B and C, respectively.

The results confirmed that the expression changes reported above (Fig. 7-7A) are mainly due to changes in the distribution of spliced versus non-spliced transcripts. Interestingly, the data showed that the expression changes observed in Cu-adapted cells grown either photomixotrophically or photoautotrophically are mainly due to changes in *GmHMA8* (Fig. 7-8A, lane 3 and 6) and *NSP GmHMA8* (Fig. 7-8B, lane 3 and 6) expression compared with control cells (Fig. 7-8A, lane 1 and 4; Fig. 7-8B, lane 1 and 4), being these changes stronger in cells grown photoautotrophically.

.

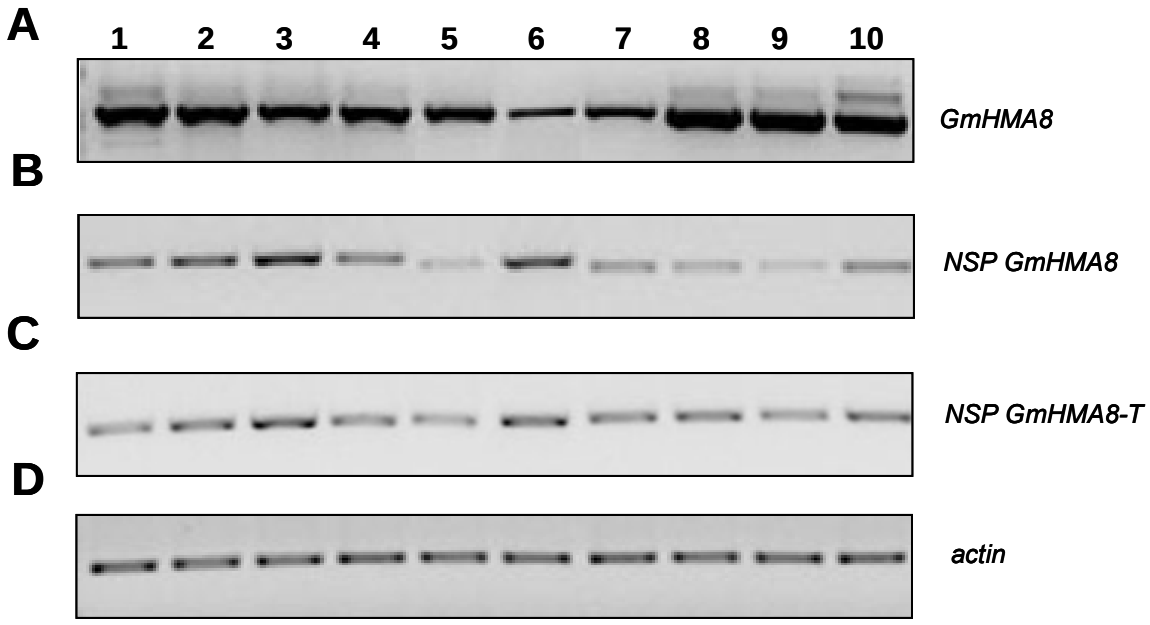

Fig. 7-8. Copper specific response of spliced *GmHMA8* (A), *NSP GmHMA8* (B) and *NSP GmHMA8-T* (C) transcripts respectively, in soybean photosynthetic cell suspensions. Expression profile was determined by RT-PCR on RNA extracted from: *i)* control (*lane 1 and 4*); *ii)* Cu-stressed (*lane 2 and 5*); *iii)* Cu-adapted (*lane 3 and 6*); *iv)* Cu-deficient (*lane 7*); *v)* Cu-reverted cells (*lane 8, 9 and 10*). The influence of copper on *GmHMA8* expression in cells grown photomixotrophically (*lanes 1, 2, 3*) and photoautotrophically (*lanes 4, 5, 6*) is also compared. *Actin* is shown as an internal control (D). Data shown are representative of at least two independent replicates.

On the other hand, a northern blot analysis of poly(A)$^+$ RNA from control and Cu-adapted cells grown photomixotrophically was carried out to determine the expression levels of *GmHMA8* and *GmHMA8-T* mRNAs and their corresponding non-spliced transcripts *NSP GmHMA8* and *NSP GmHMA8-T*

(Fig. 7-9). The results showed two bands that hybridized with *GmHMA8* probe. The lower band could correspond with spliced *GmHMA8-T* and the higher one with spliced *GmHMA8*. This result could indicate that *NSP GmHMA8* and *NSP GmHMA8-T* transcripts were not expressed at high levels. The expression pattern observed was similar to that detected by RT-PCR analysis as shown in Fig. 7-7A. Both transcripts were down-regulated in Cu-adapted cells (Fig. 7-9, lane 2) in comparison with control ones (Fig. 7-9, lane 1).

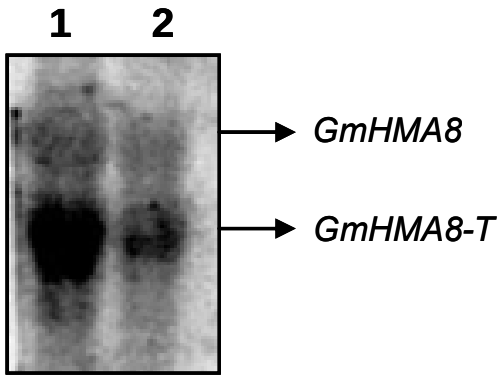

Fig. 7-9. Expression profile of *GmHMA8* transcripts in soybean photosynthetic cells grown photomixotrophically. The expression profile was determined by Northern Blot on RNA extracted from: 1) control (*lane 1*); 2) Cu-adapted cells (*lane 2*).

7.4.4. Copper increases CuZnSOD activity and *GmCCS* expression

The changes in the activity of SOD isoforms were analyzed as described by Beauchamp and Fridovich (1971) in control and in Cu-adapted cells grown photomixotrophically (Fig. 7-10A). In control cells (Fig. 7-10A, lane 1) the SOD activity mainly was due to MnSOD and FeSOD isoenzymes but in Cu-adapted cells, the CuZnSOD activity was strongly induced and the FeSOD activity was strongly repressed. The highest mobility band corresponds to the chloroplastic form (CuZnSOD2) and the other one to the cytosolic form (CuZnSOD1) (Shikanai et al., 2003).

The increase of the CuZnSOD activity was accompanied by an increase of the *GmCCS* mRNA expression in Cu-adapted cells in comparison with control ones (Fig. 7-10B). *GmCCS* encoded for the copper chaperone that

delivers copper to Cu/Zn superoxide dismutase (Cu/ZnSOD) (Abdel-Ghany et al., 2005b). This finding indicates that *GmCCS* mRNA is up-regulated by high levels of exogenous copper. These results were also independent on growth conditions (data not shown).

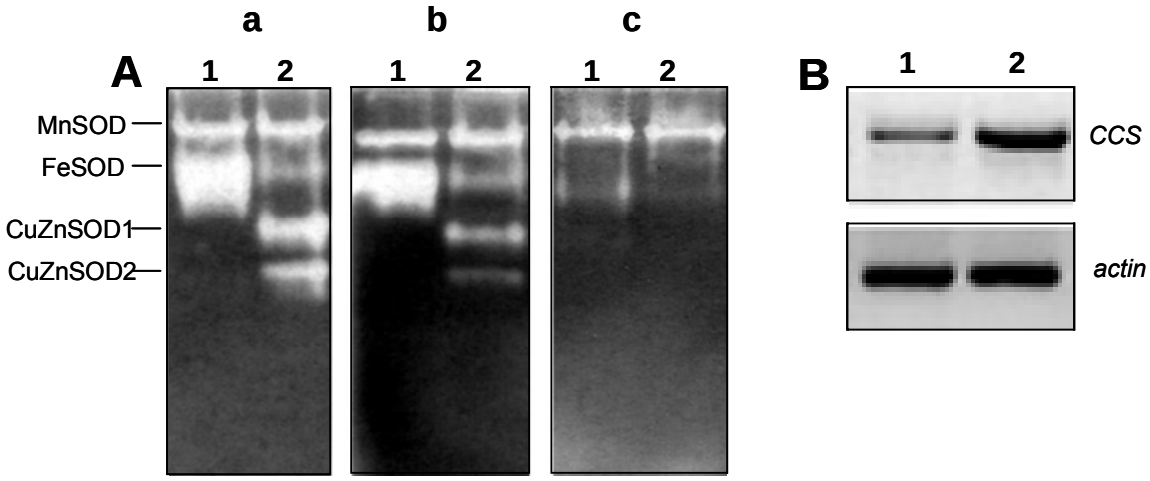

Fig 7-10. A) Native gel assays for the activity of the major SOD isoenzymes in the supernatant fraction (mainly chloroplast stroma fraction) of 18-day-old cell extract. Gels were preincubated with a) no inhibitor, b) KCN (it inhibits CuZnSOD), c) H_2O_2 (it inhibits both CuZnSOD and FeSOD), *Lane 1*; control cells; *lane 2*; Cu-adapted cells. B) Expression analysis of *GmCCS* in control (*lane 1*) and Cu-adapted cells (*lane 2*).

7.5. DISCUSSION

Using a screening with degenerated oligonucleotides we identified two different sequences of HMA8 in soybean (*GmHMA8* and *GmHMA8-T*), homologues to PacS and *At*HMA8 (PAA2) transporters (Tottey et al., 2001; Abdel-Ghany et al., 2005b). The results presented in this work suggested that *GmHMA8* and *GmHMA8-T* most probably are two independent genes because they had different 3' untranslated regions (3'-UTR) and different intron sequences in their non-spliced transcripts (*NSP GmHMA8* and *NSP GmHMA8-T*). However, we cannot absolutely exclude the possibility that both sequences correspond with two different alleles of a single copy gene, one corresponding with the mature form of *Gm*HMA8 and the other one corresponding with a null allele.

On the other hand, we demonstrated that both *GmHMA8* and *GmHMA8-T* mRNAs are alternatively spliced. Although numerous animal genes have been identified that are developmental stage-specific alternative spliced (Green, 1991), the role of alternative splicing in gene expression in plants is a relatively new area of research. This mechanism is thought to be less prevalent in plants than in humans. However, recent computational analyses of alternative splicing in *A. thaliana* are beginning to question this assertion (Kazan, 2003). Approximately 75% of the alternatively spliced genes in humans encode proteins involved in signalling and gene regulation (Modreck and Lee, 2002). Similarly, the great majority of alternatively spliced genes in *A. thaliana* encode proteins with regulatory functions. In addition, the genes associated with various stress (biotic, water, light, salt, wounding, heavy metal, heat) responses seem to be particularly prone to alternative splicing in both plants and animals (Kazan, 2003). Among the characterized alternative splicing mechanisms in plants, it has been described that *At*CUTA, a chloroplast protein involved in copper tolerance mechanism, is regulated by alternative splicing (Burkhead et al., 2003). Assuming that alternative splicing in plants is also associated with an increased evolutionary change, alternative splicing in stress-associated regulatory genes might be useful for acquiring certain adaptative benefits that are important for survival under stress conditions.

To our knowledge, there is no publication reporting a study of alternative splicing regulation of P_{1B}-*ATPase* genes in plants. However in humans, there is evidence of post-transcriptional modifications in the Menkes and Wilson Cu-ATPases yielding alternative spliced isoforms that show tissue-specific expression (Yang et al., 1997; Reddy and Harris, 1998). One of these alternatively isoforms is found predominantly in the cytosol and it lacks a number of residues, including the β-domain, the CPx motif and the last five metal-binding domains (Yang et al., 1997). It is thought that the loss of two transmembrane domains could prevent this protein from inserting into the membrane. Thus, it has been proposed that the shortened version of the Menkes ATPase may also yield a soluble protein and may have a role in copper-binding similar to that of the metal chaperone proteins ATX1 and HAH1 (Reddy and Harris, 1998).

The present study reports the first evidence of an alternative splicing mechanism for *GmHMA8* and *GmHMA8-T* P_{1B}-ATPases. This mechanism could have a role in controlling the functional characteristics of *GmHMA8* and *GmHMA8-T* altering their sequences by inclusion or exclusion of an intron, and translation of a full-length or a truncated protein. This fact potentially leads to the generation of structurally and/or functionally distinct proteins. Although the predicted protein translated from the fully spliced *GmHMA8* mRNA is 908 amino acids in length, translation of the non-spliced transcript *NSP GmHMA8* would result in a protein lacking C-terminal end because of stop codons in all reading frames of the retained intron. In the same way, the predicted protein translated from the fully spliced *GmHMA8-T* and *NSP GmHMA8-T* mRNAs would result in a protein lacking C-terminal end but different to the previous one because of stop codon generated for the 7-bp deletion. In this case, the intron sequence is not affected because it was located downstream of deletion. However, further investigations are necessary to confirm this preliminary hypothesis. In this way, the existence of a functional truncated protein of HMA4, a member of the P_{1B}-ATPase family, was shown in the cadmium hyperaccumulator *Thlaspi caerulescens* (Bernard et al., 2004).

The copper effect on the alternative splicing pattern of *GmHMA8* and *GmHMA8-T* was also analyzed. Our data showed that the expression of full-length *GmHMA8* and *GmHMA8-T* were down-regulated and non-spliced *NSP GmHMA8* and NSP *GmHMA8-T* were up-regulated in Cu-adapted cells. This regulation pattern was stronger in cells grown photoautotrophically than in cells grown photomixotrophically. This specific regulation of the full-length *GmHMA8* in Cu-adapted cells could be explained using the model for SOD regulation and Cu delivery system in chloroplasts proposed by Abdel-Ghany and coworkers (2005a; b). These authors hypothesized that for optimal photosynthesis, chloroplasts need to have a Cu delivery system that balances the activity of lumenal plastocyanin and stromal SOD enzymes under variable metal supply, ensuring that sufficient SOD activity is present to prevent oxidative damage if plastocyanin is present and PSI can be reduced. Our results demostrated that in Cu-adapted cells: *i)* the photosynthetic activity is stimulated; *ii)* CuZnSOD is induced and *iii) GmCCS* (copper chaperone for CuZnSOD) is up-regulated (for details see chapter 3, section 3.4.2; chapter 7, section 7.4.4). Thus, the fact that

the full-length *GmHMA8* expression level decreased in Cu-adapted cells could be in agreement with the balance between photosynthesis and SOD regulation that leads to increase the activity levels of CuZnSOD and the expression of *GmCCS* mRNA (Fig. 7-10A, B) to prevent the ROS that could be generated by the stimulated photosynthesis found within chloroplasts. Interestingly, the full-length *GmHMA8* was highly down-regulated in Cu-adapted cells grown photoautotrophically in comparison with those grown photomixotrophically. This fact might respond to the balance mentioned above that could be strongly displaced towards SOD regulation in these conditions.

Surprisingly, we observed that plastocianin was accumulated in Cu-adapted cells (chapter 3, Fig. 3-3B). In principle, this finding could be in disagreement with the model proposed by Abdel-Ghany et al. (2005a; b). However, this fact might be explained by an alternative low-affinity pathway for Cu delivery in chloroplasts. A candidate for this alternative transporter in the envelope is *At*HMA1 (Seigneurin-Berny et al., 2006). It is possible that HMA1 transports divalent ions, including Cu^{2+} and probably Zn^{2+}, and subsequently targets to CuZnSOD in the plastids. In thylakoids, the alternative transport activity could be explained by the energy-independent Cu^{2+} transport proposed by Shingles et al. (2004), but the component responsible for this activity is not still described.

In conclusion, in this chapter we report that two soybean Cu-transporting ATPases could exist in soybean. The identification of these *GmHMA8* gene products as putative Cu-ATPase proteins and the alternative processing of both *GmHMA8* forms could suggest that alternative splicing is an important mechanism in the control of copper homeostasis within chloroplasts.

CAPÍTULO 8

DISCUSIÓN GENERAL

La existencia de organismos fotosintéticos (cianobacterias, algas, plantas) tolerantes a concentraciones tóxicas de Cu (80-100 μM) ha sido descrita previamente en la literatura (Rai et al., 1991; Backor y Váczi, 2002; Landjeva et al., 2003). Por otro lado, también existen estudios que describen fenómenos de tolerancia en suspensiones celulares de origen vegetal aunque son escasos y limitados (Kishinami y Widholm, 1986; Turner y Dickinson, 1993; Gori et al., 1998; Raeymakers et al., 2003).

Los datos obtenidos en esta Tesis Doctoral demuestran que las suspensiones de células fotosintéticas de soja son capaces de desarrollar tolerancia a exceso de Cu (5-50 μM) y, por tanto, constituyen un buen sistema para estudiar los mecanismos de respuesta y adaptabilidad a este estrés. Las células crecidas en condiciones de exceso de Cu acumulan altos niveles de este metal y muestran un perfil de curva de crecimiento celular similar al de las células control en condiciones de luz normal (65 $\pm$ 5 μE m^{-2} s^{-1}). Sin embargo, en condiciones de luz limitante (30 $\pm$ 5 μE m^{-2} s^{-1}) el cultivo experimenta una estimulación del crecimiento siendo 2,5-3,0 veces más rápido que en condiciones de luz normal. Esta estimulación del crecimiento celular podría explicarse por una reactivación del ciclo celular que provocaría una mayor actividad proliferativa del cultivo y una mayor división celular debida a la estimulación de la fase S de este proceso.

Las células adaptadas a Cu presentaron un mayor contenido de clorofila y una mayor actividad fotosintética. Esta estimulación de la síntesis de clorofila podría deberse a un papel regulador del Cu en este proceso. En algas verdes (*Chlamydomonas reinhardtii*) y plantas (*A. thaliana*) se ha propuesto que la síntesis de clorofila podría estar regulada por este metal (Moseley et al., 2002; Tottey et al., 2003). De acuerdo con estos resultados, se ha observado que en los mutantes *paa1* y *paa2* de *A. thaliana,* que se caracterizan por tener un transporte de Cu deficiente, se produce una reducción del contenido de clorofila y una reducción de la actividad fotosintética (Shikanai et al., 2003; Abdel-Gahny et al., 2005b).

Por otra parte, el patrón de distribución de las diferentes isoformas cloroplásticas de la enzima superóxido dismutasa (SOD) varió drásticamente en las células adaptadas a Cu. En concreto, se observó que en estas células se induce la actividad de las dos enzimas CuZnSOD cloroplástica y citosólica y

se inhibe la actividad de la enzima FeSOD, respecto a las células control. Esta alteración podría deberse a la participación del Cu como elemento regulador de las SODs tanto a nivel transcripcional como postranscripcional (Kurepa et al., 1997), o a la mayor producción de radical O_2^- en las células adaptadas a Cu como resultado de la estimulación del transporte electrónico fotosintético. A este respecto, los cloroplastos pueden considerarse potencialmente como la mayor fuente de especies reactivas de oxígeno en tejidos vegetales (Barstosz, 1997).

A la vista de estos signos de tolerancia a Cu en las suspensiones celulares de soja, nos pareció interesante estudiar la respuesta al exceso de este metal, tanto a corto ("Cu-stressed cells") como a largo plazo ("Cu-adapted cells"), para, así, profundizar en el conocimiento de los mecanismos de respuesta y adaptabilidad de estas células ante este estrés.

Los resultados mostraron que, tanto las células estresadas por Cu como las células adaptadas a Cu, tienen una organización celular similar a la de las células control ("control cells"). Esta organización celular se corresponde bien con las características estructurales específicas de las células del mesófilo de hojas jóvenes como son: *i)* la presencia de una vacuola que ocupa prácticamente todo el volumen celular; *ii)* un núcleo con forma redondeada localizado en la periferia de la célula con la cromatina en estado descondesado; *iii)* la localización de los cloroplastos en la periferia celular. Además, se detectaron características estructurales específicas de células proliferativas como son la existencia de cuerpos de Cajal (Beven et al., 1995; Testillano et al., 2005; Seguí-Simarro et al., 2006) y de puentes citoplasmáticos (Satpute et al., 2005).

Sin embargo, además de estas semejanzas se observaron cambios en determinados compartimentos subcelulares. En particular, el cloroplasto y en menor medida la vacuola fueron los dos orgánulos celulares más afectados por este metal.

Los cloroplastos tanto de las células estresadas por Cu como de las células adaptadas a Cu fueron de menor tamaño y de forma más redondeada que los de las células control. Estas modificaciones contrastan con los datos publicados en cultivos celulares de *Nicotiana tabacum* tolerantes a 100 μM de

Cu (Gori et al., 1998) y en plantas de *Triticum durum* expuestas a 10-50 μM de Cu (Ciscato et al., 1997, Quartacci et al., 2000) donde no se observaron diferencias significativas en el tamaño y forma de este orgánulo subcelular. Sin embargo, también existen trabajos donde se señalan cambios en la morfología del cloroplasto similares a los observados en las suspensiones celulares de soja tratadas con exceso de Cu. Así, en plantas de *A. thaliana* expuestas a 50 μM de Cu se ha observado que los cloroplastos son más redondeados en comparación con las plantas control (Wójcik y Tukiendorf, 2003). Además, existen evidencias experimentales en la literatura de la diferente respuesta de este orgánulo frente al tratamiento con otros metales: *i)* en plantas de rábano (*Raphanus sativus*) y de *Myriophyllum spicatum* expuestas a cadmio (Cd) (0.5-1.0 mM) se observó un aumento del tamaño del cloroplasto (Stoyanova y Tchakalova 1997; Vitoria et al., 2004); *ii)* en plantas de col (*Brassica oleracea* L.) expuestas a niquel (Ni) los cloroplastos fueron más numerosos y de menor tamaño (Molas, 2002); *iii)* en dos genotipos diferentes de plantas de soja (*Glycine max*) (PI227557 y Biloxi) el exceso de manganeso (Mn) no alteró la estructura cloroplástica (Izaguirre-Mayoral y Sinclair, 2005). Esta variabilidad en la respuesta del cloroplasto podría depender del tipo de metal aplicado y su concentración y del tiempo de exposición al mismo.

Los cloroplastos de las células estresadas y adaptadas a Cu fueron más numerosos que en las células control. Este fenómeno podría compensar la reducción del tamaño de los cloroplastos en las células tratadas con Cu, tanto estresadas como adaptadas, que ayudaría a mantener el contenido de plastidios por célula. Recientemente, se han caracterizado unos mutantes en *A. thaliana* que tienen alterado el proceso de acumulación y replicación de los cloroplastos (*arc,* "accumulation and replication of chloroplasts"). Estos mutantes tienen menor número de cloroplastos y de mayor tamaño debido a la existencia de un mecanismo de compensación (Austin II y Webber, 2005). Por otro lado, se ha propuesto que la movilidad de los cloroplastos asegura una mayor absorción de la luz y una mayor protección frente a procesos de fotoinhibición, situación que se ve favorecida cuando los cloroplastos son de menor tamaño (Jeong et al., 2002). De acuerdo con estos autores se podría pensar que la reducción del tamaño de los cloroplastos observada en las células tratadas con Cu podría responder a un mecanismo de protección.

Otra característica diferencial de los cloroplastos de las células tratadas con Cu, tanto estresadas como adaptadas, fue la ausencia de acúmulos de almidón. Este hecho contrasta con el aumento del contenido de almidón observado en plantas de *A. thaliana* y pepino (*Cucumis sativus*) tras ser tratadas con exceso de Cu (Wojick y Tukiendorf 2003; Alaoui-Sousee et al., 2004). De forma similar, el estrés causado por exceso de Cd o Ni en plántulas de arroz (*Oryza sativa*) y de col (*Brassica oleracea* L.) fue acompañado por un aumento en el contenido de carbohidratos (Moya et al., 1993; Molas, 2002). La relación existente entre la acumulación de almidón en los cloroplastos de hojas de plantas estresadas y la inhibición de la fotosíntesis está bien documentada (Foyer, 1988; Moya et al., 1993). Una acumulación del almidón podría deberse a una disminución de la utilización de asimilados en los órganos correspondientes de la planta. Por el contrario, una falta de acumulación podría ser consecuencia de un metabolismo más activo. A este respecto, es de destacar que en las células adaptadas a Cu el crecimiento celular está estimulado. Sin embargo, es interesante subrayar que el efecto del exceso de Cu sobre la acumulación de almidón se observó ya en las células estresadas y que en estas células no se observó una estimulación del crecimiento. El hecho de que el contenido de almidón disminuya fuertemente, tanto en las células estresadas por Cu como en las adaptadas a Cu, sugiere que este fenómeno se pueda considerar como una respuesta a corto plazo al estrés por este metal. Por otro lado, este fenómeno acompañó a una reducción del tamaño del cloroplasto en estas células. Recientemente se ha demostrado que la manipulación de ciertos genes implicados en la división del cloroplasto puede modificar la distribución y el tamaño de los gránulos de almidón (De Parter et al., 2006). Así, se podría pensar en establecer una posible relación entre el metabolismo del almidón en el cloroplasto y el mecanismo de división de este orgánulo.

Como ya se ha mencionado anteriormente, otro orgánulo que se vió afectado por el tratamiento con exceso de Cu fue la vacuola. La acumulación de metales en la vacuola es un mecanismo de detoxificación ampliamente conocido que ayuda a mantener la concentración adecuada del metal en los restantes compartimentos subcelulares (cloroplastos, citoplasma, núcleo) (Hall y Williams, 2003). Las células adaptadas a Cu presentaron un mayor tamaño

de la vacuola en comparación con las células control y las células estresadas por Cu. Este hecho, podría estar relacionado con el mayor contenido de Cu presente en la vacuola de las células adaptadas en comparación con las células control y estresadas.

Las modificaciones estructurales que aparecen en los cloroplastos fueron independientes del tiempo de exposición al metal, por tanto, pueden considerarse como una respuesta a corto plazo que se mantiene durante el proceso de aclimatación. Sin embargo, las modificaciones en la vacuola estarían más bien asociadas a una respuesta a largo plazo.

Es también de destacar que en las células estresadas por Cu aparecen unos depósitos extracelulares en la pared celular con alto contenido de Cu que no se observan ni en las células control ni en las células adaptadas a Cu. Este hecho parece indicar que la presencia de estos depósitos es debida a una respuesta a corto plazo que desaparece al aumentar el tiempo de exposición al metal. Depósitos extracelulares de características similares se han observado también como respuesta al estrés por cadmio (Cd) en hojas de rábano (*Raphanus sativus*) (Vitória et al., 2006). La presencia de estos depósitos extracelulares fue acompañada por un mayor contenido de citrato comparado con las células adaptadas a Cu. Esto podría deberse a que en las células estresadas el Cu estimula la síntesis de citrato durante los primeros días de tratamiento como estrategia para prevenir su toxicidad. Datos similares se han observado en cultivos celulares de *Nicotiana plumbaginifolia* tolerantes a Cu (Kishinami and Widholm, 1987).

Las estrategias descritas en la literatura para prevenir y evitar la toxicidad provocada por el exceso de metales son variadas. Como primera barrera se ha descrito que compuestos extracelulares tales como ácidos orgánicos, carbohidratos, proteínas y péptidos pueden inmovilizar el metal a nivel de la pared celular (Delhaize y Jones, 2001; Hall y Williams, 2003). Sin embargo, la importancia de estos mecanismos puede variar en función de la concentración de metal aplicada, la planta tratada y los tiempos de exposición. La excreción de ácidos orgánicos como citrato, malato y oxalato entre otros, está correlacionada con la aclimatación y tolerancia de las plantas superiores a metales (Rauser, 1999; Delhaize y Jones, 2001). En el caso del Cu, se ha observado que este metal es un eficiente inductor de la exudación de ácidos

orgánicos por la raíz (Yang et al., 2001), principalmente de citrato (Murphy et al., 1999).

Teniendo en cuenta todos los resultados expuestos anteriormente, se puede argumentar que durante el proceso de aclimatación y adaptación de las suspensiones celulares a crecer en presencia de exceso de Cu se activan diferentes mecanismos dependiendo del tiempo de exposición a dicho metal. Así, en una respuesta a corto plazo, las células estresadas por Cu evitarían la entrada del Cu inmovilizándolo en la pared celular en forma de depósitos extracelulares, posiblemente por unión a citrato entre otros compuestos. Posteriormente en una respuesta a largo plazo, las células adaptadas a Cu almacenarían el exceso de Cu principalmente en la vacuola a través de un bombeo activo y una posterior formación de complejos orgánicos (ácidos orgánicos, metalotioneínas) en su interior. Sin embargo, a la vista de las modificaciones estructurales observadas en las células estresadas, no se puede descartar la posibilidad de que en una respuesta a corto plazo, el Cu entre a la célula para ser expulsado posteriormente en forma de complejo orgánico (Gledhill et al., 1999).

A la vista de que el cloroplasto sufre importantes alteraciones durante la exposición de las suspensiones celulares al exceso de Cu y que su contenido en clorofila y actividad fotosintética también se modifica, se estudió con más detalle el efecto del exceso de este metal tanto en la ultraestructura del cloroplasto como en la actividad de desprendimiento de O_2 de estas células, así como su influencia en la estructura y función del PSII.

Las células adaptadas a Cu mostraron una estimulación de la síntesis de plastocianina en comparación con las células control. Este hecho podría estar relacionado con la acumulación de Cu observada por EDX en los cloroplastos de estas células. La variación del contenido de plastocianina en función de los niveles de Cu existentes en el medio de cultivo, está ampliamente documentada en cianobacterias y algas verdes (Merchant, 1998).

Por otro lado, las células adaptadas a Cu mostraron un mayor grado de apilamiento de la membrana tilacoidal y una mayor emisión de fluorescencia del complejo antena del PSII en comparación con las células control. Este fenómeno podría deberse a una mayor relación PSII/PSI o al mayor nivel de apilamiento tilacoidal observado y agregación del PSII (Izawa y Good, 1966;

Chow et al., 1980). La primera hipótesis puede ser descartada debido a que la relación chla/chlb permaneció constante en todas las condiciones estudiadas. Por tanto, nuestros resultados serían mejor explicados con la segunda hipótesis.

Se conoce que la organización y distribución del PSII en las lamelas granales y estromales de la membrana tilacoidal es diferente. Así mientras que en las lamelas granales el PSII se encuentra en forma de dímero, en las lamelas estromales está en forma monomérica (Bassi et al., 1995). Estos autores también han demostrado que la composición polipeptídica del complejo de desprendimiento de O_2 (OECC) del PSII tanto en estado dimérico como monomérico es similar excepto en el nivel de la proteína extrínseca de 33 kDa (OEC33) que es menor en el PSII en estado monomérico. Las preparaciones de OECC dimérico son más estables, contienen altos niveles de clorofila y exhiben mayor actividad fotosintética que el OECC monomérico (Hankamer et al., 1997). Teniendo en cuenta estos datos, los resultados obtenidos en las suspensiones celulares de soja estarían de acuerdo con una mayor presencia de PSII en estado dimérico en los tilacoides de las células adaptadas a Cu. Este hecho también podría estar asociado con el mayor grado de apilamiento tilacoidal observado en las células adaptadas a Cu (Mullineaux, 2005). Del mismo modo, en las células control debería haber una mayor proporción de PSII en estado monomérico. Esta organización del PSII en el tilacoide podría explicar el hecho que la proteína extrínseca OEC33 se encuentre unida más débilmente a los complejos del PSII en las membranas estromales de las células control comparado con aquellas de las células adaptadas a Cu.

Otro resultado interesante es que las células adaptadas a Cu presentaron un contenido de Fe ligeramente superior a las células control. Este hecho podría explicar, el aumento significativo del contenido de clorofila en las células adaptadas a Cu, así como el mayor apilamiento del tilacoide y la estimulación de la actividad fotosintética. La importancia del Fe en la formación del aparato fotosintético está ampliamente documentada (Maschner, 1995; Raven et al., 1999). Sin embargo, la estimulación de la actividad fotosintética observada en las células adaptadas a Cu no sólo puede ser explicada por un aumento del contenido de Fe.

Con el fin de conocer si los efectos observados sobre la estructura del cloroplasto y la actividad fotosintética son específicos del tratamiento con exceso de Cu o si son comunes al tratamiento con otros micronutrientes en exceso, las células de soja se crecieron también en presencia de exceso de Fe y Zn. A este respecto, aunque se observó una acumulación de Fe tanto en las células crecidas con Zn como en las células crecidas con Fe, la modificación de la morfología del cloroplasto y la estimulación de la actividad fotosintética sólo se detectó en las células tratadas con Cu. Es interesante destacar que el contenido de Cu no aumentó con los tratamientos de Fe y Zn. Así, podríamos postular que el Cu tiene un efecto positivo y específico sobre la fotosíntesis.

Para profundizar en este aspecto, se estudió la posible correlación entre la estimulación por Cu de la actividad fotosintética *in vivo* y la publicada por otros autores *in vitro* (Burda et al., 2002; 2003). Para ello, se realizaron medidas de actividad de desprendimiento de O_2 en tilacoides aislados de células control y adaptadas a Cu previamente incubados con concentraciones subtóxicas de Cu(II), Ca(II), Fe(III) y Zn(II). Los resultados indicaron que concentraciones subtóxicas de Cu son capaces de estimular la actividad de desprendimiento de O_2 de los tilacoides aislados de las células control pero no la de los tilacoides aislados de las células adaptadas a Cu. Además, se observó que la inhibición de la actividad de desprendimiento de O_2 por concentraciones tóxicas de Cu fue menor en las células adaptadas a Cu que en las células control. Estos hechos podrían explicarse por: *i)* una menor accesibilidad del sitio de unión de Cu en el PSII debido a un cambio conformacional en la proximidad del mismo; *ii)* una mayor capacidad de secuestrar metales en las células adaptadas a Cu; *iii)* una menor toxicidad del Cu debido a cambios en la ultraestructura cloroplástica o en la composición lipídica. Estos resultados permiten sugerir que el Cu desempeña un papel positivo y específico en la fotosíntesis y en particular en la estructura y en la función del PSII.

La tolerancia a exceso de Cu desarrollada en las suspensiones de células fotosintéticas de soja contrasta con los datos recogidos en la literatura en planta entera (Baszynski et al., 1988; Lidon y Henriques, 1991 y 1993; Maksymiec, 1997; Ciscato et al., 1997; Pätsikkä et al., 1998; Quartacci et al., 2000; Franklin et al., 2002; Pätsikkä et al., 2002; Panou-Filotheou y

Bosabalidis, 2004; Kopittke y Menzies, 2006). Con el fin de investigar estas diferencias, se realizó un estudio comparativo en plantas de soja crecidas en medio hidropónico y sometidas a dos tipos de tratamiento con exceso de Cu: *1)* suplementación de Cu en el medio hidropónico; *2)* aplicación de Cu en las hojas. Con el primer tratamiento las plantas desarrollaron síntomas de toxicidad: *i)* inhibición del crecimiento de raíz; *ii)* clorosis; *iii)* menor contenido de clorofila por peso seco de hoja; *iv)* disminución de la actividad fotosintética. Sin embargo, el tratamiento foliar causó la estimulación de estos parámetros de forma similar a lo observado en las suspensiones celulares de soja adaptadas a Cu. Respecto a la adquisición de micronutrientes, se observó que con el tratamiento sobre las hojas la acumulación de Cu va acompañada por un aumento del contenido de Fe y un descenso del contenido de Zn. Este hecho contrastó con lo observado en las hojas de las plantas tratadas con Cu en el medio hidropónico. El antagonismo observado entre el Cu y el Zn ya ha sido descrito por otros autores (Herbick et al., 2002; Rombolá et al., 2005), sin embargo el agonismo existente entre el Cu y el Fe demostrado en este trabajo no se había descrito anteriormente en plantas.

La diferente respuesta de las plantas de soja tras los dos tipos de tratamiento de Cu podría explicarse asumiendo que las estrategias de adquisición y transporte de Cu en hojas y raíces son distintas. Aunque la competencia entre el Cu y el Fe está ampliamente documentada en plantas superiores (Schmidt, 1999; Pätsikkä et al., 2002; Chen et al., 2004; Rombolá et al., 2005), en otros organismos como mamíferos, levaduras o cierta clases de algas se ha observado que no existe tal competencia si no que la asimilación de Fe es dependiente de Cu (Franklin et al., 2002; La Fontaine et al., 2002; De Freitas et al., 2003). Estos datos permiten proponer que la homeostasis de Cu y Fe en las suspensiones de células fotosintéticas de soja podría ser similar a la de estos organismos. Por tanto, se puede sugerir que los mecanismos de homeostasis de Cu y Fe en las suspensiones celulares y en hoja difieren de los que tienen lugar en la raíz.

Teniendo en cuenta la capacidad que tiene esta línea celular de soja a adaptarse a crecer en presencia de exceso de Cu y la influencia que este metal tiene en la estructura cloroplástica y en la maquinaria fotosintética, se planteó iniciar el estudio de los mecanismos de homeostasis de Cu en el cloroplasto a

nivel molecular. A este respecto, se identificó un transportador de Cu en soja, que se denominó *Gm*HMA8, de la familia de P-ATPasas de tipo I_B homólogo a los transportadores PacS y *At*HMA8/PAA2 de *Synechocystis* PCC 6803 y *A. thaliana*, respectivamente, que podría participar en el transporte de Cu en el cloroplasto (Tottey et al., 2001; Abdel-Gahny et al., 2005b). El alineamiento de la secuencia de *Gm*HMA8 con las secuencias de transportadores HMA8 de otras plantas mostró que su secuencia está altamente conservada, esto podría reflejar la importancia de la función realizada por esta proteína. Además, el análisis "*in silico*" de la secuencia de aminoácidos de *Gm*HMA8 indicó que posee las regiones estructurales típicas de las P-ATPasas de tipo I_B (Axelsen y Palmgrem, 2001; Argüello, 2003; Williams y Mills, 2005) y una localización subcelular teórica cloroplástica (Emanuelsson et al., 1999).

Mediante un anticuerpo específico anti-*Gm*HMA8 producido a partir de un péptido sintético de 15 aminoácidos se abordaron los experimentos de localización subcelular de este transportador. La especificidad del anticuerpo anti-*Gm*HMA8 fue contrastada tanto en cloroplastos intactos y tilacoides aislados de células y plantas de soja como en cloroplastos de *Lotus corniculatus* var. *japonicus*. En todos los casos se detectó un único polipéptido de aproximadamente 180-200 kDa de masa molecular aparente que podría corresponder al transportador objeto de estudio. Sin embargo, el peso molecular aparente obtenido experimentalmente, tanto para *Gm*HMA8 como para *Lc*HMA8, resultó ser mayor que el calculado de forma teórica, 97 kDa y 95 kDa, respectivamente. Esta diferencia de tamaño podría deberse a que este transportador migra en el gel de acrilamida diferente a lo esperado (See y Jackowski, 1990) o a la presencia de formas oligoméricas.

Ensayos de inmunofluorescencia demostraron que el transportador de Cu, *Gm*HMA8, está localizado en el cloroplasto. Posteriores ensayos de inmuno-oro con este anticuerpo permitieron localizar de una forma más precisa este transportador en la membrana tilacoidal. Este hecho nos permite sugerir que *Gm*HMA8 podría estar implicado en el transporte de Cu al lumen tilacoidal. Estos datos concuerdan con la localización previa propuesta para *At*HMA8 (PAA2) por Abdel-Gahny et al. (2005b) en protoplastos de *A. thaliana*. Estos autores demostraron la localización tilacoidal de *At*HMA8 (PAA2) mediante un experimento de importe de proteínas usando sólamente un fragmento de la

proteína que contenía el péptido señal. Por tanto, es importante destacar que en este trabajo es la primera vez que se ha descrito la localización de este transportador utilizando un método más directo al disponer de un anticuerpo específico del mismo. El análisis cuantitativo de la distribución de las partículas de oro en la membrana tilacoidal indicó que el 73.9% de las partículas aparecen en grupos de 2-4 unidades. Este tipo de distribución agrupada podría indicar la presencia del transportador *Gm*HMA8 en zonas discretas de la membrana tilacoidal. Este hecho estaría de acuerdo con la idea actual acerca de la heterogeneidad existente en las membranas tilacoidales las cuales contienen regiones con funciones especializadas. Por otro lado, esta distribución también sugiere que este transportador podría tener una estructura oligomérica. Actualmente, los estudios estructurales de transportadores de membrana de Cu son muy limitados. Sin embargo, recientemente se ha propuesto una estructura trimérica para el transportador de Cu *h*CTR1 de humanos (Aller y Unger, 2006). Estos autores han sugerido la formación de un canal en el medio de la estructura trimérica por el que podría transportarse el metal. Este transportador es homólogo al transportador de Cu COPT1 de *A. thaliana* que participa en la adquisición del Cu del suelo, en el desarrollo del polen y en los mecanismos de elongación de la raíz (Sancenón et al., 2004). Para comprender la implicación que tiene la organización estructural observada para *Gm*HMA8 en su función serán necesarios estudios estructurales posteriores más específicos.

Un análisis más en profundidad de los clones obtenidos tras la realización del cribado del ADNc de las suspensiones de células fotosintéticas de soja mediante cebadores degenerados mostró la existencia de un nuevo mensajero homólogo al transportador *Gm*HMA8 previamente identificado que se denominó *GmHMA8-T*. Este nuevo mensajero se encontró tanto en células como en plantas de soja y podría codificar a una proteína truncada homóloga a *Gm*HMA8 con una función similar o complementaria a este transportador. Esta proteína truncada estaría formada únicamente por el segundo dominio citoplasmático de la proteína nativa *Gm*HMA8 lo cual podría indicar que se trata de una proteína soluble y que podría actuar como una cuprochaperona. Sin embargo, para confirmar la funcionalidad de este nuevo mensajero serían necesarios posteriores ensayos de transformación en plantas transgénicas o en

mutantes de levadura. A este respecto, se ha demostrado la existencia de una proteína truncada del transportador HMA4, miembro de la familia de P-ATPasas de tipo I_B, en la planta hiperacumuladora *Thlaspi caerulescens* (Bernard et al., 2004).

El estudio de la regulación de la expresión de *GmHMA8* y *GmHMA8-T* se realizó mediante PCR reversa y mostró que ambos genes están regulados por un mecanismo de "splicing" alternativo (Itoh et al., 2004). Por tanto, a nivel de mensajero existen dos transcritos para *GmHMA8* (*GmHMA8* y *NSP GmHMA8*) y otros dos transcritos para *GmHMA8-T* (*GmHMA8-T* y *NSP GmHMA8-T*), donde NSP significa "non-spliced". Aunque la existencia de genes regulados por mecanismos de "splicing" alternativo está ampliamente documentada en humanos y animales (Green, 1991; Modreck y Lee, 2002), sólo recientemente se ha estudiado en plantas (Kazan, 2003). Al igual que ocurre en humanos y animales, los genes regulados por este tipo de mecanismo que han sido identificados en plantas codifican proteínas que realizan funciones de regulación y señalización en el metabolismo celular. Curiosamente, muchos de los genes identificados tanto en animales como en plantas, están asociados con algún tipo de estrés. Entre los ejemplos caracterizados en plantas se encuentra una proteína cloroplástica soluble involucrada en los mecanismos de tolerancia a Cu (Burkhead et al., 2003). El mecanismo de "splicing" alternativo en genes que participan en algún tipo de estrés podría ser una herramienta muy útil para desarrollar mecanismos de adaptación y supervivencia.

A día de hoy no hay ninguna evidencia experimental de la existencia de una regulación por "splicing" alternativo de los genes que codifican a los transportadores de la familia de P_{1B}-ATPasas de plantas. Por tanto, es de señalar que esta es la primera vez que se demuestra este tipo de regulación postranscripcional. Diversos trabajos han demostrado la regulación por "splicing" alternativo y la funcionalidad de las formas no procesadas de las Cu-ATPasas involucradas en las enfermedades de Menkes y Wilson en humanos (Yang et al., 1997; Reddy y Harris, 1998). Estos autores observaron que una de las isoformas generadas por el "splicing" era funcional aunque carecía de una serie de dominios estructurales importantes y característicos de las P-ATPasas. Así, propusieron que esta isoforma se encontraba localizada en el citosol y que

podría actuar como una cuprochaperona. Teniendo en cuenta estos trabajos, podemos sugerir que la regulación por "splicing" alternativo de *GmHMA8 y GmHMA8-T* podría generar proteínas de función y estructura diferentes. Mientras que la hipotética proteína codificada por el mensajero *NSP GmHMA8* carecería del extremo C-terminal de la proteína nativa *Gm*HMA8, la proteína codificada por el mensajero *NSP GmHMA8-T* sería idéntica a la generada por el mensajero *GmHMA8-T* ya que la delección de 7-pb que genera el codón stop se encuentra localizada en la secuencia antes del intrón (ver Fig. 7-5). Sin embargo, al igual que se ha comentado para *GmHMA8-T*, habría que realizar ensayos de transformación en plantas transgénicas o en mutantes de levaduras para confirmar la funcionalidad de esta proteína.

En este trabajo también se ha investigado si los dos mensajeros identificados, *GmHMA8* y *GmHMA8-T*, corresponden a dos alelos de un gen de copia única o si por el contrario son dos genes independientes. Para ello, se han utilizado dos estrategias: *i)* la digestión con la enzima de restricción *Acc*I específica de *GmHMA8-T*; *ii)* el análisis de la secuencia intrónica de las formas no procesadas de *GmHMA8* y *GmHMA8-T.* Los resultados mostraron que *GmHMA8* y *GmHMA8-T* poseen diferentes regiones no codificantes en el extremo 3' (región 3'-UTR) y diferencias importantes en la secuencia de los intrones de las dos formas no procesadas *NSP GmHMA8* y *NSP GmHMA8-T*. Estos resultados se obtuvieron tanto en suspensiones celulares como en plantas de soja. A la vista de ello, es probable que *GmHMA8* y *GmHMA8-T* correspondan a dos genes independientes cuya existencia podría deberse a un fenómeno de duplicación del genoma durante la evolución.

En la actualidad, sólo existe un trabajo que aporta datos funcionales del transportador de Cu HMA8 en *A. thaliana* mediante la utilización de dos mutantes, *paa2-1* y *paa2-2*, deficientes en el transporte de Cu en el cloroplasto (Abdel-Ghany et al., 2005a). Estos autores han propuesto que este transportador está codificado por un gen de copia única y que los mutantes obtenidos son debidos a una mutación recesiva.

El análisis de la regulación de la expresión de *GmHMA8* y *GmHMA8-T* también reveló que en las células adaptadas a Cu los niveles de mensajero de *GmHMA8* y *GmHMA8-T* disminuyen significativamente en comparación con los de las células control mientras que los de *NSP GmHMA8* y *NSP GmHMA8-T*

aumentan. Este tipo de regulación sugiere que el Cu actúa como elemento regulador negativo de la expresión de ambos genes modificando el patrón de "splicing" alternativo observado en las células control. Esta podría ser una respuesta para evitar la acumulación excesiva del metal en el lumen tilacoidal. Los niveles de expresión de estos cuatro mensajeros en las células estresadas por Cu no experimentaron cambios significativos con respecto a los de las células control. En las células deficientes de Cu se observó un patrón de regulación similar al de las células adaptadas a Cu, pero con cambios menos pronunciados. En condiciones de supresión del estrés, la expresión de estos mensajeros se activó hasta llegar a niveles de expresión similares a los de las células control. Este tipo de regulación por Cu a nivel transcripcional se ha observado anteriormente en otros genes que participan en la homeostasis de Cu en plantas, como por ejemplo las metalochaperonas *CCH* y *CCS* y el transportador de Cu de alta afinidad *COPT1* de *A. thaliana* (Himelblau et al., 1998; Mira et al., 2000; Sancenón et al., 2003, 2004; Abdel-Ghany et al., 2005b).

En resumen, la identificación de los dos mensajeros *Gm*HMA8 y *Gm*HMA8-T en soja, y su regulación por "splicing" alternativo y Cu permite sugerir que la regulación tanto a nivel transcripcional como postranscripcional podría ser esencial en el control de la homeostasis de Cu en el cloroplasto.

De acuerdo con los datos de localización subcelular, topología y regulación del transportador *Gm*HMA8 presentados en este trabajo y junto con los datos aportados por otros autores, se presenta un modelo de la función celular que realizaría este transportador en la homeostasis de Cu en el cloroplasto (Fig. 8-1).

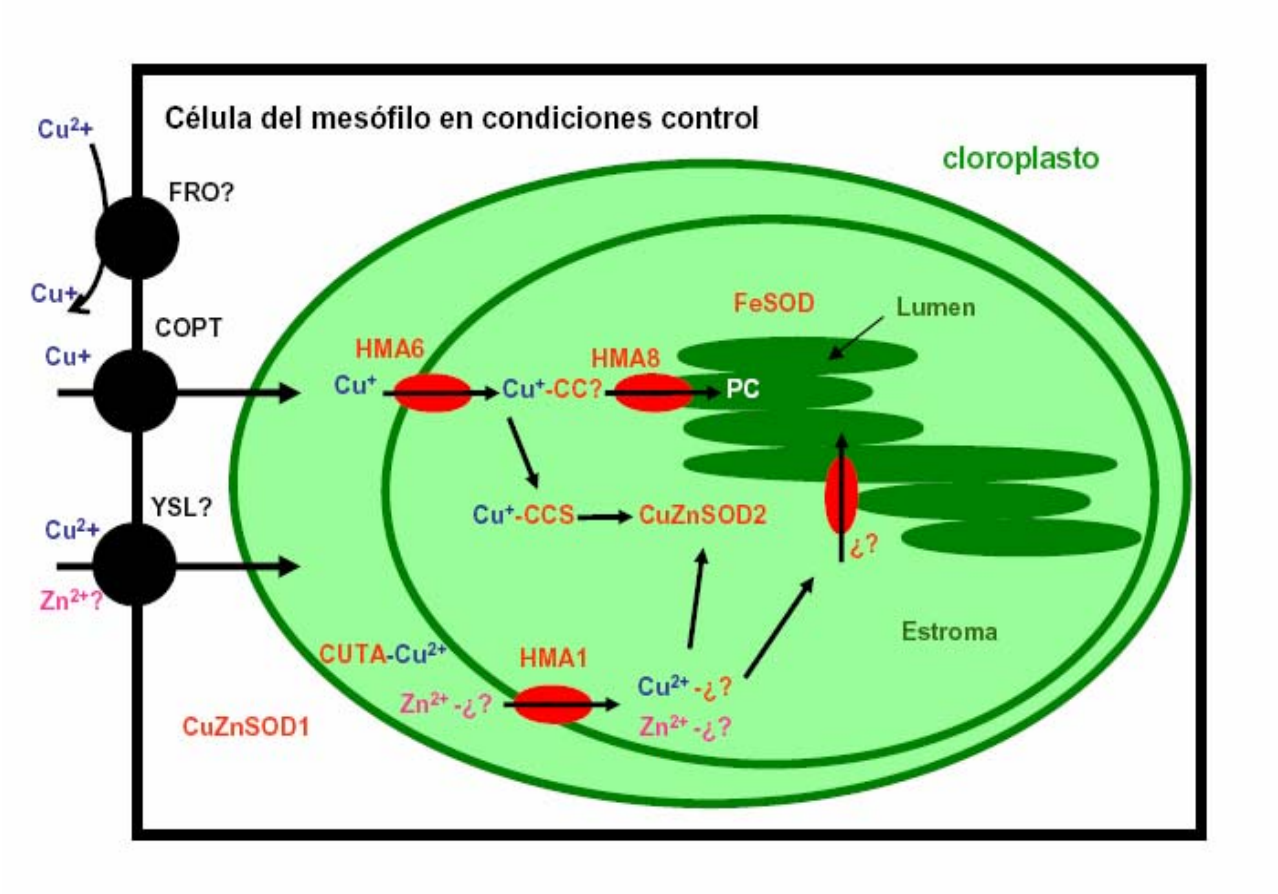

Fig. 8-1. Modelo de la función realizada por el transportador HMA8 en la homeostasis de Cu en el cloroplasto. El Cu^{2+} podría reducirse a Cu^{+} por una reductasa de la familia FRO y ser posteriormente transportado al interior celular por un transportador de la familia COPT. El Cu es posteriormente transportado al estroma cloroplástico a través de HMA6 donde se dirige a: *i)* la plastocianina por medio de una cuprochaperona desconocida (CC) y el transportador HMA8; *ii)* la CuZnSOD por medio de la cuprochaperona CCS. En condiciones control, los mensajeros CuZnSOD1, CuZnSOD2 y CCS se transcriben. En estas condiciones la CuZnSOD2 se encarga de eliminar los radicales O_2^- generados por el transporte electrónico fotosintético y el transportador HMA8 transporta el Cu al lumen tilacoidal donde es suminitrado a la plastocianina. Recientemente se ha propuesto un mecanismo alternativo de transporte de baja afinidad de Cu en el cloroplasto, concretamente de Cu^{2+}. De esta manera, el Cu^{2+} podría entrar a la célula a través de un transportador de la familia YSL para ser transportado posteriormente al estroma cloroplástico a través del transportador HMA1 que interaccionaría con la proteína CUTA del espacio intermembrana. También mediante un mecanismo similar, HMA1 podría ser el encargado de suministrar el Cu, e incluso el Zn, a la CuZnSOD2. El responsable del tranporte de Cu^{2+} al lumen tilacoidal permanece todavía sin identificar.

Según el modelo de regulación de la homeostasis de Cu en el cloroplasto propuesto por Abdel-Ghany et al. (2005a; b), debe existir un equilibrio entre el mecanismo de transporte y distribución de Cu a las cuproproteínas cloroplásticas para que el proceso fotosintético sea óptimo. Es decir, debe existir un equilibrio entre la actividad de la plastocianina en el lumen tilacoidal y las actividades de las superóxido dismutasas (CuZnSOD y FeSOD) en el estroma cloroplástico, asegurando así un nivel adecuado de plastocianina para que el PSI pueda reducirse y una actividad superóxido dismutasa suficiente como para poder eliminar los radicales O_2^- generados en la cadena de transporte electrónico fotosintético. El buen funcionamiento de este equilibrio estaría regulado por la activación o inactivación de la FeSOD y la CuZnSOD, y por la regulación de la cuprochaperona CCS cloroplástica en respuesta a Cu.

En las células adaptadas a Cu se observó: *i)* una reducción de la actividad FeSOD y un aumento de la actividad CuZnSOD; *ii)* una reducción de la expresión del transportador *GmHMA8* y *iii)* un aumento de la expresión de la cuprochaperona *GmCCS*. Si a estos resultados se suman la mayor actividad fotosintética y el mayor contenido de Cu en el cloroplasto observado en estas condiciones, se puede sugerir que en condiciones de exceso de Cu el equilibrio propuesto se desplazaría hacia la síntesis de CuZnSOD y de su cuprochaperona CCS para proteger al cloroplasto del daño oxidativo que provocarían los radicales O_2^- generados por la mayor actividad fotosintética. Sin embargo, en estas condiciones también se observó un aumento del contenido de plastocianina que contrasta con el desplazamiento del equilibrio propuesto en el modelo anterior de Abdel-Ghany et al. (2005a; b). Este hecho, sin embargo podría explicarse en base a la existencia de un mecanismo alternativo de transporte de Cu de baja afinidad al cloroplasto a través de otros transportadores. A este respecto, recientemente se ha identificado una proteína soluble llamada *At*CUTA localizada en el espacio intermembranal del cloroplasto y un nuevo transportador de Cu llamado *At*HMA1, que se encuentra localizado en su membrana interna que podría interaccionar con *At*CUTA y transportar el Cu (incluso el Zn) a la CuZnSOD cloroplástica (Burkhead et al., 2003; Seigneurin-Berny et al., 2006; Pilon et al., 2006). En el tilacoide, este

mecanismo de transporte alternativo podría explicarse en base al estudio realizado por Shingles et al. (2004). Estos autores propusieron la existencia de al menos dos transportadores de Cu en la membrana tilacoidal y sugirieron que podrían pertenecer a la familia HMA y/o a la familia ZIP. A día de hoy, uno de ellos sería el transportador HMA8 (PAA2) identificado en *A. thaliana* (Abdel-Ghany et al. 2005b), sin embargo quedaría al menos otro transportador por identificar.

Los resultados obtenidos en las células de soja deficientes de Cu no mostraron cambios significativos en el nivel de expresión de *GmHMA8* en comparación con el de las células control. Este hecho contrasta con el modelo de regulación de la homeostasis de Cu propuesto por Abdel-Ghany et al. (2005a) en condiciones de deficiencia de Cu que sugiere que el equilibrio en estas condiciones se desplazaría hacia la síntesis de plastocianina para asegurar el óptimo funcionamiento de la cadena de transporte electrónico fotosintético. Según este modelo, el resultado esperado en las suspensiones celulares de soja hubiera sido un aumento de la expresión de *GmHMA8*. Esta divergencia puede ser debida a: *i)* que el tratamiento en condiciones de deficiencia de Cu aplicado no ha sido suficiente para observar un desplazamiento del equilibrio; *ii)* la existencia de un mecanismo alternativo de transporte de Cu de baja afinidad tal como el descrito anteriormente.

Por otro lado, es importante destacar que en las células estresadas por Cu, al igual que en las células deficientes a Cu, los niveles de expresión de *GmHMA8* no se modificaron significativamente con respecto a los de las células control. Por tanto, se podría sugerir que el desplazamiento del equilibrio en uno u otro sentido estaría asociado con una respuesta al exceso o defecto de Cu a largo plazo, más que a una respuesta a corto plazo.

CAPÍTULO 9

CONCLUSIONES

1. Las suspensiones de células fotosintéticas de soja son capaces de tolerar altas concentraciones de Cu (5-50 μM). En estas condiciones las células acumulan altos niveles de este metal y tienen un crecimiento celular similar al de las células control en condiciones de luz normal (65 ± 5 μE m^{-2} s^{-1}) y 2,5 - 3 veces más rápido en condiciones de luz limitante (30 ± 5 μE m^{-2} s^{-1}). Las células adaptadas al exceso de Cu presentaron cambios en la estructura y ultraestructura del cloroplasto, un mayor contenido de clorofila y una mayor actividad fotosintética. Los resultados indican que el Cu desempeña un papel positivo y específico en la fotosíntesis y en particular en la estructura y en la función del fotosistema II.

2. Las suspensiones de células fotosintéticas de soja desarrollaron diferentes mecanismos de respuesta durante el proceso de aclimatación y adaptación a crecer en presencia de exceso de Cu. En una respuesta a corto plazo, las células evitaron la entrada de este metal inmovilizándolo en la pared celular en forma de depósitos extracelulares, posiblemente por unión a citrato entre otros compuestos. En una respuesta a largo plazo, las células almacenaron el Cu principalmente en la vacuola.

3. La acumulación de Cu en las suspensiones celulares de soja está acompañada de un aumento del contenido de Fe y una disminución del contenido de Zn. Estos hechos difieren de lo observado en plantas de soja crecidas en medio hidropónico suplementado con exceso de Cu donde hay una competencia entre la adquisición del Cu y el Fe y un aumento del contenido de Zn. Sin embargo, son coincidentes con lo observado en plantas donde las hojas han sido tratadas con exceso de Cu. Estos resultados indican que posiblemente las estrategias de adquisición y transporte de Cu en las suspensiones celulares y en las células del mesófilo de hojas son distintas a las que tienen lugar en las células de raíz.

4. Se han identificado dos mensajeros del transportador de Cu HMA8 en soja, llamados *GmHMA8* y *GmHMA8-T,* que podrían corresponder a dos genes independientes. *GmHMA8* resultó tener una homología del 45% y del 83% con los transportadores PacS de *Synechocystis* PCC 6803 y *At*HMA8/PAA2 de *A. thaliana*, respectivamente, y codifica a una proteína de 97 kDa que contiene todos los dominios característicos y específicos de la familia P_{1B}-ATPasa de transportadores de metales pesados. *GmHMA8-T* resultó tener una homología del 30% con PacS y del 83% con *At*HMA8 y podría codificar a una proteína truncada de 20 kDa con una función similar o complementaria al transportador *Gm*HMA8.

5. Estudios de localización subcelular de *Gm*HMA8 demostraron que este transportador se encuentra localizado en la membrana tilacoidal del cloroplasto formando pequeños “clusters” de 2-4 unidades. Por tanto, este transportador podría estar implicado en el transporte de Cu al lumen tilacoidal. Por otro lado, el análisis de esta proteína mediante electroforesis desnaturalizante reveló un peso molecular aparente de aproximadamente 2 veces superior al teóricamente calculado. Estos resultados podrían sugerir una organización oligomérica para este transportador.

6. El estudio de la regulación de la expresión de *GmHMA8* y *GmHMA8-T* mostró que están regulados por un mecanismo de “splicing” alternativo que genera dos mensajeros, *NSP GmHMA8* y *NSP GmHMA8-T*, respectivamente, que contienen un intrón sin procesar. El patrón de distribución de estos cuatro mensajeros fue dependiente de la presencia de Cu y de las condiciones del medio de cultivo. Por tanto, se ha propuesto que el Cu actúa como elemento regulador de la expresión de estos genes y que la regulación por “splicing” alternativo podría ser esencial en el control de la homeostasis de Cu en el cloroplasto.

CAPÍTULO 10

BIBLIOGRAFÍA

Abadía J, Nishio JN, Monge E, Montañés L, Heras L (1985). Mineral composition of peach leaves affected by iron chlorosis. *Journal of Plant Nutrition* **8**: 965-975.

Abdel-Ghany SE, Burkhead JL, Gogolin KA, Andrés-Colás N, Bodecker JR, Puig S, Peñarrubia L, Pilon M (2005a). AtCCS is a functional homolog of the yeast copper chaperone Ccs1/Lys7. *FEBS Letters* **579**: 2307-2312.

Abdel-Ghany SE, Müller-Moulé P, Niyog iKK, Pilon M, Shikanai T (2005b). Two P-type ATPases are required for copper delivery in *Arabidopsis thaliana* chloroplasts. *The Plant Cell* **17**: 1-19.

Achila D, Banci L, Bertini I, Brunce J, Ciofi-Baffoni S, Huffman DL (2006). Structure of human Wilson protein domains 5 and 6 and their interplay with domain 4 and the copper chaperone HAH1 in copper uptake. *Proceedings of the National Academy of Sciences USA* **103**: 5729-5734.

Alaoui-Sossé B, Genet P, Vinit-Dunand F, Toussaint M-L, Epron D, Badot P-M (2004). Effect of copper on growth in cucumber plants (*Cucumis sativus*) and its relationships with carbohydrate accumulation and changes in ion contents. *Plant Science* **166**: 1213-1218.

Alfonso M, Montoya G, Cases R, Rodríguez R, Picorel R (1994). Core antenna complexes, CP43 and CP47, of higher plant photosystem II. Spectral properties, pigment stoichiometry, and amino acid composition. *Biochemistry* **33**: 10494-10500.

Alfonso M, Pueyo J, Gaddour K, Etienne A-L, Kirilovsky D, Picorel R (1996). Induced new mutation of D1 Serine-268 in soybean photosynthetic cell cultures produced atrazine resistance, increased stability of S2QB- and S3QB- states, and increased sensitivity to light stress. *Plant Physiology* **112**: 1499-1508.

Ali MB, Singh N, Shohael AM, Hahn EJ, Paek K-Y (2006). Phenolics metabolism and lignin synthesis in root suspension cultures of *Panax ginseng* in response to copper stress. *Plant Science* **171**: 147-154.

Allan AC, Maddumage R, Simons JL, Neill SO, Ferguson IB (2006). Heat-induced oxidative activity protects suspension-cultured plant cells from low temperature damage. *Functional Plant Biology* **33**: 67-76.

Aller SG, Unger VM (2006). Projection structure of the human copper transporter CTR1 at 6-Å resolution reveals a compact trimer with a novel channel-like architecture. *Proceedings of the National Academy of Sciences USA* **103**: 3627-3632.

Alonso JM, Hiramaya T, Roamn G, Nourizadeh S, Ecker JR (1999). EIN2, a bifunctional transducer of ethylene and stress response in *Arabidopsis*. *Science* **284**: 2148-2152.

Altschul SF, Lipman DJ (1990). Protein database searches for multiple alignments. *Proceedings of the National Academy of Sciences USA* **87**: 5509-5513.

Anderson JM (1999). Insights into the consequences of grana stacking of thylakoid membranes in vascular plants: a personal perspective. *Australian Journal of Plant Physiology* **26**: 625-639.

Andrés-Colás N, Sancenón V, Rodríguez-Navarro S, Thiele DJ, Ecker JR, Puig S, Peñarrubia L (2006). The Arabidopsis heavy metal P-type ATPase HMA5 interacts with metallochaperones and functions in copper detoxification of roots. *The Plant Journal* **45**: 225-236.

Arellano J, Lázaro JJ, López-Gorgé J, Barón M (1995). The donor side of PSII as the copper-inhibitory binding site. *Photosynthesis Research* **45**: 127-137.

Argüello JM (2003). Identification of ion-selectivity determinants in heavy-metal transport P1B-type ATPases. *Journal of Structural Biology* **195**: 93-108.

Arnon DI (1950). Dennis Robert Hoagland: 1884-1949. *Science* **112**: 739-742.

Arnon H (1949). Copper enzymes in isolated chloroplast. Polyphenoloxidase in Beta vulgaris. *Plant Physiology* **24**: 1-15.

Aro EM, Virgin I, Andersson B (1993). Photoinhibition of photosystem II. Inactivation, protein damage and turnover. *Biochimica et Biophysica Acta* **1143**: 113-134.

Austin II J, Webber AN (2005). Photosynthesis in *Arabidopsis thaliana* mutants with reduced chloroplast number. *Photosynthesis Research* **85**: 373-384.

Axelsen KB, Pamgrem MG (1998). Evolution of substrate specificities in the P-type ATPase superfamily. *Journal of Molecular Evolution* **46**: 84-101.

Axelsen KB, Palmgrem MG (2001). Inventory of the superfamily of P-type ion pumps in Arabidopsis. *Plant Physiology* **126**: 696-706.

Backor M, Váczi P (2002). Copper tolerance in the lichen photobiont *Trebouxia erici* (Chlorophyta). *Environmental and Experimental Botany* **48**: 11–20.

Baker DE, Senef JP (1995). Copper. In: Alloway BJ (Ed.). *Heavy Metals in Soils*. Academic and Professional, London, pp. 179-205.

Balandín T, Castresana C (2002). AtCOX17, an Arabidopsis homolog of the yeast copper chaperone COX 17. *Plant Physiology* **129**: 1852-1857.

Barany I, González-Melendi P, Mityko J, Fadón B, Risueño MC, Testillano PS (2005). Microspore-derived embryogenesis in *Capsicum annuum*: subcellular rearrangements through development. *Biology of the Cell* **97**: 709-722.

Barón M, Arellano J, López-Gorgé J (1995). Copper and photosystem II: A controversial relationship. *Physiologia Plantarum* **94**: 174-180.

Barr R, Crane FL (1976). Organization of electron transport in photosystem II of spinach chloroplasts according to chelator inhibition sites. *Plant Physiology* **57**: 450-453.

Bartosz G (1997). Oxidative stress in plants. *Acta Physiologiae Plantarum* **19**: 47-64.

Bassi R, Marquardt J, Lavergne J (1995). Biochemical and functional properties of photosystem II in agranal membranes from maize mesophyll and bundle sheath chloroplasts. *European Journal of Biochemistry* **233**: 709-719.

Baszynski T, Tukendorf A, Ruszkowska M, Shórzynska E, Maksymiec W (1988). Characterisitics of the photosyntetic apparatus of copper non-tolerant spinach exposed to excess copper. *Journal of Plant Physiology* **132**: 708-713.

Bell PF, Chaney RL, Angle JS (1991). Determination of copper activity required by maize using chelator-buffered nutrient solution. *Soil Science Society of America Journal* **55**: 7824-7828.

Bernal M, Roncel M, Ortega JM, Picorel R, Yruela I (2004). Copper effect on the cytochrome b_{559} of photosystem II under photoinhibitory conditions. *Physiologia Plantarum* **120**: 686-694.

Bernal M, Ramiro MV, Cases R, Picorel R, Yruela I (2006). Excess copper effect on growth, chloroplast ultrastructure, oxygen-evolution activity and chlorophyll fluorescence in *Glycine max* cell suspensions. *Physiologia Plantarum* **127**: 312-325.

Bernard C, Roosens N, Czernic P, Lebrun M, Verbruggen N (2004). A novel CPx-ATPase from cadmium hyperacumulator *Thlaspi caerulescens*. *FEBS Letters* **569**: 140-148.

Bertrand M, Poirier I (2005). Photosynthetic organisms and excess of metals. *Photosynthetica* **43**: 345-353.

Beuchamp CH, Fridovich I (1971). Superoxide dismutase improved assays and an assay applicable to acrylamide gels. *Analytical Biochemistry* **44**: 276–287.

Beven AF, Simpson GG, Brown JW, Shaw PJ (1995). The organization of spliceosomal components in the nuclei of higher plants. *Journal of Cell Science* **108**: 509-518.

Bidwell SD, Crawford SA, Woodrow IE, Sommer-Knudsen., Marshall AT (2004). Sub-cellular localization of Ni in the hyperaccumulator, *Hybanthus floribundus* (Lindley) F. Muell. *Plant Cell and Environment* **27**: 705-716.

Bienfait HF (1988). Mechanisms in Fe deficiency reactions of higher plants. *Journal of Plant Nutrition* **11**: 605-629.

Bonilla I (2000). Introducción a la nutrición mineral de las plantas. Los elementos minerales. In: Azcón-Bieto J, Talón M (Eds.). *Fundamentos de Fisiología Vegetal*. McGraw Hill Interamericana, Barcelona, España, pp. 83-97.

Bradford M (1976). A rapid and sensitive method for the quantitation of microgram quantities of protein utilizing the principle of dye binding. *Analitical Biochemistry* **72**: 248-259.

Brown SL, Chaney RL, Angle JS, Baker AJM (1995). Zinc and cadmium uptake of *Thlaspi caerulescens* gown in nutrient solution. *Soil Science Society of America Journal* **59**: 125-133.

Brun LA, Maillet J, Hinsinger P, Pepin M (2001). Evaluation of copper availability to plants in copper-contaminated vineyard soils. *Environmental Pollution* **111**: 293-302.

Burda K, Kruk J, Strzalka K, Schimd GH (2002). Stimulation of oxygen evolution in photosystem II by copper. *Zeitschrift für Naturforschung* **57c**: 853-857.

Burda K, Kruk J, Schmid GH, Strzalka K (2003). Inhibition of oxygen evolution in photsystem II by Cu (II) ions is associated with the oxidation of cytochrome b_{559}. *Biochemical Journal* **371**: 103-102.

Burge C, Karlin S (1997). Prediction of complete gene structures in human genomic DNA. *Journal of Molecular Biology* **268**: 78-94.

Burkhead JL, Abdel-Ghany SE, Morrill JM, Pilon-Smits E, Pilon M (2003). The *Arabidopsis thaliana CUTA* gene encodes an evolutionary conserved copper binding chloroplast protein. *The Plant Journal* **34**: 856-867.

Chen Y, Shi J, Tian G, Zheng S, Lin Q (2004). Fe deficiency induces Cu uptake and accumulation in *Commelina communis*. *Plant Science* **166**: 1371-1377.

Chichiricco G, D'Alessandro A, Avigliano L (1989). Immunohistochemical localisation of ascorbate oxidase in *Cucurbita pepo medullosa*. *Plant Science* **64**: 61-66.

Chow WS, Melis A, Anderson JM (1980). Adjustments of the photosystem stoichiometry in chloroplasts improve the quantum efficiency of photosynthesis. *Proceedings of the National Academy of Sciences USA* **87**: 7502-7506.

Chu CC, Lee WC, Guo WY, Pan SM, Chen LJ, Li HM, Jinn TL (2005). A copper chaperone for superoxide dismutase that confers three types of copper/zinc superoxide dismutase activity in Arabidopsis. *Plant Physiology* **139**: 425-436.

Ciscato M, Valcke R, Van Loven K, Clijsters H, Navari-Izzo F (1997). Effects of in vivo copper treatment on the photosynthetic apparatus of two *Triticum durum* cultivars with different stress sensitivity. *Physiologia Plantarum* **100**: 901-908.

Clemens S (2001). Molecular mechanisms of plant metal tolerance and homeostasis. *Planta* **212**: 475-486.

Clemens S, Palmgren MG, Krämer U (2002). A long way ahead: understanding and engineering plant metal accumulation. *Trends in Plant Science* **7**: 309-315.

Cobbett C, Goldsbrough P (2002). Phytochelatins and metallothioneins: Roles in heavy metal detoxification and homeostasis. *Annual Review of Plant Biology* **53**: 159-182.

Cohen CK, Norvell WA, Kochian LV (1997). Induction of the root cell plasma membrane ferric reductase. *Plant Physiology* **114**: 1061-1069.

Company P, González-Bosch C (2003). Identification of a copper chaperone from tomato fruits infected with *Botrytis cinerea* by differential display. *Biochemical & Biophysical Research Communications* **304**: 825-830.

Cona A, Rea G, Angelini R, Federico R, Tavladoraki P (2006). Functions of amine oxidases in plant development and defense. *Trends in Plant Science* **11**: 80-88.

Cuypers A, Vangronsveld J, Clijsters H (2000). Biphasic effect of copper on the ascorbate-glutathione pathway in primary leaves of *Phaseolus vulgaris* seedlings during the early stages of metal assimilation. *Physiologia Plantarum* **110**: 512-517.

De Freitas J, H. W, Kim JH, Poynton H, Fox T, C. V (2003). Yeast, a model organism for iron and copper metabolism studies. *Biometals* **16**: 185-197.

De los Ríos A, Ascaso C, Wierzchos J, Fernández-Valiente E, Quesada A (2004). Microstructural Characterization of Cyanobacterial Mats from the McMurdo Ice Shelf, Antarctica. *Applied and Environmental Microbiology* **70**: 569-580.

De Parter S, Caspers M, Kottenhagen M, Miema H, ter Stege R, de Vetten N (2006). Manipulation of starch granule size distribution in potato tubers by modulation of plastid division. *Plant Biotechnology Journal* **4**: 123-134.

De Rienzo F, Gabdoulline RR, Menziani MC, Wade RC (2000). Blue copper proteins: a comparative analysis of their molecular interaction properties. *Protein Science* **9**: 1439-1454.

De Silva DM, Askwith CC, Kaplan J (1996). Molecular mechanisms of iron uptake in eukariotes. *Physiological Reviews* **76**: 31-47.

De Vos CHR, Vonk MJ, Vooijs R, Schat H (1992). Glutathione depletion due to copper-induced phytochelatin synthesis causes oxidative stress in *Silene cucubalus*. *Plant Physiology* **98**: 853-858.

De Vos CHR, Bookum WMT, Vooijs R, Schat H, De Kok LJ (1993). Effect of copper on faty acid composition and peroxidation of lipids in the roots of copper tolerant and sensitive *Silene cucubalus*. *Plant Physiology and Biochemistry* **31**: 151-158.

Delhaize PREE, Jones DL (2001). Function and mechanism of organic anion exudation from plant roots. *Annual Review of Plant Physiology and Plant Molecular Biology* **52**: 527-560.

Didonato RJ, Roberts LA, Sanderson T, Eisley RB, Walker EL (2004). *Arabidopsis yelow stripe-like2 (YSL2)*: a metal regulated gene encoding a plasma membrane transporter of nicotianamine-metal complexes. *The Plant Journal* **39**: 403-414.

Dmitriev O, Tsivkovskii R, Abildgaard F, Morgan CT, Markley JL, Lutsenko S (2006). Solution structure of the N-domain of Wilson disease protein: Distinct nucleotide-binding environment and effects of disease mutations. *Proceedings of the National Academy of Sciences USA* **103**: 5302-5307.

Dong J, Kim ST, Lord EM (2005). Plantacyanin plays a role in reproduction in arabidopsis. *Plant Physiology* **138**: 778-789.

Drazkiewicz M, Skórzynska-Polit E, Krupa Z (2003). Response of the ascorbate-glutathione cycle to excess copper in *Arabidopsis thaliana* (L.). *Plant Science* **164**: 195-202.

Drazkiewicz M, Skórzynska-Polit E, Krupa Z (2004). Copper-induced oxidative stress and antioxidant defence in *Arabidopsis thaliana*. *Biometals* **17**: 379-387.

Droppa M, Horvath G (1990). The role of copper in photosynthesis. *Plant Science* **9**: 111-123.

Eide D, Broderius M, Fett J, Guerinot ML (1996). A novel iron-regulated metal transporter from plants identified by functional expression in yeast. *Proceedings of the National Academy of Sciences USA* **93**: 5624-5628.

Emanuelsson O, Nielsen H, Von Heijne G (1999). ChloroP, a neural metwork-based method for predicting chloroplast transit peptides and their cleavage sites. *Protein Science* **8**: 978-984.

Eren E, Argüello JM (2004). Arabidopsis HMA2, a divalent heavy metal-transporting P_{1B}-ATPase, is involved in cytoplamic Zn^{2+} homeostasis. *Plant Physiology* **136**: 3712-3723.

Ernst WHO, Verkleji JAC, Schat H (1992). Metal tolerance in plants. *Acta Botanica Neerlandica* **41**: 229-248.

Falconi M, Desideri A (2002). Molecular modeling and dynamics of copper proteins. In: Masaro EJ (Ed.). *Handbook of copper farmacology and toxicology*. Humana Press, Totowa, N.J., pp. 81-101.

Fernandes JC, Henriques FS (1991). Biochemical, physiological and structural effects of excess copper on plants. *Botanical Review* **57**: 246-273.

Fernández JA, Maldonado JM (2000). Absorción y transporte de nutrientes minerales. In: Azcón-Bieto J, Talón M (Eds.). *Fundamenos de Fisiología Vegetal*. McGraw-Hill Interamericana, Barcelona, España, pp. 99-112.

Fornazier RF, Ferreira RR, Pereira GJG, Molina SMG, Smith RJ, Lea PJ, Azevedo RA (2002). Cadmium stress in sugar cane callus cultures: Effect on antioxidant enzymes. *Plant Cell, Tissue and Organ Culture* **71**: 125-131.

Fortes AM, Coronado MJ, Testillano PS, Risueño MC, Pais MS (2004). Expression of Lipoxigenase during organogenic nodule formation from hoop internodes (*Humulus lupulus* var. Nugget). *Journal of Histochemistry and Cytochemistry* **52**: 227-241.

Fox TC, Guerinot ML (1998). Molecular biology of cation transport in plants. *Annual Review of plant physiology in plant molecular bilogy* **49**: 669-696.

Foyer C (1988). Feedback inhibition of photosynthesis through source-sink regulation in leaves. *Plant Physiology and Biochemistry* **26**: 483-492.

Franklin N, Stauber JL, R.P. L, Petocz P (2002). Toxicity of metal mixtures to a tropical fresh-water alga (*Chlorella* sp). The effect of interactions between copper, cadmium and zinc on metal cell binding and uptake. *Environmental Toxicology and Chemistry* **21**: 2412-2422.

Friedland AJ (1990). The movement of metals through soils and ecosystems. In: Shaw AJ (Ed.). *Heavy metal tolerance in plants: evolutionary aspects*. CRC Press, Inc., Boca Raton, Florida, pp. 7-37.

García Luis A, Guardiola JL (2000). Transporte en el floema. In: Azcón-Bieto J, Talón M (Eds.). *Fundamentos de Fisiología Vegetal*. McGraw-Hill Interamericana, Barcelona, España, pp. 65-82.

Gerdemann C, Eicken B, Krebs B (2002). The Crystal Structure of Catechol Oxidase: New Insight into the Function of Type-3 Copper Proteins. *Accounts of Chemical Research* **35**: 183-191.

Gledhill M, Nimmo M, Hill SJ (1999). The release of copper-complexing ligands by the brown alga *Fucus vesiculosus* (phaeophyceae) in response to increasing total copper levels. *Journal of Phycology* **35**: 501-509.

Gori P, Schiff S, Santandrea G, Bennici A (1998). Response of *in vitro* cultures of *Nicotiana tabacum* L. to copper stress and selection of plants from Cu-tolerant callus. *Plant Cell, Tissue and Organ Culture* **53**: 161-169.

Graham RD (1979). Absorption of copper by plant roots. *Plant Cell and Environment* **2**: 139-143.

Gratão PL, Polle A, Lea PJ, Azebedo RA (2005). Making the life of heavy metal-stressed plants a little easier. *Functional Plant Biology* **32**: 481-494.

Gravot A, Lieutaud A, Verret F, Auroy P, Vavasseur A, Richaud P (2004). AtHMA3, a plant P_{1B}-ATPase, functions as a Cd/Pb transporter in yeast. *FEBS Letters* **561**: 22-28.

Green MR (1991). Biochemical mechanisms of constitutive and regulated pre-mRNA splicing. *Annual Review of Cell Biology* **7**: 559-599.

Grusak MA, Pezeshgi S (1996). Shoot-to-root signal transmission regulates root Fe (III) reductase activity in the *dgl* mutant of pea. *Plant Physiology* **110**: 329-334.

Guerinot ML (2000). The ZIP family of metal transporters. *Biochimica et Biophysica Acta* **1465**: 190-198.

Guo W-J, Bundithya W, Goldsbrough P (2003). Characterization of the *Arabidopsis* metallothionenin gene family: tissue-specific expression and induction during senescence and in response to copper. *New Phytologist* **159**: 369-381.

Gupta M, Cuypers A, Vangronsveld J, Clijsters H (1999). Copper affects the enzymes of the ascorbate-glutathiones cycles and its related metabolites in the roots of *Phaseolus vulgaris*. *Physiologia Plantarum* **106**: 262-267.

Halcrow MA, Knowles PF, Phillips SE (2001). Copper proteins in the transport and activation of dioxygen, and the reduction of inorganic molecules. In: Bertini I, Sigel A, Sigel H (Eds.). *Handbook of Metalloproteins*. CRC Press, Basel, Switzerland, pp. 709-762.

Hall JL (2002). Cellular mechanisms for heavy metal detoxification and tolerance. *Journal of Experimental Botany* **53**: 1-11.

Hall JL, Williams LE (2003). Transition metal transporters in plants. *Journal of Experimental Botany* **54**: 2601-2613.

Halliwell B, Gutteridge JMC (1989). Free radicals in biology and medicine. In., Claredon Press, Oxford, UK.

Hankamer B, Nield J, Zheleva D, Boekema E, Jansson S, Barber J (1997). Isolation and biochemical characterisation of monomeric and dimeric photosystem II complexes from spinach and their relevance to the organisation of photosystem II in vivo. *European Journal of Biochemistry* **243**: 422-429.

Hashimoto A, Ettinger WF, Yamamoto Y, Theg SM (1997). Assembly of the newly imported oxygen-evolving complex subunits in isolated chloroplasts: sites of assembly and mechanisms of binding. *The Plant Cell* **9**: 441-452.

Hasset R, Kosman DJ (1995). Evidence for Cu (II) reduction as a component of copper uptake by *Saccharomyces cerevisiae*. *Journal of Biological Chemistry* **270**: 128-134.

Hayashi R, Morohashi Y (1993). Phytochrome control of the development of ascorbate oxidase activity in mustard (*Sinapis alba*) cotyledons. *Plant Physiology* **102**: 1237–1241.

Herbik A, Bölling C, Buckhout TJ (2002). The involvement of a multicopper oxidase in iron uptake by the green algae *Chlamydomonas reinhardtii*. *Plant Physiology* **130**: 2039-2048.

Hill KL, Hasset R, Kosman D, Merchant S (1996). Regulated copper uptake in *Chlamydomonas reinhardtii* in response to copper availability. *Plant Physiology* **112**: 697-704.

Himelblau E, Mira H, Su-Ju L, Cizenski Culotta V, Peñarrubia L, Amasino RM (1998). Identification of a funcional homolog of the yeast copper homeostasis gene *ATX1* from *Arabidopsis*. *Plant Physiology* **117**: 1227-1234.

Himelblau E, Amasino RM (2000). Delivering copper within plant cells. *Current Opinion in Plant Biology* **3**: 205-210.

Himelblau E, Amasino RM (2001). Nutrients mobilized from leaves of *Arabidopsis thaliana* during leaf senescence. *Journal of Plant Physiology* **158**: 1317-1323.

Hipkins MF, Baker N (1984). Photosynthesis energy transduction. 1 Practical Aproach. Oxford University Press.

Hiramaya T, Kieber JJ, N. H, Kogan M, Guzman P, Nourizadeh S, Alonso JM, Dailey WP, Dancis A, Ecker JR (1999). RESPONSIVE-TO-ANTAGONIST1, a Menkes/Wilson disease-related copper transporter, is required for ethylene signaling in *Arabidopsis*. *Cell* **97**: 383-393.

Howe CJ, Schlarb-Ridley BG, Wastl J, Purton S, Bendall DS (2006). The novel cythocrome c_{6A} of chloroplasts: a case of evolutionary bricolage? *Journal of Experimental Botany* **57**: 13-22.

Hussain D, Haydon MJ, Wang Y, Wong E, Sherson SM, Young J, Camakaris J, Harper JE, Cobbet CS (2004). P-type ATPases heavy metal transporters with roles in essential zinc homeostasis in *Arabidopsis*. *Plant Cell* **16**: 1327-1339.

Izaguirre-Mayoral ML, Sinclair TR (2005). Soybean genotypic difference in growth, nutrient accumulation an ultrastructure in response to manganese and iron supply in solution culture. *Annals of Botany* **96**: 149-158.

Izawa S, Good NE (1966). Effects of salt and electron transport on the conformation of isolated chloroplasts. II. Electron microscopy. *Plant Physiology* **41**: 544-552.

Jasiewicz C (1981). The effect of copper and application of different forms of nitrogen on some physiological indices of maize. *Acta Agraria et Silvestria Agraria* **20**: 95-106.

Jegerschöld C, Arellano J, Schöder WP, Van Kam PJM, Barón M, Styring S (1995). Copper (II) inhibition of electron transfer through photosystem II studied by EPR spectroscopy. *Biochemistry* **34**: 12747-12754.

Jeong WJ, Park YI, Suh K, Raven JA, Yoo OJ, Liu JR (2002). A large population of small chloroplasts in tobacco leaf cells allows more effective movement than a few enlarged chloroplasts. *Plant Physiology* **129**: 112-121.

Jiang W, Liu D, Liu X (2001). Effect of copper on root growth, cell division and nucleolus of *Zea mays*. *Biologia Plantarum* **44**: 105-109.

Jonak C, Nakagami H, Hirt H (2004). Heavy metal stress. Activation of distinct mitogen-activated protein kinase pathways by copper and cadmium. *Plant Physiology* **136**: 3276-3283.

Jungmann J, Reins H-A, Lee J, Romeo A, Hasset R, Kosman D, Jentsch S (1993). MAC1, a nuclear regulatory protein related to Cu-dependent transcription factors is involved in Cu / Fe utilization and stress resistance in yeast. *EMBO Journal* **12**: 5051-5056.

Kabata-Pendias A, Pendias H (2001). Trace elements in soil and plants. Boca Raton, FL CRC Press.

Kaim W, Rall J (1996). Copper, a "modern bioelement". *Angewandte Chemie International Edition* **35**: 43-60.

Kanamaru K, Kashiwagi S, Mizuno T (1994). A copper-transporting P-type ATPase found in the thylakoid membrane of the cyanobacterium *Synechococcus* species PCC7942. *Molecular Microbiolgy* **13**: 369-377.

Kazan K (2003). Alterantive splicing and proteome diversity in plants: the tip of iceberg has just emerged. *Trends in Plant Science* **8**: 468-471.

Kirchhoff H, Hinz H-J, Rösgen J (2003). Aggregation and fluorescence quenching of chlorophyll a of the light-harvesting complex II from spinach in vitro. *Biochimica et Biophysica Acta* **1606**: 105-116.

Kishinami I, Widholm JM (1986). Selection of copper and zinc resistant *Nicotiana plumbaginifolia* cell suspension cultures. *Plant Cell Physiology* **27**: 1263-1268.

Kishinami I, Widholm JM (1987). Characterization of Cu and Zn resistant *Nicotiana plumbaginifolia* suspension cultures. *Plant Cell Physiology* **28**: 203-210.

Koch KA, Peña MM, Thiele DJ (1997). Copper-binding motifs in catalysis,transport, detoxification and signaling. *Chemistry & Biology* **4**: 549-560.

Kochian LV (1991). Mechanisms of micronutrient uptake and translocation in plants. In: Segoe S (Ed.). *Micronutrients in Agriculture*. SSSA, Madison, Wi, USA, pp. 229-295.

Kochian LV, Hoekenga OA, Pineros MA (2004). How do crop plants tolerate acid soils? -Mechanisms of aluminium tolerance and phosphorous efficiency. *Annual Review of Plant Biology* **55**: 459-493.

Kopittke PM, Menzies NW (2006). Effect of Cu on growth of cowpea (*Vigna unguiculata*). *Plant and Soil* **279**: 287-296.

Koster AJ, Klumperman J (2003). Electron microscopy in cell biology: integrating structure and function. *Nature Reviews Molecular Cell Biology* **4**: SS6-SS10.

Krämer U, Clemens S (2006). Functions and homeostasis of zinc, copper, and nickel in plants. In: Tamás MJ, Martinoia E (Eds.). *Molecular Biology of Metal Homeostasis and Detoxification from Microbes to Man*. Springer, pp. 214-272.

Kruk J, Burda K, Jemiota-Rzmínska M, Strzalka K (2003). The 33 kDa protein of photosystem II is a low-affinity calcium and lanthanide-binding protein. *Biochemistry* **42**: 14862-14867.

Kühlbrandt W (2004). Biology, structure and mechanim of P-type ATPases. *Nature* **5**: 282-294.

Kuo WT, Tang TK (1998). Effect of G6PDH overexpression in NIH3T3 cells treated with tert-butyl hydroperoxide of paraquat. *Free Radical Biology & Medicine* **24**: 1130-1138.

Kuper J, Llamas A, Hecht HJ, Mendel RR, Schwarz G (2004). Structure of the molybdopterin-bound Cnx1G domain links molybdenum and copper metabolism. *Nature* **430**: 803-806.

Küpper H, Küpper F, Spiller M (1996). Environmental relevance of heavy metal substituted chlorophylls using the example of water plants. *Journal of Experimental Botany* **47**: 259-266.

Küpper H, Šetlik I, Šetliková E, Ferimazova N, Spiller M, Küpper FC (2003). Copper-induced inhibition of photosynthesis: limiting steps of in vivo copper chlorophyll formation in *Scenedemus quadricauda*. *Functional Plant Biology* **30**: 1187-1196.

Kurepa J, Montagu MV, Inzé D (1997). Expression of *sodCp* and *sodB* genes in *Nicotiana tabacum*: effects of light and copper excess. *Journal of Experimental Botany* **48**: 2007-2014.

La Fontaine S, Quinn JM, Nakamoto SS, Page MD, Göhre V, Moseley JL, Kropat J, S. M (2002). Copper-dependent iron assimilation pathway in the model photosynthetic eukaryote *Chlamydomonas reinhardtii*. *Eukariotic Cell* **1**: 736-757.

Laemmli UK (1970). Cleavage of structural proteins during the assembly of the head of bacteriophage. *Nature* **227**: 680-685.

Landjeva S, Merakchijska-Nikolova M, Ganeva G (2003). Copper toxicity tolerance in *Aegilops* and *Haynaldia* seedlings. *Biologia Plantarum* **46**: 479-480.

Lepp NW (2004). Copper. In: Shtangeeva I (Ed.). *Trace and Ultratrace Elements in Plants and Soils*. WITpress, Russia, pp. 129-148.

Li L, Cheng X, Ling HQ (2004). Isolation and characterization of Fe (III)-reductase gene *LeFRO1* in tomato. *Plant Molecular Biology* **5**: 125-136.

Liao MT, Hedley MJ, Woolley DJ, Brooks RR, Nichols MA (2000). Copper uptake and trnaslocation in chicory (*Cichorium intybus* L. cv Grasslands Puna) and tomato (*Lycopersicom esculetum* Mill. cv Rondy) plants growth in NFT system. II. The role of nicotianamine and histidine in xylem sap copper transport. *Plant and Soil* **223**: 243-252.

Lidon FC, Henriques FS (1991). Limiting step on photosynthesis of rice plants treated with varing copper levels. *Journal of Plant Physiology* **138**: 115-118.

Lidon FC, Henriques FS (1993). Changes in the thylakoid membrane polypeptide patterns triggered by excess Cu in rice. *Photosynthethica* **28**: 109-117.

Lightbody JJ, Krogmann DW (1967). Isolation and properties of plastocyanin from *Anabaena variabilis*. *Biochimica et Biophysica Acta* **131**: 508-515.

Lin C-C, Chen L-M, Liu Z-H (2005). Rapid effect of copper on lignin biosynthesis in soybean roots. *Plant Science* **168**: 855-861.

Lindley PF (2001a). Multi-copper oxidases. In: Bertini I, Sigel A, Sigel H (Eds.). *Handbook of Metalloproteins*. CRC Press, Basel, Switzerland, pp. 763-812.

Lindley PF (2001b). Proteins of various functions containing copper. In: Bertini I, Sigel A, Sigel H (Eds.). *Handbook of Metalloproteins*. CRC Press, Basel, Switzerland, pp. 857-880.

Llorens N, Arola L, Blade C, Mas A (2000). Effects of copper exposure upon nitrogen metabolism in tissue-cultured *Vitis vinifera*. *Plant Science* **160**: 159-163.

Loneragan JF (1981). Distribution and movement of copper in plants. In: Loneragan JF, Robson AD (Eds.). *Copper in Soils and Plants*. Academic Press, New York, pp. 165-188.

López-Millán AF, Musetti V, Stephens BW, Li CM, Grusak MA (2005). Identification and characterization of an Fe (III) reductase, *Mt*FRO1, in *Medicago truncatula*. In. *2005 Legume Congress*, Assilomar, CA (USA).

Luna CM, González CA, Trippi VS (1994). Oxidative damage caused by an excess of copper in oat leaves. *Plant Cell Physiology* **35**: 11-15.

Macnair MR (1993). The genetic of metal tolerance in vacular plants. *New Phytologist* **124**: 541-559.

Maksymiec W, Russa R, Urbanik-Sypniewska T, Baszynski T (1994). Effect of excess Cu on the photosynthetic apparatus of runner bean leaves treated at two different growth stages. *Physiologia Plantarum* **91**: 715-721.

Maksymiec W (1997). Effect of copper on cellular processes in higher plants. *Photosynthethica* **34**: 321-341.

Mariano ED, Jorge RA, Keltjens WG (2005). Metabolism and root exudation of organic acid anions under aluminium stress. *Brazilian Journal of Plant Physiology* **17**: 157-172.

Markossian KA, Kurganov BI (2003). Copper chaperones, intracellular copper trafficking proteins. Function, structure and mechanism of action. *Biochemistry (Moscow)* **68**: 827-837.

Marschner H (1995). Mineral nutrition of higher plants. Academic Press, Boston, USA.

Marusek CM, Trobaugh NM, Flurkey WH, Inlow JK (2006). Comparative analysis of polyfenol oxidase from plant and fungal species. *Journal of Inorganic Biochemistry* **100**: 108-123.

Mench M, Morel JL, Guckert A (1988). Action des métaux [Cd (II), Cu (II), Pb (II), Zn (II)] sur la production d'exsudats racinaires solubles chez le maïs (*Zea mays* L.). *Agronomie* **8**: 237-241.

Mench M (1990). Transfert des oligo-éléments du sol à la racine et absorption. *Comptes Rendus Académie d'Agriculture de France* **76**: 17-30.

Mendel RR (2005). Molybdenum: biological activity and metabolism. *Dalton Transactions* **21**: 3404-3409.

Merchant S (1998). Synthesis of metalloproteins involved in photosynthesis: plastocyanin and cytochromes. In: Rochaix J-D, Goldschmidt-Clermont M, Merchant S (Eds.). *The molecular biology of chloroplasts and mithocondria in Clamydomonas*. Kluwer Academiv Publishers, The Netherlands, pp. 598-609.

Merchant S, Dreyfuss BW (1998). Posttranslational assembly of photosynthetic metalloproteins. *Annual Review of Plant Physiology and Plant Molecular Biology* **49**: 25-51.

Merchant S, Allen M, Ericksson M, Kropat J, Moseley JL, Quinn J, Tottey S (2004). Metabolic adaptation in a photosynthetic eukaryote to nutritional copper deficiency occurs through a novel DNA binding protein, Crr1. In. *Trace Element Metabolism: Integrating Basic and Applied Research, FASEB Summer Research Conferences*, Snowmass, Colorado, USA.

Mills RF, Krijger JL, Baccarini PJ, Hall JL, Williams LE (2003). Functional expression of AtHMA4, a P_{1B}-type ATPase of the Zn/Co/Cd/Pb subclass. *The Plant Journal* **35**: 164-176.

Mills RF, Francini A, Ferreira da Rocha PSC, Baccarini PJ, Aylett M, Krijger GC, Williams LE (2005). The plant P_{1B}-type ATPase AtHMA4 transport Zn and Cd and plays a role in detoxification of transition metals supplied at elevated levels. *FEBS Letters* **579**: 783-791.

Mira H, Martínez-García F, Peñarrubia L (2001a). Evidence for the plant-specific intercellular transport of the Arabidopsis copper chaperone CCH. *The Plant Journal* **25**: 521-528.

Mira H, Vilar M, Perez-Paya E, Peñarrubia L (2001b). Functional and conformational properties of the exclusive of the C-domain from the Arabidopsis copper chaperone (CCH). *Biochemical Journal* **367**: 545-549.

Mira H, Martínez N, Peñarrubia L (2002). Expression of a vegetative-storage-protein gene from Arabidopsis is regulated by copper, senescence and ozone. *Planta* **214**: 939-946.

Mithöfer A, Schulze B, Boland W (2004). Biotic and heavy metal stress response in plants. *FEBS Letters* **566**: 1-5.

Modreck B, Lee C (2002). A genomic view of alternative splicing. *Nature Genetics* **30**: 13-19.

Mohanty N, Vass I, Demeter S (1989). Copper toxicity affects photosystem II electron transport at the secondary quinone acceptor Q_B. *Plant Physiology* **108**: 29-38.

Molas J (2002). Changes of chloroplast ultraestructure and total chlorophyll concentration in cabbage leaves by excess of organic Ni(II) complexes. *Environmental and Experimental Botany* **47**: 115-126.

Molina-Heredia FP, Wastl J, Navarro JA, Bendall DS, Hervás M, Howe CJ, De La Rosa MA (2003). Photosynthesis: a new function for an old cytochrome? *Nature* **424**: 33-34.

Moseley JL, Quinn J, Eriksson M, Merchant S (2000). The *Crd1* gene encodes a putative di-iron enzyme required for photosystem I accumulation in copper deficiency and hypoxia in *Chlamydomonas reinhardtii*. *EMBO Journal* **19**: 2139-2151.

Moseley JL, Page MD, Alder NP, Ericksson M, Quinn J, Soto F, Theg SM, Hippler M, Merchant S (2002). Reciprocal expression of two candidate di-iron enzymes affecting photosystem I and light-harvesting complex accumulation. *The Plant Cell* **14**: 673-688.

Moya JL, Ros R, Picazo I (1993). Influence of cadmium and nickel on growth, net photosynthesis and carbohydrate distribution in rice plants. *Photosynthesis Research* **36**: 75-80.

Mukherjee I, Campbell NH, Ash JS, Connolly EL (2006). Expression profiling of the Arabidopsis ferric chelate reductase (*FRO*) gene family reveals differential regulation by iron and copper. *Planta* **223**: 1-13.

Mullineaux CW (2005). Function and evolution of grana. *Trends in Plant Science* **10**: 521-525.

Murphy A, Taiz L (1995). Comparison of metallothionein gene expression and non-protein thiols in ten *Arabidopsis* ecotypes. Correlation with copper tolerance. *Plant Physiology* **109**: 945-954.

Murphy A, Eisenger WR, Shaff JE, Kochian LV, Taiz L (1999). Early-copper induced leakage of K^+ from *Arabidopsis* seedlings is mediated by ion channels and coupled to citrate efflux. *Plant Physiology* **121**: 1375-1382.

Murphy KA, Kuhle RA, Fischer AM, Anterola AM, Grimes HD (2005). The functional status of paraveinal mesophyll vacuoles changes in response to altered metabolic conditions in soybean leaves. *Functional Plant Biology* **32**: 335-344.

Nagler M, Eliade E, Zinca N (1973). Morphological and physiological reactions of vines to fungicide treatment. *Analele Institutului de Cercetari pentru Protectis Plantelor* **11**: 261-267.

Nakamura K, Go N (2005). Function and molecular evolution of multicopper blue proteins. *Cellular and Molecular Life Science* **61**: 926-937.

Navari-Izzo F, Quartacci MF, Pinzino C, Dalla VF, Sgherri CLM (1998). Thylakoid-bound and stromal antioxidative enzymes in wheat treated with excess copper. *Physiologia Plantarum* **104**: 630-638.

Nerssissian AM, Shipp EL (2002). Blue copper-binding domains. *Advances in Protein Chemistry* **60**: 271-340.

Nield J, Hankamer B, Zheleva D, Hodges ML, Boekema EJ, Barber J (1995). Biochemical characterisation of PSII-LHCII complexes associated with and lacking the 33 kDa subunit. In: Mathis P (Ed.). *Photosynthesis: from Light to Biosphere*. Dordrecht: Kluwer Academic Publishers, pp. 361-364.

Norvell WA, Welch RM, Adams ML, Kochian LV (1993). Reduction of Fe (III), Mn (II), and Cu (II) chelates by roots of pea (*Pisum sativum* L.) or soybean (*Glycine max*). *Plant and Soil* **155/156**: 123-126.

O' Brien TP, McCully ME (1981). The study of plant structure principles and selected methods. Termarcarphi Pty. Ltd., Melbourne, Australia, pp. 357.

Ouariti O, Boussama N, Zarrouk M, Cherif A, Ghorbal MH (1997). Cadmium- and copper-induced changes in tomato membrane lipids. *Phytochemistry* **45**: 1343-1350.

Ouzounidou G, Moustakas M, Strasser RJ (1997). Sites of action of copper in the photosynthetic apparatus of maize leaves: kinetic analysis of chlorophyll fluorescence, oxygen evolution, absorption changes and thermal dissipation as monitored by photoacoustic signals. *Australian Journal of Plant Physiology* **24**: 81-90.

Pålsgård E, Lindh U, Roomans GM (1994). Comparative study of freeze-substitution techniques for X-ray microanalysis of biological tissue. *Microscopy Research and Technique* **28**: 254-258.

Panou-Filotheou H, Bosabalidis AM (2004). Root structural aspects associated with copper toxicity in oregano (*Origanum vulgare* subsp. *hirtum*). *Plant Science* **166**: 1497-1504.

Parker DR, Ruscitti T, McCue KF, Ow DW (2001). Reevaluating the free-ion activity of trace metal toxicity toward higher plants: experimental evidence with copper and zinc. *Environmental Toxicology and Chemistry* **20**: 899-906.

Pätsikkä E, Aro EM, Tyystjarvi E (1998). Increase in the quantum yield of phoinhibition contributes to copper toxicity in vivo. *Plant Physiology* **117**: 619-627.

Pätsikkä E, Aro E-M, Tyystjarvi E (2001). Mechanism of copper-enhanced photoinhibition in thylakoid membranes. *Physiologia Plantarum* **113**: 142-150.

Pätsikkä E, Kairavuo M, Šeršen F, Aro E-M, Tyystjärvi E (2002). Excess copper predisposes photosystem II to photoinhibition in vivo by outcompeting iron and causing decrease in leaf chlorophyll. *Plant Physiology* **129**: 1359-1367.

Phung LT, Ajlani G, KaselKorn R (1994). P-type ATPase from the cyanobacterium *Synechococcus* 7942 related to the human Menkes and Wilson disease gene products. *Proceedings of the National Academy of Sciences USA* **91**: 9651-9654.

Pich A, Scholz G, Stephan UW (1994). Iron-dependent changes of heavy metals, nicotianamine, and citrate in different plant organs and in the xylem exudate of two tomato genotypes. Nicotianamine as possible copper translocator. *Plant and Soil* **61**: 323-326.

Pich A, Scholz G (1996). Translocation of copper and other mcronutrients in tomato plants (*Lycopersicom esculetum* Mill.): nicotianamine-stimulated copper transport in the xylem. *Journal of Experimental Botany* **47**: 41-47.

Pilon M, Abdel-Ghany SE, Cohu CM, Gogolin KA, Ye H (2006). Copper cofactor delivery in plant cells. *Current Opinion in Plant Biology* **9**: 1-8.

Pilon-Smits E, Pilon M (2002). Phytorremediation of metals using transgenic plants. *Critical Reviews in Plant Science* **21**: 439-456.

Prasad MNV, Strzalka K (1999). Impact of heavy metals on photosynthesis. In: Prasad MNV, Hagemeyer J (Eds.). *Heavy Metal Stress in Plants*. Springer Publisher, Berlin, pp. 117-138.

Puig S, Thiele DJ (2002). Molecular mechanisms of copper uptake and distribution. *Current Opinion in Chemical Biology* **6**: 171-180.

Quartacci MF, Pinzino C, Sgherri CLM, Vecchia FD, Navari-Izzo F (2000). Growth in excess of copper induces changes in the lipid composition and fluidity of PSII-enriched membranes in wheat. *Physiologia Plantarum* **108**: 87-93.

Quartacci MF, Cosi E, Navari-Izzo F (2001). Lipids and NADPH-dependent superoxide production in plasma membrane vesicles from roots of wheat grown under copper deficiency or excess. *Journal of Experimental Botany* **52**: 77-84.

Rae TD, Schmidt PJ, Pufahl RA, Culotta VC, O'Halloran TV (1999). Undetectable intracellular free copper: the requirement of a copper chaperone for superoxide dismutase. *Science* **284**: 805-808.

Raeymaekers T, Potters G, Asard H, Guisez Y, Horemans N (2003). Copper-mediated oxidative burst in *Nicotiana tabacum* L. cv. Bright Yellow 2 cell suspension cultures. *Protoplasma* **221**: 93-100.

Rai LC, Mallick N, Singh JB, Kumar HD (1991). Physiological and biochemical characteristics of a copper tolerant and a wild type strain of *Anabaena doliolum* under copper stress. *Journal of Plant Physiology* **138**: 68-74.

Rai V, Khatoon S, Bisht SS, Mehrotra S (2005). Effect of cadmium on growth, ultramorphology of leaf and secondary metabolites of *Physllanthus amarus* Schum. and Thonn. *Chemosphere* **61**: 1644-1650.

Rashid A, Camm EL, Ekramoddoullah AK (1994). Molecular mechanism of action of Pb^{2+} and Zn^{2+} on water oxidizing complex of photosystem II. *FEBS Letters* **350**: 296-298.

Rauser WE (1999). Structure and function of metal chelators produced by plants. The case for organic acids, amino acids, phytin, and metallothioneins. *Cell Biochemistry and Biophysics* **31**: 19-48.

Raven JA, Evans MCW, Korb RE (1999). The role of trace metals in photosynthetic electron transport in O_2-evolving organisms. *Photosynthesis Research* **60**: 111-149.

Reddy MCM, Harris ED (1998). Multiple transcripts coding for the Menkes gene: evidence for alternative splicing of Menkes mRNA. *Biochemical Journal* **334**: 71-77.

Reichman SM, Menzeis NW, Asher CJ, Mulligan DR (2006). Responses of four Australian tree species to toxic concentrations of copper in solution culture. *Journal of Plant Nutrition* **29**: 1127-1141.

Renganathan M, Bose S (1990). Inhibition of photosystem II activity by Cu(II) ion. Choice of buffer and reagent is critical. *Photosynthesis Research* **23**: 95-99.

Rensing M, Ghosh M, Rosen BP (1999). Families of soft-metal-ion-transporting ATPases. *Journal of Bacteriology* **181**: 5891-5897.

Risueño MC, Medina FJ (1986). The nucleolar structure in plant cells. *Cell Biology Review* **7**: 1-140.

Risueño MC, Testillano PS, González-Melendi P (1998). The use of cryomethods for plant biology studies. In: Calderón-Benavides HA, Yacamán MJ (Eds.). *Electron Microscopy 98*. Inst. Physics, Publ., Bristol Philadelphia, pp. 3-4.

Robinson NJ, Procter CM, Connolly EL, Guerinot ML (1999). A ferric-chelate reductase for iron uptake from soils. *Nature* **397**: 694-697.

Rodríguez FI, Esch JJ, Hall AE, Binder BM, Schaller GE, Bleecker AB (1999). A copper cofactor for ethylene receptor ETR1 from Arabidopsis. *Science* **283**: 996-998.

Rogers SMD, Ogren WL, Widholm JM (1987). Photosynthetic characteristics of a photoautotrophic cell suspension culture of soybean. *Plant Physiology* **84**: 1451-1456.

Roitsch T, Sinha AK (2002). Application of photoautotrophic suspensions cultures in plant science. *Photosynthetica* **40**: 481-492.

Rombolà AD, Gogorcena Y, Larbi A, Morales F, Balde E, Marangoni B, Tagliavini M, Abadía J (2005). Iron deficiency-induced changes in carbon fixation and leaf elemental composition of sugar beet (*Beta vulgaris*) plants. *Plant and Soil* **27**: 39-45.

Roncel M, Ortega JM, Losada M (2001). Factors determining the special redox properties of photosynthetic cythocrome b_{559}. *European Journal of Biochemistry* **268**: 4961-4968.

Rozak PR, Seiser RM, Wacholtz WF, Wise RR (2002). Rapid, reversible alterations in spinach thylakoid appression upon changes in light intensity. *Plant Cell and Environment* **25**: 421-429.

Ruzsa SM, Scandalios JG (2003). Altered Cu metabolism and differential transcription of Cu/Zn*Sod* genes in a Cu/ZnSOD-deficient mutant of maize: evidence for a Cu-responsive transcription factor. *Biochemistry* **42**: 1508-1516.

Salim R, Al-Subu MM, Douleh A, Chenavier L, Hagemeyer J (1992). Effects of root and foliar treatments on carrot plants with lead and cadmium on the growth, uptake and the distribution of metals in treated plants. *Journal of Environmental Science Health Part A* **27**: 1739-1758.

Sambrook J, Russel DW (2001). Molecular Cloning - A laboratory manual. Cold Spring Harbor, New York: Cold Spring Harbor Laboratory Press.

Sancenón V, Puig S, Mira H, Thiele DJ, Peñarrubia L (2003). Identification of a copper transporter family in *Arabidopsis thaliana*. *Plant Molecular Biology* **51**: 577-587.

Sancenón V, Puig S, Mateu-Andrés I, Dorcey E, Thiele DJ, Peñarrubia L (2004). The *Arabidopsis* copper transporter COPT1 functions in root elengation and pollen development. *Journal of Biological Chemistry* **279**: 15348-15355.

Sandmann G, Böger P (1980). Copper-mediated lipid peroxidation processes in photosynthetic membranes. *Plant Physiology* **66**: 797-800.

Sandmann G, Böger P (1983). Enzymological function of heavy metals and their role in electron transfer processes of plants. In. *Encyclopedia of Plant Physiology, New series. Physiological Plant Ecology III: Responses to Chemical and Biological Environment*. Springer-Verlag, Berlin, pp. 246-300.

Sandström B (2001). Micronutrient interactions: effects on absorption and bioavailability. *British Journal of Nutrition* **85**: 181-185.

Satpute GK, Long H, Seguí-Simarro JM, Risueño MC, Testillano PS (2005). Cell architecture during gametophytic and embryogenic microspore development in *Brassica napus* L. *Acta Physiologiae Plantarum* **27**: 665-674.

Sazinsky MH, Agarwal S, Argüello JM, Rosenzweig AC (2006). Structure of the actuator domain from the *Archaeoglobus fulgidus* Cu^{+}-ATPase. *Biochemistry* **45**: 9949-9955.

Sazinsky MH, Mandal AK, Argüello JM, Rosenzweig AC (2006). Structure of the ATP binding domain from the *Archaeoglobus fulgidus* Cu^{+}-ATPase. *Journal of Biological Chemistry* **281**:11161-11166.

Schaaf G, Schikora A, Haberle J, Vert G, Ludewig U, Briat J, Curie C, von Wiren N (2005). A putative function for the arabidopsis Fe-Phytosiderophore transporter homolog AtYSL2 in Fe and Zn homeostasis. *Plant Cell Physiology* **46**: 762-774.

Schat H, Vooijs R (1997). Multiple tolerance and co-tolerance to heavy metals in *Silene vulgaris*: A co-segregation analysis. *New Phytologist* **136**: 489-496.

Schlarb-Ridley BG, Nimmo RH, Purton S, Howe CJ, Bendall DS (2006). Cytochrome c_{6A} is a funnel for thiol oxidation in the thylakoid lumen. *FEBS Letters* **580**: 2166-2169.

Schmidt W (1999). Mechanisms and regulation of reduction-based iron uptake in plants. *New Phytologist* **141**: 1-26.

Schröder WP, Arellano JB, Bittner T, Barón M (1994). Flash-induced absorption spectroscopy studies of copper interaction with photosystem II in higher plants. *Journal of Biological Chemistry* **52**: 32865-32870.

Schubert TS (1982). Copper deficiency of plants. *Plant Pathology Circular* **241**.

Schwacke R, Schneider A, Van der Graaff E, Fischer K, Catoni E, Desimone M, Frommer WB, Flügge UI, Kunze R (2003). ARAMEMNON, a novel database for Arabidopsis integral membrane proteins. *Plant Physiology* **131**: 16-26.

See YP, Jackowski G (1990). Estimating molecular weights of polypeptides by SDS gel electrophoresis. In: Creighton TE (Ed.). *Protein structure a practical approach*. IRL Press, Oxford University Press, pp. 1-19.

Seguí-Simarro JM, Testillano PS, Risueño MC (2003). Hsp70 and Hsp90 Change Their Expression and in situ Localization After Microspore Embryogenesis Induction in *Brassica napus* cv. Topas. *Journal of Structural Biology* **142**: 379-391.

Seguí-Simarro JM, Testillano PS, Jouannic S, Henry Y, Risueño MC (2005). MAP kinases are developmentally regulated during stress-induced microspore embryogenesis in *Brassica napus*. *Histochemistry of Cell Biology* **123**: 541-551.

Seguí-Simarro JM, Bárány I, Suárez R, Fadón B, Testillano PS, Risueño MC (2006). Nuclear bodies domain changes with microspore reprogramming to embryogenesis. *European Journal of Histochemistry*: 35-44.

Seigneurin-Berny D, Gravot A, Auroy P, Mazard C, Kraut A, Finazzi G, Grunwald D, Rappaport F, Vavasseur A, Joyard J, Richaud P, Rolland NJBC (2006). HMA1, a new Cu-ATPase of the chloroplast envelope, is essential for growth under adverse light conditions. *Journal of Biological Chemistry* **28**: 2882-2892.

Sersen K, Králová K, Bumbálová A, Svajlenova O (1997). The effect of Cu (II) ions bound with tridentade Schiff base ligands upon the photosynthetic apparatus. *Journal of Plant Physiology* **151**: 299-305.

Shikanai T, Müller-Moulé P, Munekage Y, Niyogi KK, Pilon M (2003). PAA1, a P-type ATPase of Arabidopsis, functions in copper transport in chloroplasts. *The Plant Cell* **15**:1333-1346.

Shingles R, Wimmers LE, McCarty RE (2004). Copper transport across pea thylakoid membranes. *Plant Physiology* **135**: 145-151.

Silva MS, Fortes AM, Testillano PS, Risueño MC, Pais S (2004). Differential expression and cellular localization of ERKs during organogenic nodule formation from internodes of *Humulus lupulus* var. Nugget. *European Journal of Cell Biology* **83**: 425-433.

Solioz M, Vulpe C (1996). CPx-ATPases: A class of P-type ATPases that pump heavy metals. *Trends in Biochemical Science* **21**: 237-241.

Sommer A, Ne'eman E, Steffens JC, Mayer AM, Harel E (1994). Import, targeting, and processing of a plant polyphenol oxidase. *Plant Physiology* **105**: 1301-1311.

Stacey MG, Koh S, Becker J, Stacey G (2002). AtOPT3, a member of the oligopeptide transporter family, is essential for embryo development in Arabidopsis. *The Plant Cell* **14**: 2799-2811.

Stoyanova DP, Tchakalova FS (1997). Cadmium-induced ultrastructural changes in chloroplasts of the leaves and ítems parenchyma in *Myriophyllum spicatum* L. *Photosynthetica* **34**: 241-248.

Sugiura M, Takeda Y (2000). Nucleic Acids. In: Buchanan BB, Gruissem W, Jones RL (Eds.). *Biochemistry & Molecular Biology of Plants*. American Society of Plant Physiology, Rockville, Maryland, USA, pp. 260-310.

Testilllano PS, González Melendi P, Ahmadian P, Fadon B, Risueño MC (1995). The immunolocalization of nuclear antigens during the pollen developmental program and the induction of pollen embryogenesis. *Experimental Cell Research* **221**: 41-54.

Testillano PS, González-Melendi P, Coronado MJ, Seguí JM, Moreno. MA, Risueño MC (2005). Differentiating plant cells switched to proliferation remodel the functional organization of nuclear domains. *Cytogenetic and Genome Research* **109**: 166-174.

Tewari RK, Kumar P, Sharma PN (2006). Antioxidant responses to enhanced generation of superoxide anion radical and hydrogen peroxide in the copper-stresses mulberry plants. *Planta* **223**: 1145-1153.

Thomas JC, Davies EC, Malick FK, Endreszi C, Williams CR, Abbas M, Petrella S, Swisher K, Perron M, Edwards R, Osenkowski P, Urbanczyk N, Wiesend WN, Murray KS (2003). Yeast metallothionein in transgenic tobacco promotes copper uptake from contaminated soils. *Biotechnology Progress* **19**: 273-280.

Thompson JD, Higgins DG, Gibson TJ (1994). CLUSTAL W: improving the sensitivity of progressive multiple sequence alignment through sequence weighting, position-specific gap penalties and weight matrix choice. *Nucleic Acids Research* **22**: 4673-4680.

Tiffin LO (1972). Translocation of micronutrients in plants. In: Mortvedt JJ, Giordano PM, Lindsay WL (Eds.). *Micronutrients in Agriculture*. Americam Society of Agronomy, Madison, pp. 199-229.

Tong PY, Ling BY, Gao FL, Wang JH, Li ZQ, Di SH (1995). A study on the effects of copper fertilizer on the growth, development and yield structure of maize. *Beijing Agricultural Sciences* **13**: 36-39.

Tottey S, Borrelly GP, Robinson PJ, Rich PR, Robinson NJ (2001). Two menkes-type ATPases supply copper for photosynthesis in *Synechocystis* PCC 6803. *The Journal of Biological Chemistry* **276**: 999-1004.

Tottey S, Rich PR, Rondet S, Robinson NJ (2002). A copper metallochaperone for photosynthesis and respiration reveals metal-specific targets, interaction with an importer and alternative sites for copper acquisition. *Journal of Biological Chemistry* **277**: 5490-5497.

Tottey S, Block MA, Allen M, Westergren T, Albrieux C, Scheller HV, Merchant S, Jensen PE (2003). Arabidopsis CHL27, located in both envelope and thylakoid membranes, is required for the synthesis of protochlorophyllide. *Proceedings of the National Academy of Sciences USA* **100**: 16119-16124.

Toyoshima C, Nakasako M, Nomura H, Ogawa H (2000). Crystal structure of the calcium pump of sarcoplasmic reticulum at 2.6 Å resolution. *Nature* **405**: 647-655

Toyoshima C, Nomura H (2002). Structural changes in the calcium pump accompanying the dissociation of calcium. *Nature* **418**: 605-611.

Treeby M, Marschner H, Römheld V (1989). Mobilization of iron and other micronutrient cations from a calcareus soil by plant-borne, microbial, and synthetic metal chelators. *Plant and Soil* **114**: 217-226.

Trindade LM, Horvath BM, Bergervoet MJE, Visser RGF (2003). Isolation of a gene encoding a copper chaperone for the copper/zinc superoxide dismutase and characterization of its promoter in potato. *Plant Physiology* **133**: 618-629.

Turner AP, Dickinson NM (1993). Copper tolerance of *Acer-pseudoplatanus* L. (sycamore) in tissue-culture. *New Phytologist* **123**: 523-530.

Van Dorssen RJ, Plijter JJ, Dekker JP, den Ouden A, Amesz J, Van Gorkom HJ (1987). Spectroscopic properties of chloroplasts grana membranes and the core of photosystem II. *Biochimica et Biophysica Acta* **890**: 134-143.

Van Hoof NA, Hassinen VH, Hakvoort HW, Ballintijn KF, Schat H, Verkleij JA, Ernst WH, Karelampi SO, Tervahauta AI (2001). Enhanced copper tolerance in *Silene vulgaris* (Moench) Garcke populations from copper mines is associated with increased transcript levels of a 2b-type metallothionein gene. *Plant Physiology* **126**: 1519-1526.

Van Vliet C, Andersen CR, Cobbett CS (1995). Copper-sensitive mutant of *Arabidopsis thaliana*. *Plant Physiology* **109**: 871-878.

Van Wijk KJ, Bingsmark S, Aro EM, Andersson B (1995). In vitro synthesis and assembly of photosystem II core proteins. The D1 protein can be incorporated into photosystem II in isolated chloroplasts and thylakoids. *Journal of Biological Chemistry* **270**: 25685-25695.

Verret F, Gravot A, Auroy P, Leonhardt N, Pascale D, Nussaume L, Vavasseur A, Richaud P (2004). Overexpression of AtHMA4 enhances root-to-shoot translocation of zinc and cadmium and plant metal tolerance. *FEBS Letters* **576**: 306-312.

Verret F, Gravot A, Auroy P, Preveral S, Forestier C, Vavasseur A, Richaud P (2005). Heavy metal transport by AtHMA4 involves the N-terminal degenerated metal binding domain and the C-terminal His11 stretch. *FEBS Letters* **579**: 1515-1522.

Vila AJ, Fernández CO (2001). Copper in electron-transfer proteins. In: Bertini I, Sigel A, Sigel H (Eds.). *Handbook of Metalloproteins*. CRC Press, Basel, Switzerland, pp. 813-856.

Vitória AP, Rodriguez APM, Cunha M, Lea PJ, Azevedo RA (2004). Structural changes in radish seedlings (*Raphanus sativus*) exposed to cadmium. *Biologia Plantarum* **47**: 561-568.

Vitória AP, Cunha M, Azevedo RA (2006). Ultraestructural changes of radish leaf exposed to cadmium. *Environmental and Experimental Botany* **58**: 47-52.

Wastl J, Bendall DS, Howe CJ (2002). Higher plants contain a modified cytochrome c_6. *Trends in Plant Science* **7**: 244-245.

Wastl J, Purton S, Bendall DS, Howe CJ (2004). Two forms of cytochrome c_6 in a single eukaryote. *Trends in Plant Science* **9**: 474-476.

Waters BM, Blevins DG, Eide DJ (2002). Characterization of FRO1, a pea ferric-chelate reductase involved in root iron acquisition. *Plant Physiology* **129**: 85-94.

Weckx JED, Clijsters HMM (1996). Oxidative damage and defense mechanisms in primary leaves of *Phaseolus vulgaris* as aresult of root assimilation of toxic amounts of copper. *Physiologia Plantarum* **96**: 506-512.

Weigel M, Varotto C, Pesaresi P, Finazzi G, Rappaport F, Salamini F, Leister D (2003a). Plastocyanin is indispensable for photosynthetic electron flow in *Arabidopsis thaliana*. *Journal of Biological Chemistry* **278**: 31286-31286.

Weigel M, Pesaresi P, Leister D (2003b). Tracking the function of the cytochrome c_6-like protein in higher plants. *Trends in Plant Science* **8**: 513-517.

Welch RM, Norvell WA, Schaefer SC, Shaff JE, Kochian LV (1993). Induction of iron (III) and copper (II) reduction in pea (*Pisum sativum* L.) roots by Fe and Cu status: Does the root-cell plasmalemma Fe (III)-chelate reductase perform a general role in regulating cation uptake? *Planta* **190**: 555-561.

Williams LE, Pittman JK, Hall JL (2000). Emerging mechanisms for heavy metal transport in plants. *Biochimica et Biophysica Acta* **1465:** 104-126.

Williams LE, Mills RF (2005). P_{1B}-ATPases - an ancient family of transition metal pumps with diverse functions in plants. *Trends in Plant Sciences* **10**: 491-502.

Wintz H, Vulpe C (2002). Plant copper chaperones. *Biochemical Society Transactions* **30**: 732-735.

Wintz H, Fox T, Wu Y-Y, Feng V, Chen W, Chang H-S, Zhu T, Vulpe C (2003). Expression profiles of *A. thaliana* in mineral deficiencies reveal novel transporters involved in metal homeostasis. *Journal of Biological Chemistry* **278**: 47644-47653.

Woeste KE, Kieber JJ (2000). A strong loss-of-function mutation in RAN1 results in constitutive activation of the ethylene response pathway as well as a rosette-lethal phenotype. *The Plant Cell* **12**: 443-455.

Wójcik M, Tukiendorf A (2003). Response of wild type of *Arabidopsis thaliana* to copper stress. *Biologia Plantarum* **46**: 79-84.

Yang H, Wong JW, Yang ZM, Zhou LX (2001). Ability of *Arogyrom elongatum* to accumulate the single metal of cadmium, copper, nickel, and lead and root exudation of organic acids. *Journal of Environmental Science* **13**: 368-375.

Yang XL, Miura N, Kawarada K, Terada K, Petru-khin CT, Gilliam T, Sugiyama GT (1997). Two forms of Wilson disease protein produced by alternative splicing are localized in distinct cellular compartments. *Biochemical Journal* **326**: 897-902.

Yen MR, Tseng YH, Saier MH (2001). Maize yellow stripe1, an iron-phytosiderophore uptake transporter, is a member of the oligopeptide transporter (OPT) transporter. *Microbiology* **147**: 2881-2883.

Yi Y, Guerinot ML (1996). Genetic evidence that induction of Fe (III) chelate reductase activity is neccessary for iron uptake under iron deficency. *The Plant Journal* **10**: 835-844.

Yruela I, Montoya G, Alonso PJ, Picorel R (1991). Identification of the pheophytin-Qa-Fe domain of the redicing side of photosystem II as the Cu(II)-inhibitory binding site. *The Journal of Biological Chemistry* **266**: 22847-22850.

Yruela I, Montoya G, Picorel R (1992). The inhibitory mechanism of Cu on the photosystem II electron transport from higher plants. *Photosynthesis Research* **33**: 227-233.

Yruela I, Alfonso M, Ortiz de Zarate I, Montoya G, Picorel R (1993). Precise location of the Cu(II)-inhibitory binding site in higher plant and bacterial photosyntetic reaction center as probed by light-induced absorption changes. *The Journal of Biological Chemistry* **268**: 1684-1689.

Yruela I, Gatzen G, PIcorel R, Holzwarth AR (1996a). Cu (II)-inhibitory effect on photosystem II from higher plants. A picosecond time-resolved fluorescence study. *Biochemistry* **35**: 9469-9474.

Yruela I, Pueyo JJ, Alonso PJ, PIcorel R (1996b). Photoinhibition of photosystem II from Higher plants: effect of copper inhibition. *The Journal of Biological Chemistry* **271**: 27408-27415.

Yruela I, Alfonso M, Barón M, Picorel R (2000). Copper effect on the protein composition of photosystem II. *Physiologia Plantarum* **110**: 551-557.

Yruela I (2005). Copper in plants. *Brazilian Journal of Plant Physiology* **17**: 145-156.

Zhao H, Eide D (1996). The yeast *ZRT1* gene encodes the zinc transporter protein of a high-affinity uptake system induced by zinc limitation. *Proceedings of the National Academy of Sciences USA* **93**: 2454-2458.

Zhu H, Shipp E, Sanchez RJ, Liba A, Stine JE, Hart PJ, Gralla EB, Nerssisian AM, Valentine JS (2000). Cobalt (2+): binding to human and tomato copper chaperone for superoxide dismutase: implications for the metal ion transfer mechanism. *Biochemistry* **39**: 5413-5421.

Zuppini A, Bugno V, Baldan B (2006). Monitoring programmed cell death triggered by mild heat shock in soybean-cultures cells. *Functional Plant Biology* **33**: 617-627.

CAPÍTULO 11

ANEXO

11.1. PUBLICACIONES

Bernal M, Roncel M, Ortega JM, Picorel R, Yruela I (2004).
Copper effect on the cytochrome b_{559} of photosystem II under photoinhibitory conditions. *Physiologia Plantarum* 120: 686-694.

Bernal M, Ramiro MV, Cases R, Picorel R, Yruela I (2006).
Excess copper effect on growth, chloroplast ultrastructure, oxygen-evolution activity and chlorophyll fluorescence in *Glycine max* cell suspensions. *Physiologia Plantarum* 127: 312-325.

Bernal M, Cases R, Picorel R, Yruela I (2006).
Foliar and root Cu supply affect differently Fe and Zn uptake and photosynthetic activity in soybean plants. *Environmental and Experimental Botany (en prensa)*.

Bernal M, Testillano PS, Risueño MC, Yruela I (2006).
Excess copper induces structural changes in cultured photosynthetic soybean cells. *Functional Plant Biology (en prensa).*

Bernal M, Testillano PS, Alfonso M, Risueño MC, Picorel R (2006).
Identification and subcellular of the soybean copper P_{1B}-ATPase *Gm*HMA8 transporter. *Journal of Structural Biology (en prensa).*

Bernal M, Alfonso M, Picorel R, Yruela I (2006).
Idenfication of two copper *HMA8* P-ATPase mRNAs in soybean: Analysis of their response to copper and their splicing regulatory mechanism (en preparación).